

# **Cyclic (Alkyl)(Amino)Carbene (CAAC)–Mercury(II) Complexes and Their Catalytic Activity in Hydroamination Reactions**

**Bhupendra Goswami**

*A dissertation submitted for the partial fulfilment of  
BS-MS dual degree in Science*



**Department of Chemical Sciences**

**Indian Institute of Science Education and Research Mohali**

**April 2017**

*Dedicated to my parents*

## Certificate of Examination

This is to certify that the dissertation titled “Cyclic (Alkyl)(Amino)Carbene (CAAC)–Mercury(II) Complexes and their Catalytic Activity in Hydroamination Reactions” submitted by Mr. Bhupendra Goswami (Reg. No. MS12059) for the partial fulfilment of BS-MS dual degree programme of the Institute, has been examined by the thesis committee duly appointed by the Institute. The committee finds the work done by the candidate satisfactory and recommends that the report be accepted.

**Dr. Sanjay Singh**  
*Associate Professor*  
*IISER Mohali*  
(Supervisor)

**Dr. Sugumar Venkataramani**  
*Assistant Professor*  
*IISER Mohali*

**Dr. S. S. V. Ramasastry**  
*Assistant Professor*  
*IISER Mohali*

Date:

## Declaration

The work presented in this dissertation has been carried out by me under the guidance of Dr. Sanjay Singh at the Department of Chemical Sciences, Indian Institute of Science Education and Research Mohali. This work has not been submitted in part or in full for a degree, a diploma, or a fellowship to any other university or institute. Whenever contributions of others are involved, every effort is made to indicate this clearly, with due acknowledgement of collaborative research and discussions. This thesis is a bonafide record of original work done by me and all sources listed within have been detailed in the bibliography.

**Bhupendra Goswami**

Date:

Place:

In my capacity as the supervisor of the candidate's project work, I certify that the above statements by the candidate are true to the best of my knowledge.

**Dr. Sanjay Singh**

*Associate Professor  
Department of Chemical Sciences  
Indian Institute of Science Education and Research Mohali  
(Supervisor)*

Date:

Place:



## Acknowledgement

I would like to express my sincere gratitude towards my supervisor Dr. Sanjay Singh for his kind support, guidance, motivation and interest to my project entitled '**Cyclic (Alkyl)(Amino)Carbene (CAAC)–Mercury(II) Complexes and their Catalytic Activity in Hydroamination Reactions**'. Without his help and guidance the project would not have been possible. I am very thankful to him for teaching me experimental skills and also for the course work which I have done with him helped me a lot to understand many basic concepts of chemistry. The confidence and guidance with which he guided me throughout the project requires no elaboration. I will always be thankful to him for his support, patience and for his motivation during my project.

I would also like to thank my thesis committee members Dr. R. VijayaAnand, Dr. S. S. V. Ramasastry and Dr. Sugumar Venkataramani for their valuable inputs, support and suggestions.

My sincere thanks to Mr. Deependra Bawari for his help throughout the execution of this project and at difficult times as well. I owe him for the experimental techniques that he taught me during this project. I would also like to thank my lab mates Mr. Sandeep Rawat, Ms. Mamta Bhandari, Mr. Sandeep Kumar Thakur and Ms. Chandrakala Negi for keeping me motivated and for maintaining cheerful and peaceful atmosphere in lab.

I am thankful to IISER Mohali for providing me with the instrumental and other infrastructural facilities during the course of my project.

At last, I would like to thank my parents, my brother and sisters and my friends for their motivation to accomplish my work.

## Contents

List of Figures	iii
List of Charts	iii
List of Tables	iii
List of Schemes	iv
Notations and Abbreviations	v
Abstract	vii
1. Introduction	1
1.1. Structure and properties of stable carbenes: Metal complex thereof and beyond	1
1.2. An overview of hydroamination reaction	9
2. Results and Discussion	13
2.1. <i>Synthesis and characterization of [CAACH]<sup>+</sup>[HgCl<sub>3</sub>]<sup>-</sup> (1)</i>	
2.2. <i>Synthesis and characterization of [CAAC·HgCl(μ-Cl)]<sub>2</sub> (2)</i>	
2.3. <i>Synthesis and characterization of [CAAC·HgBr(μ-Br)]<sub>2</sub> (3)</i>	
2.4. <i>Synthesis and characterization of [CAAC·HgI(μ-I)]<sub>2</sub> (4)</i>	
2.5. <i>Synthesis and characterization of [(CAAC<sup>cy</sup>)<sub>2</sub>Hg(H<sub>2</sub>O)]<sup>2+</sup>2[NO<sub>3</sub>]<sup>-</sup> (5)</i>	
2.6. <i>Synthesis and characterization of [(CAAC<sup>cy</sup>)<sub>2</sub>Hg]<sup>2+</sup>[Hg<sub>2</sub>Br<sub>6</sub>]<sup>2-</sup> (6)</i>	
2.7. <i>Intermolecular hydroamination reactions using [CAAC<sup>cy</sup>·HgBr(μ-Br)]<sub>2</sub> as a catalyst</i>	

<b>3. Experimental Section</b>	<b>25</b>
3.1. General	25
3.2. Single crystal X-ray structure determination	25
3.3. <i>Preparation of [CAACH]<sup>+</sup>[HgCl<sub>3</sub>]<sup>-</sup> (1)</i>	25
3.4. <i>Preparation of [CAAC·HgCl(μ-Cl)]<sub>2</sub> (2)</i>	26
3.5. <i>Preparation of [CAAC·HgBr(μ-Br)]<sub>2</sub> (3)</i>	26
3.6. <i>Preparation of [CAAC·HgI(μ-I)]<sub>2</sub> (4)</i>	27
3.7. <i>Preparation of [(CAAC<sup>cy</sup>)<sub>2</sub>Hg(H<sub>2</sub>O)]<sup>2+</sup>2[NO<sub>3</sub>]<sup>-</sup> (5)</i>	27
3.8. <i>Preparation of [(CAAC<sup>cy</sup>)<sub>2</sub>Hg]<sup>2+</sup>[Hg<sub>2</sub>Br<sub>6</sub>]<sup>2-</sup> (6)</i>	28
3.9. <i>Preparation of aromatic imines (7-27)</i>	31
<b>4. Conclusion</b>	<b>37</b>
<b>5. Future Directions</b>	<b>38</b>
<b>6. References</b>	<b>39</b>
<b>Supporting Information</b>	<b>44</b>

## List of Figures and Charts

<b>Fig 1.1.</b> Possible geometry with electronic configuration of carbenes.	<b>1</b>
<b>Fig 1.2.</b> Schematic representation of NHCs, CAACs, BACs, ADACs and AAACs.	<b>4</b>
<b>Fig 1.3.</b> CAAC as better electron donor than NHC.	<b>5</b>
<b>Fig 1.4.</b> Group 12 metal complexes of NHCs and CAACs	<b>8</b>
<b>Fig 1.5.</b> Examples of bioactive natural products accessible via hydroamination or-amidation reactions	<b>9</b>
<b>Fig 2.1.</b> Single crystal X-ray structure of $[\text{CAACH}]^+[\text{HgCl}_3]^-$ ( <b>1</b> )	<b>13</b>
<b>Fig 2.2.</b> Single crystal X-ray structure of $[\text{CAAC}\cdot\text{HgCl}(\mu\text{-Cl})]_2$ ( <b>2</b> )	<b>15</b>
<b>Fig 2.3.</b> Single crystal X-ray structure of $[\text{CAAC}\cdot\text{HgBr}(\mu\text{-Br})]_2$ ( <b>3</b> )	<b>16</b>
<b>Fig 2.4.</b> Single crystal X-ray structure of $[\text{CAAC}\cdot\text{HgI}(\mu\text{-I})]_2$ ( <b>4</b> )	<b>18</b>
<b>Fig 2.5.</b> Single crystal X-ray structure of $[(\text{CAAC}^{\text{cy}})_2\text{Hg}(\text{H}_2\text{O})]^{2+}2[\text{NO}_3]^-$ ( <b>5</b> )	<b>19</b>
<b>Fig 2.6.</b> Single crystal X-ray structure of $[(\text{CAAC}^{\text{cy}})_2\text{Hg}]^{2+}[\text{Hg}_2\text{Br}_6]^{2-}$ ( <b>6</b> )	<b>20</b>
<b>Chart 1.1.</b> Major Application of NHCs	<b>3</b>

## List of Tables

<b>Table 2.1.</b> Substrate scope of intermolecular hydroamination reactions.	<b>23</b>
<b>Table 3.1.</b> Crystal data and structure refinement details of complexes <b>1-6</b> .	<b>28</b>

## List of Schemes

<b>Scheme 1.1.</b> Frontier orbitals for carbene carbon atom	<b>2</b>
<b>Scheme 1.2.</b> Stereoselective addition of carbenes with alkene	<b>2</b>
<b>Scheme 1.3.</b> Small molecules activation by CAAC	<b>6</b>
<b>Scheme 1.4.</b> Hydroamination of alkene by primary amines	<b>10</b>
<b>Scheme 1.5.</b> Hydroamination of alkynes by primary amines	<b>10</b>
<b>Scheme 1.6.</b> Proposed mechanism for Hg(II) catalyzed hydroamination of aromatic amines and aromatic alkynes.	<b>12</b>
<b>Scheme 2.1.</b> Synthesis of $[\text{CAACH}]^+[\text{HgCl}_3]^-$ ( <b>1</b> ).	<b>13</b>
<b>Scheme 2.2a.</b> Route attempted for synthesis of the adduct $[\text{CAAC}\cdot\text{HgCl}(\mu\text{-Cl})]_2$ ( <b>2</b> ).	<b>13</b>
<b>Scheme 2.2b.</b> Synthesis of the adduct $[\text{CAAC}\cdot\text{HgCl}(\mu\text{-Cl})]_2$ ( <b>2</b> ).	<b>15</b>
<b>Scheme 2.3.</b> Synthesis of the adduct $[\text{CAAC}\cdot\text{HgBr}(\mu\text{-Br})]_2$ ( <b>3</b> ).	<b>16</b>
<b>Scheme 2.4.</b> Synthesis of the adduct $[\text{CAAC}\cdot\text{HgI}(\mu\text{-I})]_2$ ( <b>4</b> ).	<b>17</b>
<b>Scheme 2.5.</b> Synthesis of $[(\text{CAAC}^{\text{cy}})_2\text{Hg}(\text{H}_2\text{O})]^{2+}2[\text{NO}_3]^-$ ( <b>5</b> ).	<b>18</b>
<b>Scheme 2.6.</b> Synthesis of $[(\text{CAAC}^{\text{cy}})_2\text{Hg}]^{2+}[\text{Hg}_2\text{Br}_6]^{2-}$ ( <b>6</b> ).	<b>20</b>
<b>Scheme 2.7.</b> General intermolecular hydroamination reaction.	<b>22</b>

## Notations and Abbreviations

Ac	Acetyl group (CH <sub>3</sub> C(O))
Å	Angstrom
Ar	Aryl
AP	Atomic probe
calcd	Calculated
$\delta$	Chemical shift in ppm
$J$	Coupling constant
Cy	Cyclohexyl
°	Degree (angle)
°C	Degree Celsius
decomp.	Decomposition
DMSO	Dimethyl sulfoxide
d	Doublet
DMSO-d <sub>6</sub>	Deuterated dimethyl sulfoxide
ES	Electron spray ionization
Hz	Hertz
HRMS	High resolution mass spectrometry
IR	Infrared spectroscopy
$\tilde{\nu}$	Wave number
m/z	Mass/charge
MS	Mass spectrometry
MHz	Mega hertz
Mp	Melting point
Me	Methyl group (CH <sub>3</sub> )
m	Multiplet

NMR	Nuclear magnetic resonance
Z	No. of molecules in the unit cell
ppm	Parts per million
s	Singlet
t	Triplet
THF	Tetrahydrofuran
V	Volume

## Abstract

The unprecedented low valent metal compounds, highly active catalysts are the outcome of the stabilization offered by the appended carbenes to the metal centers. A modified version of NHCs named as cyclic (alkyl)(amino)carbenes (CAACs) discovered by Bertrand in 2005, have surpassed the notion of routine carbene chemistry due to more nucleophilic ( $\sigma$ -donating) as well as electrophilic ( $\pi$ -accepting) nature than those of diamino carbenes. The present work deals with the syntheses of adducts of Cyclic (Alkyl)(Amino)Carbene (CAACs) with  $\text{HgX}_2$  salts. As an initial trial, when  $\text{Hg}(\text{OAc})_2$  was reacted with  $[\text{CAACH}]^+[\text{Cl}]^-$  the ionic complex,  $[\text{CAACH}]^+[\text{HgCl}_3]^-$  (**1**) was isolated. In subsequent attempts, the reaction of insitu generated free carbene was carried out with  $\text{HgX}_2$  salts that smoothly yield the CAAC-Hg(II) adducts as  $[\text{CAAC}\cdot\text{HgCl}(\mu\text{-Cl})_2]$  (**2**),  $[\text{CAAC}\cdot\text{HgBr}(\mu\text{-Br})_2]$  (**3**),  $[\text{CAAC}\cdot\text{HgI}(\mu\text{-I})_2]$  (**4**). In an effort to substitute the halide with a weakly coordinating anion, a cationic mercury species,  $[(\text{CAAC}^{\text{cy}})_2\text{Hg}(\text{H}_2\text{O})]^{2+}2[\text{NO}_3]^-$  (**5**) was also obtained. This product was isolated by reacting  $\text{AgNO}_3$  with the previously synthesized complex by Singh and co-workers  $[\text{CAAC}^{\text{cy}}\cdot\text{HgBr}(\mu\text{-Br})_2]$  (**3.1**) in DMSO. When the same reaction was performed in dry THF a two coordinated cationic mercury complex,  $[(\text{CAAC}^{\text{cy}})_2\text{Hg}]^{2+}[\text{Hg}_2\text{Br}_6]^{2-}$  (**6**) was isolated. After the successful synthesis of some of these adducts, their application in the hydroamination reactions between aromatic amines and terminal alkynes has been explored. The catalytic ability of  $[\text{CAAC}^{\text{cy}}\cdot\text{HgBr}(\mu\text{-Br})_2]$  (**3.1**) in intermolecular hydroamination has been explored in detail.



## 1. Introduction

### 1.1. Structure and Properties of stable carbenes: Metal complexes thereof and beyond

The term carbene was first introduced by Doering in organic chemistry in 1950s and by Fisher in the area of organometallic chemistry in 1964. Carbene is a neutral divalent species having six valence electrons, where four electrons are used in two covalent bonds leaving two nonbonded electrons. Carbenes are coordinatively unsaturated due to the incomplete octet and are traditionally considered as highly reactive species. Carbenes can have either linear or bent geometry which depends on the degree of hybridization at the carbon. Carbenes can be classified as singlet or triplet depending on their electronic states. Singlet carbenes have filled and vacant orbital thereby shows both nucleophilic as well as electrophilic character (i.e., ambiphilic character) while the triplet carbene have two unpaired electrons thereby show biradicaloid character. (Fig 1.1.)

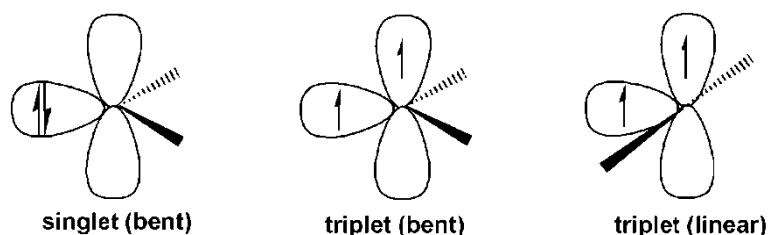
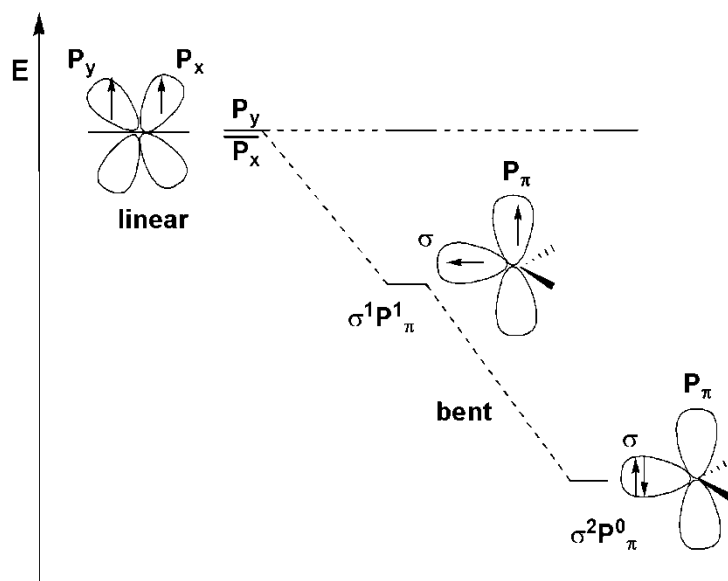


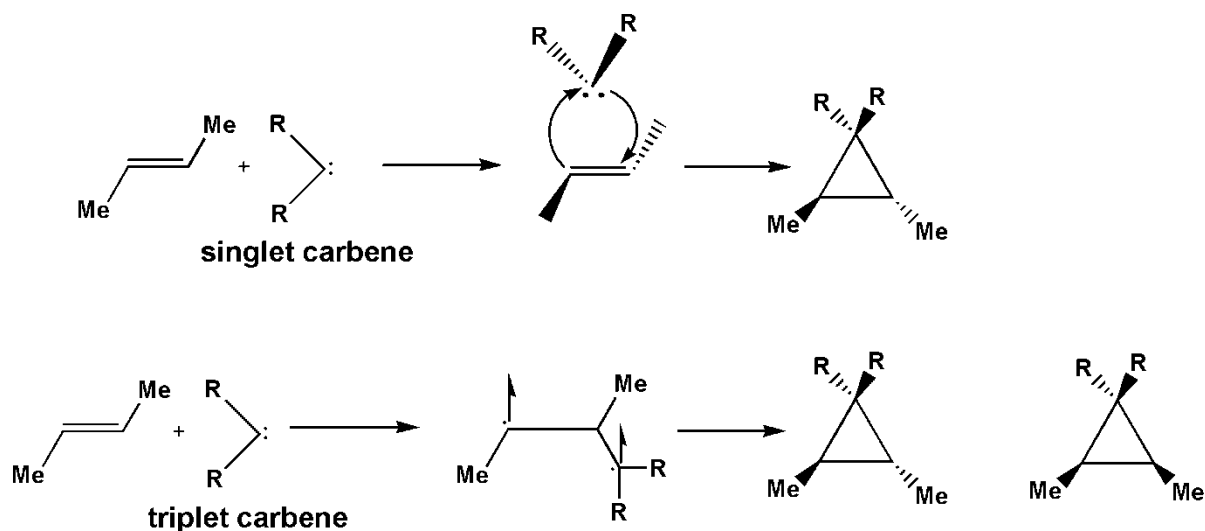
**Fig 1.1.** Possible geometries and electronic configurations of carbenes.

The linear geometry have sp-hybridized carbene centre having P<sub>x</sub> and P<sub>y</sub> degenerate orbitals. On bending the angle at the carbene carbon from linear (sp) the carbene adopts sp<sup>2</sup>-type hybridization and the degeneracy of both P<sub>x</sub> and P<sub>y</sub> orbitals break and the P<sub>x</sub> orbital becomes more stabilized since it acquires more s character therefore it is called as σ orbital. While the P<sub>y</sub> orbital remains almost unchanged and it is called as P<sub>π</sub> orbital. The linear geometry is an extreme case and generally it is not observed. So the frontier orbitals of carbene are depicted by σ and P<sub>π</sub>. (Scheme 1.1).<sup>[1]</sup>



**Scheme 1.1.** Frontier orbitals for carbene carbon atom (Adapted from *Angew. Chem. Int. Ed.* **2008**, *47*, 3122-3172).

The spin state of carbene can be examined by reaction of carbene with alkene results in the formation of cyclopropane derivative. A one step mechanism is possible for singlet carbene thereby affording single cyclopropane product. In the case of triplet carbenes due to intermediary of diradicals, the cyclopropanes formed will be mixtures of two different isomers, which are shown in Scheme 1.2. [2]



**Scheme 1.2.** Stereospecific addition of carbenes with an alkene.

Apart from this, the ground state spin multiplicity of carbenes depend on the relative energy of  $\sigma$  and  $P_\pi$  orbitals. Large  $\sigma$ - $P_\pi$  separation ( $\geq 2\text{eV}$ ) impose singlet ground state spin multiplicity and  $\sigma$ - $P_\pi$  separation of ( $\leq 1.5\text{eV}$ ) implies triplet ground state spin multiplicity. [3]

The  $\sigma$ - $P_\pi$  separation is affected by the inductive effect of the substituents. If the substituents are  $\sigma$  electron withdrawing then it will stabilize the  $\sigma$  nonbonding orbital by increasing the s character leaving the  $P_\pi$  orbital remaining same thus increases  $\sigma$ - $P_\pi$  energy separation leading to the singlet state of the carbene. In contrast,  $\sigma$ -electron donating substituents favour triplet ground state.<sup>[3]</sup>

Prior to 1960, it was considered that carbene is too reactive to be isolated which precluded the efforts to investigate carbene chemistry. This assumption got breakthrough in early 1960's when Wanzlick<sup>[4]</sup> investigated the stability and reactivity of N-heterocyclic carbenes (NHCs) for first time. Shortly thereafter, Wanzlick proposed the first application of NHC as a ligand for metal (mercury) complexes.<sup>[5]</sup> NHCs are defined as heterocyclic species containing a carbene carbon and at least one nitrogen atom within the ring structure.

Despite the discovery of NHC its use as a ligand to bind with transition metals chemistry remained dormant for 23 years until 1991 when Arduengo and co-workers showed for the first time the isolation, storability and crystallinity of NHCs. NHCs show strong  $\sigma$  donor ability like other neutral ligands such as phosphines, ethers and can be considered as a better alternative to phosphines in organometallic and organic chemistry because of easy preparation and possibilities to tune the steric and electronic properties whereas, phosphines are unstable in presence of air. In short, the major applications of NHCs have been summarized in Chart 1.1.<sup>[6]</sup>

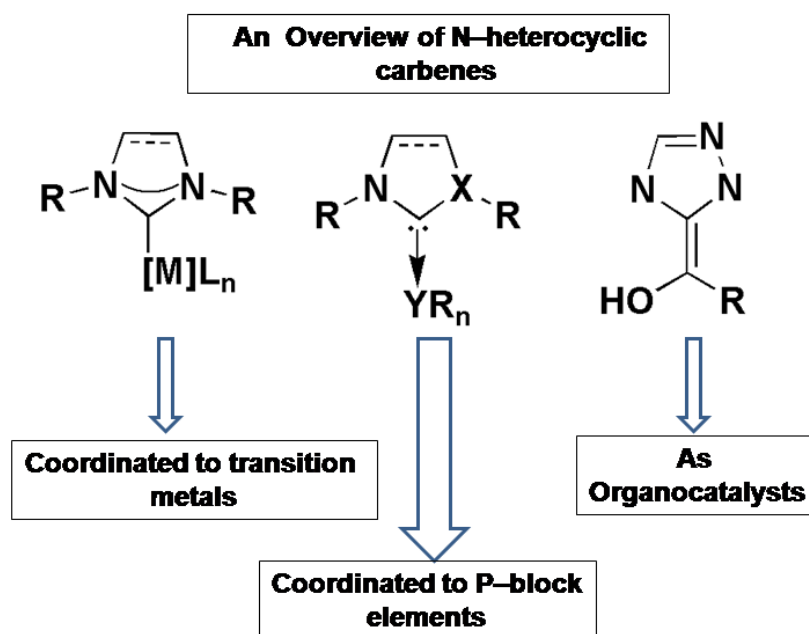


**Chart 1.1.** Major applications of NHCs (Adapted from *Nature*, 2014, 510, 485-496).

NHCs have been used as spectator ligands in 2<sup>nd</sup> and 3<sup>rd</sup> generation Grubbs catalyst for olefin metathesis reaction. There are also reports on hydrogenation reactions catalyzed by NHC-iridium complexes, hydrosilylation reactions catalysed by NHC-platinum complexes, NHC-palladium complexes as catalyst for cross-coupling reactions, Heck olefination of haloarenes and the asymmetric hydrosilylation of acetophenone.<sup>[7]</sup>

More recently, NHCs have been used in metal-free polymer synthesis which includes aliphatic polyesters, polyethers, polysiloxanes, polyurethans, polymethacrylates, poly( $\alpha$ -peptoids).<sup>[8]</sup> Apart from this NHCs have also been used to isolate low-coordinate metal complexes.<sup>[9]</sup> In 1994, Arduengo *et al.* reported on the first synthesis of  $[\text{NHC}]_2\text{M}^0$  [M = Ni, Pt] complex containing two coordinate metal(0).<sup>[10]</sup> This was followed by the syntheses of  $[\text{NHC}]_2\text{Pd}^0$ <sup>[11]</sup> and cationic complexes  $[\text{NHC}]_2\text{M}^+\text{X}^-$  [M = Cu<sup>12a</sup>, Au<sup>12b</sup>, Co<sup>12c</sup>, Ni<sup>12d</sup>] with two coordinate M<sup>I</sup>. Thereafter many transition metal complexes with NHC were known. In 2008, the isolation of unusual Si=Si by Robinson and co-workers demonstrated that NHCs are not just limited to transition metals but also highly useful for main group elements.<sup>[13]</sup>

Other similar NHCs like cyclic(alkyl)(amino)carbene (CAACs), bis(amino)cyclopropenylidene (BACs), acyclic di(amino)carbenes (ADACs), acyclic (alkyl)(amino)carbene (AAACs) (Fig 1.2) have also been explored recently.<sup>[14]</sup> Among these carbenes, the cyclic carbenes are less nucleophilic than acyclic carbenes and the BACs are most nucleophilic carbenes. The reason for being more nucleophilic nature of acyclic carbenes is their wider bond angles that reduce the s character of the lone pair. Similarly, also the acyclic carbenes are more electrophilic than their cyclic counterparts due to the free rotation of the amino group in CAAC one of the N atoms of NHC is replaced by one  $\sigma$ -donating quaternary C atom. As a result the HOMO-LUMO energy gap is smaller in CAAC when compared with that of NHC.<sup>[15]</sup> Consequently, CAAC is a stronger  $\sigma$ -donor and better  $\pi$ -acceptor than NHC.

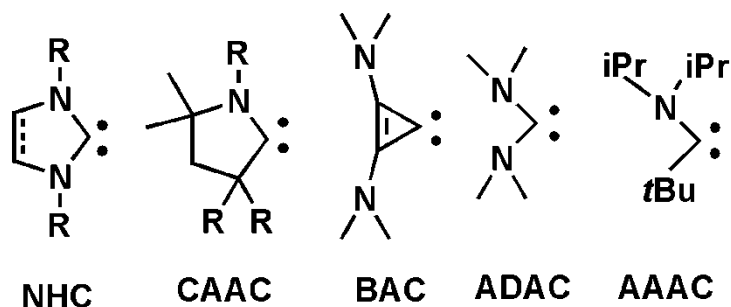


**Fig 1.2.** Schematic representation of NHCs, CAACs, BACs, ADACs and AAACs.

These differences were quantified by computational studies, where it was found that the HOMO of CAACs is slightly higher, and the singlet-triplet gap slightly smaller, than those of NHCs (HOMO: ~ -4.9 vs -5.2 eV;  $\Delta E_{S/T}$  : ~ 45 vs 68 kcal.mol<sup>-1</sup>) (Fig 1.3).<sup>[16]</sup> The difference in electronic property of NHC and CAAC was further quantified by measuring the CO stretching frequency of the complex [RhCl(CO)<sub>2</sub>(L)] where L = NHC and CAAC.

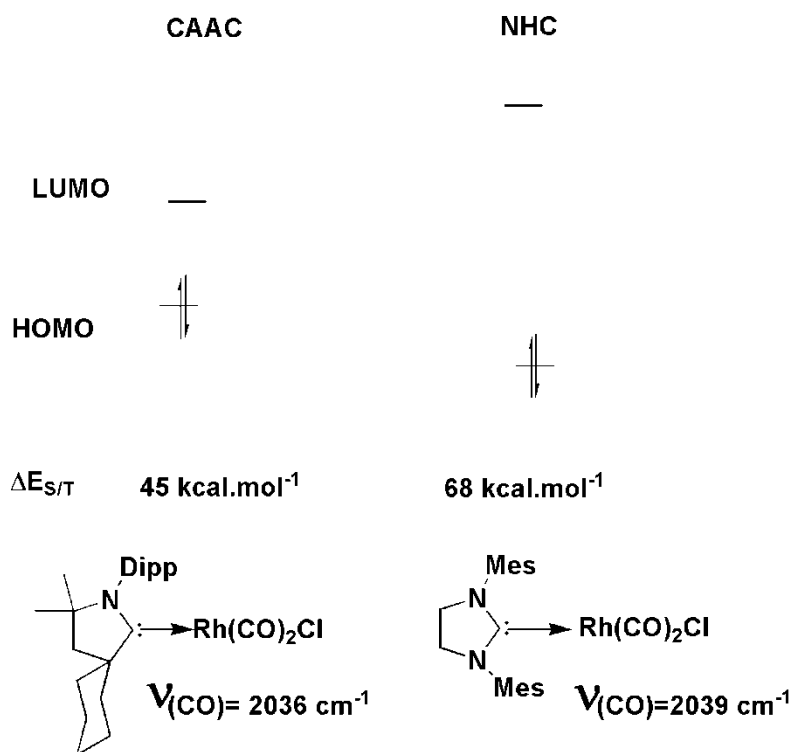
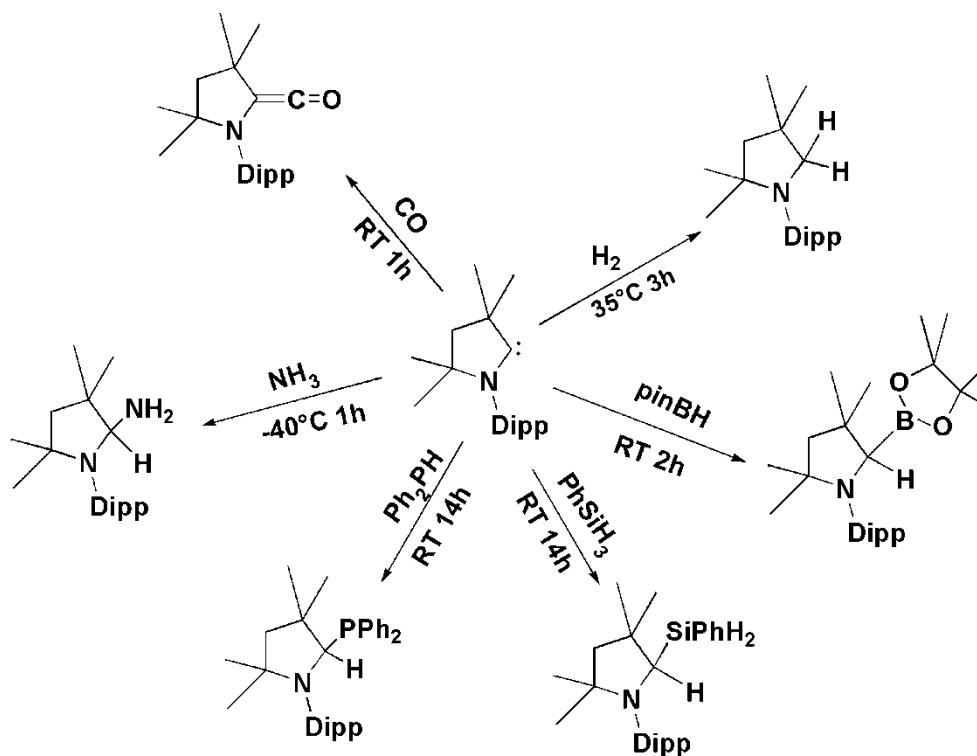


**Fig 1.3.** CAAC as better electron donor than NHC.

The work in this thesis deals with the advanced version of NHC carbene named as cyclic (alkyl)(amino)carbene (CAAC) discovered by Bertrand and co-workers in 2005.<sup>[17]</sup> Due to stronger  $\sigma$  donation ability of CAAC than NHC, its Palladium complex [PdCl(All)(CAAC)] where (All = Allyl) shows strong catalytic efficiency for the  $\alpha$ -arylation of ketones and aldehydes. CAACs have been so efficient to isolate the low coordinate metal complexes, which are not isolable with other ligands. CAAC stabilizes a diverse area of metal complexes ranging from main group to transition metals creating enormous interest in comparison to NHCs. Both NHCs and CAACs are able to stabilize many transition elements (M = Cr, Mn, Fe, Co, Ni, Cu, Zn, Ag, Au) in their different oxidation states which play key role in various transformations.<sup>[18]</sup> Because of smaller singlet-triplet gap and stronger electrophilicity of CAAC, it has been used to activate small molecules, and enthalpically stronger bonds under mild conditions (Scheme 1.3) such as CO<sup>[19]</sup>, H<sub>2</sub><sup>[20]</sup>, P<sub>4</sub><sup>[21]</sup> when CAAC reacts with P<sub>4</sub> it opens it in a linear P<sub>4</sub> unit whereas, when NHC react with P<sub>4</sub> it gives

aggregation of P<sub>4</sub> into P<sub>12</sub>. CAAC can also activate enthalpically strong bonds like B-H<sup>[22]</sup>, P-H<sup>[23]</sup> and even NH<sub>3</sub><sup>[24]</sup> which is a difficult task for transition metal centers and NHC as well.



**Scheme 1.3.** Small molecules activation by CAAC.

Interestingly, Turner *et al.* have recently shown that CAACs can also activate sp, sp<sup>2</sup> and sp<sup>3</sup> hybridized C-H bonds.<sup>[25]</sup> CAAC based carbenes have been used to stabilize electron rich main group elements based species like nucleophilic borane (H-B:), which can be regarded as parent borylene stabilized by two CAACs, in contrast to classical borane which is Lewis acid in nature interestingly borylene stabilized by CAACs shows Lewis basic property and isoelectronic to NH<sub>3</sub>. Similarly CAACs have been used to stabilize radical and radical cation of borylene (H-B:) based species<sup>[26]</sup>, triatomic silicon(0).<sup>[27]</sup> CAACs are also known to stabilize zero valent diphosphorus and diphosphonium radical cation.<sup>[28]</sup> CAAC has also been employed to stabilize the isolation of different oxidation states of antimony compounds (0,+1).<sup>[29]</sup>

Transition metals with zero oxidation states are known to be isolated using CAACs for example, bis(CAAC)M complexes of Au,<sup>[30]</sup> Cu,<sup>[31]</sup> Co & Fe,<sup>[32]</sup> Ni,<sup>[33]</sup> Mn<sup>[34]</sup> and Zn<sup>[35]</sup> have been isolated where the metal M is in zero oxidation state. Other low coordinate metal complexes with 14-electron species of rhodium and palladium<sup>[36]</sup> have also been isolated which were otherwise unable to be stabilized by classical NHCs and phosphines. CAAC is

also able to stabilize the cationic CAAC-Au complexes which have been used as a catalyst for hydroamination reactions of ammonia and secondary amines with internal or terminal alkynes.<sup>[37]</sup> (A brief introduction about hydroamination reactions will be discussed in Section 1.2 of introduction). The CAAC-ruthenium complex is seen as an excellent catalyst for ethanolysis of methyl oleate, when NHC was replaced with the CAAC back in Grubbs catalyst.<sup>[38a]</sup>

Although CAACs have better basicity than NHCs, which make them poor leaving group so in principle CAACs are poor candidate for organocatalysis. But this drawback of CAACs have been overcome by their conformational flexibility of alkyl substituents on quaternary carbon atom whereas NHC has excessive steric hindrance present in their skeleton which makes the typical organocatalysis steps (i.e., oxidative addition, transmetalation and reductive elimination) less favorable thus NHC shows less catalytic activity than CAAC.

Since the greater  $\pi$  accepting property of CAAC compared to NHC, and also the lower ability to serve as  $d_{\pi}$  donors for group 12 metals in comparison to other transition metals, isolation of group 12 metal complexes with CAAC can be considered as a challenging and interesting task. Therefore, we focused on the synthesis of group 12 metal complexes of CAACs with Zn, Cd, and Hg halides. In group 12 also Zn and Cd shows homologous chemistry but the Hg diverges from it. Apart from this, Hg is noble due to its neutral character however the Zn and Cd are very electropositive. The halides of group 12,  $\text{HgCl}_2$  forms linear molecules whereas,  $\text{ZnCl}_2$  and  $\text{CdCl}_2$  have typical ionic structures in molecules in their crystal structures. Because of these many divergences in group 12 metals (metal halides), one can expect different behavior that carbene chemistry has to deal with these metal complexes. Fig 1.4 below depicts some known metal complexes of group 12 with CAACs parallel to NHCs.

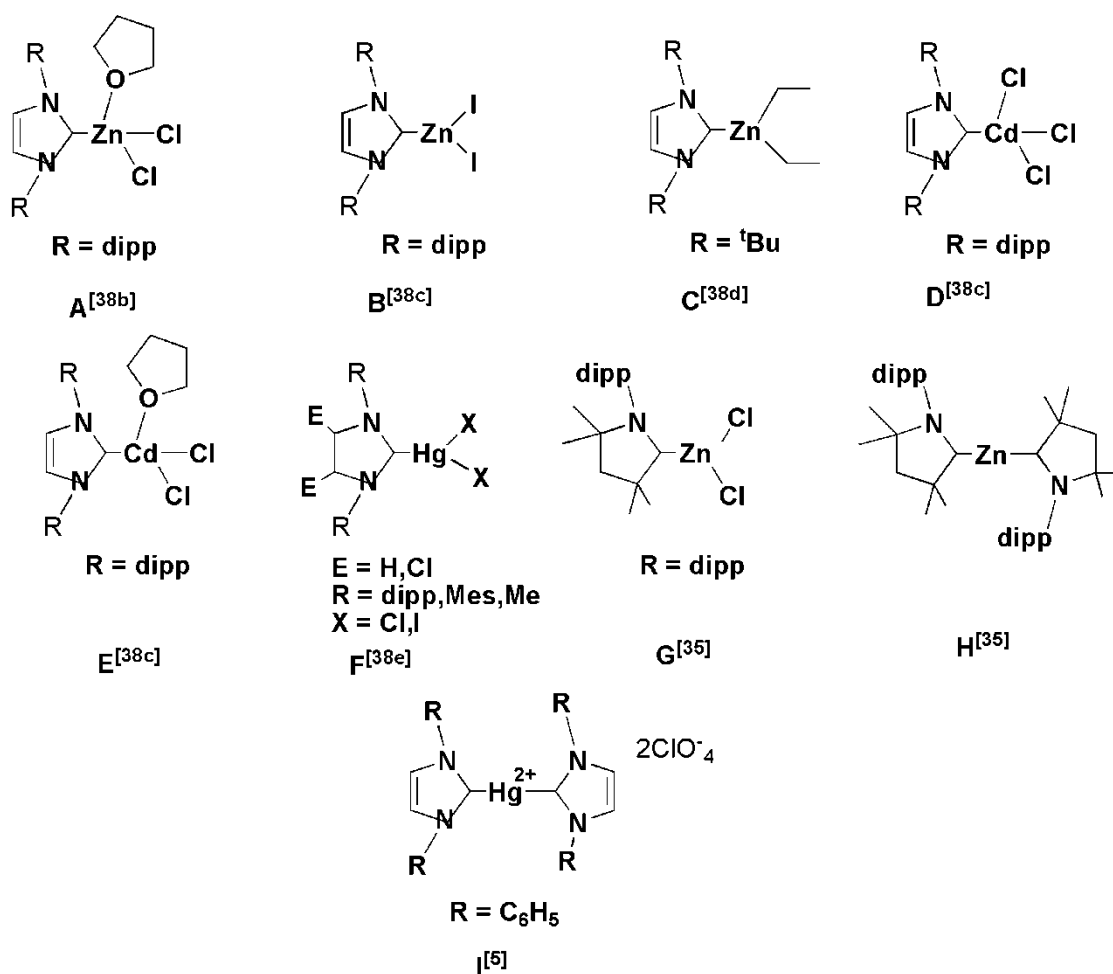


**Fig 1.4.** Group 12 metal complexes of NHCs and CAACs.

It was found that, while NHC complexes of all (i.e., Zn, Cd and Hg) group 12 metals were known (structures **A-E** and **I**, Fig 1.4.), the CAAC complexes were reported with Zn only (structure **G** and **H**, Fig 1.4.).

Following these directions, we were able to synthesize, during the work of this dissertation, the first CAAC-mercury(II) complexes. We have discussed the preparation, isolation and characterization the following complexes,  $[\text{CAACH}]^+[\text{HgCl}_3]^-$  (**1**),  $[\text{CAAC} \cdot \text{HgCl}(\mu\text{-Cl})]_2$  (**2**),  $[\text{CAAC} \cdot \text{HgBr}(\mu\text{-Br})]_2$  (**3**),  $[\text{CAAC} \cdot \text{HgI}(\mu\text{-I})]_2$  (**4**),  $[(\text{CAAC}^{\text{cy}})_2\text{Hg}(\text{H}_2\text{O})]^{2+}2[\text{NO}_3]^-$  (**5**) and  $[(\text{CAAC}^{\text{cy}})_2\text{Hg}]^{2+}[\text{Hg}_2\text{Br}_6]^{2-}$  (**6**). These compounds have been characterized thoroughly using NMR, HRMS, IR and single crystal X-ray diffraction techniques.



## 1.2. An overview of hydroamination reaction

The molecules containing C-N bonds can be considered as very useful building blocks in organic synthesis and constitute important part of many biologically active molecules. In spite of various methods, hydroamination route is the most atom efficient and green process to achieve this kind of functionality in molecules. Hydroamination is an addition reaction in which an N-H unit of a nucleophile (nucleophile can be primary amine, secondary amine or ammonia) is added to unsaturated system of carbon such as alkene, alkyne or allene, which results in the cleavage of N-H bond and formation of C-N and C-H bonds.

The products obtained by hydroamination reactions are very useful and find many applications. Enamides based on N-vinylpyrrolidone (NVP) which are produced via hydroamination of 2-pyrrolidone and acetylene under high pressure.<sup>[39-41]</sup> NVP serves as monomer in radical polymerization for synthesizing numerous functional polymers and copolymers.<sup>[42,43]</sup> These polymers/copolymers show compatibility with biological systems, they are nontoxic, stable within a wide pH range, and soluble in hydrophilic as well as lipophilic systems. Apart from this enamines/imines and enamides are also used for synthesis of chiral amines, amides, amino acids. Hydroamination reactions have also been employed to synthesize natural products or synthetic drugs (Fig.1.5.)

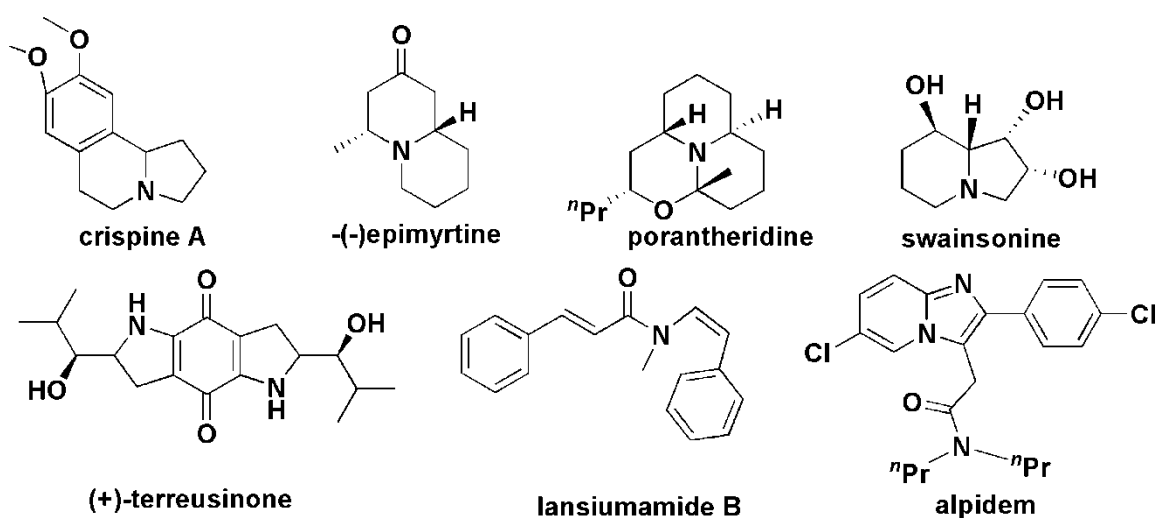
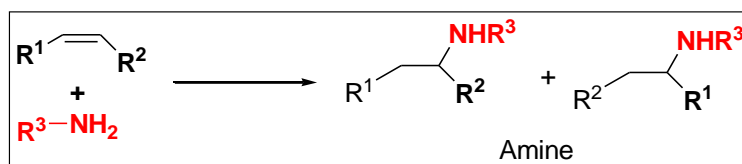


**Fig 1.5.** Examples of bioactive natural products accessible via hydroamination or amidation reactions, (Figure adapted from *Chem. Rev.* **2015**, *115*, 2596–2697).

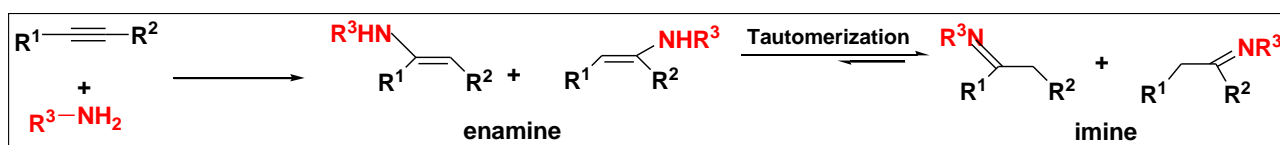
These bioactive drugs show their activity in anticancer, antibacterial, antiviral, anti-inflammatory, anti-HIV, for the treatment of asthma, viral hepatitis and anxiety. But these kinds of reactions do not occur at normal conditions, since hydroamination reactions are

addition reactions so they are slightly exothermic or thermoneutral in nature.<sup>[44,45]</sup> The entropy of this reaction is also negative.<sup>[46,47]</sup> Combining these two facts the  $\Delta G$  of the reaction is positive even at high temperature which implies that the reaction does not occur on its own even at high temperature and shifts the equilibrium back towards starting material. Moreover, there is kinetic issue also associated with this kind of transformation, because the high electron density of nucleophile and  $\pi$ -electron density of the multiple bonds repel each other. So to perform hydroamination reaction non catalytically either it requires a strong acids that can protonate the C-C multiple bond which facilitates the attack of N-nucleophile<sup>[48-49]</sup> or strong base which can deprotonate the N-nucleophile, so it can add to the C-C multiple bond more easily.<sup>[50-54]</sup>

Interestingly, metal based catalysts can play both the roles either by coordinating to the C-C multiple bond thus facilitating the C-N bond formation or by removal of proton bound to nitrogen thus allowing C-C multiple bonds to insert. Another issue is the regioselectivity during reaction this is challenging task for internal alkenes (Scheme1.4) and alkynes (Scheme1.5). With alkenes it gives the amine product which can be based on either Markovnikov or anti-Markovnikov selectivity. Similarly with alkyne, we can get either type of enamines depending on whether it follows Markovnikov or anti-Markovnikov based selectivity which can readily tautomerize to give corresponding imines. The rate of tautomerization of enamines to imines is faster in case of aromatic-alkynes and aromatic amines. In catalytic reaction, the preferred regioselectivity strongly depends on the catalytic pathway, the substrate combination and catalyst system combination of all these factors decides the regioselectivity of the products. It was observed that late transition metal based catalysts in hydroaminations of terminal alkynes with primary aromatic amines usually lead to Markovnikov products.



**Scheme1.4.** Hydroamination of alkene by primary amines.

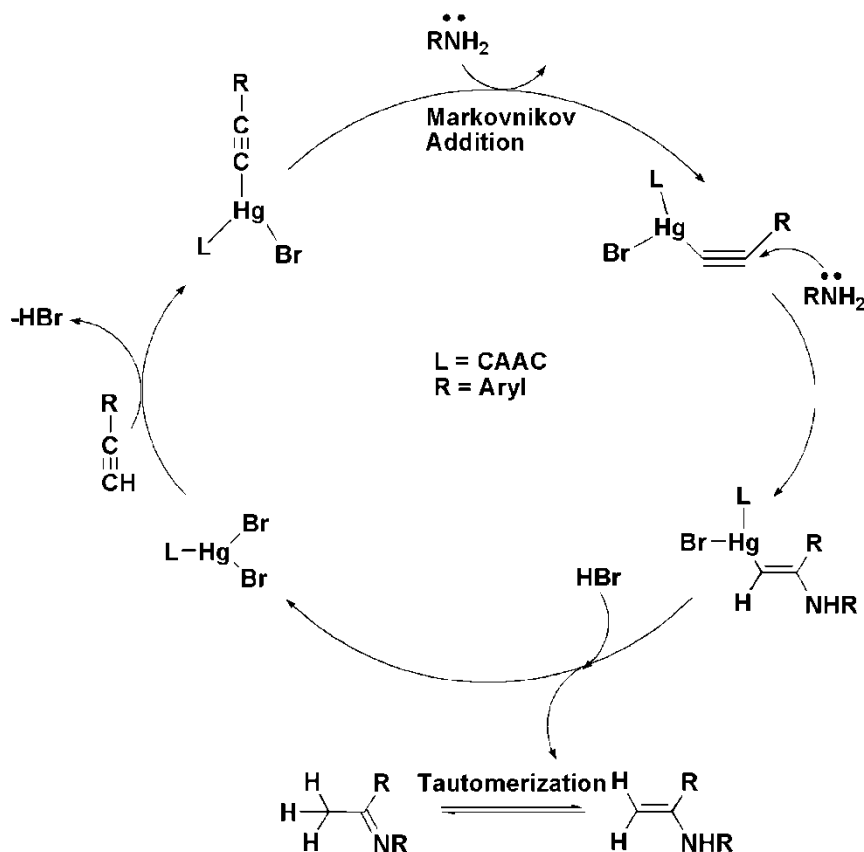


**Scheme 1.5.** Hydroamination of alkynes by primary amines.

The first catalyst for intramolecular hydroamination reactions was reported by Marks and co-workers in 1989 using metallocene complexes of earth metals (lanthanum, lutetium and samarium).<sup>[55]</sup> Later on many catalysts were reported which are based on early transition metals (e.g., Ti or Zr) or lanthanide/actinide which show high activity in the addition of N-H across carbon based unsaturated system.<sup>[56-59a]</sup> However, these catalysts show high oxophilicity and are susceptible to air and moisture and also have low functional group tolerance.

To overcome these problems associated with the early transition metal based catalysts, the use of late transition metals became desirable which shows higher functional group tolerance and lower air and moisture sensitivity. The mechanism of action in hydroamination catalyzed by late transition metal complexes is delineated via alkyne activation pathway.<sup>[59b,59c]</sup> Many different catalysts have been developed for specific transformations. The Au(I) and Au(III)<sup>[60,61]</sup> and Ag(I)<sup>[62,63]</sup> complexes have been studied extensively for hydroamination reactions of alkenes, alkynes and allenes. Gold catalyst have also been very efficient with TON (turn over number) of 95000.<sup>[64]</sup> A number of gold(I) complexes have proved to be efficient catalyst in hydroamination of aryl and alkyl amines. The versatility of NHC carbene has found many applications in gold catalysis and homogeneous catalyst active in the hydroamination with ammonia. Bertrand *et al.* in 2009 reported gold(I) complexes stabilized by CAAC ligands, which were tested as efficient catalysts for the hydroamination of non-activated alkynes and this also occurs via alkyne activation pathway.<sup>[65-68a]</sup>

In recent years, zinc complexes as catalysts in hydroamination reactions have become an active area of research due to their low cost, nontoxic nature and high tolerance towards polar functional group. Zinc triflate was the first zinc compounds to be used in hydroamination reaction as a catalyst.<sup>[68b]</sup> Roesky and co-workers have recently reported cationic zinc organyls as precatalysts for intermolecular hydroamination which do not require any co-catalyst and interestingly shows high catalytic activity.<sup>[68c]</sup> Specially, for HgCl<sub>2</sub> catalyzed hydroamination reactions no inner sphere attack of Hg(II) was observed but the activated complex of mercury (HgCl<sub>2</sub>) with terminal alkyne was observed.<sup>[68d]</sup> Following these literature reports following catalytic cycle, involving Hg(II) complexes, can be proposed:



**Scheme 1.6.** Proposed mechanism for Hg(II) catalyzed hydroamination of aromatic alkynes with aromatic amines.

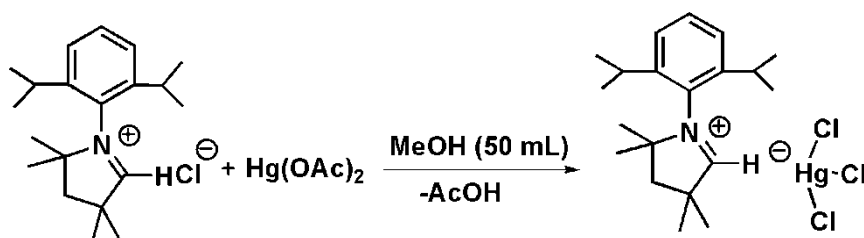
The reactivity of aromatic amines in metal-catalyzed hydroaminations is higher as compared to aliphatic amines, because they coordinate less strongly to the metal catalysts, and are more easily transferred to the alkyne triple bond thus facilitates the conversion.

A lot of fascinating mercury based catalyst were known in the time frame of 1940-1990.<sup>[69]</sup> To the best of our knowledge, early known mercury based catalysts are  $\text{HgCl}_2$ ,<sup>[70]</sup>  $\text{Hg}(\text{OTf})_2$ ,<sup>[71]</sup> and  $\text{Hg}(\text{OAc})_2$ .<sup>[72]</sup> However, there are many disadvantages associated with these catalysts such as, in the hydroamination catalyzed by  $\text{HgCl}_2$  disproportionate amount of alkyne:amine (1:5) in contrast to reactions with 1:1 of reactive species and also it affords mixture of E and Z isomers of the products with (<5%) enamine contamination. In addition to this hydroamination by  $\text{HgCl}_2$  proceeds above 60°C leading to the deposition of mercury and other side reactions. In the case of  $\text{Hg}(\text{OAc})_2$  we need a stoichiometric amount of catalyst (i.e., alkyne : amine :  $\text{Hg}(\text{OAc})_2 = 1:1:1$ ). So to investigate the catalytic activity of our newly synthesized  $[\text{CAAC}^{\text{cy}} \cdot \text{HgBr}(\mu\text{-Br})_2]$  (**3.1**) in hydroamination reactions we have performed intermolecular hydroamination with various aromatic amines and aromatic alkynes which gave Markovnikov products.

## 2. Results and Discussion

### 2.1. Synthesis and characterization of [CAACH]<sup>+</sup>[HgCl<sub>3</sub>]<sup>-</sup> (**1**):

It is known that the reaction of imidazolium salts [NHCH]<sup>+</sup>Cl<sup>-</sup> with Hg(OAc)<sub>2</sub> afford the expected dicationic species [(NHC)<sub>2</sub>·Hg]<sup>2+</sup>2Cl<sup>-</sup>.<sup>[5]</sup> Therefore, similar to NHCs it was anticipated to isolate the [(CAAC)<sub>2</sub>Hg]<sup>2+</sup>2Cl<sup>-</sup> between the reaction of Hg(OAc)<sub>2</sub> with two equivalents of [CAACH]<sup>+</sup>Cl<sup>-</sup>. However, when a 2:1 mixture of [CAACH]<sup>+</sup>Cl<sup>-</sup> and Hg(OAc)<sub>2</sub> was stirred in methanol at room temperature, the air and moisture stable crystalline salt [CAACH]<sup>+</sup>[HgCl<sub>3</sub>]<sup>-</sup> (**1**) was obtained (Scheme2.1). Compound **1** is soluble in MeOH and DMSO and it is partially soluble in chlorinated solvents.



**Scheme 2.1.** Synthesis of [CAACH]<sup>+</sup>[HgCl<sub>3</sub>]<sup>-</sup> (**1**).

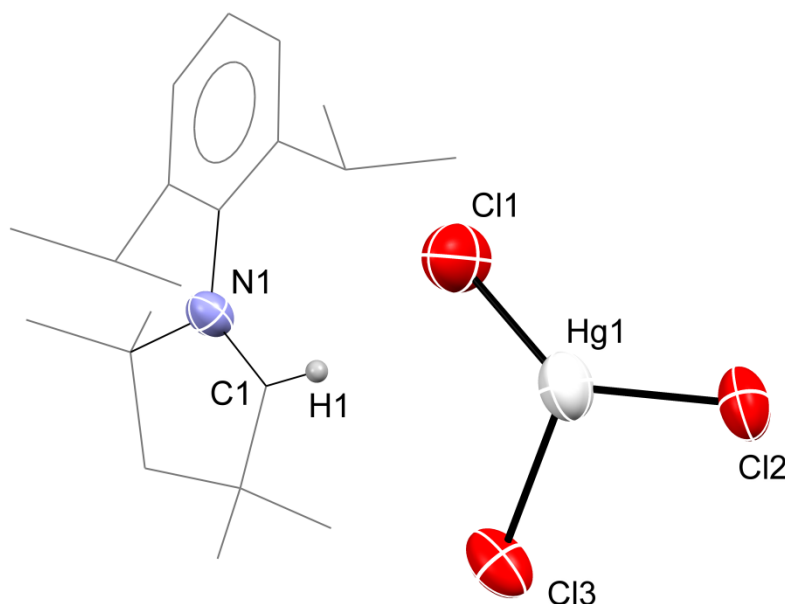
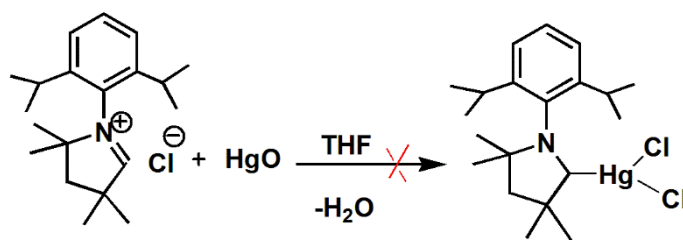


**Fig 2.1.** Single crystal X-ray structure of [CAACH]<sup>+</sup>[HgCl<sub>3</sub>]<sup>-</sup> (**1**). Ellipsoids are shown at 50 % probability levels. All hydrogen atoms except at C1 have been omitted for clarity. Selected bond lengths [Å] and bond angles [°]: Hg1-Cl1 2.372(3), Hg1-Cl2 2.363(2), Hg1-Cl3 2.666(4); Cl1-Hg1-Cl2 132.11(4), Cl2-Hg1-Cl3 103.80(3), Cl1-Hg1-Cl3 107.42(3).

The  $^1\text{H}$  NMR spectrum of **1** showed the aldiminium hydrogen to resonate at 9.40 ppm as compared to 10.28 ppm reported for the same hydrogen in  $[\text{CAACH}]^+\text{Cl}^-$ . In the  $^{13}\text{C}$  NMR spectrum of **1** the carbenoid carbon showed a change in chemical shift from 193.7 ppm (reported for  $[\text{CAACH}]^+\text{Cl}^-$ ) to 193.0 ppm. Therefore, it was clear that the product of this reaction was an ionic compound and not the expected dicationic salt  $[(\text{CAAC})_2\text{Hg}]^{2+}[\text{2Cl}]^-$ . The HRMS spectrum of **1** showed a signal at  $m/z = 306.8733$  corresponding to  $[\text{HgCl}_3]^-$  as the counter anion (later also confirmed by single crystal X-ray diffraction studies) (Fig 2.1). X-ray quality crystals of **1** were obtained by keeping its methanol solution at 4 °C. The single crystal X-ray structure of **1** showed that this molecule crystallizes in the monoclinic system with the  $P2_1/n$  space group and consists of discrete ion-pairs. The counter anion  $[\text{HgCl}_3]^-$  exists in the dimeric form with distorted tetrahedral geometry around Hg(II) centers and the two  $[\text{CAACH}]^+$  cations provide the electrical neutrality.

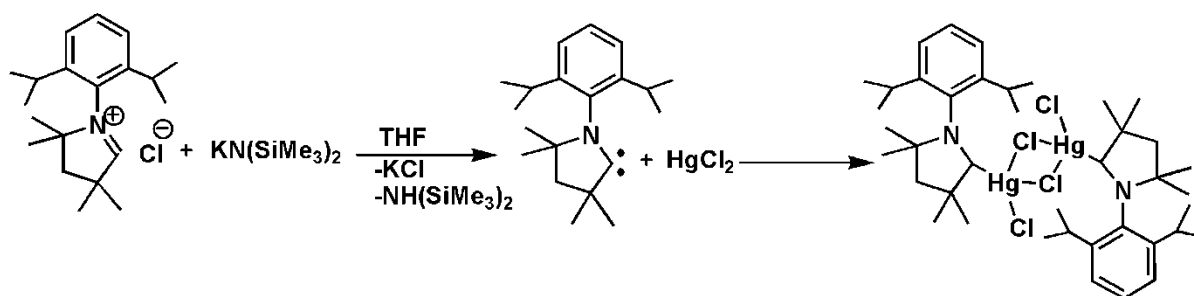
## 2.2. Synthesis and characterization of $[\text{CAAC}\cdot\text{HgCl}(\mu\text{-Cl})]_2$ (**2**):

As reported in the literature for the reaction of  $[\text{NHCH}]^+\text{Cl}^-$  salt with HgO to form the  $\text{NHC}\cdot\text{HgCl}_2$  adduct<sup>[38e]</sup> the similar reaction of HgO with  $[\text{CAACH}]^+\text{Cl}^-$  should also give  $\text{CAAC}\cdot\text{HgCl}_2$  adduct. However, this strategy of reacting  $[\text{CAACH}]^+\text{Cl}^-$  with HgO did not work (Scheme 2.2a). This led us to adopt another route where the free carbene was generated insitu and reacted with  $\text{HgCl}_2$  that gave the expected adduct  $[\text{CAAC}\cdot\text{HgCl}(\mu\text{-Cl})]_2$  (**2**) (Scheme 2.2b).



**Scheme 2.2a.** Route attempted for synthesis of the adduct  $[\text{CAAC}\cdot\text{HgCl}(\mu\text{-Cl})]_2$  (**2**).

The free carbene (CAAC) was generated in THF from the reaction of  $[\text{CAACH}]^+\text{Cl}^-$  with  $\text{K}[\text{N}(\text{SiMe}_3)_2]$  in equal amounts. This insitu generated free carbene was reacted with equimolar amount of  $\text{HgCl}_2$  to afford the complex,  $[\text{CAAC}\cdot\text{HgCl}(\mu\text{-Cl})]_2$  (**2**) (Scheme 2.2b) which was isolated as air and moisture stable colorless crystals on storing the mother liquor at room temperature. Compound **2** is partially soluble in DMSO and insoluble in most of the chlorinated and hydrocarbon solvents.



**Scheme 2.2b.** Synthesis of the adduct  $[\text{CAAC}\cdot\text{HgCl}(\mu\text{-Cl})_2]$  (**2**).

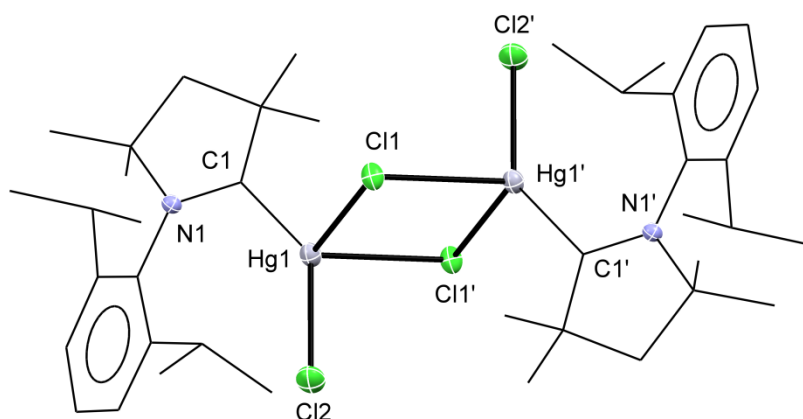
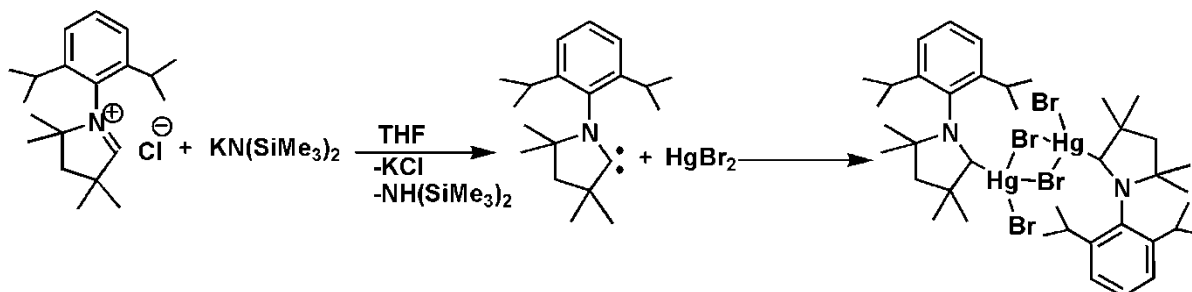


**Fig 2.2.** Single crystal X-ray structure of  $[\text{CAAC}\cdot\text{HgCl}(\mu\text{-Cl})_2]$  (**2**). Ellipsoids are shown at 50 % probability. All hydrogen atoms have been omitted for clarity. Selected bond lengths [ $\text{\AA}$ ] and bond angles [ $^\circ$ ]: Hg1-Cl1 2.689(5), Hg1-Cl1' 2.704(8), Hg1-Cl2 2.389(6), Hg1-C1 2.113(2); Cl1-Hg1-Cl1' 87.86(4), Hg1-Cl1-Hg1' 92.14(3), Cl1-Hg1-Cl2 97.97(6), C1-Hg1-Cl1 110.27(4), C1-Hg1-Cl2 140.78(6).

Formation of complex **2** could be confirmed by the disappearance of the singlet (otherwise observed for the aldiminium hydrogen for the precursor  $[\text{CAACH}]^+\text{Cl}^-$ ) at 10.32 ppm in the  $^1\text{H}$  NMR spectrum. Additionally, a new signal arising in  $^{13}\text{C}$  NMR spectrum of **2** at 245.0 ppm corresponds to  $\text{C}_{\text{carbene}}\text{-Hg}$  adduct. The HRMS spectrum of **2** revealed a signal at  $m/z = 1079.3512$  (cal: 1079.3481) corresponding to  $[\text{M-Cl-2H}]^+$ . The molecular structure of **2** was determined by the single crystal X-ray diffraction method that showed the Cl bridged dimer for **2**. This is contrary to the adducts of  $\text{NHC-HgCl}_2$  which were found to be monomers in the solid state.<sup>[32]</sup> Mercury atoms in complex **2** adopt distorted tetrahedral geometry consisting of one CAAC unit, a terminal Cl and two bridged Cl ligands. The  $\text{C}_{\text{carbene}}\text{-Hg}$  bond distance in **2** (2.113(2)  $\text{\AA}$ ) is slightly longer due to higher coordination number around Hg(II) in **2** compared to that observed for the monomeric NHC-mercury complex  $(1,3\text{-}(2,6\text{-}i\text{Pr}_2\text{C}_6\text{H}_3)_2\text{-C}_3\text{N}_2)\cdot\text{HgCl}_2$  with C-Hg distance of 2.090(4)  $\text{\AA}$ .<sup>[38e]</sup>

### 2.3. Synthesis and characterization of [CAAC·HgBr(μ-Br)]<sub>2</sub> (3):

In a manner similar to the synthesis of complex **2**, the *in situ* generated free CAAC carbene was reacted with equimolar amount of HgBr<sub>2</sub> to afford the complex, [CAAC·HgBr(μ-Br)]<sub>2</sub> (**3**) as air and moisture stable colorless crystals from the mother liquor at room temperature.



**Scheme 2.3.** Synthesis of the adduct [CAAC·HgBr(μ-Br)]<sub>2</sub> (**3**).

Complex **3** is partially soluble in DMSO and is insoluble in most of the chlorinated and hydrocarbon solvents. Formation of complex **3** could be confirmed by the disappearance of the singlet (otherwise observed for the aldiminium hydrogen for the precursor [CAACH]<sup>+</sup>Cl<sup>-</sup>) at 10.32 ppm in the <sup>1</sup>H NMR spectrum whereas the carbene (C<sub>carbene</sub>-Hg) signal in the <sup>13</sup>C NMR spectrum could not be observed due to its low solubility. The HRMS spectrum of **3** revealed the presence of a signal at *m/z* = 1211.1899 (calcd. 1211.1831) that corresponds to the [M-Br-2H]<sup>+</sup> fragment.

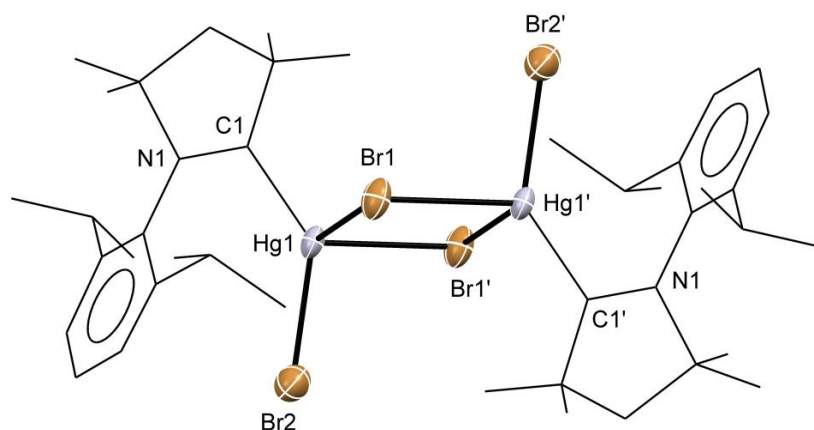


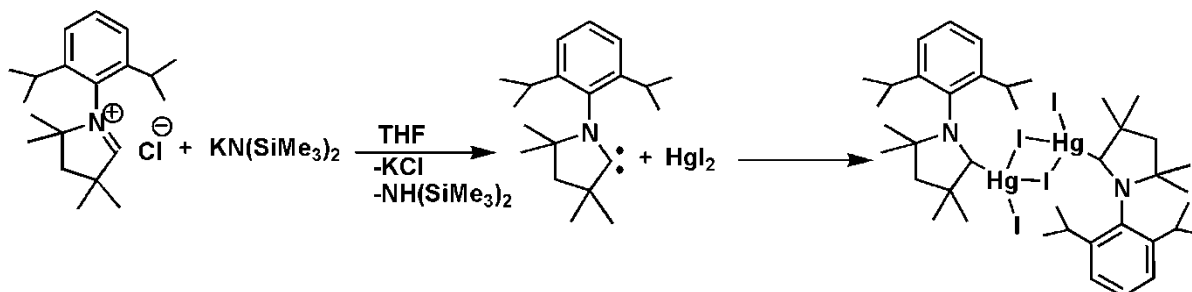
**Fig 2.3.** Single crystal X-ray structure of [CAAC·HgBr(μ-Br)]<sub>2</sub> (**3**). Ellipsoids are shown at 50 % probability. All hydrogen atoms have been omitted for clarity. Selected bond lengths [Å] and bond angles [°]: Hg1-Br1 2.780(3), Hg1-Br1' 2.783(7), Hg1-Br2 2.492(4), Hg1-C1 2.175(4); Br1-Hg1-Br1' 90.13(4), Hg1-Br1-Hg1' 89.87(5), Br1-Hg1-Br2 100.19(6), C1-Hg1-Br1 109.84(4), C1-Hg1-Br2 137.38(6).



Single crystal X-ray structure confirmed the dimeric nature of complex **3** in the solid state as  $[\text{CAAC}\cdot\text{HgBr}(\mu\text{-Br})]_2$  (**3**) (Fig 2.3). The crystal data of **3** are given in Table 3.1. The structural features of complex **3**, including the dimer formation was identical to the adduct  $[\text{CAAC}\cdot\text{HgCl}(\mu\text{-Cl})]_2$  (**2**). The  $C_{\text{carbene}}\text{-Hg}$  distance of 2.175(4) Å is comparable to that of complex **2** (2.113(2) Å).

#### 2.4. Synthesis and characterization of $[\text{CAAC}\cdot\text{HgI}(\mu\text{-I})]_2$ (**4**):

Following a procedure similar to that adopted for complexes **2** and **3**, the  $\text{HgI}_2$  adduct of CAAC,  $[\text{CAAC}\cdot\text{HgI}(\mu\text{-I})]_2$  (**4**) was also synthesized. Colorless air and moisture stable crystals of  $[\text{CAAC}\cdot\text{HgI}(\mu\text{-I})]_2$  (**4**) were obtained at room temperature which were partially soluble in DMSO and is insoluble in chlorinated and hydrocarbon solvents.



**Scheme 2.4.** Synthesis of the adduct  $[\text{CAAC}\cdot\text{HgI}(\mu\text{-I})]_2$  (**4**).

The formation of complex **4** was confirmed by the disappearance of the characteristic singlet for the aldiminium hydrogen in its  $^1\text{H}$  NMR spectrum whereas other signals were in accordance with the structure of the CAAC skeleton. The signal for the carbene carbon ( $C_{\text{carbene}}\text{-Hg}$ ) could not be observed in the  $^{13}\text{C}$  NMR spectrum probably due to low solubility of complex **4**. The HRMS spectrum of complex **4** revealed a signal at  $m/z = 1353.1576$  (cal: 1353.1450) for  $[\text{M-I-4H}]^+$  attributing its dimeric nature.

The molecular structure of **4** was determined by the single crystal X-ray diffraction method that showed the I bridged dimer for **4** (Fig 2.4). This is similar to the adducts of  $\text{NHC}\text{-HgI}_2$  which were also found to be dimeric in the solid state.<sup>[38e]</sup> Mercury atoms in complex **4** adopt distorted tetrahedral geometry consisting of one CAAC unit, a terminal I and two bridged I ligands. The  $C_{\text{carbene}}\text{-Hg}$  bond distance in **4** (2.170(8) Å) is similar to that observed for the dimeric NHC-mercury complex  $[(1,3\text{-Me}_2\text{-4,5-Cl}_2\text{-C}_3\text{N}_2)\cdot\text{HgI}(\mu\text{-I})]_2$  with C-Hg distance of 2.126(9) Å.<sup>[38e]</sup>

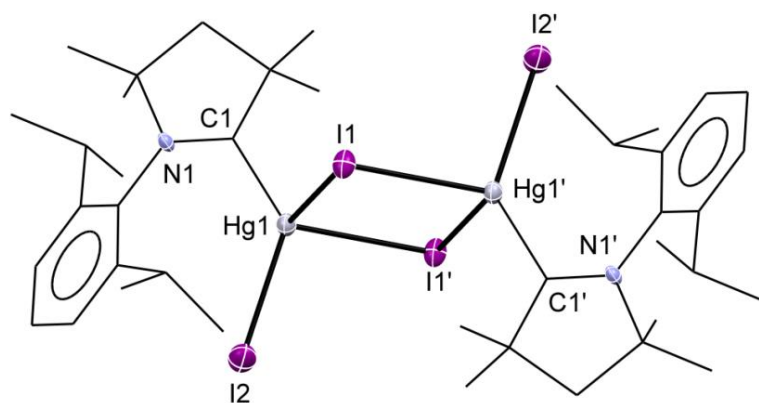
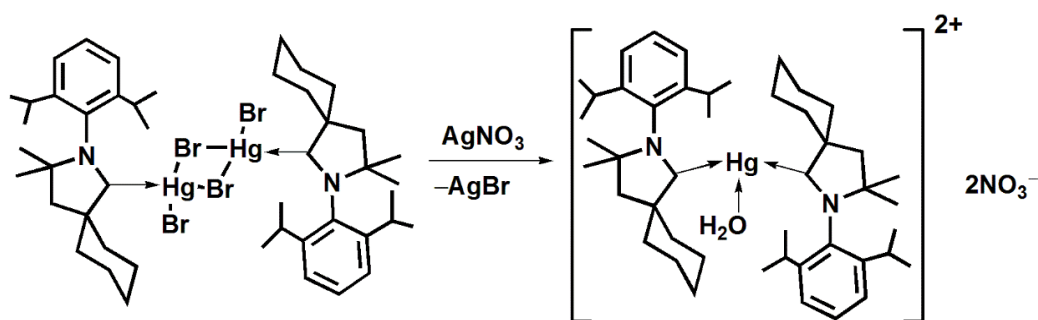


**Fig 2.4.** Single crystal X-ray structure of  $[\text{CAAC}\cdot\text{HgI}(\mu\text{-I})_2]$  (**4**). Ellipsoids are shown at 50 % probability. All hydrogen atoms have been omitted for clarity. Selected bond lengths [ $\text{\AA}$ ] and bond angles [ $^\circ$ ]: Hg1-I1 2.965(5), Hg1-I1' 2.924(7), Hg1-I2 2.676(3), Hg1-C1 2.170(8); I1-Hg1-I1' 91.58(4), Hg1-I1-Hg1' 88.42(7), I1-Hg1-I2 100.34(3), C1-Hg1-I1 100.31(3), C1-Hg1-I2 132.66(5).

## 2.5. Synthesis and characterization of $[(\text{CAAC}^{\text{cy}})_2\text{Hg}(\text{H}_2\text{O})]^{2+}2[\text{NO}_3]^-$ (**5**):

As discussed above, the reaction of  $[\text{CAACH}]^+\text{Cl}^-$  with  $\text{Hg}(\text{OAc})_2$  in 2:1 in methanol is expected to produce dicationic complex,  $[(\text{CAAC}^{\text{cy}})_2\text{Hg}]^{2+}$  however, in the present case the colorless crystals of  $[\text{CAACH}]^+[\text{HgCl}_3]^-$  (**1**) were obtained. Therefore, to synthesize the expected cationic complex of mercury with CAAC an indirect route was adopted by reacting  $[\text{CAAC}^{\text{cy}}\cdot\text{HgBr}(\mu\text{-Br})_2]$  with  $\text{AgNO}_3$ . This reaction was tested on NMR scale in 1:2 molar ratio of  $[\text{CAAC}^{\text{cy}}\cdot\text{HgBr}(\mu\text{-Br})_2]$  and  $\text{AgNO}_3$  in  $\text{DMSO-d}_6$ .



**Scheme 2.5.** Synthesis of  $[(\text{CAAC}^{\text{cy}})_2\text{Hg}(\text{H}_2\text{O})]^{2+}2[\text{NO}_3]^-$  (**5**).

Formation of the complex  $[(\text{CAAC}^{\text{cy}})_2\text{Hg}(\text{H}_2\text{O})]^{2+}2[\text{NO}_3]^-$  (**5**) can be considered as a simple salt metathesis reaction on removal of  $\text{AgBr}$ . The  $^1\text{H}$  NMR spectrum of **5** showed a signal at 3.54 ppm which was later seen (in the single crystal X-ray structure) as the water molecule

coordinated with mercury. Moreover, the carbene signal for **5** (237.71 ppm) in  $^{13}\text{C}$  NMR spectrum was observed as slight upfield shifted in comparison to **3** (244.59 ppm). It is noteworthy that there are some reports where dicationic, bis(NHC) mercury salts of the type  $[(\text{NHC})_2\text{Hg}]^{2+}$  have been derived but all these routes either involve the reaction of mercury acetate with an imidazolium salt. The HRMS spectrum of **5** revealed the presence of  $[\text{M}+\text{Na}-2\text{NO}_3]^+$  at  $m/z = 897.5538$  (cal. 897.5571).

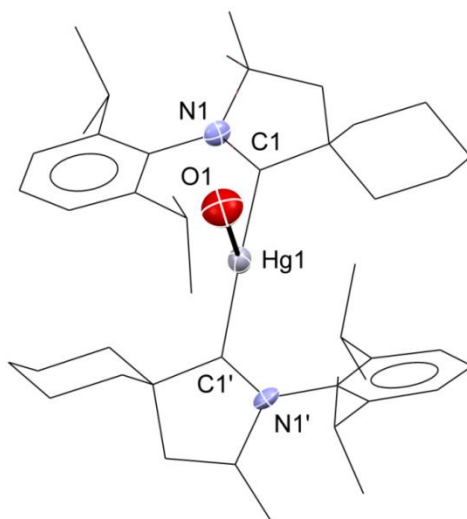


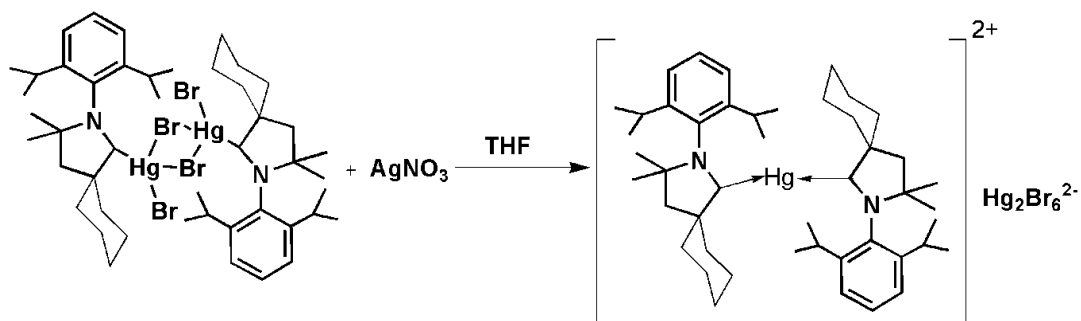
**Fig 2.5.** Single crystal X-ray structure of  $[(\text{CAAC}^{\text{cy}})_2\text{Hg}(\text{H}_2\text{O})]^{2+}2[\text{NO}_3]^-$  (**5**). Ellipsoids are shown at 50 % probability. Two nitrate ions and all hydrogen atoms have been omitted for clarity. Selected bond lengths [Å] and bond angles [°]: Hg1-C1 2.094(5), Hg1-O1 2.502(3); C1-Hg1-C1' 171.60(4), C1-Hg1-O1 94.20(5).

The crystal data of compound **5** is given in Table 3.1. The single crystals of compound **5** were obtained from the concentrated mother liquor at room temperature in one week. Compound **5** crystallizes in the monoclinic system with  $C_{21/c}$  space group. The structure for **5** shows that the mercury atom is coordinated to two CAAC units in a linear fashion. A water molecule is also coordinated to this mercury centre constituting a T-shaped geometry around the Hg centre. The  $\text{C}_{\text{carbene}}\text{-Hg}$  bond length of 2.094(5) Å for **5** is slightly shorter than that of its precursor **3** (2.15(5) Å) whereas, it is almost similar to  $[(\text{NHC})_2\text{Hg}]^{2+}$  2.073(6).<sup>[5]</sup>

## 2.6. Synthesis and characterization of $[(\text{CAAC}^{\text{cy}})_2\text{Hg}]^{2+}[\text{Hg}_2\text{Br}_6]^{2-}$ (**6**):

Unlike the dicationic mercury complex,  $[(\text{CAAC}^{\text{cy}})_2\text{Hg}(\text{H}_2\text{O})]^{2+}2[\text{NO}_3]^-$  (**5**), where a water molecule was connected to the mercury atom, our effort to get two coordinated biscarbene dicationic mercury species centred on the reaction of  $[\text{CAAC}^{\text{cy}}\cdot\text{HgBr}(\mu\text{-Br})]_2$  (**3.1**) with  $\text{AgNO}_3$  in 1:2 molar ratio in dry THF. This reaction afforded a mixture of two products from

which colorless crystals of  $[(\text{CAAC}^{\text{cy}})_2\text{Hg}]^{2+}[\text{Hg}_2\text{Br}_6]^{2-}$  (**6**) were obtained in small yield. Surprisingly, the  $^{13}\text{C}$  NMR spectrum of this mixture gave a single peak for the carbene carbon. Due to limited solubility of this mixture it was difficult to ascertain the composition of other product in the mixture with the aid of multinuclear NMR measurements.



**Scheme 2.6.** Synthesis of  $[(\text{CAAC}^{\text{cy}})_2\text{Hg}]^{2+}[\text{Hg}_2\text{Br}_6]^{2-}$  (**6**).

A careful inspection of the  $^1\text{H}$  NMR spectrum of the crude reaction mixture showed that the  $\text{C}_{\text{carbene}}\text{-Hg}$  bonds for these products are intact. The fate of  $\text{NO}_3^-$  ions and the formation of  $[\text{Hg}_2\text{Br}_6]^{2-}$  ion are unclear at this stage. It may be possible that some of the  $\text{HgBr}_2$  released from **3.1** binds with  $\text{Br}^-$  ions to form the anion  $[\text{Hg}_2\text{Br}_6]^{2-}$  according to the reaction shown below. Moreover, it may also be possible that the other product may contain  $\text{NO}_3^-$  as counter ions.

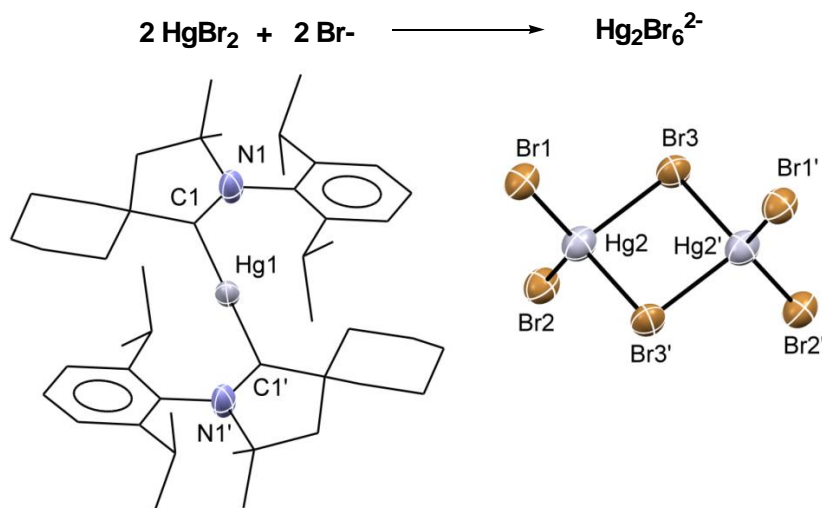


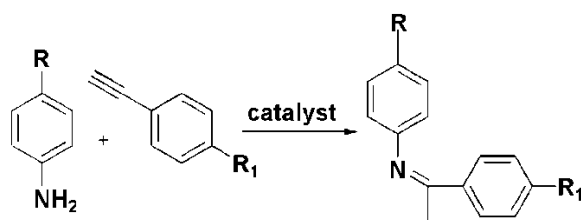
**Fig 2.6.** Single X-ray crystal structure of  $[(\text{CAAC}^{\text{cy}})_2\text{Hg}]^{2+}[\text{Hg}_2\text{Br}_6]^{2-}$  (**6**). Ellipsoids have been shown at 50 % probability. All hydrogen atoms have been omitted for clarity. Selected bond lengths [ $\text{\AA}$ ] and bond angles [ $^\circ$ ]: Hg1-C1 2.098(4), Hg2-Br1 2.513(4), Hg2-Br3 2.684(5), Hg2-Br3' 2.828(2); C1-Hg1-C1' 180.00(3), Br1-Hg2-Br2 126.00(6), Br1-Hg2-Br3 111.40(3), Br2-Hg2-Br3' 104.26(5), Br1-Hg2-Br3' 93.64(3), Hg2-Br3-Hg2' 86.36(6).

Complex **6** crystallizes in the orthorhombic system with *Pnmm* space group. In contrast to the cationic complex  $[(\text{CAAC}^{\text{cy}})_2\text{Hg}(\text{H}_2\text{O})]^{2+}2[\text{NO}_3]^-$  (**5**) where one water molecule was coordinated to mercury atom (C1-Hg1-C1' 171.60(4)°) the structure for **6** shows that the mercury atom is coordinated to two CAAC units in an exact linear fashion (C1-Hg1-C1' 180.00(3)°). Unlike, **5** the cationic complex **6** consist of  $[\text{Hg}_2\text{Br}_6]^{2-}$  as counter anion. The  $\text{C}_{\text{carbene}}\text{-Hg}$  bond length in **6** (2.098(4) Å) is slightly smaller than that of precursor **3** (2.175(4) Å) whereas, it is almost similar to that of dication **5** (2.094(5) Å) and  $[(\text{NHC})_2\text{Hg}]^{2+}$  2.073(6).<sup>[5]</sup>

## 2.7. Intermolecular hydroamination reactions using $[\text{CAAC}^{\text{cy}}\cdot\text{HgBr}(\mu\text{-Br})]_2$ as a catalyst

Simple salts of mercury,  $\text{Hg}(\text{OAc})_2$  and  $\text{HgCl}_2$  were used as a catalysts at the outset of hydroamination reactions however; with the advent of modern transition metal-based catalysts these became obsolete perhaps due to the toxicity of mercury. In the first case where  $\text{Hg}(\text{OAc})_2$  showed limited catalytic activity (because the stoichiometric amount of catalyst was required), in the latter case  $\text{HgCl}_2$  has been known catalyst for a long time but demands a disproportionate amount of alkynes and amines (20:100) with other issues (i) gives the enamines as a mixture of *Z*- and *E*-isomers and the products are always contaminated by < 5% of the isomer having a terminal double bond ( $\text{R} = \text{R}^2\text{CH}_2$ ); (ii) higher temperatures lead to the side reactions causing the destruction of the catalyst after 1 hour. All these facts prompted us to look back in the past to develop a mercury based catalyst where the deposition of mercury can be precluded.

Complex  $[\text{CAAC}^{\text{cy}}\cdot\text{HgBr}(\mu\text{-Br})]_2$  (**3.1**)<sup>[73]</sup> was tested as a catalyst for the intermolecular hydroamination reactions. The hydroamination reaction of phenylacetylene with aniline was carried out to observe the desired conversion. On employing 1.63 mol% of complex **3.1** and 1.5 mmol each of aniline and phenylacetylene in THF, a substantial conversion (60.2 %) of phenylacetylene occurred after 8 h on refluxing THF solution. The reaction gave the selective formation of the imine *N*-(1-phenylethylidene)-aniline (**7**) with Markonikov regioselectivity without side products. The formation of (**7**) was confirmed by the emerging of a singlet in <sup>1</sup>H NMR at 2.28 ppm and 17.44 ppm in <sup>13</sup>C NMR in aliphatic region due to the newly originated CH<sub>3</sub> group (it was not present in precursors) and the shifting of meta protons of phenylacetylene (from 7.48 ppm to 8.03 ppm) in <sup>1</sup>H NMR, also supported by their corresponding signals in <sup>13</sup>C NMR. The formation of this hydroamination product was also supported by the signal at 196.1120 in HRMS spectrum having good agreement with the experimental data (cal. 196.1126).



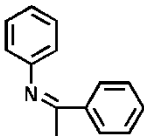
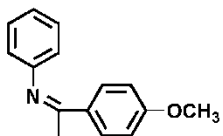
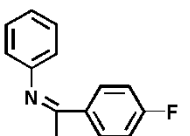
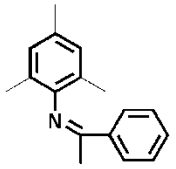
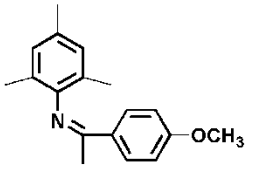
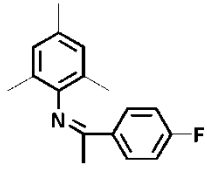
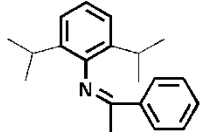
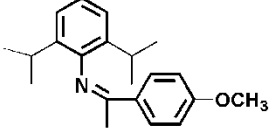
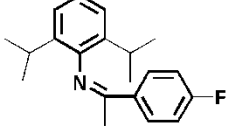
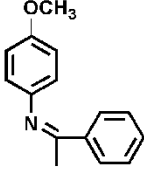
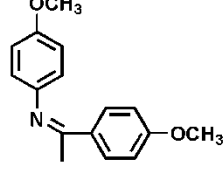
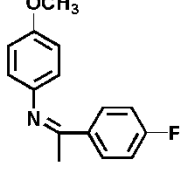
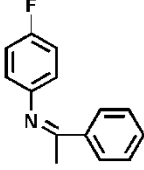
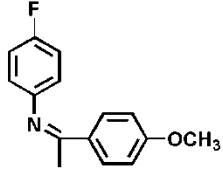
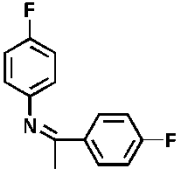
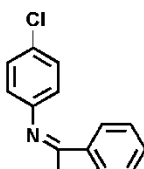
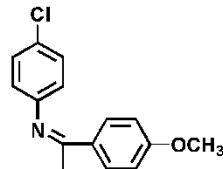
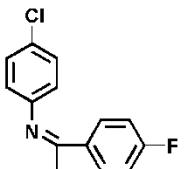
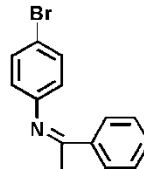
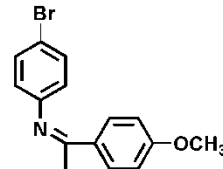
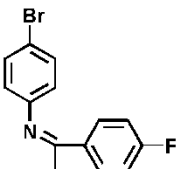
**Scheme 2.7.** General intermolecular hydroamination reaction.

Motivated from this result the hydroamination reaction of various substituted phenylacetylene with various substituted aniline was carried out to understand the effect of substituents on reactivity. Although terminal aromatic alkynes gave expected imines but the aliphatic alkynes and disubstituted aromatic alkynes was of failure.

With an optimized set of conditions the scope of other phenylacetylenes and anilines bearing different functional groups were evaluated, with same amount (1.63 %) of complex  $[\text{CAAC}^{\text{cy}} \cdot \text{HgBr}(\mu\text{-Br})_2]$  (**3.1**). A combination of phenylacetylene derivatives including phenylacetylene and *p*-methoxyphenylacetylene, with aniline, 2,4,6-trimethylaniline, 2,6-diisopropylaniline, *p*-methoxyaniline, *p*-floroaniline, *p*-chloroaniline, *p*-bromoaniline afforded formation of their corresponding imines as Markonikov product in good to excellent yields whereas, reaction of *p*-florophenylacetylene with above anilines produced lower conversion (Table 4.1). On observing reaction of diphenylacetylene, 1-phenyl-1-propyne and styrene with above anilines couldn't give any fruitful result even after modifying the conditions and catalyst amount. As expected on altering the substituent (electron donating) on aniline which enhance the nucleophilicity of amino group, reaction of phenylacetylene with 2,4,6-trimethylaniline (75 %) gave better conversion than aniline (60.2 %) even at room temperature whereas, the reaction with 2,6-diisopropylaniline (56.8 %) gave lower conversion which is perhaps due to the bulkiness of the substituents on phenyl ring. The use of *p*-methoxyaniline (15.5 %) however gave less yield as expected to give higher yield because of better donating property, in the same way an expected routine was observed on using *p*-floroaniline (100 %), *p*-chloroaniline (50.0 %), *p*-bromoaniline (14.3 %) with phenylacetylene.

On using *p*-methoxyphenylacetylene, as expected decrease in electrophilicity of the acetylene, its reaction with alkyl substituted anilines also showed a decent conversion (2,4,6-trimethylaniline (69.0 %), 2,6-diisopropylaniline (76.3 %) whereas,

**Table 2.1** Substrate scope of intermolecular hydroamination reactions.

		
4.5% (RT, 14h) 60.2% (reflux, 8h)	35.0% (RT, 7h) 48.0% (reflux, 10h)	10.0% (RT, 4h) 21.3% (reflux, 8h)
		
66.6% (RT, 8h) 75.0% (reflux, 8h)	13.7% (RT, 10h) 69.0% (reflux, 10h)	No reaction (RT, 8h) 14.8% (reflux, 8h)
		
21.56% (RT, 7.5h) 56.8% (reflux, 8h)	16.0% (RT, 5h) 76.3% (reflux, 10h)	No reaction (RT, 8h) 22.5% (reflux, 10h)
		
6.3% (RT, 7.3h) 15.5% (reflux, 12h)	72.5% (RT, 8h) 100% (reflux, 10h)	7.4% (RT, 4h) 12.0% (reflux, 8h)
		
20.0% (RT, 7.5h) 100% (reflux, 11.0h)	38.0% (RT, 3.5h) 100% (reflux, 10h)	5.8% (RT, 4h) 14.7% (reflux, 8h)
		
1% (RT, 7.5h) 50.0% (reflux, 12h)	78.3% (RT, 4h) 90.0% (reflux, 4h)	10.6% (RT, 13h) 28.0% (reflux, 24h)
		
No reaction (RT, 6h) 14.3% (reflux, 11h)	87.0% (RT, 8h) 87.0% (reflux, 10h)	5.2% (RT, 4h) 20.0% (reflux, 8h)

unexpectedly very good conversion was observed on reaction with *p*-methoxyaniline (100 %), *p*-floroaniline (100 %), *p*-chloroaniline (90.0 %), *p*-bromoaniline (87.0 %) at even room temperature in lesser time. The use of *p*-florophenylacetylene with all above mentioned aromatic amines afforded the lower yield than the other two above mentioned aromatic alkynes.

### 3. Experimental Section:

#### 3.1. General

All manipulations were performed under nitrogen/argon atmosphere using Schlenk or glove box techniques. All chemicals were purchased from Sigma-Aldrich and used without further purification. The starting material cyclic (alkyl)(amino)carbene salt, [CAACH]<sup>+</sup>Cl<sup>-</sup> was prepared by following the reported procedure.<sup>[34]</sup> IR spectra of the complexes were recorded in the range 4000–400 cm<sup>-1</sup> with a Perkin–Elmer Lambda 35-spectrophotometer. The <sup>1</sup>H and <sup>13</sup>C spectra were recorded with a Bruker 400 MHz spectrometer with TMS as external reference; chemical shift values are reported in ppm. High-resolution mass spectrometry was performed with Waters SYNAPT G2-S instrument.

#### 3.2. Single crystal X-ray structural determination

Single crystal X-ray diffraction data of **1-6** were collected using a RigakuXtaLAB mini diffractometer equipped with Mercury375M CCD detector. The data were collected with graphite monochromatic MoK $\alpha$  radiation ( $\lambda = 0.71073 \text{ \AA}$ ) at 100.0(2) K using scans. During the data collection the detector distance was 50 mm (constant) and the detector was placed at  $2\theta = 29.85^\circ$  (fixed) for all the data sets. The data collection and data reduction were done using Crystal Clear suite.<sup>[75]</sup> The crystal structures were solved by using either OLEX2<sup>[76]</sup> or WINGX package using SHELXS-97<sup>[77]</sup> and the structure were refined using SHELXL-97 2008. All non-hydrogen atoms were refined anisotropically. All the graphics were generated using Mercury 3.2.

#### 3.3. Preparation of [CAACH]<sup>+</sup>[HgCl<sub>3</sub>]<sup>-</sup> (**1**)

A mixture of [CAACH]<sup>+</sup>Cl<sup>-</sup> salt (0.64 g, 2.0 mmol) and mercury acetate (Hg(OAc)<sub>2</sub>) (0.32 g, 1.0 mmol) was taken in a 50 mL solution of methanol. The resulting suspension was stirred at room temperature for overnight. The solution was filtered and subsequently kept for crystallization after concentrating the solution. Colorless crystals were grown at room temperature. Yield: 0.35 g, 58.9%. Mp: 228–230 °C. **IR** (Nujol, cm<sup>-1</sup>)  $\tilde{\nu}$  : 3060, 3012, 2971, 2808, 1441, 1460, 1392, 1371, 1347, 1207, 1128, 1056, 933, 807, 766, 653, 561, 485, 420. **<sup>1</sup>H**



**NMR** (400 MHz, CD<sub>3</sub>OD):  $\delta$  = 9.40 (s, 1H, CH=N), 7.60 (t, 1H, *p*Ar-H, <sup>3</sup>*J*<sub>H-H</sub> = 8 Hz), 7.49 (d, 2H, *m*Ar-H, <sup>3</sup>*J*<sub>H-H</sub> = 8 Hz), 2.78 (sept, 2H, CH(CH<sub>3</sub>)<sub>2</sub>, <sup>3</sup>*J*<sub>H-H</sub> = 8.0 Hz), 2.50 (s, 2H, CH<sub>2</sub>), 1.62 (s, 6H, CH<sub>3</sub>), 1.57 (s, 6H, CH<sub>3</sub>), 1.38 (d, 6H, CH(CH<sub>3</sub>)<sub>2</sub>, <sup>3</sup>*J*<sub>H-H</sub> = 8.0 Hz), 1.13 (d, 6H, CH(CH<sub>3</sub>)<sub>2</sub>, <sup>3</sup>*J*<sub>H-H</sub> = 8.0 Hz). **<sup>13</sup>C NMR** (100 MHz, CD<sub>3</sub>OD):  $\delta$  = 193.7 (N=CH), 145.9 (*C*<sub>ortho</sub>), 133.3 (*C*<sub>para</sub>), 126.7 (*C*<sub>ipso</sub>), 85.9 (CCH<sub>3</sub>), 30.9, 28.6 CH(CH<sub>3</sub>)<sub>2</sub>, 26.3 (CH<sub>3</sub>), 26.2 (CH<sub>3</sub>), 22.2. **HRMS (AP<sup>+</sup>)**: *m/z* calcd for HgCl<sub>3</sub>: 306.8772 [M-CAACH]<sup>+</sup>; found: 306.8566.

### 3.4. Preparation of [CAAC·HgCl(μ-Cl)]<sub>2</sub> (2)

A mixture of [CAACH]<sup>+</sup>Cl<sup>-</sup> (0.32 g, 1.0 mmol) and potassium bis(trimethylsilyl)amide (0.2 g, 1.0 mmol) was taken in 20 mL THF. The resulting suspension was stirred at room temperature for 2 h. The solution was filtered to remove KCl and subsequently added to HgCl<sub>2</sub> (0.27 g, 1.0 mmol). The resulting suspension was stirred at room temperature for overnight. The solution was filtered, concentrated and subsequently kept for crystallization. Yield: 0.37 g, 67 %. Mp: 252–255°C. **IR** (KBr, cm<sup>-1</sup>)  $\tilde{\nu}$  : 2967, 2868, 1634, 1555, 1463, 1388, 1371, 1320, 1203, 1125, 1050, 807, 776, 564. **<sup>1</sup>H NMR** (400 MHz, DMSO-d<sub>6</sub>):  $\delta$  = 7.56-7.36 (m, 3H, *m*- and *p*-H), 2.69 (sept, 2H, CH(CH<sub>3</sub>)<sub>2</sub>, <sup>3</sup>*J*<sub>H-H</sub> = 6.4 Hz), 2.32 (s, 2H, CH<sub>2</sub>), 1.42 (s, 6H, CH<sub>3</sub>), 1.25 (d, 6H, CH(CH<sub>3</sub>)<sub>2</sub>, <sup>3</sup>*J*<sub>H-H</sub> = 6.4), 1.20 (d, 6H, CH(CH<sub>3</sub>)<sub>2</sub>, <sup>3</sup>*J*<sub>H-H</sub> = 6.4). **<sup>13</sup>C NMR** (100 MHz, DMSO-d<sub>6</sub>):  $\delta$  = 245.5 (C-Hg), 148.3, 144.5 (*C*<sub>ortho</sub>), 132.8 (*C*<sub>para</sub>), 130.6, 125.5, 123.7, 84.4, 67.6, 54.7, 48.2, 28.6, 28.4, 27.3, 26.5, 23.5. **HRMS (AP<sup>+</sup>)**: *m/z* calcd for C<sub>40</sub>H<sub>62</sub>Cl<sub>3</sub>Hg<sub>2</sub>N<sub>2</sub>: 1079.3512 [M-Cl-2H]<sup>+</sup>; found: 1079.3481; *m/z* calcd for C<sub>20</sub>H<sub>31</sub>Cl<sub>1</sub>HgN<sub>1</sub>: 522.1844 [M/2-HCl]<sup>+</sup>; found: 522.1822.

### 3.5. Preparation of [CAAC·HgBr(μ-Br)]<sub>2</sub> (3)

A mixture of [CAACH]<sup>+</sup>Cl<sup>-</sup> salt (0.5 g, 1.38 mmol) and potassium bis(trimethylsilyl)amide (0.28 g, 1.4 mmol) was taken in THF (25 mL). The resulting suspension was stirred at room temperature for 2 h. The solution was filtered to remove KCl and subsequently added to mercuric iodide (HgBr<sub>2</sub>) (0.496 g, 1.38 mmol). The resulting suspension was stirred at room temperature for overnight. The solution was filtered and the precipitate obtained was washed with acetonitrile to give whitish solid. The colorless crystals were grown in DMSO solution at room temperature. Yield: 0.45 g, 69 %. Mp: 256–258 °C. **IR** (KBr, cm<sup>-1</sup>)  $\tilde{\nu}$  : 2968, 2928, 2867, 1550, 1462, 1390, 1370, 1325, 1205, 1125, 1052, 1008, 807, 771, 566. **<sup>1</sup>H NMR** (400 MHz, DMSO-d<sub>6</sub>):  $\delta$  = 7.51 (t, 1H, *p*Ar-H, <sup>3</sup>*J*<sub>H-H</sub> = 8 Hz), 7.41 (d, 2H, *m*Ar-H, <sup>3</sup>*J*<sub>H-H</sub> = 8 Hz), 2.69 (sept, 2H, CH(CH<sub>3</sub>)<sub>2</sub>, <sup>3</sup>*J*<sub>H-H</sub> = 8 Hz), 2.25 (s, 2H, CH<sub>2</sub>), 1.62 (s, 6H, CH<sub>3</sub>), 1.44 (s, 6H, CH<sub>3</sub>), 1.25 (t, 12H, CH(CH<sub>3</sub>)<sub>2</sub>, <sup>3</sup>*J*<sub>H-H</sub> = 8 Hz). **<sup>13</sup>C NMR** (100 MHz, DMSO-d<sub>6</sub>):  $\delta$  = 144.3 (*C*<sub>ortho</sub>), 132.8 (*C*<sub>para</sub>), 130.7 (*C*<sub>ipso</sub>), 125.75 (*C*<sub>meta</sub>), 84.3

(NCCH<sub>3</sub>), 55.0(CH<sub>2</sub>), 48.81, 28.57, 27.41, 26.80, 23.75. **HRMS (AP<sup>+</sup>):** *m/z* calcd for C<sub>40</sub>H<sub>62</sub>N<sub>2</sub>Hg<sub>2</sub>Br<sub>3</sub>: 1211.1831: [M–Br–2H]<sup>+</sup>; found: 1211.1899.

### 3.6 Preparation of [CAAC·HgI(μ-I)]<sub>2</sub> (4)

A mixture of [CAACH]<sup>+</sup>Cl<sup>–</sup> (0.32 g, 1.0 mmol) and potassium bis(trimethylsilyl)amide (0.2 g, 1.0 mmol) was taken in 20 mL THF. The resulting suspension was stirred at room temperature for 2 h. The solution was filtered to remove KCl and subsequently added to HgI<sub>2</sub> (0.45 g, 1.0 mmol). The resulting suspension was stirred at room temperature for overnight. The solution was filtered, concentrated and subsequently kept for crystallization. Colorless crystals were obtained at room temperature in overnight. Yield: 0.49 g, 66 %. Mp: 263–265 °C (decomposed). **IR** (Nujol, cm<sup>–1</sup>)  $\tilde{\nu}$ : 2968, 2928, 2871, 1550, 1458, 1390, 1370, 1321, 1205, 1124, 803, 775, 662. **<sup>1</sup>H NMR** (400 MHz, DMSO–d<sub>6</sub>):  $\delta$  = 7.51 (t, 1H, *p*Ar–H, <sup>3</sup>*J*<sub>H–H</sub> = 8 Hz), 7.40 (d, 2H, *m*Ar–H, <sup>3</sup>*J*<sub>H–H</sub> = 8 Hz), 2.68 (sept, 2H, CH(CH<sub>3</sub>)<sub>2</sub>, <sup>3</sup>*J*<sub>H–H</sub> = 8 Hz), 2.26 (s, 2H, CH<sub>2</sub>), 1.59 (s, 6H, CH<sub>3</sub>), 1.43 (s, 6H, CH<sub>3</sub>), 1.25 (d, 6H, CH(CH<sub>3</sub>)<sub>2</sub>, <sup>3</sup>*J*<sub>H–H</sub> = 8 Hz), 1.22 (d, 6H, CH(CH<sub>3</sub>)<sub>2</sub>, <sup>3</sup>*J*<sub>H–H</sub> = 8 Hz). **<sup>13</sup>C NMR** (100 MHz, DMSO–d<sub>6</sub>):  $\delta$  = C–Hg could not be observe, 144.9 (*C*<sub>ortho</sub>), 133.2 (*C*<sub>para</sub>), 131.2 (*C*<sub>ipso</sub>), 126.2 (*C*<sub>meta</sub>), 85.0 (CCH<sub>3</sub>), 67.5, 55.1, 48.8, 29.0, 28.8, 27.6, 26.9, 26.0, 23.9. **HRMS (AP<sup>+</sup>):** *m/z* calcd for C<sub>40</sub>H<sub>60</sub>I<sub>3</sub>Hg<sub>2</sub>N<sub>2</sub>:1353.1450 [M–I–4H]<sup>+</sup> found:1353.1576; *m/z* calcd for C<sub>20</sub>H<sub>31</sub>I<sub>1</sub>Hg<sub>1</sub>N<sub>1</sub>: 614.1237 [M/2–HI]; found: 614.1211.

### 3.7 Preparation of [(CAAC<sup>cy</sup>)<sub>2</sub>Hg(H<sub>2</sub>O)]<sup>2+</sup>2[NO<sub>3</sub>]<sup>–</sup> (5)

A mixture of **3.1** (0.02 g, 0.03 mmol) and AgNO<sub>3</sub> (0.01 g, 0.06 mmol) was taken in NMR tube in 0.5 mL of DMSO–d<sub>6</sub>. The NMR tube was kept for crystallization after a few days colorless crystals of [(CAAC<sup>cy</sup>)<sub>2</sub>Hg(H<sub>2</sub>O)]<sup>2+</sup>2[NO<sub>3</sub>]<sup>–</sup> were observed. Yield: 0.04 g, 20 %. Mp: 215–217 °C. **IR** (Nujol, cm<sup>–1</sup>)  $\tilde{\nu}$ : 2973, 2935, 2859, 1590, 1469, 1446, 1382, 1318, 1143, 1052, 931, 810, 779, 594. **<sup>1</sup>H NMR** (400 MHz, DMSO–d<sub>6</sub>):  $\delta$  = 7.69 (t, 2H, *p*Ar–H, <sup>3</sup>*J*<sub>H–H</sub> = 8 Hz), 7.62 (d, 4H, *m*Ar–H, <sup>3</sup>*J*<sub>H–H</sub> = 8 Hz), 3.54 (s, 2H, H<sub>2</sub>O), 2.73 (sept, 4H, CH(CH<sub>3</sub>)<sub>2</sub>, <sup>3</sup>*J*<sub>H–H</sub> = 8 Hz), 2.38 (s, 4H, CH<sub>2</sub>), 1.47 (s, 12H, CH<sub>3</sub>), 1.25 (d, 12H, CH(CH<sub>3</sub>)<sub>2</sub>, <sup>3</sup>*J*<sub>H–H</sub> = 4 Hz), 1.11 (d, 12H, CH(CH<sub>3</sub>)<sub>2</sub>, <sup>3</sup>*J*<sub>H–H</sub> = 4 Hz). **<sup>13</sup>C NMR** (100 MHz, DMSO–d<sub>6</sub>):  $\delta$  = 237 (C–Hg), 145.0 (*C*<sub>ortho</sub>), 132.4 (*C*<sub>para</sub>), 127.0 (*C*<sub>meta</sub>), 88.0 (CCH<sub>3</sub>), 58.5, 43.2, 34.7, 28.8, 28.5, 27.8, 24.0, 20.6. **HRMS (AP<sup>+</sup>):** *m/z* calcd for C<sub>46</sub>H<sub>76</sub>HgN<sub>2</sub>NaO: 897.5571 [M+Na–2NO<sub>3</sub>]<sup>+</sup>; found: 897.5538.

### 3.8 Preparation of [(CAAC<sup>cy</sup>)<sub>2</sub>Hg]<sup>2+</sup>[Hg<sub>2</sub>Br<sub>6</sub>]<sup>2–</sup> (6):

A mixture of **3.1**(0.61 g, 1.1 mmol) and AgNO<sub>3</sub> (0.37 g, 2.2 mmol) was taken in 30mL

THF. The resulting suspension was stirred at room temperature for 6 h. The solution was filtered and filtrate was kept for crystallization. Colorless crystals were obtained at room temperature in overnight. **<sup>1</sup>H NMR** (400 MHz, CDCl<sub>3</sub>):  $\delta$  = 7.61–7.54 (m, 2H, Ar–H), 7.42 (d, 1H, Ar–H, <sup>3</sup>J<sub>H–H</sub> = 8 Hz), 7.34 (d, 2H, Ar–H, <sup>3</sup>J<sub>H–H</sub> = 8 Hz), 2.79 (sept, 2H, CH(CH<sub>3</sub>)<sub>2</sub>, <sup>3</sup>J<sub>H–H</sub> = 8 Hz), 2.70 (sept, 2H, CH(CH<sub>3</sub>)<sub>2</sub>, <sup>3</sup>J<sub>H–H</sub> = 8 Hz), 2.41 (s, 2H, CH<sub>2</sub>), 2.30 (s, 6H), 1.77–1.66 (m, 9H), 1.53 (d, 12H, CH(CH<sub>3</sub>)<sub>2</sub>), 1.34 (d, 7H, CH(CH<sub>3</sub>)<sub>2</sub>, <sup>3</sup>J<sub>H–H</sub> = 8 Hz), 1.28 (d, 12H, CH(CH<sub>3</sub>)<sub>2</sub>), 1.21 (d, 7H, CH(CH<sub>3</sub>)<sub>2</sub>), 1.07 (m, 3H). **<sup>13</sup>C NMR** (100 MHz, CDCl<sub>3</sub>):  $\delta$  = 241.7 (C–Hg), 145.9 (C<sub>ortho</sub>), 144.8, 133.1 (C<sub>para</sub>), 132.7, 132.0, 131.9 (C<sub>ipso</sub>), 126.7, 126.3 (C<sub>meta</sub>), 86.9, 84.9 (CCH<sub>3</sub>), 68.1, 59.8, 59.3, 45.5, 45.1, 36.4, 33.8, 29.9, 29.7, 29.4, 27.1, 26.94, 25.7, 25.0, 24.7, 24.3, 23.6, 21.4.

**Table 3.1. Crystal data and structure refinement details of complexes 1-6.**

Compound <sup>[a]</sup>	1	2	3	4	5	6
Chemical formula	C <sub>23</sub> H <sub>36</sub> C <sub>13</sub> HgN	C <sub>18</sub> H <sub>29</sub> C <sub>12</sub> HgN	C <sub>20</sub> H <sub>31</sub> HgBr <sub>2</sub> N	C <sub>20</sub> H <sub>31</sub> HgI <sub>2</sub> N	C <sub>23</sub> H <sub>35</sub> Hg <sub>0.5</sub> N <sub>2</sub> O <sub>3.50</sub>	C <sub>23</sub> H <sub>34</sub> Br <sub>3</sub> Hg <sub>1.50</sub> N
Molar mass	633.47	530.91	753.87	753.87	499.83	1060.35
Crystal system	Monoclinic	Monoclinic	Monoclinic	Monoclinic	Monoclinic	Orthorhombic
Space group	<i>P</i> 2 <sub>1</sub> / <i>n</i>	<i>P</i> 2 <sub>1</sub> / <i>n</i>	<i>P</i> 2 <sub>1</sub> / <i>n</i>	<i>P</i> 2 <sub>1</sub> / <i>n</i>	<i>C</i> 2/ <i>c</i>	<i>P</i> <i>n</i> <i>n</i> <i>m</i>
<i>T</i> [K]	100.0(2)	100.0(2)	298	298	298	298
<i>a</i> [Å]	14.5279(10)	9.2281(11)	9.367(3)	9.5075(16)	21.351(3)	15.901(3)
<i>b</i> [Å]	11.5471(8)	14.4065(13)	14.355(5)	14.2113(17)	10.5581(11)	12.099(2)
<i>c</i> [Å]	15.7316(10)	15.6797(17)	15.850(6)	16.619(2)	21.185(2)	14.057(3)
$\alpha$ [°]	90	90	90	90	90	90
$\beta$ [°]	105.650(3)	91.901(6)	91.681(15)	91.675(7)	106.150(4)	90
$\gamma$ [°]	90	90	90	90	90	90
<i>V</i> [Å <sup>3</sup> ]	2541.2(3)	2083.4(4)	2130(11)	2244.5(5)	4587.3(9)	2704.4(9)
<i>Z</i>	4	4	4	4	8	4
<i>D</i> (calcd.) [g·cm <sup>-3</sup> ]	1.656	1.693	2.189	2.189	1.447	2.125
$\mu$ (Mo- <i>K</i> $\alpha$ ) [mm <sup>-1</sup> ]	6.381	7.642	9.611	9.611	3.419	12.957
Index range	-17 ≤ <i>h</i> ≤ 16	-10 ≤ <i>h</i> ≤ 10	-12 ≤ <i>h</i> ≤ 12	-11 ≤ <i>h</i> ≤ 11	-25 ≤ <i>h</i> ≤ 25	-18 ≤ <i>h</i> ≤ 15
	-13 ≤ <i>k</i> ≤ 11	-17 ≤ <i>k</i> ≤ 17	-18 ≤ <i>k</i> ≤ 18	-16 ≤ <i>k</i> ≤ 16	-12 ≤ <i>k</i> ≤ 11	-10 ≤ <i>k</i> ≤ 14
	-18 ≤ <i>l</i> ≤ 18	-18 ≤ <i>l</i> ≤ 18	-20 ≤ <i>l</i> ≤ 20	-19 ≤ <i>l</i> ≤ 19	-25 ≤ <i>l</i> ≤ 24	-16 ≤ <i>l</i> ≤ 16
Reflections collected	4599	3654	3956	3956	11558	7595
Independent reflections	4178	3130	3751	3751	6536	5227
Data/restraints/parameters	4599/0/263	3130/0/225	3751/0/225	3751/0/225	6536/0/273	5227/0/149
<i>R</i> 1, <i>wR</i> 2 [ <i>I</i> > 2 $\sigma$ ( <i>I</i> ) <sup>[a]</sup>	0.0219, 0.0573	0.0479, 0.1141	0.0453, 0.1382	0.0453, 0.1382	0.0352, 0.0899	0.0655, 0.1690
<i>R</i> 1, <i>wR</i> 2 (all data) <sup>[a]</sup>	0.0250, 0.0589	0.0582, 0.1297	0.0468, 0.1419	0.0468, 0.1419	0.0394, 0.1075	0.0967, 0.2014
GOF	1.067	1.107	1.082	1.082	1.167	1.084

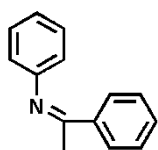
$$[a] R1 = \frac{\sum |F_o| - |F_c|}{\sum |F_o|}, wR2 = \left[ \frac{\sum w(|F_o|^2 - |F_c|^2)^2}{\sum w|F_o|^2} \right]^{1/2}$$

### 3.9 Preparation of aromatic imines (7-27):

**General procedure for hydroamination:** A Schlenk flask was charged with amine (1.5 mmol), alkyne (1.5 mmol) and the catalyst, **3.1** (1.63 mol%) in 20 mL THF. The reaction was monitored by TLC and NMR. After the completion of reaction all volatiles were evaporated under vacuum and the compound was extracted with hexane.

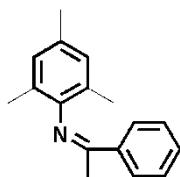
**NMR data of Intermolecular hydroamination reactions of aromatic alkynes with aromatic amines:**

#### Synthesis of *N*-(1-phenylethylidene)-aniline (**7**)<sup>[78]</sup>



Phenylacetylene (0.164 mL, 1.5 mmol) was added to a mixture of aniline (0.137 mL, 1.5 mmol) and [CAAC<sup>cy</sup>·HgBr(μ-Br)]<sub>2</sub>, (**3.1**) (28 mg, 0.071 mmol, 1.63 mol%) taken in a Schlenk flask in 20 mL THF. The resulting solution was reflux for 8 h. The volatiles were then removed under reduced pressure and the resulting residue was extracted with hexane to remove the catalyst. This extract was evaporated under vacuum and the oily material was purified by column chromatography on silica gel (eluent petroleum ether/ethyl acetate 4:1+2% triethylamine) under non-inert conditions to give **7** as yellow oil. **<sup>1</sup>H NMR** (400 MHz, CDCl<sub>3</sub>): δ = 8.03 (d, 2H, ArH, <sup>3</sup>J<sub>H-H</sub> = 8 Hz), 7.50 (s, br, 3H, ArH), 7.40 (t, 2H, ArH, <sup>3</sup>J<sub>H-H</sub> = 8 Hz), 7.14 (t, 1H, ArH, <sup>3</sup>J<sub>H-H</sub> = 8 Hz), 6.85 (d, 2H, ArH, <sup>3</sup>J = 8 Hz), 2.28 (s, 3H, N=CCH<sub>3</sub>); **<sup>13</sup>C NMR** (100 MHz, CDCl<sub>3</sub>): δ = 165.5 (NCCH<sub>3</sub>), 151.72 (CAr), 139.5 (CAr), 130.5 (CAr), 129.3 (CAr), 129.0 (CAr), 128.4 (CAr), 123.3 (CAr), 119.4 (CAr) 17.4 (CH<sub>3</sub>). **HRMS (ESI<sup>+</sup>):** *m/z* calcd for C<sub>14</sub>H<sub>14</sub>N: 196.1126 [M]<sup>+</sup>; found: 196.1120.

#### Synthesis of *N*-(1-phenylethylidene)-2,4,6-trimethylaniline (**8**)<sup>[79]</sup>

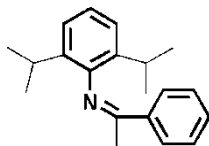


**<sup>1</sup>H NMR** (400 MHz, CDCl<sub>3</sub>): δ = 8.05 (d, 2H, ArH, <sup>3</sup>J<sub>H-H</sub> = 8 Hz), 7.50 (s, br, 3H, ArH), 6.90 (s, br, 2H, ArH), 2.32 (s, 3H, N=CCH<sub>3</sub>), 2.10 (s, 3H, CH<sub>3</sub>), 2.03 (s, 6H, CH<sub>3</sub>); **<sup>13</sup>C NMR**

(100MHz, CDCl<sub>3</sub>):  $\delta$  = 165.5 (NCCH<sub>3</sub>), 146.6 (CAr), 139.4 (CAr), 132.0 (CAr), 130.5 (CAr), 128.9 (CAr), 128.5 (CAr), 127.2 (CAr), 125.7 (CAr), 20.9 (CH<sub>3</sub>), 18.0 (CH<sub>3</sub>), 17.5 (CH<sub>3</sub>).

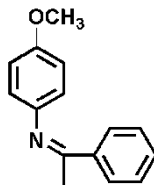
**HRMS (ESI<sup>+</sup>):**  $m/z$  calcd for C<sub>17</sub>H<sub>20</sub>N: 238.1596 [M]<sup>+</sup>; found: 238.1584.

#### Synthesis of *N*-(1-phenylethylidene)-2,6-diisopropylaniline (9)<sup>[79]</sup>



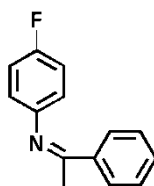
**<sup>1</sup>H NMR** (400 MHz, CDCl<sub>3</sub>):  $\delta$  = 8.06 (d, 2H, ArH, <sup>3</sup>J<sub>H-H</sub> = 8 Hz), 7.51 (s, br, 3H, ArH), 7.18 (d, 2 H, ArH, <sup>3</sup>J = 8 Hz), 7.11 (d, 1H, ArH), 2.78 (sept, 2H, CH(CH<sub>3</sub>)<sub>2</sub>, <sup>3</sup>J<sub>H-H</sub> = 8 Hz), 2.13 (s, 3H, N=CCH<sub>3</sub>), 1.17 (t, 12H, CH(CH<sub>3</sub>)<sub>2</sub>, <sup>3</sup>J<sub>H-H</sub> = 8 Hz); **<sup>13</sup>C NMR** (100 MHz, CDCl<sub>3</sub>):  $\delta$  = 164.9 (NCCH<sub>3</sub>), 146.8 (CAr), 140.3 (CAr), 136.2 (CAr), 132.3 (CAr), 130.5 (CAr), 128.5 (CAr), 127.3 (CAr), 123.4 (CAr), 123.1 (CAr), 28.3 (CH(CH<sub>3</sub>)<sub>2</sub>), 23.4 (CH(CH<sub>3</sub>)<sub>2</sub>), 23.1 (CH(CH<sub>3</sub>)<sub>2</sub>), 18.3 (CH<sub>3</sub>). **HRMS (ESI<sup>+</sup>):**  $m/z$  calcd for C<sub>20</sub>H<sub>26</sub>N: 288.2055 [M]<sup>+</sup>; found: 288.2065.

#### Synthesis of *N*-(1-phenylethylidene)-*p*-methoxyaniline (10)<sup>[78]</sup>



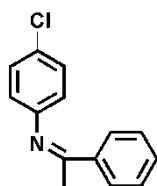
**<sup>1</sup>H NMR** (400 MHz, CDCl<sub>3</sub>):  $\delta$  = 7.97 (d, 2H, ArH, <sup>3</sup>J<sub>H-H</sub> = 8 Hz), 7.46 (m, 3H, ArH), 6.92 (d, 2H, ArH, <sup>3</sup>J = 8 Hz), 6.74 (d, 2H, ArH, <sup>3</sup>J = 8 Hz), 3.82 (s, 3H, OCH<sub>3</sub>), 2.26 (s, 3H, N=CCH<sub>3</sub>); **<sup>13</sup>C NMR** (100 MHz, CDCl<sub>3</sub>):  $\delta$  = 165.8 (NCCH<sub>3</sub>), 156.1 (CAr), 144.5 (CAr), 139.5 (CAr), 130.2 (CAr), 128.2 (CAr), 127.0 (CAr), 120.7 (CAr), 114.1 (CAr), 55.3 (OCH<sub>3</sub>), 17.2 (CH<sub>3</sub>). **HRMS (ESI<sup>+</sup>):**  $m/z$  calcd for C<sub>15</sub>H<sub>16</sub>NO: 226.1232 [M]<sup>+</sup>; found: 226.1220.

#### Synthesis of *N*-(1-phenylethylidene)-*p*-fluoroaniline (11)<sup>[78]</sup>



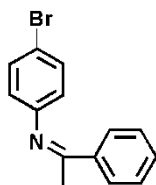
**<sup>1</sup>H NMR** (400 MHz, CDCl<sub>3</sub>):  $\delta$  = 7.96 (d, 2H, ArH, <sup>3</sup>J<sub>H-H</sub> = 8 Hz), 7.46 (s, br, 3H, ArH), 7.05 (t, 2H, ArH, <sup>3</sup>J<sub>H-H</sub> = 8 Hz), 6.75 (m, 2H, ArH), 2.24 (s, 3H, N=CCH<sub>3</sub>); **<sup>13</sup>C NMR** (100 MHz, CDCl<sub>3</sub>):  $\delta$  = 166.3 (NCCH<sub>3</sub>), 160.2 (CAr), 157.1 (CAr), 147.4 (CAr), 130.4 (CAr), 129.1 (CAr), 127.1 (CAr), 120.6 (CAr), 115.9 (CAr), 115.34 (CAr), 16.9 (CH<sub>3</sub>); **<sup>19</sup>F NMR** (376.4 MHz, CDCl<sub>3</sub>):  $\delta$  = -121.24. **HRMS (ESI<sup>+</sup>)**: *m/z* calcd for C<sub>14</sub>H<sub>12</sub>NFNa: 236.0851 [M]<sup>+</sup>; found: 236.0840.

#### Synthesis of *N*-(1-phenylethylidene)-*p*-chloroaniline (12)<sup>[80a,80b]</sup>



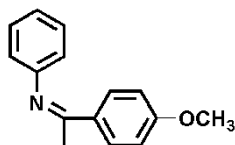
**<sup>1</sup>H NMR** (400 MHz, CDCl<sub>3</sub>):  $\delta$  = 7.97 (d, 2H, ArH, <sup>3</sup>J<sub>H-H</sub> = 8 Hz), 7.47 (d, 3H, ArH, <sup>3</sup>J<sub>H-H</sub> = 8 Hz), 7.31 (d, 2H, ArH, <sup>3</sup>J<sub>H-H</sub> = 8 Hz), 6.75 (d, 2H, ArH, <sup>3</sup>J<sub>H-H</sub> = 8 Hz), 2.24 (s, 3H, N=CCH<sub>3</sub>); **<sup>13</sup>C NMR** (100 MHz, CDCl<sub>3</sub>):  $\delta$  = 166.4 (CAr), 150.3 (CAr), 139.3 (CAr), 130.8 (CAr), 129.2 (CAr), 128.5 (CAr), 127.3 (CAr), 120.9 (CAr), 17.6 (CH<sub>3</sub>). **HRMS (ESI<sup>+</sup>)**: *m/z* calcd for C<sub>14</sub>H<sub>13</sub>ClN: 230.0737 [M]<sup>+</sup>; found: 230.0742.

#### Synthesis of *N*-(1-phenylethylidene)-*p*-bromoaniline (13)<sup>[80a,80b]</sup>



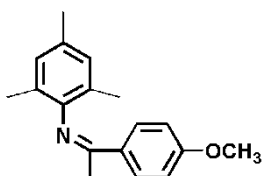
**<sup>1</sup>H NMR** (400 MHz, CDCl<sub>3</sub>):  $\delta$  = 8.00 (d, 2H, ArH, <sup>3</sup>J<sub>H-H</sub> = 8 Hz), 7.50 (m, 4H, ArH), 6.73 (d, 2H, ArH), 2.25 (s, 3H, N=CCH<sub>3</sub>); **<sup>13</sup>C NMR** (100 MHz, CDCl<sub>3</sub>):  $\delta$  = 166.4 (CAr), 150.4 (CAr), 138.9 (CAr), 130.6 (CAr), 128.3 (CAr), 127.1 (CAr), 121.2 (CAr), 120.9 (CAr), 17.4 (CH<sub>3</sub>). **HRMS (ESI<sup>+</sup>)**: *m/z* calcd for C<sub>14</sub>H<sub>13</sub>BrN: 274.0231 [M]<sup>+</sup>; found: 274.0243.

#### Synthesis of *N*-(1-(*p*-methoxyphenyl)ethylidene)aniline (14)<sup>[78]</sup>



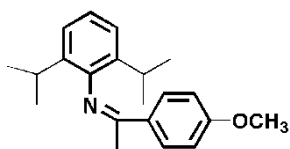
**<sup>1</sup>H NMR** (400 MHz, CDCl<sub>3</sub>):  $\delta$  = 8.00 (d, 2H, ArH, <sup>3</sup>J<sub>H-H</sub> = 8 Hz), 7.39 (t, 2H, ArH, <sup>3</sup>J<sub>H-H</sub> = 8 Hz), 7.12 (t, 1H, ArH, <sup>3</sup>J<sub>H-H</sub> = 8 Hz), 6.99 (d, 2H, ArH, <sup>3</sup>J<sub>H-H</sub> = 8 Hz), 6.86 (d, 2H, ArH, <sup>3</sup>J<sub>H-H</sub> = 8 Hz), 3.85 (s, 3H, OCH<sub>3</sub>), 2.22 (s, 3H, N=CCH<sub>3</sub>); **<sup>13</sup>C NMR** (100 MHz, CDCl<sub>3</sub>):  $\delta$  = 164.4 (NCCH<sub>3</sub>), 161.4 (CAr), 151.8 (CAr), 132.0 (CAr), 128.8 (CAr), 122.9 (CAr), 119.5 (CAr), 113.5 (CAr), 55.2 (OCH<sub>3</sub>), 17.0 (CH<sub>3</sub>). **HRMS (ESI<sup>+</sup>)**: *m/z* calcd for C<sub>14</sub>H<sub>16</sub>NO: 226.1232 [M]<sup>+</sup>; found: 226.1211.

#### Synthesis of *N*-(1-(*p*-methoxyphenyl)ethylidene)-2,4,6-trimethylaniline (15)



**<sup>1</sup>H NMR** (400 MHz, CDCl<sub>3</sub>):  $\delta$  = 8.17 (d, 2H, ArH, <sup>3</sup>J<sub>H-H</sub> = 8 Hz), 7.10 (d, 2H, ArH, <sup>3</sup>J<sub>H-H</sub> = 8 Hz), 7.03 (s, 2H, ArH), 3.95 (s, 3H, OCH<sub>3</sub>), 2.45 (s, 3H, CH<sub>3</sub>), 2.17 (s, br, 9H, CH<sub>3</sub> and N=CCH<sub>3</sub>); **<sup>13</sup>C NMR** (100 MHz, CDCl<sub>3</sub>):  $\delta$  = 164.2 (NCCH<sub>3</sub>), 161.3 (CAr), 146.6 (CAr), 140.1 (CAr), 131.70 (CAr), 128.5 (CAr), 125.6 (CAr), 113.4 (CAr), 55.1 (OCH<sub>3</sub>), 20.64 (CH<sub>3</sub>), 17.83 (CH<sub>3</sub>), 17.42 (CH<sub>3</sub>). **HRMS (ESI<sup>+</sup>)**: *m/z* calcd for C<sub>18</sub>H<sub>22</sub>NO: 268.1689 [M]<sup>+</sup>; found: 268.1701.

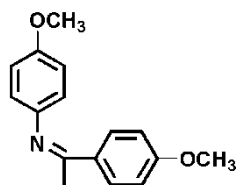
#### Synthesis of *N*-(1-(*p*-methoxyphenyl)ethylidene)-2,6-diisopropylaniline (16)



**<sup>1</sup>H NMR** (400 MHz, CDCl<sub>3</sub>):  $\delta$  = 8.18 (d, 2H, ArH, <sup>3</sup>J<sub>H-H</sub> = 8 Hz), 7.57 (d, 1H, ArH, <sup>3</sup>J<sub>H-H</sub> = 8 Hz), 7.20 (m, 2H, ArH), 7.12 (d, 2H, ArH, <sup>3</sup>J = 8 Hz), 6.95 (d, 1H, ArH, <sup>3</sup>J = 8 Hz), 3.96 (s, 3H, OCH<sub>3</sub>), 2.95 (sept, 2H, CH(CH<sub>3</sub>)<sub>2</sub>, <sup>3</sup>J<sub>H-H</sub> = 8 Hz), 2.23 (s, 3H, N=CCH<sub>3</sub>), 1.31 (t, 12H, CH(CH<sub>3</sub>)<sub>2</sub>, <sup>3</sup>J<sub>H-H</sub> = 8 Hz); **<sup>13</sup>C NMR** (100 MHz, CDCl<sub>3</sub>):  $\delta$  = 163.9 (NCCH<sub>3</sub>), 161.5 (CAr), 146.9 (CAr), 136.2 (CAr), 133.5 (CAr), 131.7 (CAr), 128.7 (CAr), 122.90 (CAr), 113.90 (CAr), 113.63 (CAr), 55.18 (OCH<sub>3</sub>), 28.32 (CH(CH<sub>3</sub>)<sub>2</sub>), 23.97 (CH(CH<sub>3</sub>)<sub>2</sub>), 23.22 (CH(CH<sub>3</sub>)<sub>2</sub>), 17.8 (CH<sub>3</sub>). **HRMS (ESI<sup>+</sup>)**: *m/z* calcd for C<sub>21</sub>H<sub>28</sub>NO: 310.2171 [M]<sup>+</sup>; found: 310.2157.

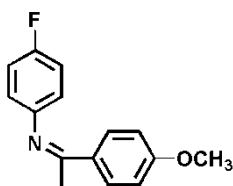


### Synthesis of *N*-(1-(*p*-methoxyphenyl)ethylidene)-*p*-methoxyaniline (17)<sup>[78]</sup>



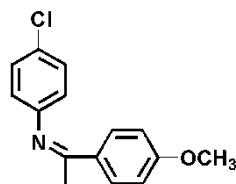
**<sup>1</sup>H NMR** (400 MHz, CDCl<sub>3</sub>):  $\delta$  = 7.93 (d, 2H, ArH, <sup>3</sup>*J*<sub>H-H</sub> = 8 Hz), 6.94 (d, 2H, ArH, <sup>3</sup>*J* = 8 Hz), 6.90 (d, 2H, ArH, <sup>3</sup>*J* = 8 Hz), 6.74 (d, 2H, ArH, <sup>3</sup>*J* = 8 Hz), 3.86 (s, 3H, OCH<sub>3</sub>), 3.81 (s, 3H, OCH<sub>3</sub>), 2.22 (s, 3H, N=CCH<sub>3</sub>); **<sup>13</sup>C NMR** (100MHz, CDCl<sub>3</sub>):  $\delta$  = 165.1 (NCCH<sub>3</sub>), 161.5 (CAr), 155.9 (CAr), 145.1 (CAr), 132.5 (CAr), 128.9 (CAr), 121.0 (CAr), 114.3 (CAr), 113.7 (CAr), 55.6 (OCH<sub>3</sub>), 55.5 (OCH<sub>3</sub>), 17.3 (CH<sub>3</sub>). **HRMS (ESI<sup>+</sup>)**: *m/z* calcd for C<sub>16</sub>H<sub>16</sub>NO<sub>2</sub>: 256.1338 [M+2H]<sup>+</sup>; found: 256.1325.

### Synthesis of *N*-(1-(*p*-methoxyphenyl)ethylidene)-*p*-floroaniline (18)<sup>[81]</sup>



**<sup>1</sup>H NMR** (400 MHz, CDCl<sub>3</sub>):  $\delta$  = 7.93 (d, 2H, ArH, <sup>3</sup>*J*<sub>H-H</sub> = 8 Hz), 7.04 (t, 2H, ArH, <sup>3</sup>*J*<sub>H-H</sub> = 8 Hz), 6.95 (d, 2H, ArH, <sup>3</sup>*J*<sub>H-H</sub> = 8 Hz), 6.73 (m, 2H, ArH), 3.87 (s, 3H, OCH<sub>3</sub>), 2.20 (s, 3H, N=CCH<sub>3</sub>); **<sup>13</sup>C NMR** (100 MHz, CDCl<sub>3</sub>):  $\delta$  = 165.7 (NCCH<sub>3</sub>), 161.7 (CAr), 160.5 (CAr), 158.2 (CAr), 147.9 (d, CAr), 132.2 (CAr), 128.9 (CAr), 121.0 (d, CAr), 115.7 (d, CAr), 113.7 (CAr), 55.5 (OCH<sub>3</sub>), 17.3 (CH<sub>3</sub>); **<sup>19</sup>F NMR** (376.4 MHz, CDCl<sub>3</sub>):  $\delta$  = -121.57. **HRMS (ESI<sup>+</sup>)**: *m/z* calcd for C<sub>15</sub>H<sub>15</sub>FNO: 244.1138 [M]<sup>+</sup>; found: 244.1127.

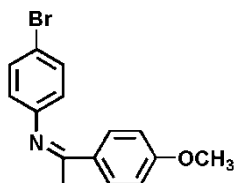
### Synthesis of *N*-(1-(*p*-methoxyphenyl)ethylidene)-*p*-chloroaniline (19)<sup>[81]</sup>



**<sup>1</sup>H NMR** (400 MHz, CDCl<sub>3</sub>):  $\delta$  = 7.92 (d, 2H, ArH, <sup>3</sup>*J*<sub>H-H</sub> = 8 Hz), 7.06 (d, 2H, ArH, <sup>3</sup>*J*<sub>H-H</sub> = 8 Hz), 6.92 (d, 2H, ArH, <sup>3</sup>*J*<sub>H-H</sub> = 8 Hz), 6.58 (d, 2H, ArH, <sup>3</sup>*J*<sub>H-H</sub> = 8 Hz), 3.84 (s, 3H, OCH<sub>3</sub>), 2.54 (s, 3H, N=CCH<sub>3</sub>); **<sup>13</sup>C NMR**(100 MHz, CDCl<sub>3</sub>):  $\delta$  = 165.3 (NCCH<sub>3</sub>), 145.1 (d, CAr),

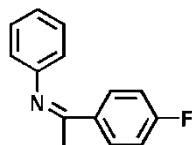
130.6 (CAr), 129.1 (CAr), 123.0 (CAr), 121.1 (CAr), 116.3 (CAr), 113.7 (CAr), 55.5 (OCH<sub>3</sub>), 26.4 (CH<sub>3</sub>). **HRMS (ESI<sup>+</sup>):** *m/z* calcd for C<sub>15</sub>H<sub>15</sub>ClNO: 260.0842 [M]<sup>+</sup>; found: 260.1217.

#### Synthesis of *N*-(1-(*p*-methoxyphenyl)ethylidene)-*p*-bromoaniline (20)



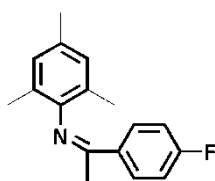
**<sup>1</sup>H NMR** (400 MHz, CDCl<sub>3</sub>):  $\delta$  = 7.91 (d, 2H, ArH, <sup>3</sup>*J*<sub>H-H</sub> = 8 Hz), 7.42 (d, 2H, ArH, <sup>3</sup>*J*<sub>H-H</sub> = 8 Hz), 6.93 (d, 2H, ArH, <sup>3</sup>*J*<sub>H-H</sub> = 8 Hz), 6.66 (d, 2H, ArH, <sup>3</sup>*J*<sub>H-H</sub> = 8 Hz), 3.82 (s, 3H, OCH<sub>3</sub>), 2.16 (s, 3H, N=CCH<sub>3</sub>); **<sup>13</sup>C NMR** (100 MHz, CDCl<sub>3</sub>):  $\delta$  = 165.03 (NCCH<sub>3</sub>), 161.6 (CAr), 150.8 (CAr), 131.8 (CAr), 128.8 (CAr), 121.4 (CAr), 113.6 (CAr), 113.5 (CAr), 55.2 (OCH<sub>3</sub>), 17.1 (CH<sub>3</sub>). **HRMS (ESI<sup>+</sup>):** *m/z* calcd for C<sub>15</sub>H<sub>15</sub>BrNNaO: 312.0188 [M+Na]<sup>+</sup>; found: 312.0222.

#### Synthesis of *N*-(1-(*p*-fluorophenyl)ethylidene)aniline (21)<sup>[78]</sup>



**<sup>1</sup>H NMR** (400MHz, CDCl<sub>3</sub>):  $\delta$  = 8.00 (m, 2H, ArH), 7.38 (t, 2H, ArH, <sup>3</sup>*J*<sub>H-H</sub> = 8 Hz), 7.14 (m, 3H, ArH), 6.80 (m, 2H, ArH) 2.23 (s, 3H, N=CCH<sub>3</sub>); **<sup>13</sup>C NMR** (100 MHz, CDCl<sub>3</sub>):  $\delta$  = 165.6 (NCCH<sub>3</sub>), 164.3 (CAr), 151.5 (CAr), 135.7 (CAr), 129.1 (CAr), 123.4 (CAr), 119.5 (CAr), 115.4 (CAr), 17.3 (CH<sub>3</sub>); **<sup>19</sup>F NMR** (376.4 MHz, CDCl<sub>3</sub>):  $\delta$  = -105.29. **HRMS (ESI<sup>+</sup>):** *m/z* calcd for C<sub>14</sub>H<sub>13</sub>NF: 214.1032 [M]<sup>+</sup>; found: 214.1023.

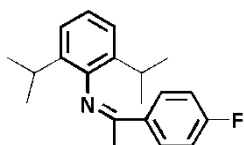
#### Synthesis of *N*-(1-(*p*-fluorophenyl)ethylidene)-2,4,6-trimethylaniline (22)<sup>[82]</sup>



**<sup>1</sup>H NMR** (400 MHz, CDCl<sub>3</sub>):  $\delta$  = 8.03 (m, 2H, ArH), 7.14 (t, 2H, ArH, <sup>3</sup>*J*<sub>H-H</sub> = 8 Hz), 6.92 (s,

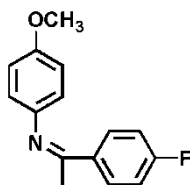
2H, ArH), 2.34 (s, 3H, N=CCH<sub>3</sub>) 2.06 (s, 3H, CH<sub>3</sub>), 2.04 (s, 6H, CH<sub>3</sub>); <sup>13</sup>C NMR (100 MHz, CDCl<sub>3</sub>): δ = 164.2 (NCCH<sub>3</sub>), 146.1 (CAr), 135.2 (CAr), 131.8 (CAr), 129.0 (CAr), 128.4(CAr), 125.4 (CAr), 115.0 (CAr), 20.5 (CH<sub>3</sub>), 17.7 (CH<sub>3</sub>), 17.1 (CH<sub>3</sub>); <sup>19</sup>F NMR (376.4 MHz, CDCl<sub>3</sub>): δ = -110.66. **HRMS (ES<sup>+</sup>):** *m/z* calcd for C<sub>17</sub>H<sub>19</sub>FN: 256.1501 [M]<sup>+</sup>; found: 256.1489.

#### Synthesis of *N*-(1-(*p*-florophenyl)ethylidene)-2,6-diisopropylaniline (23)<sup>[82]</sup>



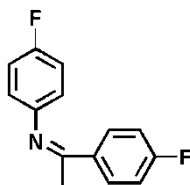
<sup>1</sup>H NMR (400 MHz, CDCl<sub>3</sub>): δ = 8.08 (m, 2H, ArH), 7.12 (m, 5H, ArH), 2.77 (sept, 2H, CH(CH<sub>3</sub>)<sub>2</sub>, <sup>3</sup>J<sub>H-H</sub> = 6.8 Hz), 2.13 (s, 3H, N=CCH<sub>3</sub>), 1.28 (m, 12H, CH(CH<sub>3</sub>)<sub>2</sub>); <sup>13</sup>C NMR (100 MHz, CDCl<sub>3</sub>): δ = 167.9 (CAr), 166.4 (NCCH<sub>3</sub>), 145.1 (CAr), 137.4 (CAr), 128.7 (CAr), 123.8 (CAr), 122.9 (CAr), 115.3 (CAr), 27.7 (CH(CH<sub>3</sub>)<sub>2</sub>), 23.6 (CH(CH<sub>3</sub>)<sub>2</sub>), 22.5 (CH<sub>3</sub>); <sup>19</sup>F NMR (376.4 MHz, CDCl<sub>3</sub>): δ = -110.19. **HRMS (ESI<sup>+</sup>):** *m/z* calcd for C<sub>20</sub>H<sub>25</sub>FN: 298.1971 [M]<sup>+</sup>; found: 298.1967.

#### Synthesis of *N*-(1-(*p*-florophenyl)ethylidene)-*p*-methoxyaniline (24)<sup>[78]</sup>



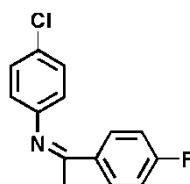
<sup>1</sup>H NMR (400 MHz, CDCl<sub>3</sub>): δ = 7.94 (m, 2H, ArH), 7.09 (t, 2H, ArH, <sup>3</sup>J<sub>H-H</sub> = 8 Hz), 6.91 (m, 2H, ArH), 6.79 (m, 2H, ArH), 3.78 (s, 3H, OCH<sub>3</sub>), 2.53 (s, 3H, CH<sub>3</sub>); <sup>13</sup>C NMR (100 MHz, CDCl<sub>3</sub>): δ = 166.7 (NCCH<sub>3</sub>), 164.3(CAr), 155.8 (CAr), 144.3 (CAr), 136.2 (CAr), 130.8 (CAr), 130.7 (CAr), 115.5 (CAr), 114.4 (CAr), 55.4 (OCH<sub>3</sub>), 17.0 (CH<sub>3</sub>); <sup>19</sup>F NMR (376.4 MHz, CDCl<sub>3</sub>): δ = -112.10. **HRMS (ES<sup>+</sup>):** *m/z* calcd for C<sub>15</sub>H<sub>15</sub>FNO: 244.1138 [M]<sup>+</sup>; found: 244.1529.

#### Synthesis of *N*-(1-(*p*-florophenyl)ethylidene)-*p*-floroaniline (25)<sup>[81]</sup>



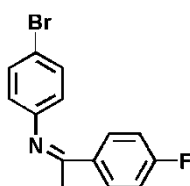
**<sup>1</sup>H NMR** (400 MHz, CDCl<sub>3</sub>):  $\delta$  = 7.97 (m, 2H, ArH), 7.12 (t, 2H, ArH, <sup>3</sup>J<sub>H-H</sub> = 8 Hz), 7.05 (t, 2H, ArH, <sup>3</sup>J<sub>H-H</sub> = 8 Hz), 6.75 (m, 2H, ArH), 2.22 (s, 3H, CH<sub>3</sub>); **<sup>13</sup>C NMR** (100 MHz, CDCl<sub>3</sub>):  $\delta$  = 165.2 (NCCH<sub>3</sub>), 160.5 (CAr), 158.3 (CAr), 147.5 (CAr), 135.6 (CAr), 129.4 (CAr), 120.8 (CAr), 115.5 (CAr), 115.3 (CAr), 17.5 (CH<sub>3</sub>); **<sup>19</sup>F NMR** (376.4 MHz, CDCl<sub>3</sub>):  $\delta$  = -110.2 and -121.1. **HRMS (ES<sup>+</sup>)**: *m/z* calcd for C<sub>14</sub>H<sub>12</sub>F<sub>2</sub>N: 232.0928 [M]<sup>+</sup>; found: 232.1329.

#### Synthesis of *N*-(1-(*p*-fluorophenyl)ethylidene)-*p*-chloroaniline (26)<sup>[81]</sup>



**<sup>1</sup>H NMR** (400 MHz, CDCl<sub>3</sub>):  $\delta$  = 7.97 (m, 2H, ArH), 7.32 (d, 2H, ArH, <sup>3</sup>J<sub>H-H</sub> = 8 Hz), 7.10 (m, 2H, ArH), 6.72 (d, 2H, ArH, <sup>3</sup>J<sub>H-H</sub> = 8 Hz), 2.21 (s, 3H, CH<sub>3</sub>); **<sup>13</sup>C NMR** (100 MHz, CDCl<sub>3</sub>):  $\delta$  = 165.1 (NCCH<sub>3</sub>), 163.2 (CAr), 150.0 (CAr), 135.4 (CAr), 129.4 (CAr), 129.4 (CAr), 123.2 (CAr), 120.9 (CAr), 115.3 (CAr), 17.5 (CH<sub>3</sub>); **<sup>19</sup>F NMR** (376.4 MHz, CDCl<sub>3</sub>):  $\delta$  = -105.24. **HRMS (ES<sup>+</sup>)**: *m/z* calcd for C<sub>14</sub>H<sub>12</sub>ClFN: 248.0642 [M]<sup>+</sup>; found: 248.0750.

#### Synthesis of *N*-(1-(*p*-fluorophenyl)ethylidene)-*p*-bromoaniline (27)



**<sup>1</sup>H NMR** (400 MHz, CDCl<sub>3</sub>):  $\delta$  = 7.95 (m, 2H, ArH), 7.45 (d, 3H, ArH, <sup>3</sup>J<sub>H-H</sub> = 8 Hz), 7.12 (t, 2H, ArH, <sup>3</sup>J<sub>H-H</sub> = 8 Hz), 6.67 (d, 2H, ArH, <sup>3</sup>J<sub>H-H</sub> = 8 Hz), 2.20 (s, 3H, CH<sub>3</sub>); **<sup>13</sup>C NMR** (100MHz, CDCl<sub>3</sub>):  $\delta$  = 165.1 (NCCH<sub>3</sub>), 163.1 (CAr), 150.4 (CAr), 135.3 (CAr), 129.4 (CAr), 129.3 (CAr), 121.3 (CAr), 115.3 (CAr), 17.4 (CH<sub>3</sub>); **<sup>19</sup>F NMR** (376.4 MHz, CDCl<sub>3</sub>):  $\delta$  = -105.16. **HRMS (ES<sup>+</sup>)**: *m/z* calcd for C<sub>14</sub>H<sub>12</sub>BrFN: 292.0137 [M]<sup>+</sup>; found: 292.0453.

#### 4. Conclusions

We have been able to prepare new CAAC-Hg(II) complexes in this work by employing insitu generated CAAC and subsequently treating it with  $\text{HgX}_2$  salts ( $X = \text{Cl, Br, I}$ ). The complexes obtained have the composition  $[\text{CAAC}\cdot\text{HgCl}(\mu\text{-Cl})]_2$  (**2**),  $[\text{CAAC}\cdot\text{HgBr}(\mu\text{-Br})]_2$  (**3**),  $[\text{CAAC}\cdot\text{HgI}(\mu\text{-I})]_2$  (**4**) and form dimeric structures in the solid state. The Hg(II) centers in these complexes adopt a distorted tetrahedral geometry and the two CAAC units are trans to each other. The previously known dimer,  $[\text{CAAC}^{\text{cy}}\cdot\text{HgBr}(\mu\text{-Br})]_2$  (**3.1**) when reacted with  $\text{AgNO}_3$  with the aim to substitute the bromides with nitrate to isolate cationic mercury species led to the formation of  $[(\text{CAAC}^{\text{cy}})_2\text{Hg}(\text{H}_2\text{O})]^{2+}2[\text{NO}_3]^-$  (**5**). A similar reaction when performed in dry THF afforded water free dicationic complex  $[(\text{CAAC}^{\text{cy}})_2\text{Hg}]^{2+}[\text{Hg}_2\text{Br}_6]^{2-}$  (**6**). All These results shows that the CAACs have different properties than NHCs, at least when coordinated to mercury(II) centers. The reaction pathways that worked well were not successful with CAACs moreover, the NHCs generally afford the monomeric adducts whereas the CAACs gave the dimmers. Moreover, the complex,  $[\text{CAAC}^{\text{cy}}\cdot\text{HgBr}(\mu\text{-Br})]_2$  (**3.1**) has been successfully used as a catalyst for the hydroamination reactions with a variety of amines and alkynes which shows Markovnikov selectivity.

## 5. Future Directions

The continuation of the current work will focus on:

1. Investigations on the catalytic cycle of intermolecular hydroamination reaction with the catalyst  $[\text{CAAC}^{\text{cy}}\cdot\text{HgBr}(\mu\text{-Br})]_2$ .
2. The intramolecular version of hydroamination can be investigated to see the feasibility of formation of indole and related molecules.
3. To isolate the adducts containing rare molecules with hard and soft mismatch of the ligands ( $\text{H}^-$ ,  $\text{F}^-$ ,  $\text{OH}^-$  etc.) with soft Hg centers as in the complexes  $[\text{CAAC}\cdot\text{HgH}_2]$  and  $[\text{CAAC}\cdot\text{Hg}(\text{OH})_2]$ .
4. Hydroamination of nitriles (addition of amines and nitriles) can also be explored.
5. The cationic complexes may turn out to be better electrophiles and thus may be capable of activating olefins for hydroamination reactions.

## 6. References:

1. Hahn, F.; Jahnke, C. M. *Angew. Chem. Int. Ed.* **2008**, *47*, 3122–3172.
2. Hoffmann, R. *J. Am. Chem. Soc.* **1968**, *90*, 1475–1485.
3. Bourissou, D.; Guerret, O.; P. Gabbai, F.; Bertrand, G. *Chem. Rev.* **2000**, *100*, 39–91.
4. Wanzlick, W. H. *Angew. Chem. Int. Ed. Engl.* **1962**, *1*, 75–80.
5. Wanzlick, H. W.; Schonherr, H. J. *Angew. Chem. Int. Ed. Engl.* **1968**, *7*, 141–142.
6. Hopkinson, M. N.; Richter, C.; Schedler, M.; Glorius, F. *Nature* **2014**, *510*, 485–496.
7. Herrmann, W. A.; Elison, M.; Fischer, J.; Kocher, C.; Artus, G. R. J. *Angew. Chem. Int. Ed. Engl.* **1995**, *34*, 2371–2374.
8. Fevre, M.; Pinaud, J.; Gnanou, J.; Vignolle, J. Daniel T. *Chem. Soc. Rev.* **2013**, *42*, 2142–2172.
9. Kuhn, A. Al-Sheikh, *Coord. Chem. Rev.* **2005**, *249*, 829–857.
10. Arduengo, A.J.; Gamper, S. F.; Calabrese, J. C.; Davidson, *J. Am. Chem. Soc.* **1994**, *116*, 4391–439.
11. Gstöttmayr, C. W. K.; Böhm, V. P. W.; Herdtweck, E.; Grosche, M.; Herrmann, W. A. *Angew. Chem. Int. Ed.* **2002**, *41*, 1363–1365.
12. (a) Arduengo, A. J. III; Dias, H. V. R.; Calabrese, J. C.; Davidson, F. *Organometallics* **1993**, *12*, 3405–3409; (b) Bonati, F.; Burini, A.; Pietroni, B. R.; Bovio, B. *J. Organomet. Chem.* **1989**, *375*, 147–160; (c) Mo, Z.; Chen, D.; Leng, X.; Deng, L. *Organometallics* **2012**, *31*, 7040–7043; (d) Poulten, R. C.; Page, M. J.; Algarra, A. G.; Le Roy, J. J.; Lopez, I.; Carter, E.; Llobet, A.; Macgregor, S. A.; Mahon, M. F.; Murphy, D. M.; Murugesu, M.; Whittlesey, M. K. *J. Am. Chem. Soc.* **2013**, *135*, 13640–13643.
13. Wang, Y. Z.; Xie, Y.; Wei, P.; King, R. B.; Schaefer, H. F.; Schleyer, P. v. R.; Robinson, G. H. *Science* **2008**, *321*, 1069–1071.
14. Soleilhavoup, M.; Bertrand, G. *Acc. Chem. Res.* **2015**, *48*, 256–266.
15. Martin, D.; Melaimi, M.; Soleilhavoup, M.; Bertrand, *Organometallics* **2011**, *30*, 5304–5313.
16. Malaimi, M.; Jazzar, R.; Soleilhavoup, M.; Bertrand, G. *Angew. Chem. Int. Ed.* **2017** (DOI10.1002/anie.201702148).
17. Lavallo, V.; Canac, Y.; Donnadiou, B.; Schoeller, W. W.; Bertrand, G. *Angew. Chem. Int. Ed.* **2006**, *45*, 3488–3491.
18. Roy, S.; Mondal, K. C.; Roesky, H. W. *Acc. Chem. Res.* **2016**, *49*, 357–369.

19. Lavallo, V.; Canac, Y.; Donnadiou, B.; Schoeller, W. W.; Bertrand, G. *Angew. Chem. Int. Ed.* **2006**, *45*, 3488–3491.
20. Frey, G. D.; Lavallo, V.; Donnadiou, B.; Schoeller, W. W.; Bertrand, G. *Science* **2007**, *316*, 439–441.
21. Masuada, J. D.; Schoeller, W. W.; Donnadiou, B.; Bertrand, G. *Angew. Chem. Int. Ed.* **2007**, *46*, 7053–7055.
22. Frey, G. D.; Masuda, J. D.; Donnadiou, B.; Bertrand, G. *Angew. Chem.* **2010**, *122*, 9634–9637.
23. Frey, G. D.; Masuda, J. D.; Donnadiou, B.; Bertrand, G. *Angew. Chem. Int. Ed.* **2010**, *49*, 9444–9447.
24. Frey, G. D.; Lavallo, V.; Donnadiou, B.; Schoeller, W. W.; Bertrand, G. *Science* **2007**, *316*, 439–441.
25. Turner, Z. R. *Chem–Eur. J.* **2016**, *22*, 11461–11468.
26. Kinjo, R.; Donnadiou, B.; Ali Celik, M.; Frenking, G.; Bertrand, G. *Science* **2011**, *333*, 610–613.
27. Mondal, K. C.; Roy, S.; Dittrich, B.; Andrada, D. M.; Frenking, G.; Roesky, H. W.; *Angew. Chem. Int. Ed.* **2016**, *55*, 3158–316.
28. Back, O.; Kuchenbeiser, G.; Donnadiou, B.; Bertrand, G. *Angew. Chem. Int. Ed.* **2009**, *48*, 5530–5533.
29. Kretschmer, R.; Ruiz, D. A.; Moore, C. E.; Rheingold, A. L.; Bertrand, G. *Angew. Chem. Int. Ed.* **2014**, *53*, 8176–8179.
30. Weinberger, D. S.; Melaimi, M.; Moore, C. E.; Rheingold, A. L.; Frenking, G.; Jerabek, P.; Bertrand, G. *Angew. Chem. Int. Ed.* **2013**, *52*, 8964–8967.
31. Weinberger, D. S.; Amin S. K. N.; Mondal, K. C.; Melaimi, M.; Bertrand, G.; C. Stuckl, A.; Roesky, H. W.; Dittrich, B.; Demeshko, S.; Schwederski, B.; Kaim, W.; Jerabek, P.; Frenking, G. *J. Am. Chem. Soc.* **2014**, *136*, 6235–6238.
32. Ung, G.; Rittle, J.; Soleilhavoup, M.; Bertrand, G.; Peters, J. C. *Angew. Chem. Int. Ed.* **2014**, *53*, 8427–8433.
33. Mondal, K. C.; Samuel, P. P.; Li, Y.; Roesky, H. W.; Roy, S.; Ackermann, L.; Sidhu, N. S.; Sheldrick, G. M.; Carl, E.; Demeshko, S.; De, S.; Parameswaran, P.; Ungur, L.; Chibotaru, L. F.; Andrada, D. M. *Eur. J. Inorg. Chem.* **2014**, 818–823.
34. Samuel, P. P.; Mondal, K. C.; Roesky, H. W.; Hermann, M.; Frenking, G.; Demeshko, S.; Meyer, F.; C. Stuckl, A.; Christian, J. H.; Dalal, N. S.; Ungur, L.; Chibotaru, L. F.; Propper, K.; Meents, A.; Dittrich, B. *Angew. Chem. Int. Ed.* **2013**, *52*, 11817–11812.



35. Singh, A. P.; Samuel, P. P.; Roesky, H. W.; Schwarzer, M. C.; Sidhu, N. S.; Dittrich, B. *J. Am. Chem. Soc.* **2013**, *135*, 7324–7329.
36. Lavallo, V.; Canac, Y.; DeHope, A.; Donnadiou, B.; Bertrand, G. *Angew. Chem. Int. Ed.* **2005**, *44*, 7236–7239.
37. Zeng, X.; Frey, G. D.; Kousar, S.; Bertrand, G.; *Chem. Eur. J.* **2009**, *15*, 3056–3060.
38. (a) Anderson, D. R.; Ung, T.; Mkrtumyan, G.; Bertrand, G.; Grubbs, R. H.; Schrodi, Y. *Organometallics* **2008**, *27*, 563–566; (b) Jayarathne, U.; Mazzacano, T. J.; Bagherzadeh, S.; Mankad, N. P. *Organometallics* **2013**, *32*, 3986–3992; (c) Al-Rafia, S. M. I.; Lummis, P. A.; Swarnakar, A. K.; Deutsch, K. C.; Ferguson, M. J.; McDonald, R.; Rivard, E. *Austr. J. Chem.* **2013**, *66*, 1235–1245; (d) Naktode, K.; Anga, S.; Kottalanka, R. K.; Nayek, H. P.; Panda, T. K. *J. Coord. Chem.* **2014**, *67*, 236–248; (e) Pelz, S.; Mohr, F. *Organometallics* **2011**, *30*, 383–385.
39. Reppe, W.; Krzihalla, H. Ger. Patent DE000000851197B, April 1944.
40. Reppe, W.; Krzihalla, H.; Dornheim, O. Ger. Patent DE000000890508B, January 17, **1939**.
41. Reppe, W.; Liebigs, J. *Ann. Chem.* **1956**, *601*, 81–138.
42. Reppe, W.; Herrle, K.; Fikentscher, H. Ger. Patent DE000000922378B, November 21, **1943**.
43. Reppe, W.; Schuster, C.; Hartmann, A. Ger. Patent DE000000737663A, January 17, **1939**.
44. Müller, T. E.; Hultsch, K. C.; Yus, M.; Foubelo, F.; Tada, M. *Chem. Rev.* **2008**, *108*, 3795–3892.
45. Pohlki, F.; Doye, S. *Chem. Soc. Rev.* **2003**, *32*, 104–114.
46. Severin, R.; Doye, S. *Chem. Soc. Rev.* **2007**, *36*, 1407–1420.
47. Haggins, J. *Chem. Eng. News* **1993**, *71*, 23–27.
48. Schlummer, B.; Hartwig, J. F. *Org. Lett.* **2002**, *4*, 1471–1474.
49. Dion, I.; Beauchemin, A. M. *Angew. Chem., Int. Ed.* **2011**, *50*, 8233–8235.
50. (a) Zhang, X.; Li, K.; Li, W. *Eur. J. Org. Chem.* **2008**, 1929; (b) Seayad, J.; Tillack, A.; Hartung, C. G.; Beller, M. *Adv. Synth. Catal.* **2002**, *344*, 795–813.
51. Rodriguez, A. L.; Koradin, C.; Dohle, W.; Knochel, P. *Angew. Chem. Int. Ed.* **2000**, *39*, 2488–2490.
52. Herrero, M. T.; de Sarralde, J. D.; SanMartin, R.; Bravo, L.; Domínguez, E. *Adv. Synth. Catal.* **2012**, *354*, 3054–3064.
53. Tzalis, D.; Koradin, C.; Knochel, P. *Tetrahedron Lett.* **1999**, *40*, 6193–6195.

54. Joshi, M.; Tiwari, R.; Verma, A. K. *Org. Lett.* **2012**, *14*, 1106–1109.
55. Gagne, R. M.; Marks, J. T. *J. Am. Chem. Soc.* **1989**, *111*, 4108–4109.
56. Hong, S.; Marks, T. J. *Acc. Chem. Res.* **2004**, *37*, 673–686.
57. Straub, B. F.; Bergman, R. G. *Angew. Chem., Int. Ed.* **2001**, *40*, 4632–4635.
58. Leitch, D. C.; Platel, R. H.; Schafer, L. L. *J. Am. Chem. Soc.* **2011**, *133*, 15453–15463.
59. (a) Manna, K.; Everett, W. C.; Schoendorff, G.; Ellern, A.; Windus, T. L.; Sadow, A. D. *J. Am. Chem. Soc.* **2013**, *135*, 7235–7250; (b) Shanbhag, G.V.; Halligudi, S. B. *J. Mol. Catal. A: Chem.* **2004**, *222*, 223–228; (c) Muller, T. E.; Pleier, A.-K. *J. Chem. Soc. Dalton Trans.* **1999**, 583–587.
60. Zeng, X. *Chem. Rev.* **2013**, *113*, 6864–6900.
61. Krause, N.; Winter, C. *Chem. Rev.* **2011**, *111*, 1994–2009.
62. Álvarez-Corral, M.; Muñoz-Dorado, M.; Rodríguez-García, I. *Chem. Rev.* **2008**, *108*, 3174–3198.
63. Weibel, J.-M.; Blanc, A.; Pale, P. *Chem. Rev.* **2008**, *108*, 3149–3173.
64. Lavallo, V.; Wright, J. H.; Tham, F. S.; Quinlivan, S. *Angew. Chem. Int. Ed.* **2013**, *52*, 3172–3176.
65. Zeng, X.; Soleilhavoup, M.; Bertrand, G. *Org. Lett.* **2009**, *11*, 3166–3169.
66. Xeng, X.; Frey, G. D.; Kousar, S.; Bertrand, G. *Chem.-Eur. J.* **2009**, *15*, 3056–3060.
67. Zeng, X.; Frey, G. D.; Kinjo, R.; Donnadiou, B.; Bertrand, G. *J. Am. Chem. Soc.* **2009**, *131*, 8690–8696.
68. (a) Zeng, X.; Kinjo, R.; Donnadiou, B.; Bertrand, G. *Angew. Chem. Int. Ed.* **2010**, *49*, 942–945; (b) Muller, T. E.; Grosche, M.; Herdtweck, E.; Pleier, A. K.; Walter, E.; Yan, Y. K; *Organometallics* **2000**, *19*, 170–183; (c) Chileck, M. A.; Hartenstein, L.; Braun, T.; Roesky, P. W.; *Chem-Eur. J.* **2015**, *21*, 2594–2602; (d) Barluenga, J.; Aznar, F.; Liz, R.; Rodes, R. *J. Chem. Soc. Perkin Trans.* **1983**, *1*, 1087–1091.
69. Hudrlik, P. F.; Hudrlik, A. M. *J. Org. Chem.* **1973**, *38*, 4254–4258.
70. Barluenga, J.; Aznar, F.; Liz, R.; Rodes, R. *J. Chem. Soc. Perkin Trans.* **1980**, *1*, 2732–2737.
71. Kurisaki, T.; Naniwa, T.; Yamamoto, H.; Imagawa, H.; Nishizawa, M. *Tetrahedron Lett.* **2007**, *48*, 1871–1874.
72. Barluenga, J.; Azanar, F. *Synthesis*, **1975**, *11*, 704–704.
73. Sabari V. R (2016) MS Dissertation on “Synthesis of Cyclic (Alkyl)(Amino) Carbene–Mercury(II) Complexes”, (IISER Mohali).

74. Liua, Q. L.; Yina, L. N.; Wua, X. M.; Fenga, J. C.; Guoa, J. H.; Songb, H. B. *Polyhedron* **2008**, *27*, 87–94.
75. CrystalClear 2.0, Rigaku Corporation, Tokyo, Japan.
76. Dolomanov, O. V.; Bourhis, L. J.; Gildea, R. J.; Howard, J. A. K.; Puschmann, H. *J. Appl. Cryst.* **2009**, *42*, 339–341.
77. Sheldrick, G. M. *Acta Crystallogr., Sect. A.* **2008**, *64*, 112–122.
78. Pham, N. N.; Dang, T. T.; Ngo, N. T.; Villinger, A.; Ehlers, P.; Langer, P. *Org. Biomol. Chem.* **2015**, *13*, 6047–6058.
79. Mir, R.; Dudding, T.; *J. Org. Chem.* **2016**, *81*, 2675–2679.
80. (a) Zhu, S., F.; Xie, J. B.; Zhang, Y. Z.; Li, S.; Zhou, Q. L. *J. Am. Chem. Soc.* **2006**, *128*, 12886–12891; (b) Barluenga, J.; Fernández, M. A.; Aznar, F.; Valdés, F.; *Chem–Eur. J.* **2004**, *10*, 494–507.
81. Cao, Z.; Cao, C. *J. Phys. Org. Chem.* **2015**, *28*, 564–569.
82. Lavallo, V.; Wright II, J. H.; Tham, F. S.; Quinliva, S. *Angew. Chem. Int. Ed.* **2013**, *52*, 3172–3176.

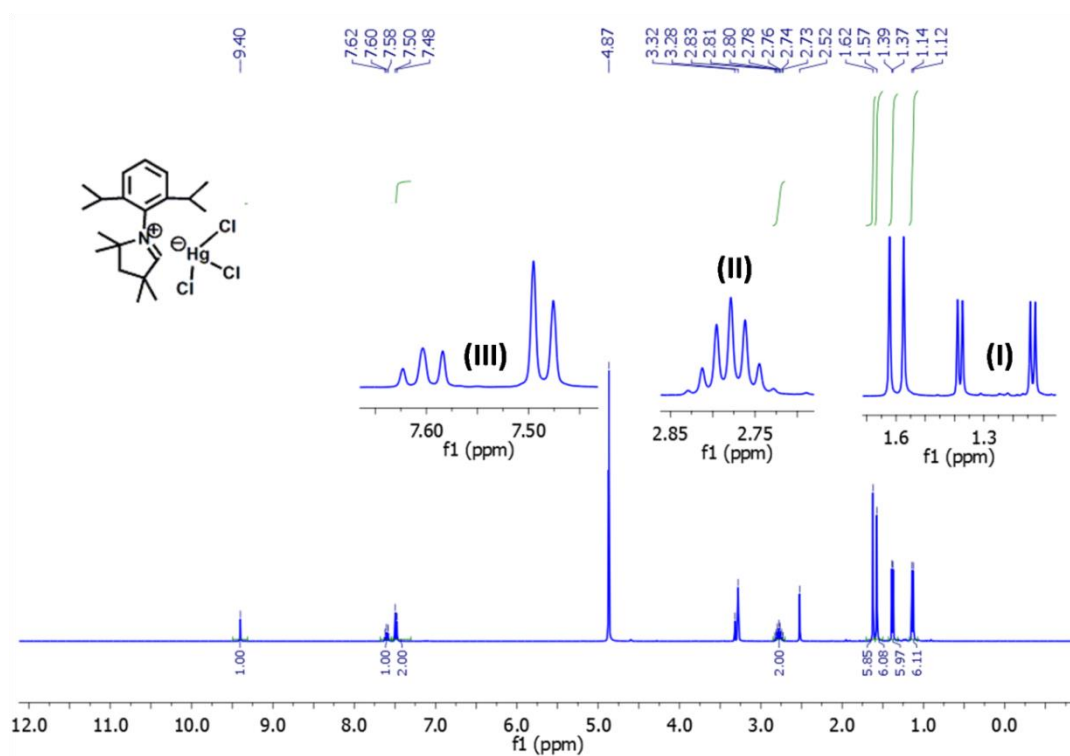
## **Supporting Information**

Heteronuclear NMR spectra ( $^1\text{H}$ ,  $^{13}\text{C}$ ), IR-spectra and HRMS spectrums of new compounds reported in this dissertation

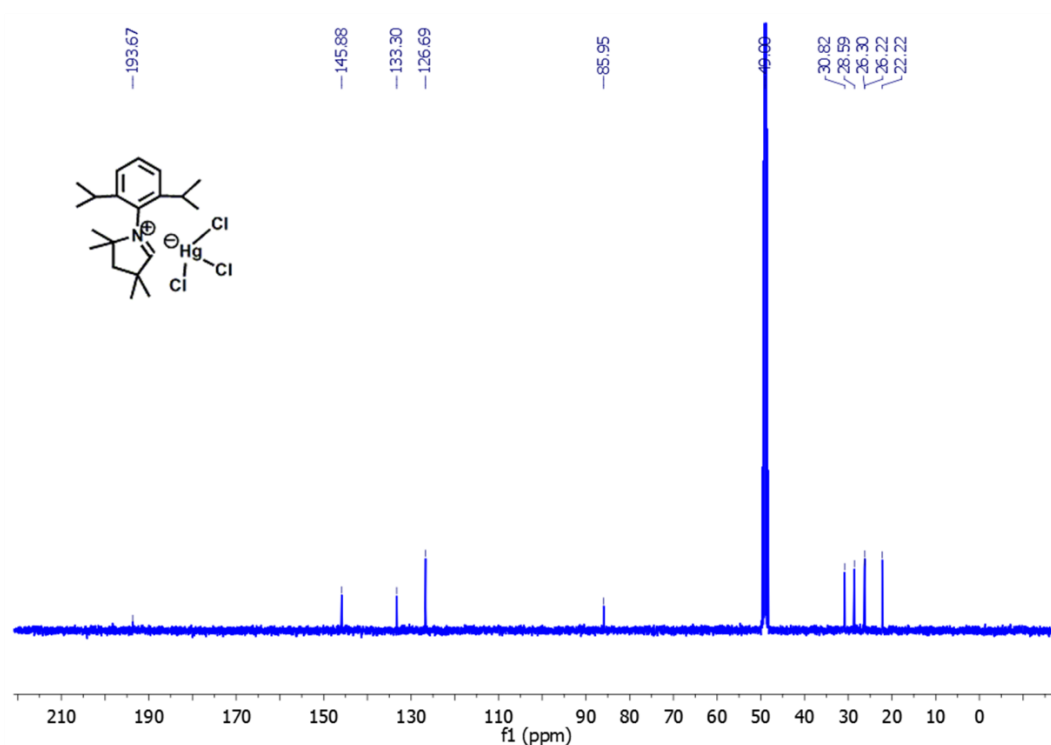
### **Contents**

<b>S1.</b>	$^1\text{H}$ NMR spectrum of $[\text{CAACH}^+][\text{HgCl}_3^-]$ ( <b>1</b> )	<b>45</b>
<b>S2.</b>	$^{13}\text{C}$ NMR spectrum of $[\text{CAACH}^+][\text{HgCl}_3^-]$ ( <b>1</b> )	<b>45</b>
<b>S3.</b>	IR spectrum of $[\text{CAACH}^+][\text{HgCl}_3^-]$ ( <b>1</b> )	<b>46</b>
<b>S4.</b>	HRMS spectrum of $[\text{CAACH}^+][\text{HgCl}_3^-]$ ( <b>1</b> )	<b>46</b>
<b>S5.</b>	$^1\text{H}$ NMR spectrum of $[\text{CAAC}\cdot\text{HgCl}(\mu\text{-Cl})_2]$ ( <b>2</b> )	<b>47</b>
<b>S6.</b>	$^{13}\text{C}$ NMR spectrum of $[\text{CAAC}\cdot\text{HgCl}(\mu\text{-Cl})_2]$ ( <b>2</b> )	<b>47</b>
<b>S7.</b>	IR spectrum of $[\text{CAAC}\cdot\text{HgCl}(\mu\text{-Cl})_2]$ ( <b>2</b> )	<b>48</b>
<b>S8.</b>	HRMS spectrum of $[\text{CAAC}\cdot\text{HgCl}(\mu\text{-Cl})_2]$ ( <b>2</b> )	<b>49</b>
<b>S9.</b>	$^1\text{H}$ NMR spectrum of $[\text{CAAC}\cdot\text{HgBr}(\mu\text{-Br})_2]$ ( <b>3</b> )	<b>49</b>
<b>S10.</b>	$^{13}\text{C}$ NMR spectrum of $[\text{CAAC}\cdot\text{HgBr}(\mu\text{-Br})_2]$ ( <b>3</b> )	<b>50</b>
<b>S11.</b>	IR spectrum of $[\text{CAAC}\cdot\text{HgBr}(\mu\text{-Br})_2]$ ( <b>3</b> )	<b>50</b>
<b>S12.</b>	HRMS spectrum of $[\text{CAAC}\cdot\text{HgBr}(\mu\text{-Br})_2]$ ( <b>3</b> )	<b>51</b>
<b>S13.</b>	$^1\text{H}$ NMR spectrum of $[\text{CAAC}\cdot\text{HgI}(\mu\text{-I})_2]$ ( <b>4</b> )	<b>51</b>
<b>S14.</b>	$^{13}\text{C}$ NMR spectrum of $[\text{CAAC}\cdot\text{HgI}(\mu\text{-I})_2]$ ( <b>4</b> )	<b>52</b>
<b>S15.</b>	IR spectrum of $[\text{CAAC}\cdot\text{HgI}(\mu\text{-I})_2]$ ( <b>4</b> )	<b>52</b>
<b>S16.</b>	HRMS spectrum of $[\text{CAAC}\cdot\text{HgI}(\mu\text{-I})_2]$ ( <b>4</b> )	<b>53</b>
<b>S17.</b>	$^1\text{H}$ NMR spectrum of $[(\text{CAAC}^{\text{cy}})_2\text{Hg}(\text{H}_2\text{O})]^{2+}2[\text{NO}_3]^-$ ( <b>5</b> )	<b>54</b>
<b>S18.</b>	$^{13}\text{C}$ NMR spectrum of $[(\text{CAAC}^{\text{cy}})_2\text{Hg}(\text{H}_2\text{O})]^{2+}2[\text{NO}_3]^-$ ( <b>5</b> )	<b>54</b>
<b>S19.</b>	IR spectrum of $[(\text{CAAC}^{\text{cy}})_2\text{Hg}(\text{H}_2\text{O})]^{2+}2[\text{NO}_3]^-$ ( <b>5</b> )	<b>55</b>
<b>S20.</b>	HRMS spectrum of $[(\text{CAAC}^{\text{cy}})_2\text{Hg}(\text{H}_2\text{O})]^{2+}2[\text{NO}_3]^-$ ( <b>5</b> )	<b>55</b>
<b>S21.</b>	$^1\text{H}$ NMR spectrum of $[(\text{CAAC}^{\text{cy}})_2\text{Hg}]^{2+}[\text{Hg}_2\text{Br}_6]^{2-}$ ( <b>6</b> )	<b>56</b>
<b>S22.</b>	$^{13}\text{C}$ NMR spectrum of $[(\text{CAAC}^{\text{cy}})_2\text{Hg}]^{2+}[\text{Hg}_2\text{Br}_6]^{2-}$ ( <b>6</b> )	<b>56</b>
<b>S23–S94</b>	Multinuclear NMR and HRMS spectrum of hydroamination products ( <b>7–27</b> )	

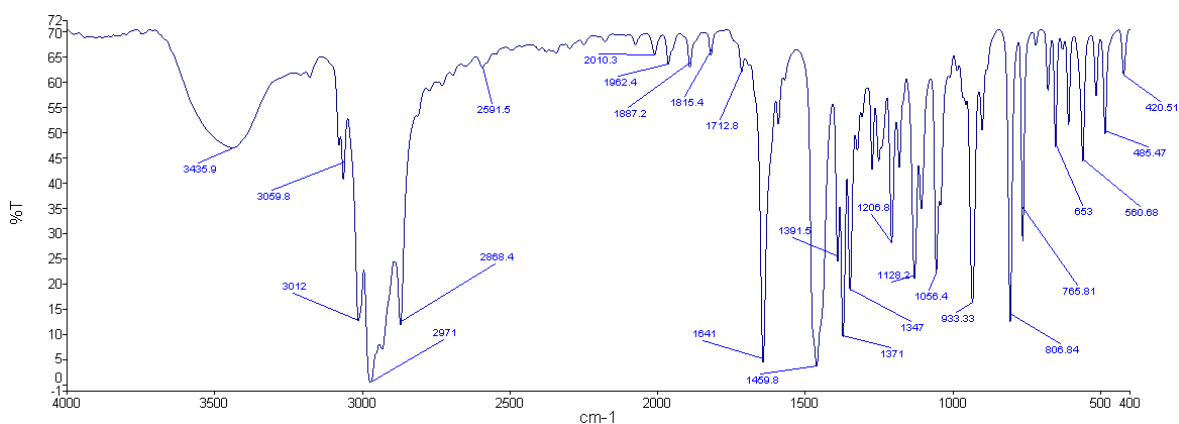
### Heteronuclear NMR spectra of [CAACH]<sup>+</sup>[HgCl<sub>3</sub>]<sup>-</sup> (1)



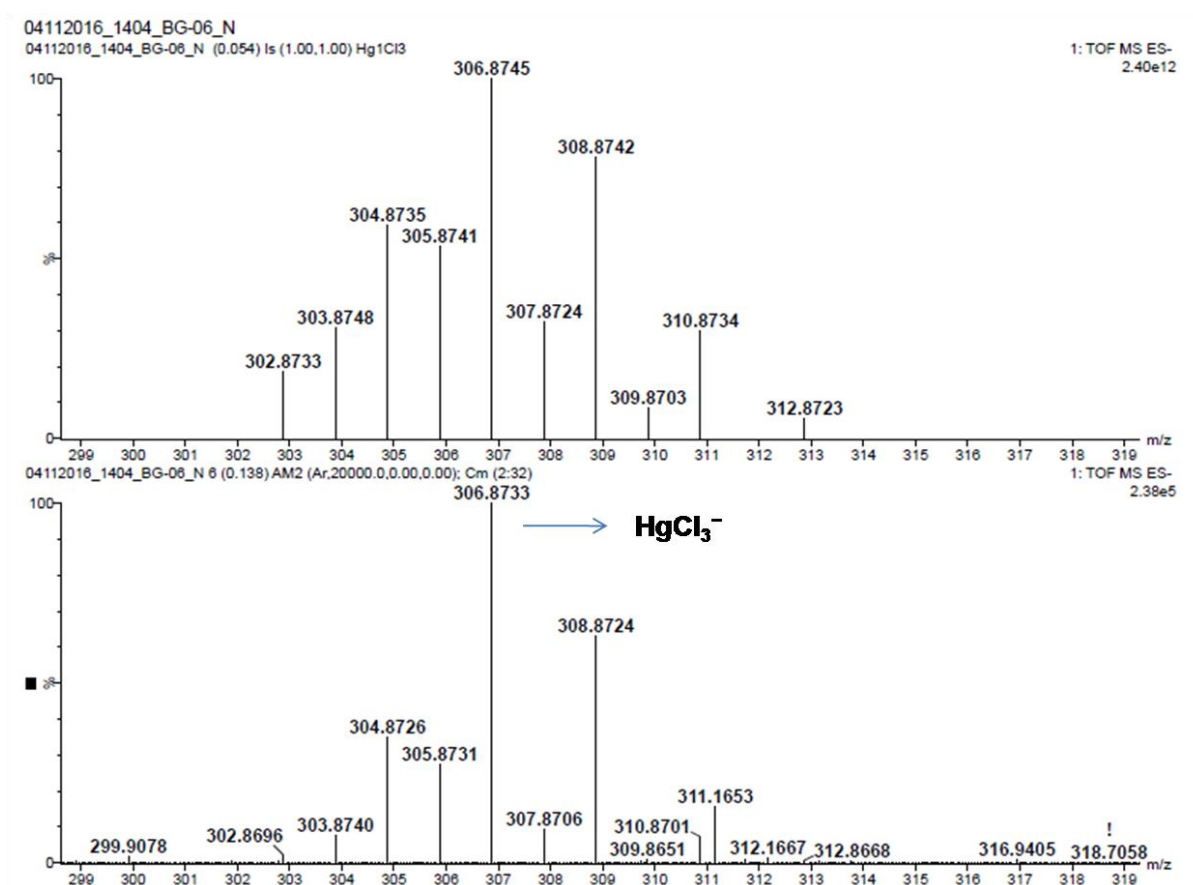
**Fig S1.** <sup>1</sup>H NMR spectrum (400 MHz, d<sub>6</sub>-DMSO) of [CAACH]<sup>+</sup>[HgCl<sub>3</sub>]<sup>-</sup> (1). Inset (I), (II) show expansion for the aliphatic region and (III) shows expansion for the selected aromatic region.



**Fig S2.** <sup>13</sup>C NMR spectrum (100 MHz, d<sub>6</sub>-DMSO) of [CAACH]<sup>+</sup>[HgCl<sub>3</sub>]<sup>-</sup> (1).

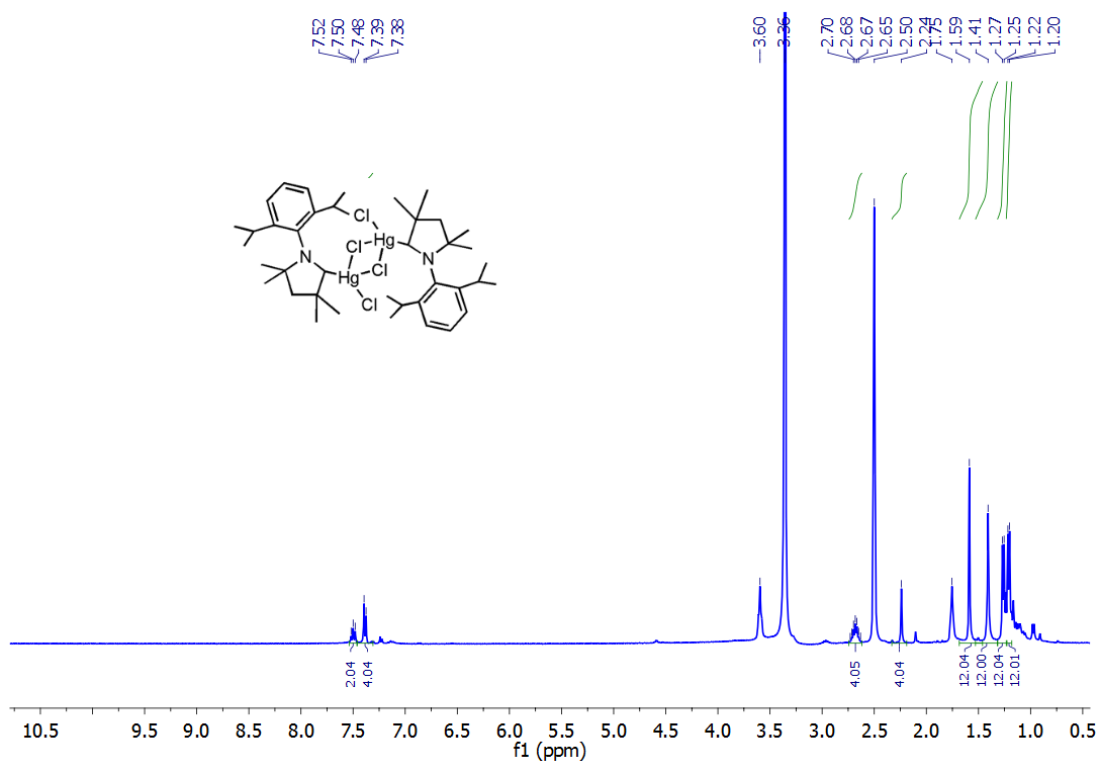


**Fig S3.** IR spectrum of [CAACH]<sup>+</sup>[HgCl<sub>3</sub>]<sup>-</sup> (1).

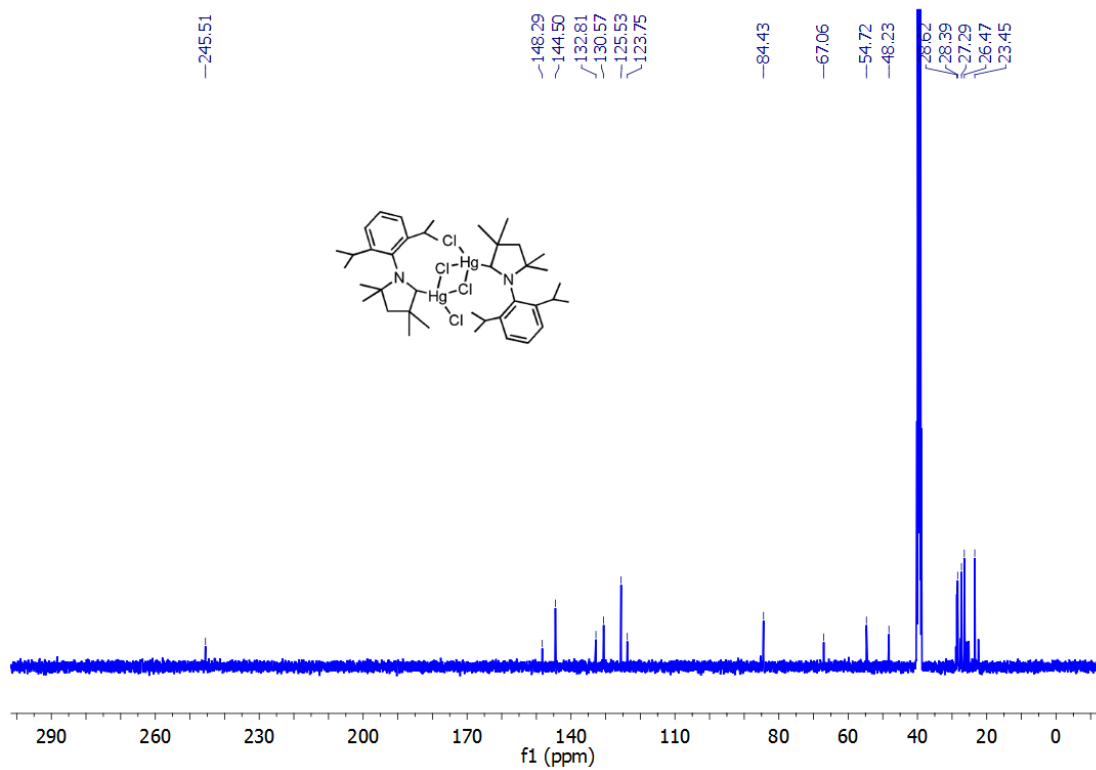


**Fig S4.** HRMS spectrum of [CAACH]<sup>+</sup>[HgCl<sub>3</sub>]<sup>-</sup> (1).

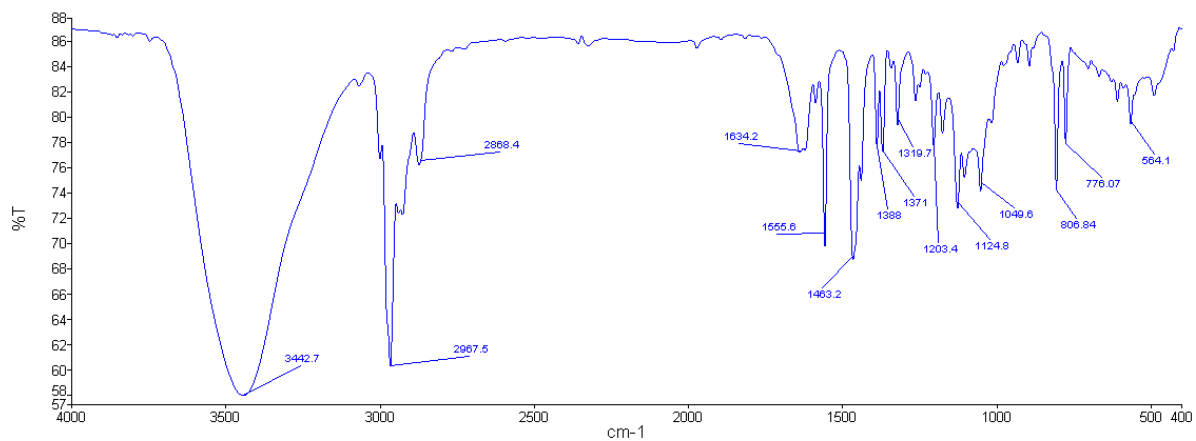
## Heteronuclear NMR spectra of [CAAC·HgCl(μ-Cl)]<sub>2</sub> (2)



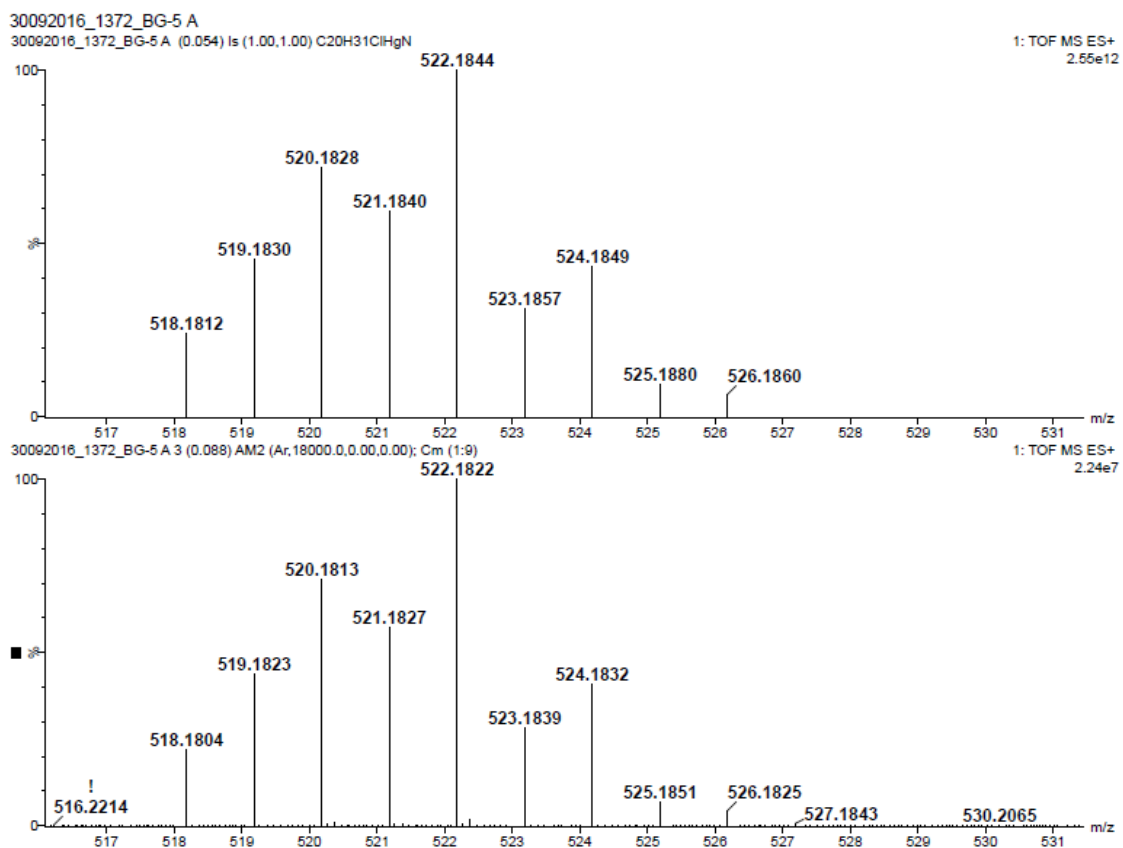
**Fig S5.** <sup>1</sup>H NMR spectrum (400 MHz, d<sub>6</sub>-DMSO) of [CAAC·HgCl(μ-Cl)]<sub>2</sub> (2).



**Fig S6.** <sup>13</sup>C NMR spectrum (100 MHz, d<sub>6</sub>-DMSO) of [CAAC·HgCl(μ-Cl)]<sub>2</sub> (2).



**Fig S7.** IR spectrum of  $[\text{CAAC} \cdot \text{HgCl}(\mu\text{-Cl})]_2$  (**2**).





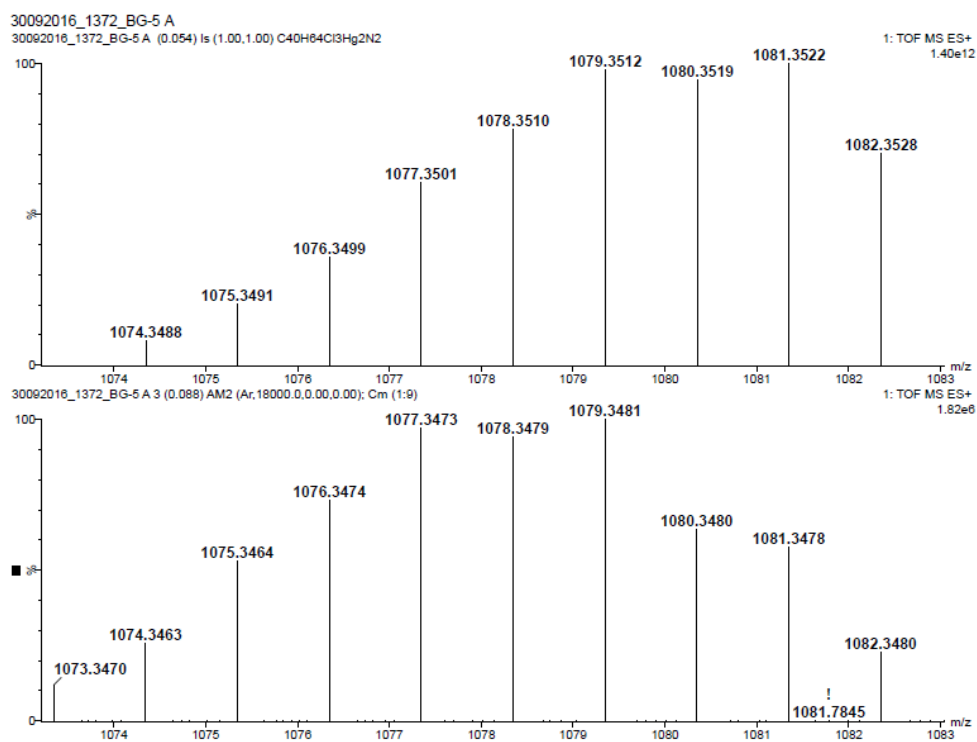


**Fig S8.** HRMS spectrum of  $[\text{CAAC} \cdot \text{HgCl}(\mu\text{-Cl})]_2$  (**2**).

**Heteronuclear NMR spectra of  $[\text{CAAC} \cdot \text{HgBr}(\mu\text{-Br})]_2$  (**3**)**

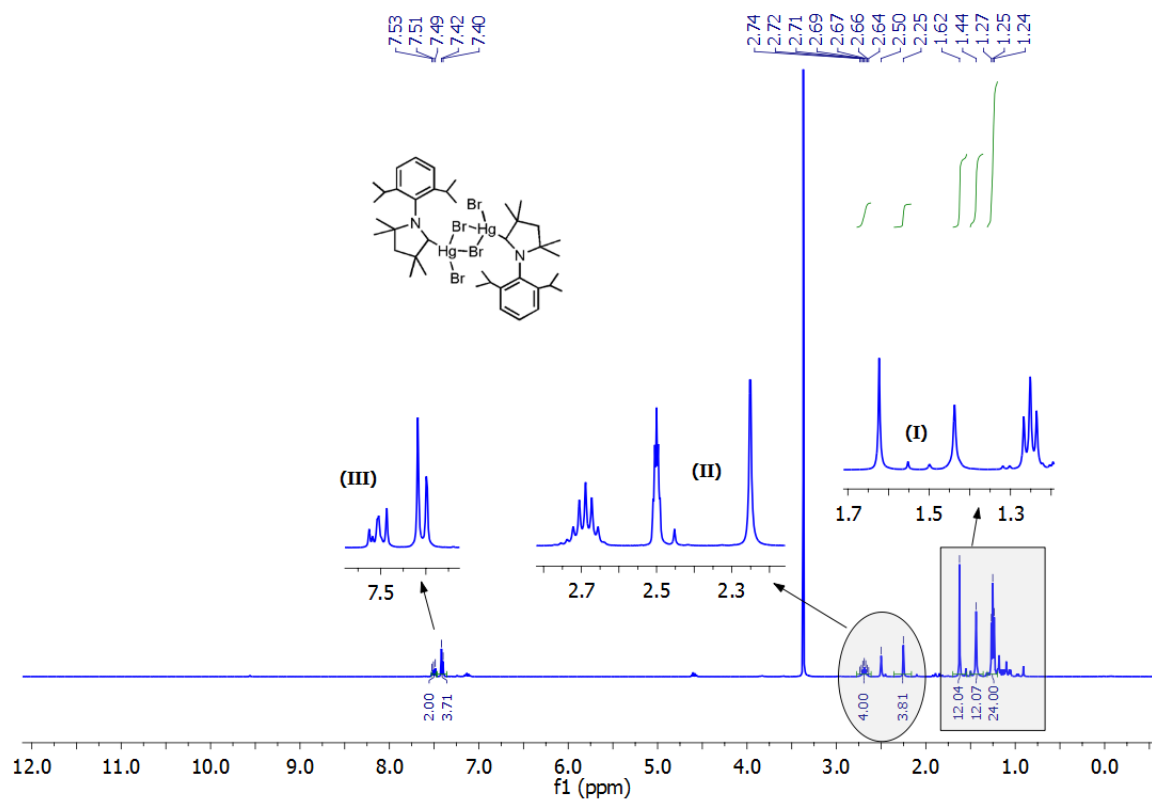


**Fig S9.**  $^1\text{H}$  NMR spectrum (400 MHz,  $\text{d}_6\text{-DMSO}$ ) of  $[\text{CAAC} \cdot \text{HgBr}(\mu\text{-Br})]_2$  (**3**).

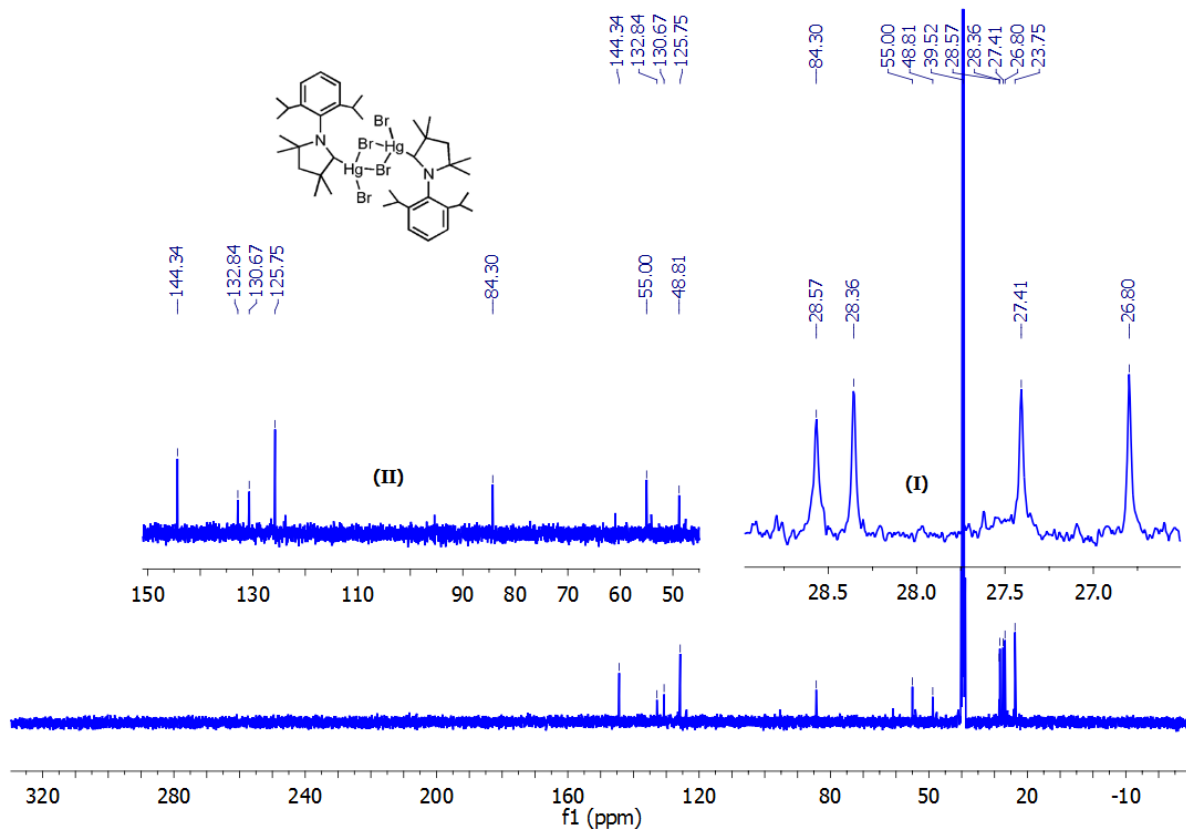


**Fig S10.**  $^{13}\text{C}$  NMR spectrum (100 MHz,  $d_6$ -DMSO) of  $[\text{CAAC} \cdot \text{HgBr}(\mu\text{-Br})]_2$  (3).

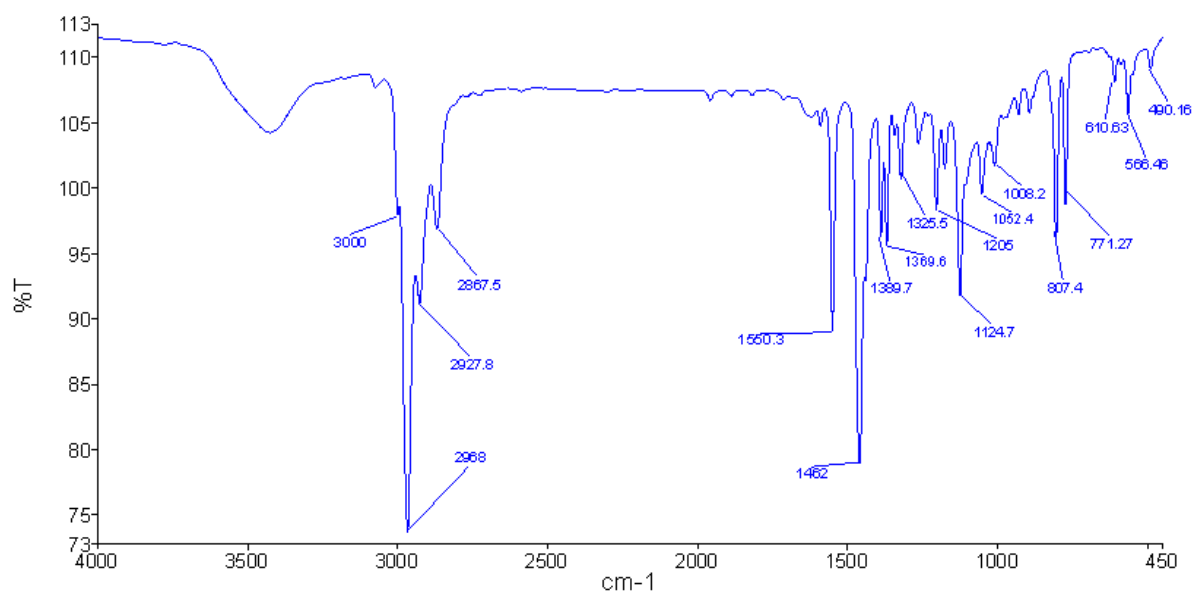
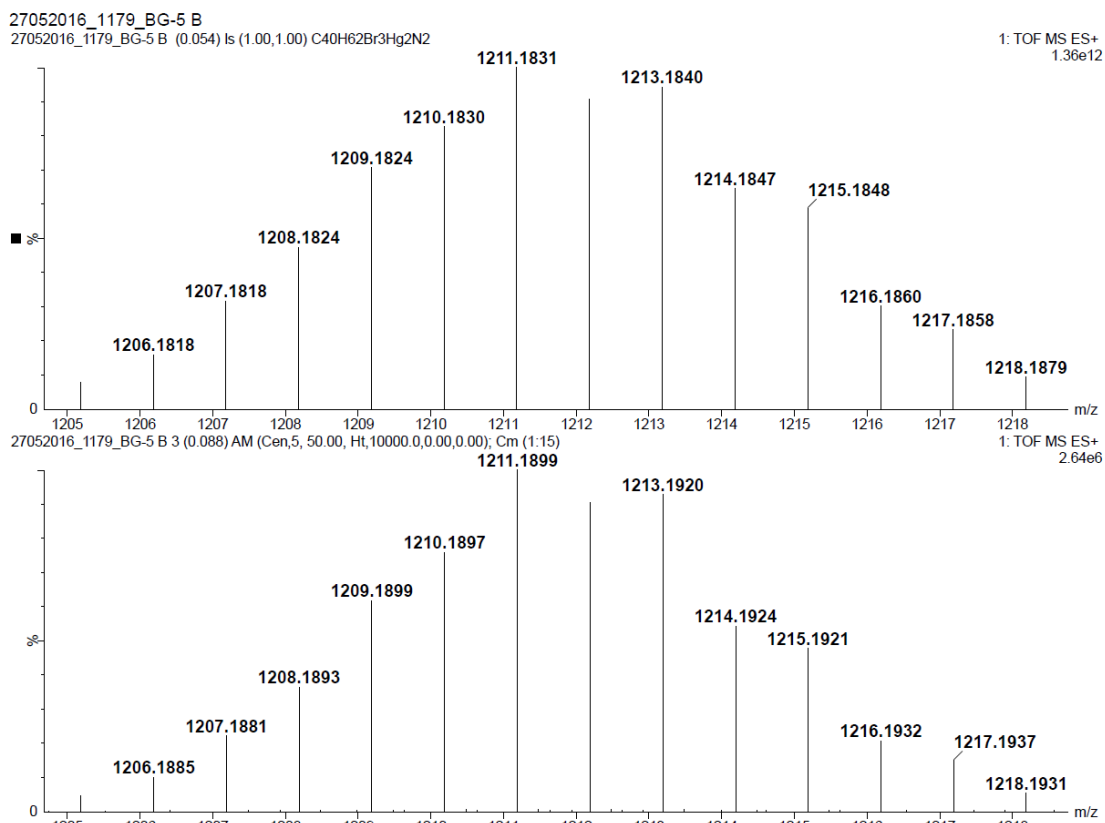


**Fig S11.** IR spectrum of  $[\text{CAAC} \cdot \text{HgBr}(\mu\text{-Br})]_2$  (3).



**Fig**

**Fig S12.** HRMS spectrum of  $[\text{CAAC}\cdot\text{HgBr}(\mu\text{-Br})]_2$  (**3**).

**Heteronuclear NMR spectra of  $[\text{CAAC}\cdot\text{HgI}(\mu\text{-I})]_2$  (**4**)**

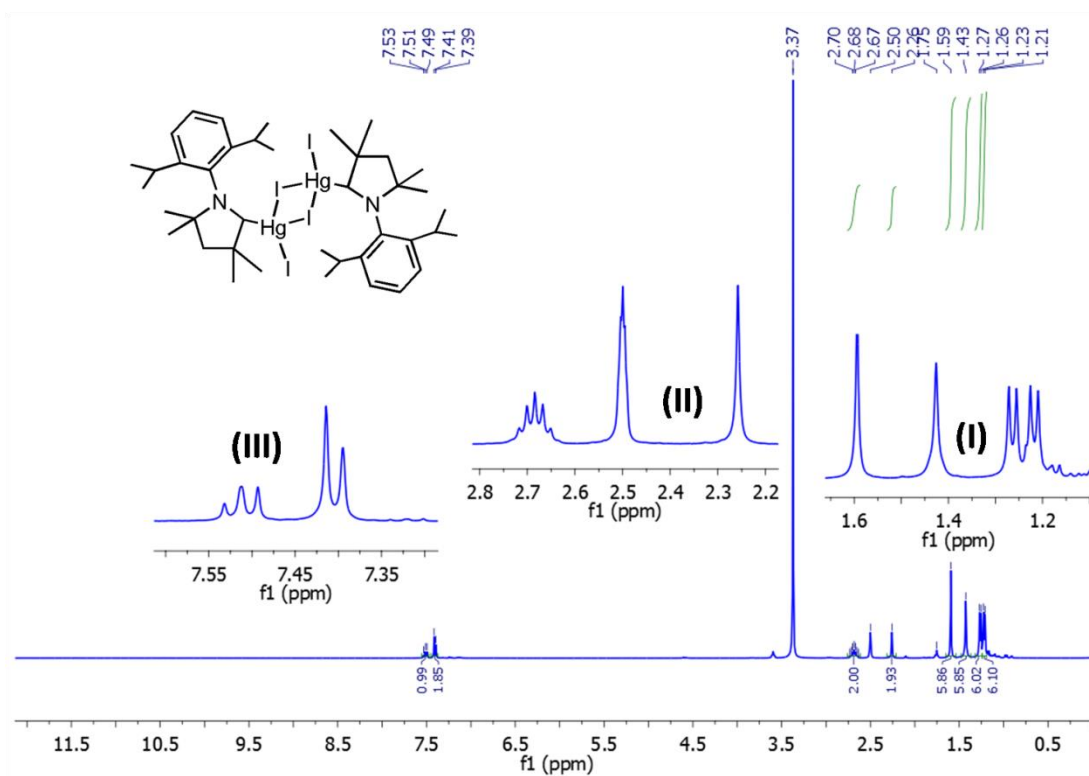


**Fig S13.**  $^1\text{H}$  NMR spectrum (400 MHz,  $d_6$ -DMSO) of  $[\text{CAAC}\cdot\text{HgI}(\mu\text{-I})]_2$  (**4**).

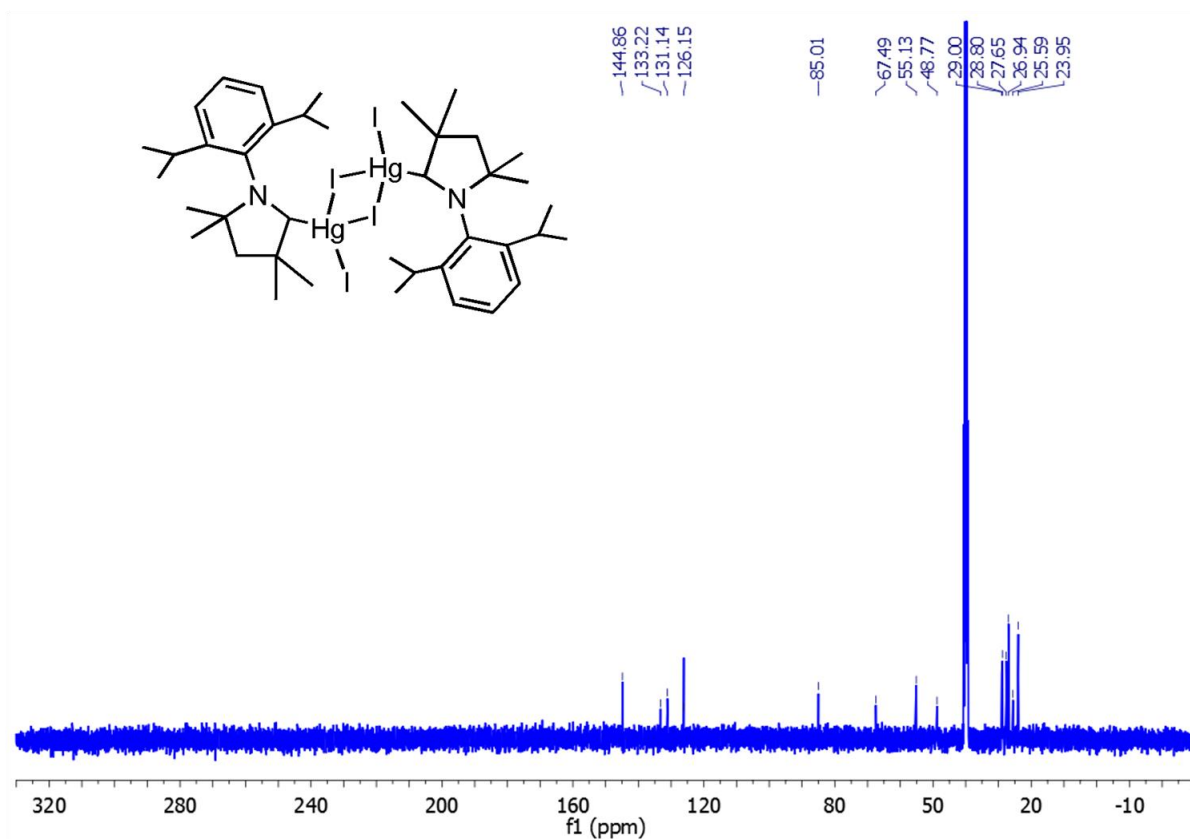


**Fig S14.**  $^{13}\text{C}$  NMR spectrum (100 MHz,  $\text{d}_6\text{-DMSO}$ ) of  $[\text{CAAC} \cdot \text{HgI}(\mu\text{-I})]_2$  (4).

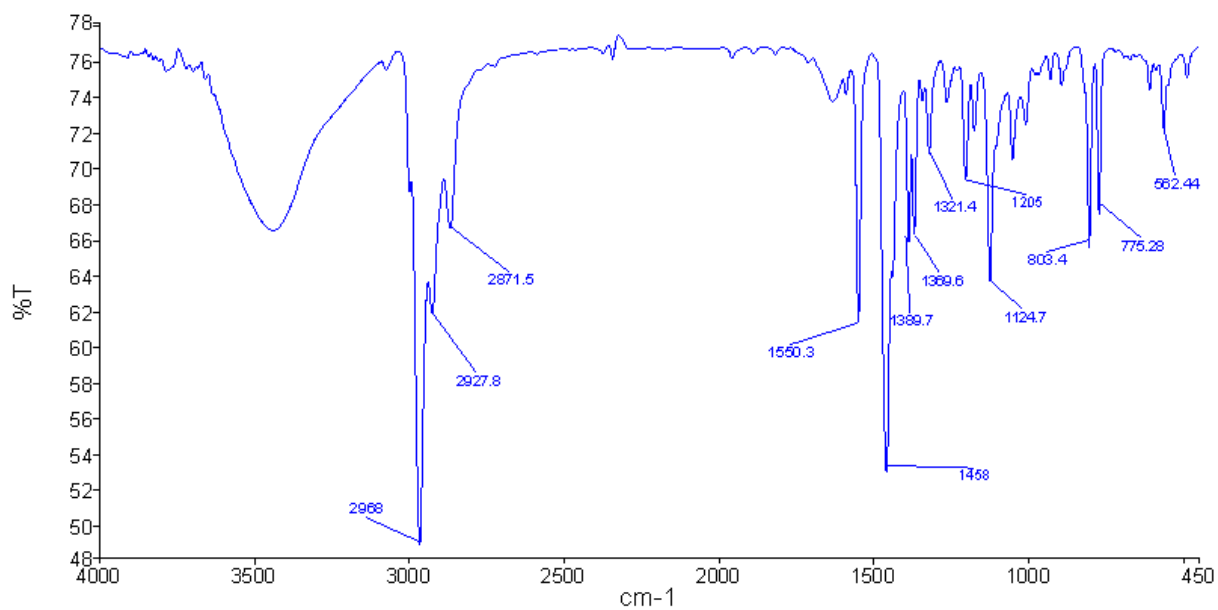


**Fig S15.** IR spectrum of  $[\text{CAAC} \cdot \text{HgI}(\mu\text{-I})]_2$  (4).

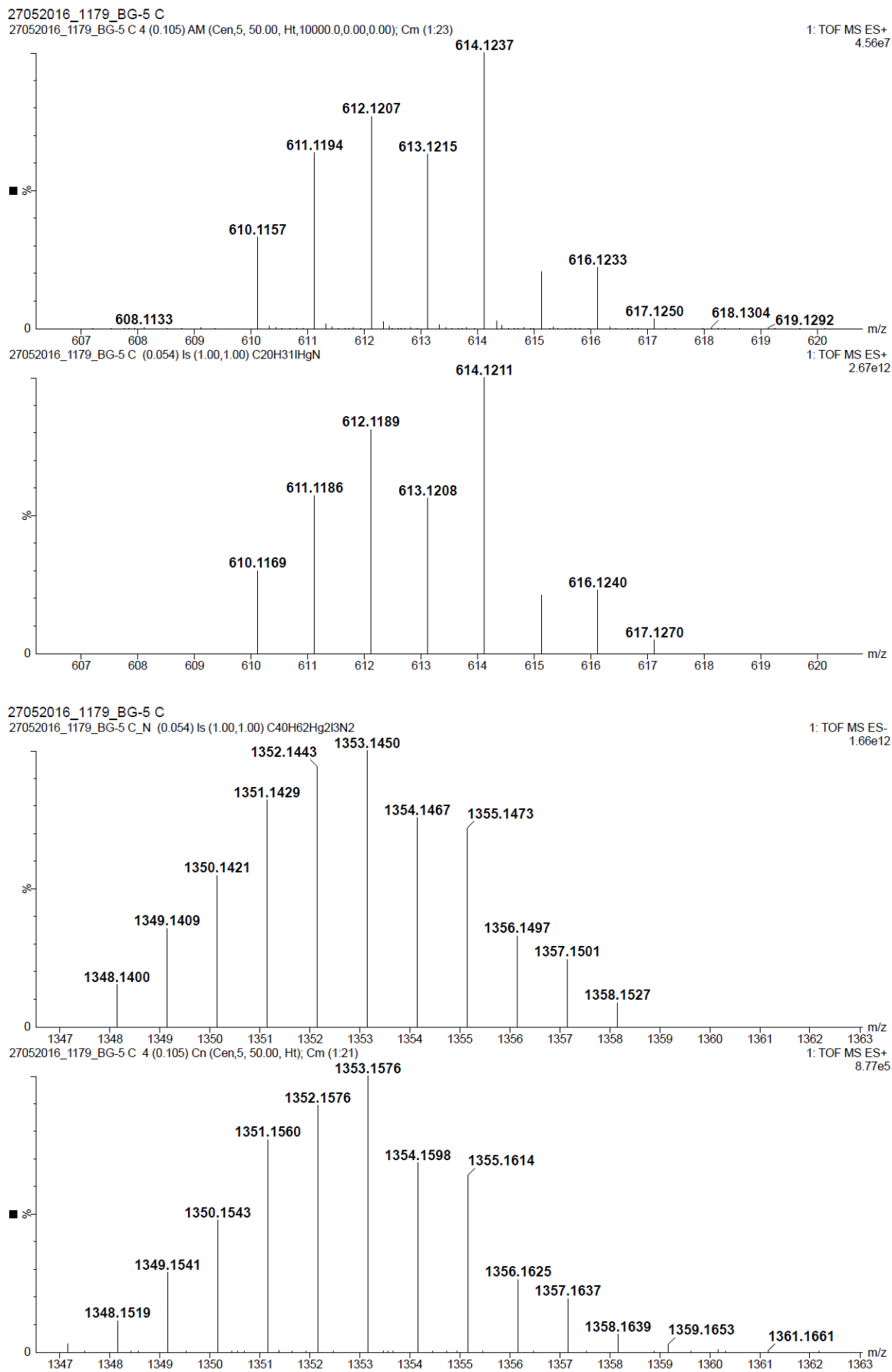


**Fig S16.** HRMS spectrum of  $[\text{CAAC} \cdot \text{HgI}(\mu\text{-I})_2]$  (**4**).

**Heteronuclear NMR spectra of  $[(\text{CAAC})_2\text{Hg}(\text{H}_2\text{O})]^{2+}2[\text{NO}_3]^-$  (5)**

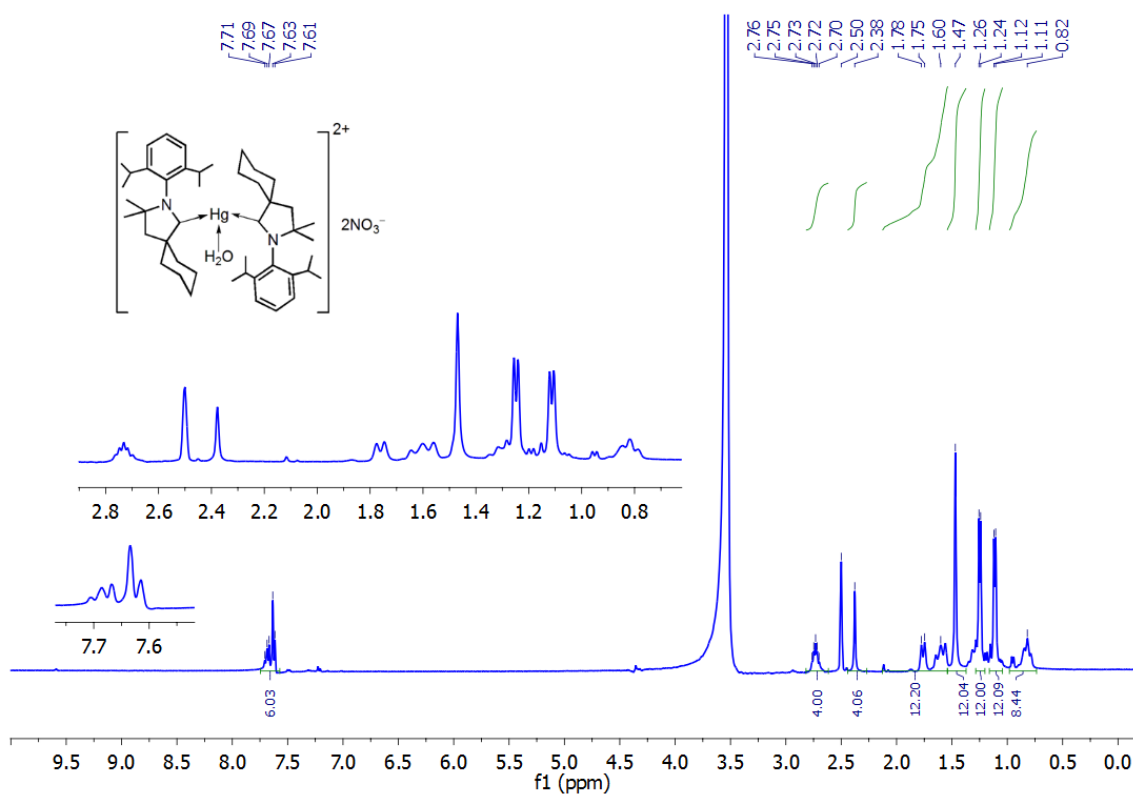


**Fig S17.**  $^1\text{H}$  NMR spectrum (400 MHz,  $d_6$ -DMSO) of  $[(\text{CAAC})_2\text{Hg}(\text{H}_2\text{O})]^{2+}2[\text{NO}_3]^-$  (5). Insets show expansion for the aliphatic and aromatic regions.

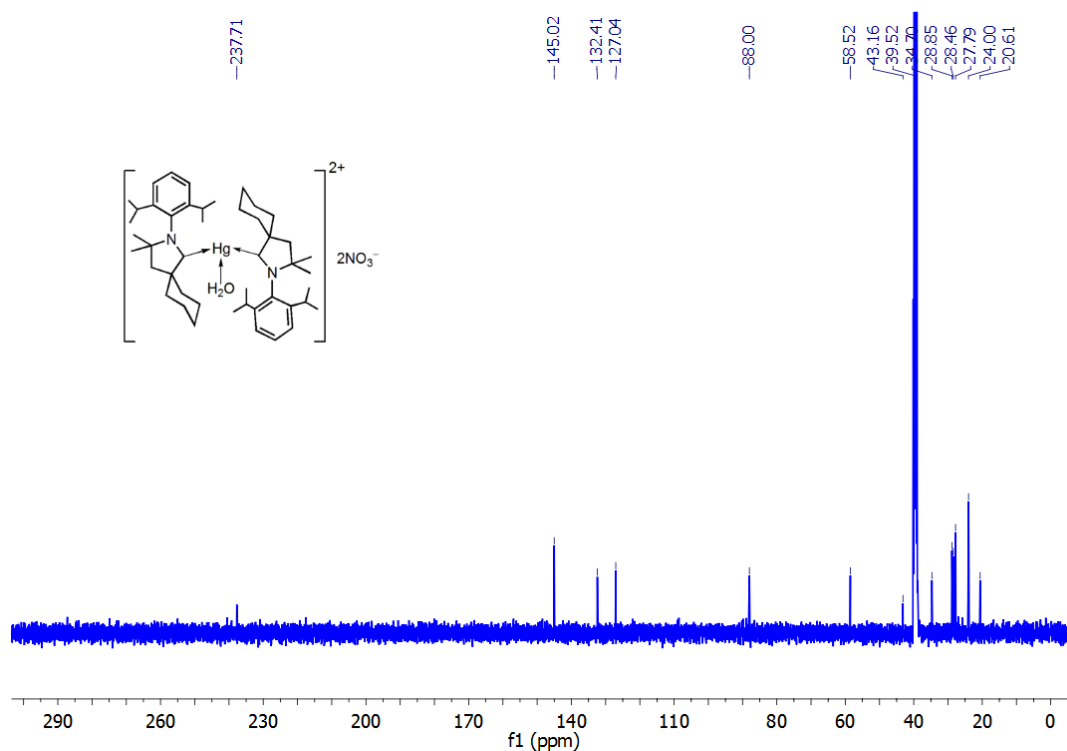


**Fig S18.**  $^{13}\text{C}$  NMR spectrum (100 MHz,  $d_6$ -DMSO) of  $[(\text{CAAC})_2\text{Hg}(\text{H}_2\text{O})]^{2+}2[\text{NO}_3]^-$  (5).

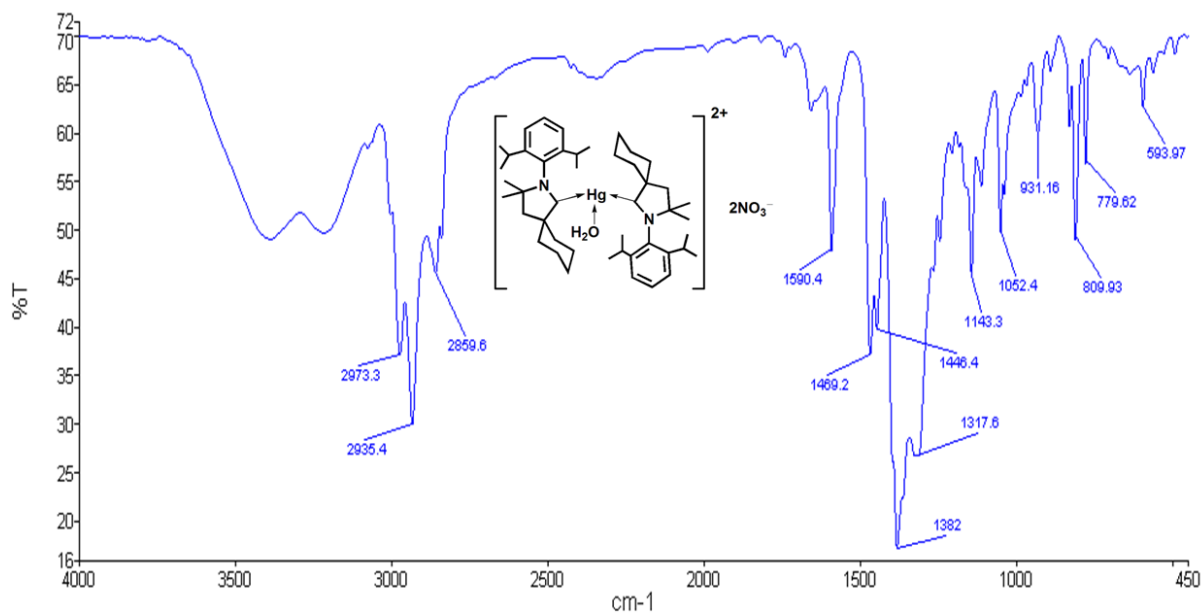


**Fig S19.** IR spectrum of  $[(\text{CAAC})_2\text{Hg}(\text{H}_2\text{O})]^{2+} 2[\text{NO}_3]^-$  (**5**).

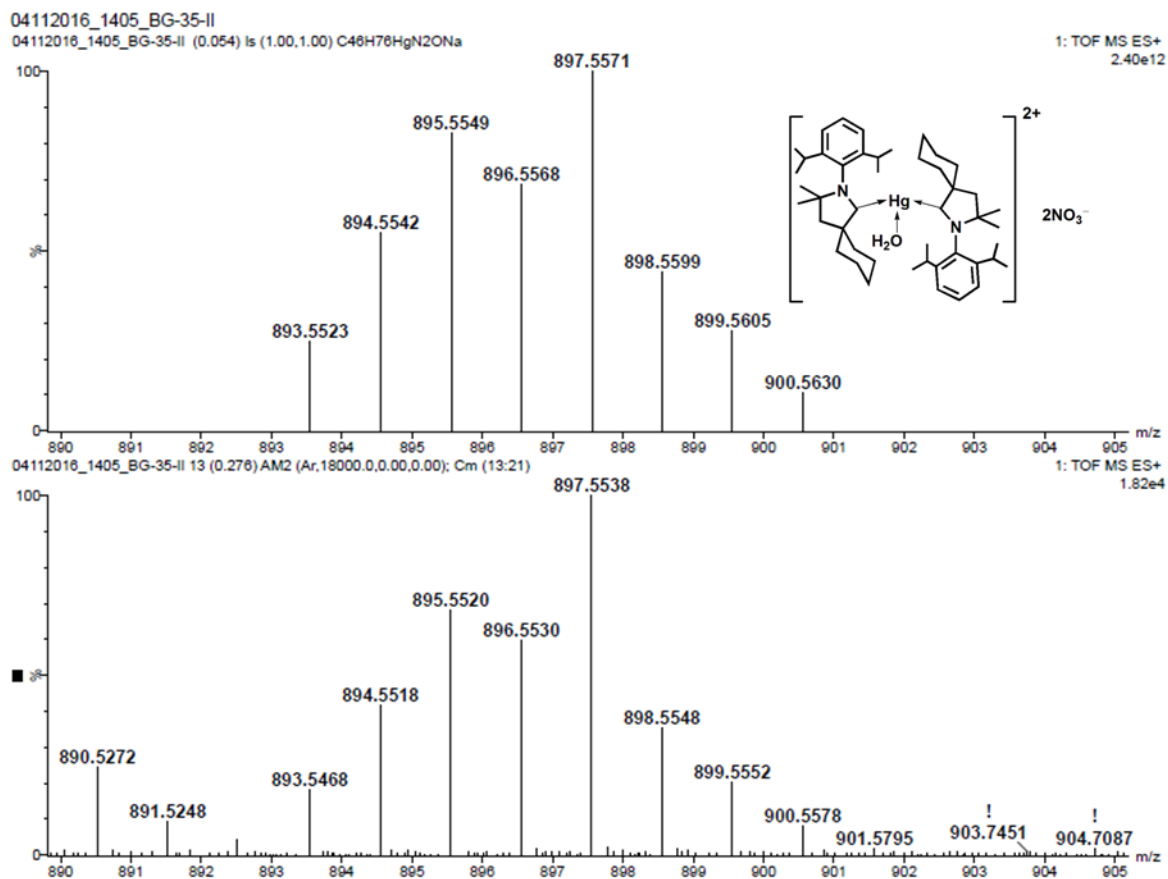


**Fig S20.** HRMS spectrum of  $[(\text{CAAC})_2\text{Hg}(\text{H}_2\text{O})]^{2+} 2[\text{NO}_3]^-$  (**5**).

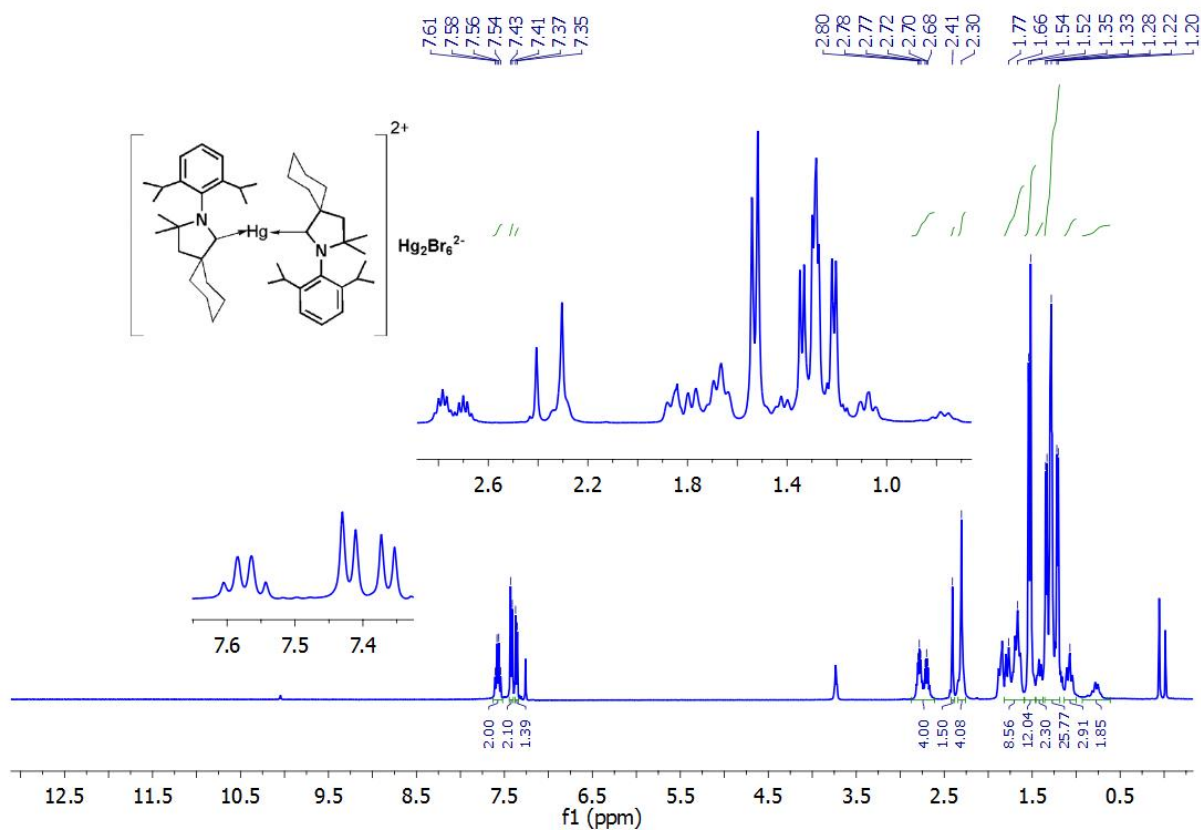


**Fig S21.**  $^1\text{H}$  NMR spectrum (400 MHz,  $d_6$ -DMSO) of  $[(\text{CAAC}^{\text{cy}})_2\text{Hg}]^{2+}[\text{Hg}_2\text{Br}_6]^{2-}$  (6).

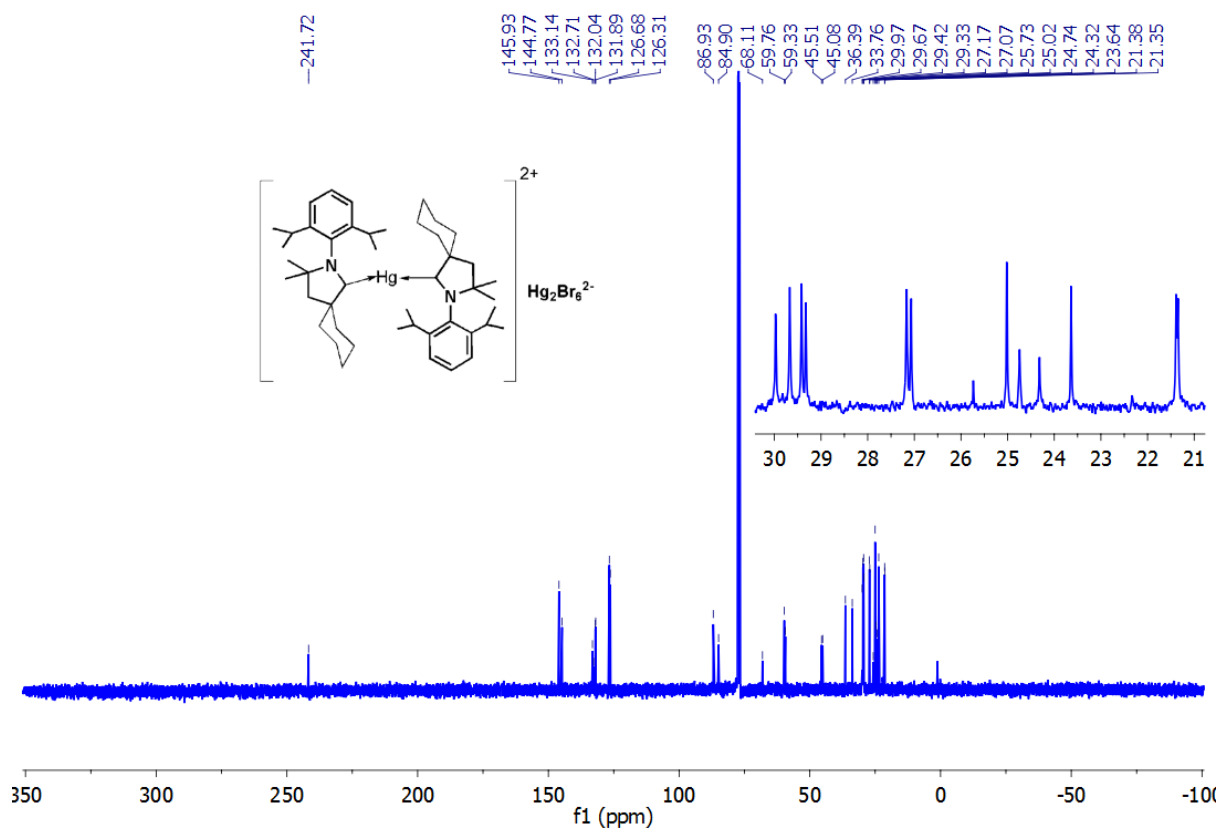


**Fig S22.**  $^{13}\text{C}$  NMR spectrum (100 MHz,  $d_6$ -DMSO) of  $[(\text{CAAC}^{\text{cy}})_2\text{Hg}]^{2+}[\text{Hg}_2\text{Br}_6]^{2-}$  (6).



**NMR and HRMS spectra of hydroamination products:**

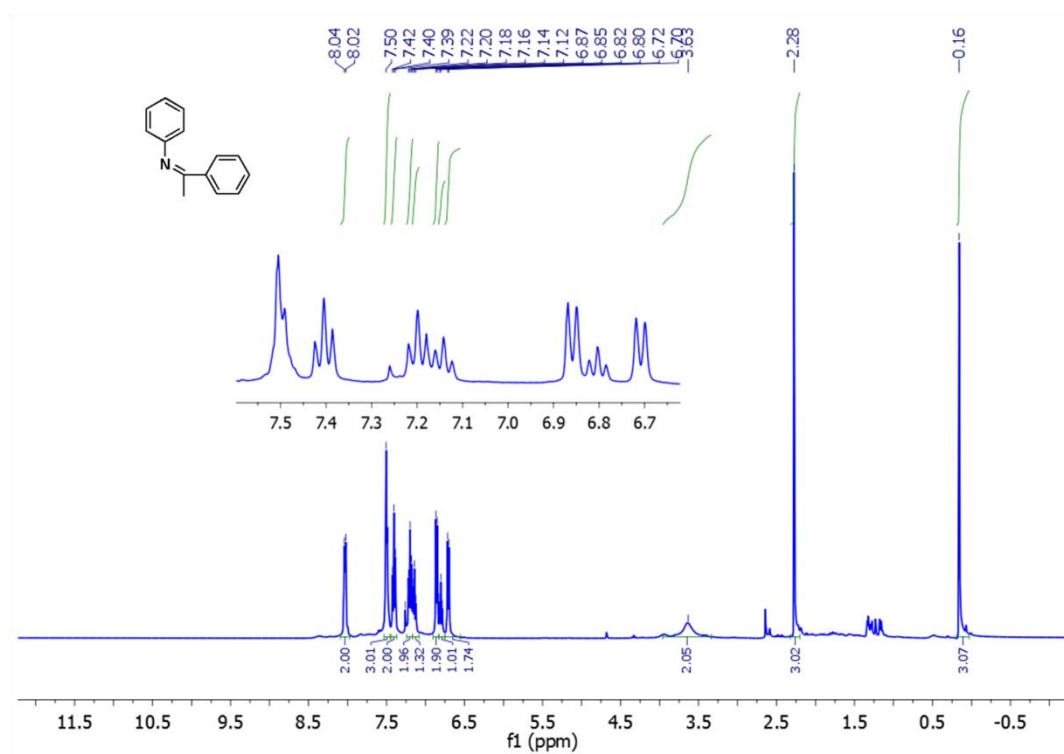


**Fig S23.** <sup>1</sup>H NMR spectrum (400 MHz, CDCl<sub>3</sub>) of *N*-(1-phenylethylidene)aniline (**7**).

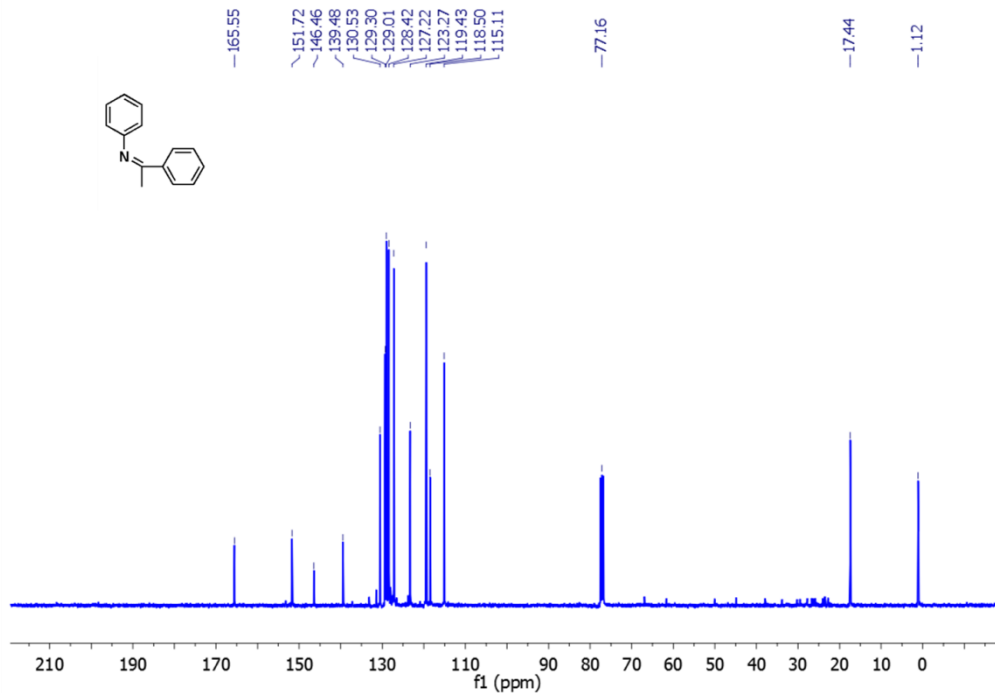


**Fig S24.** <sup>13</sup>C NMR spectrum (100 MHz, CDCl<sub>3</sub>) of *N*-(1-phenylethylidene)aniline (**7**).

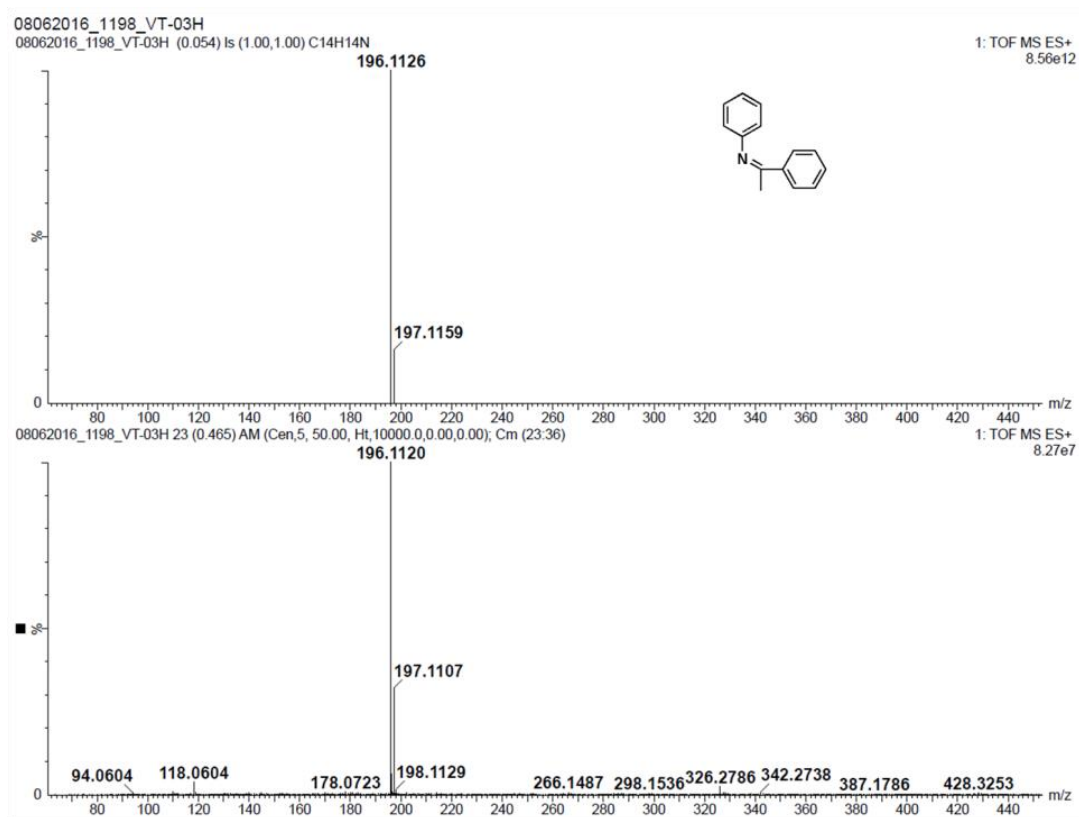


**Fig S25.** HRMS spectrum of *N*-(1-phenylethylidene)aniline (**7**).

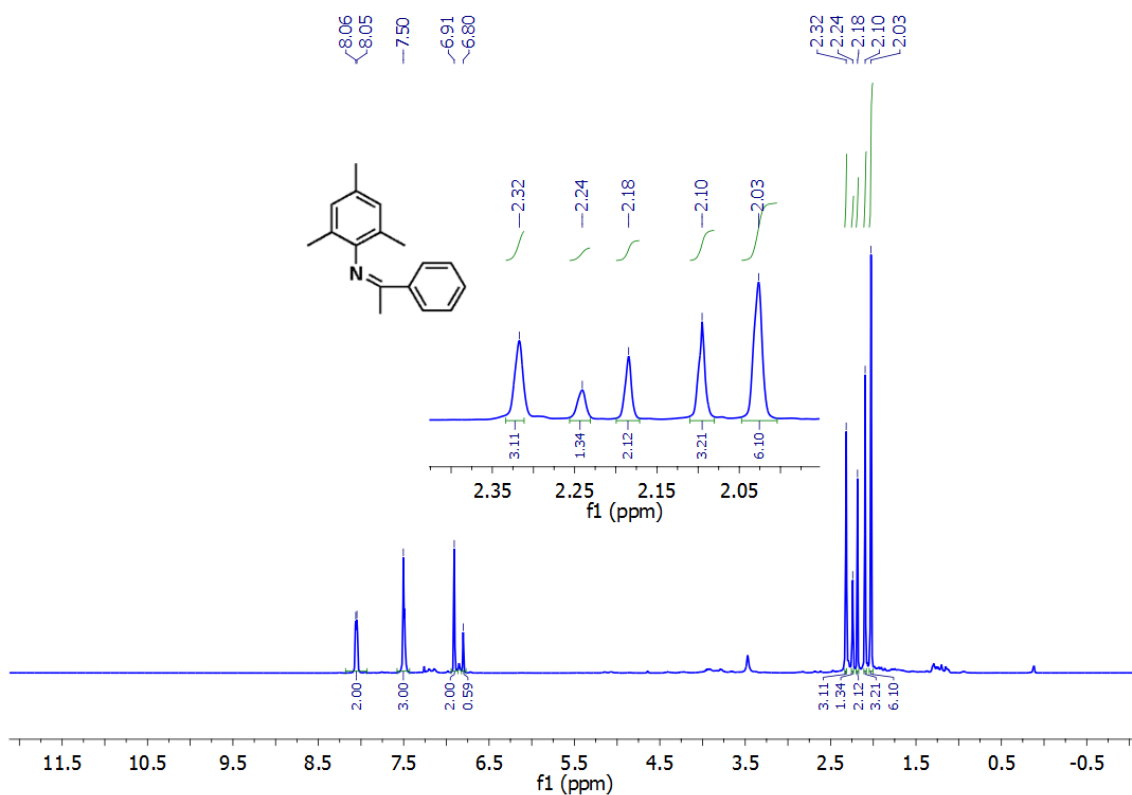


**Fig S26.**  $^1\text{H}$  NMR spectrum (400 MHz,  $\text{CDCl}_3$ ) of *N*-(1-phenylethylidene)-2,4,6-trimethylaniline (**8**).

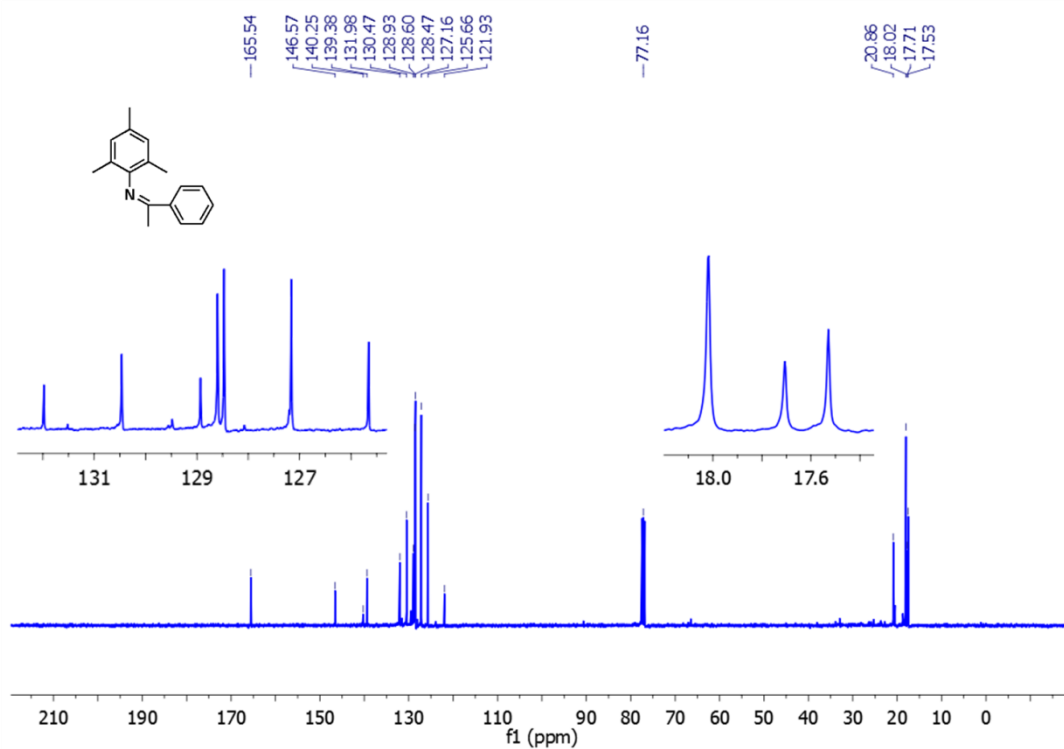


**Fig S27.** <sup>13</sup>C NMR spectrum (100 MHz, CDCl<sub>3</sub>) of *N*-(1-phenylethylidene)-2,4,6-trimethylaniline (**8**).

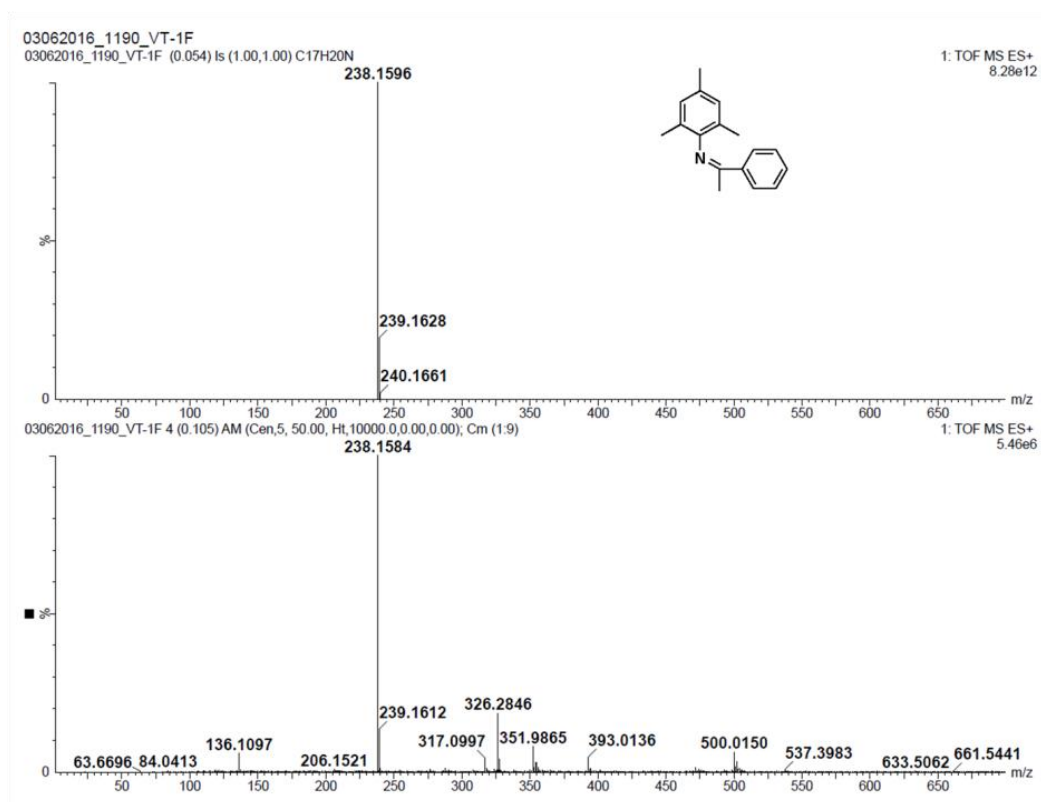


**Fig S28.** HRMS spectrum of *N*-(1-phenylethylidene)-2,4,6-trimethylaniline (**8**).

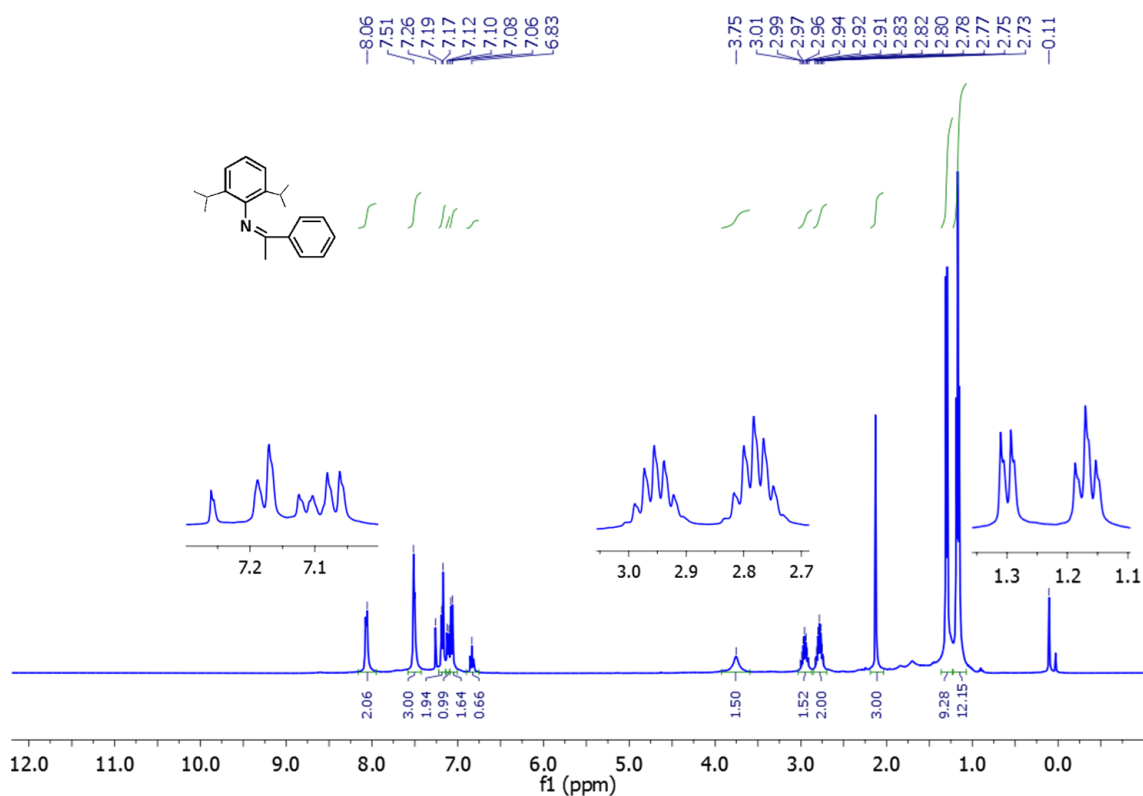


**Fig S29.** <sup>1</sup>H NMR spectrum (400 MHz, CDCl<sub>3</sub>) of *N*-(1-phenylethylidene)-2,6-diisopropylaniline (**9**).

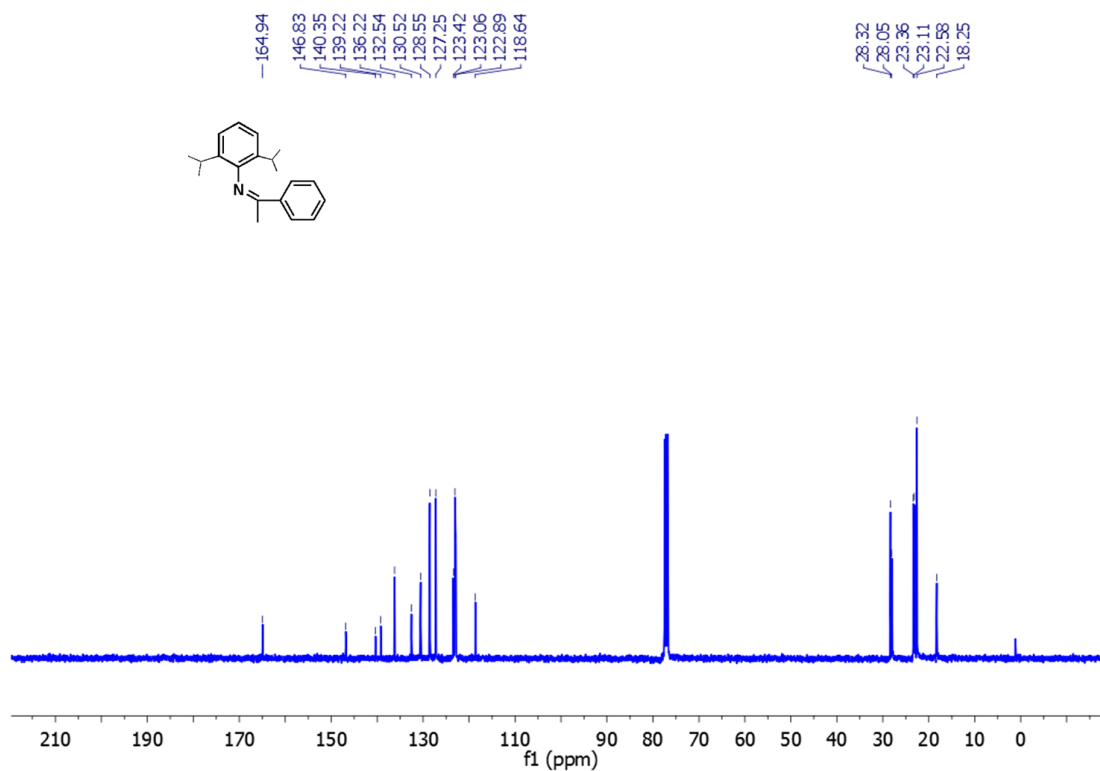


**Fig S30.** <sup>13</sup>C NMR spectrum (100 MHz, CDCl<sub>3</sub>) of *N*-(1-phenylethylidene)-2,6-diisopropylaniline (**9**).

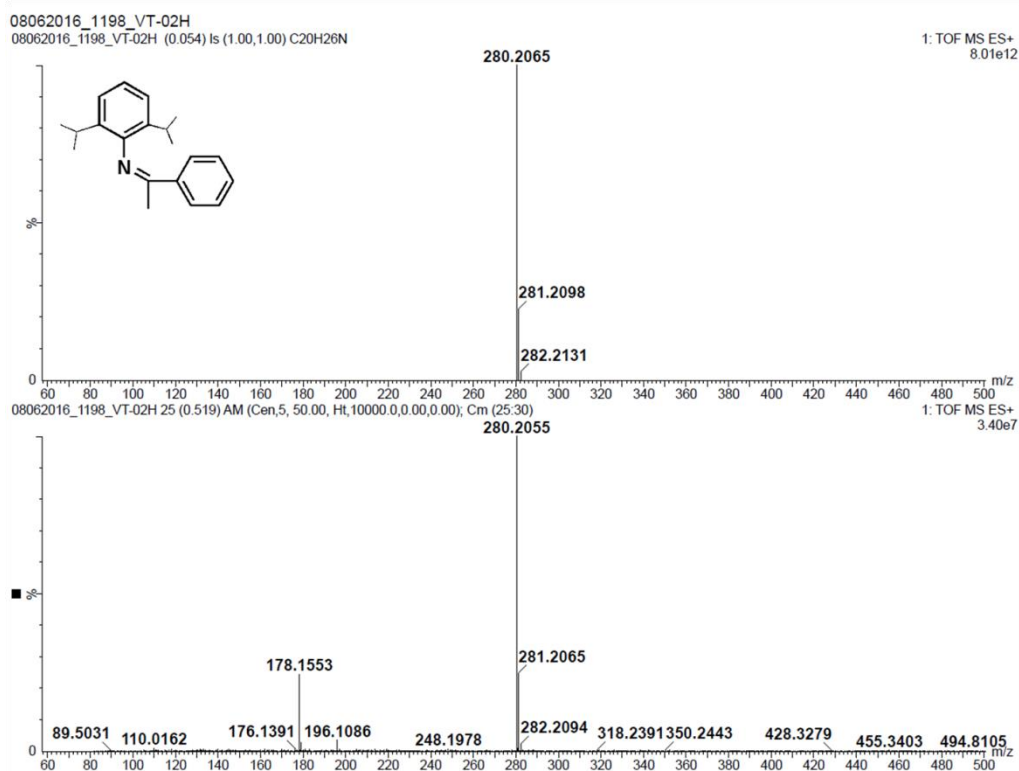


**Fig S31.** HRMS spectrum of *N*-(1-phenylethylidene)-2,6-diisopropylaniline (**9**).

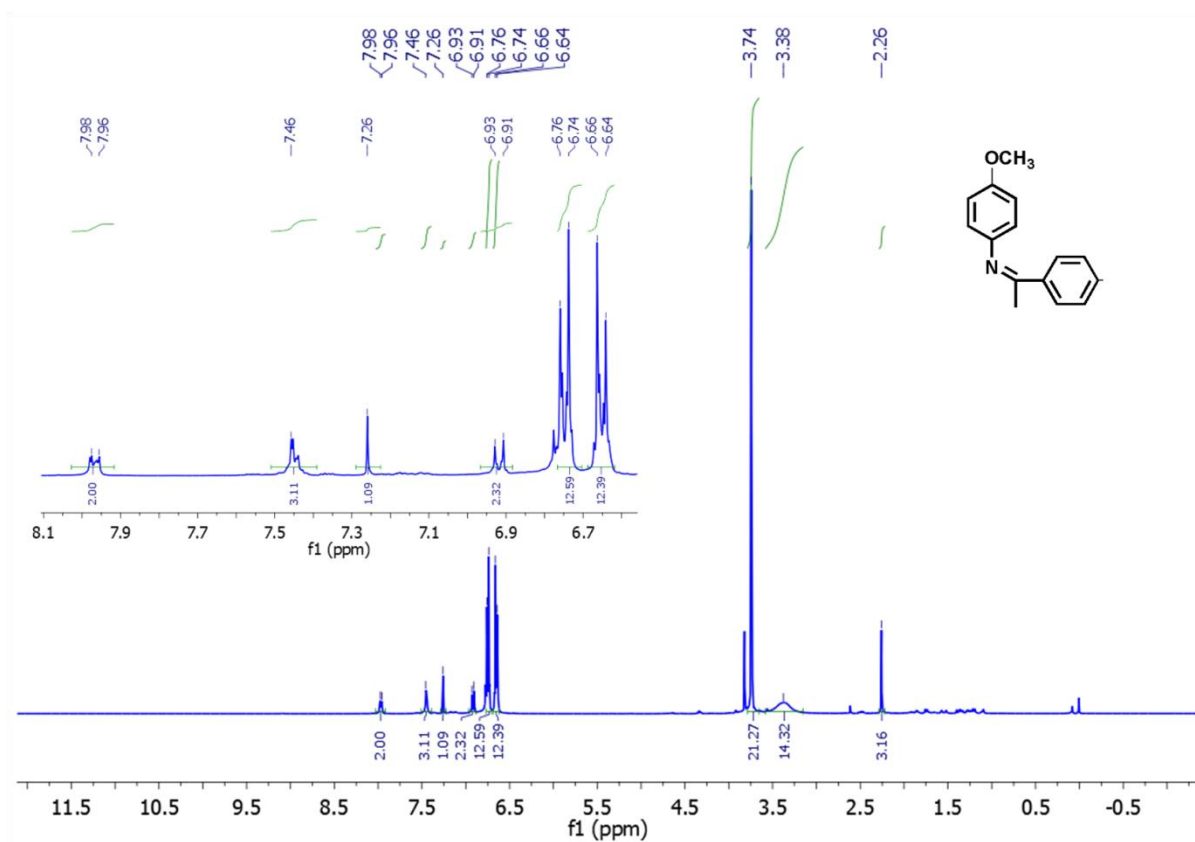


**Fig S32.** <sup>1</sup>H NMR spectrum (400 MHz, CDCl<sub>3</sub>) of *N*-(1-phenylethylidene)-*p*-methoxyaniline (**10**).

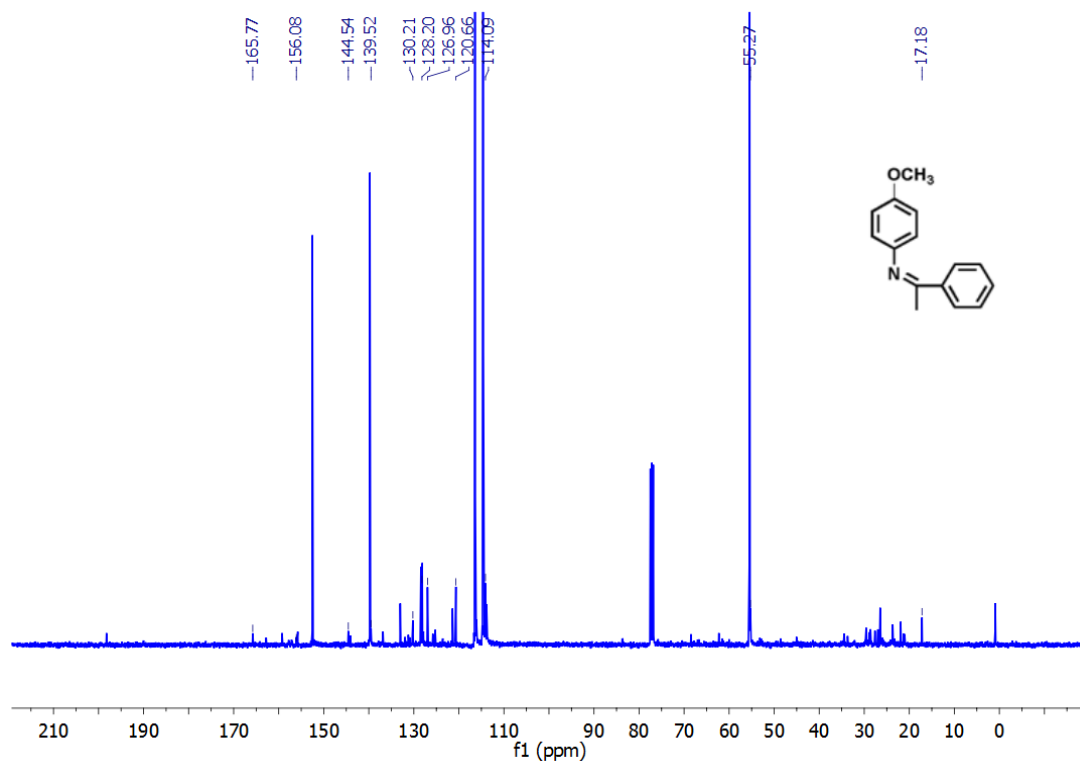


**Fig S33.**  $^{13}\text{C}$  NMR spectrum (100 MHz,  $\text{CDCl}_3$ ) of *N*-(1-phenylethylidene)-*p*-methoxyaniline (**10**).

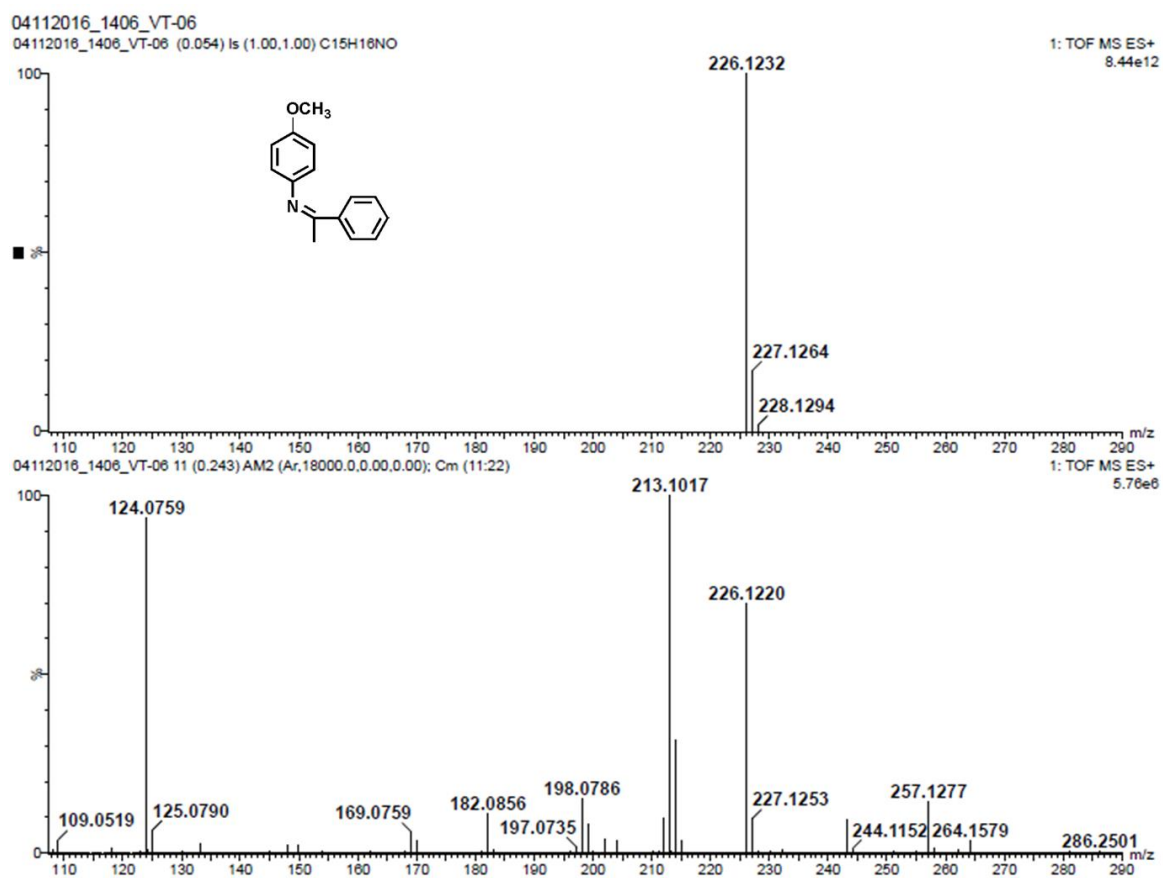


**Fig S34.** HRMS spectrum of *N*-(1-phenylethylidene)-*p*-methoxyaniline (**10**).

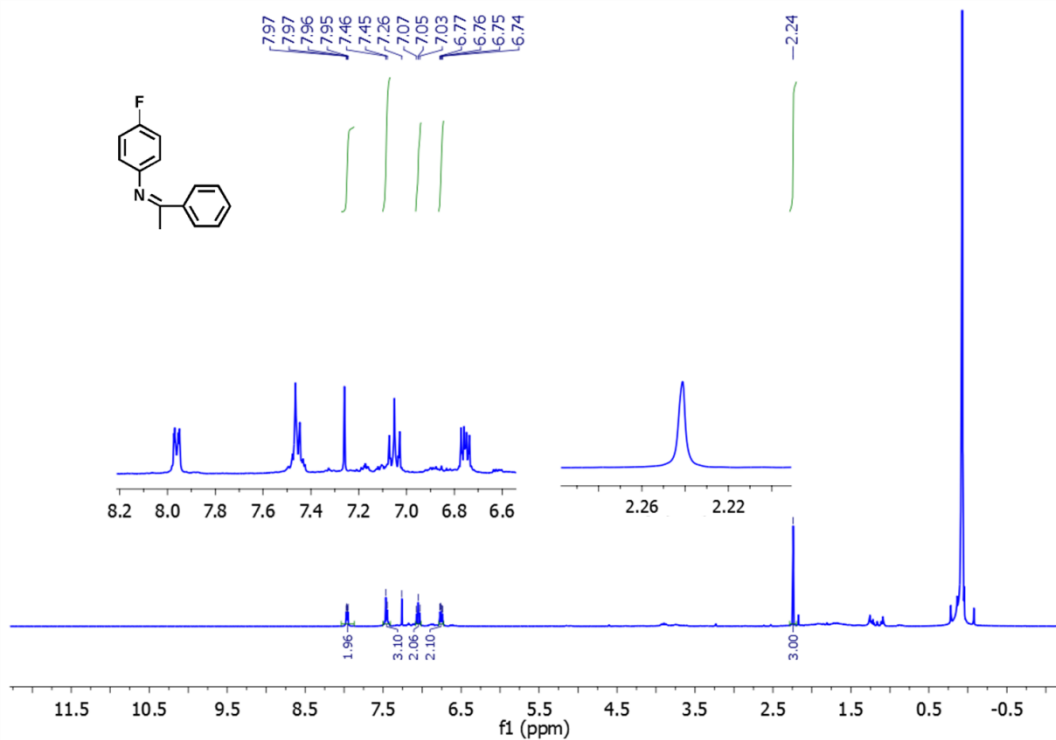


**Fig S35.** <sup>1</sup>H NMR spectrum (400 MHz, CDCl<sub>3</sub>) of *N*-(1-phenylethylidene)-*p*-floroaniline (11).

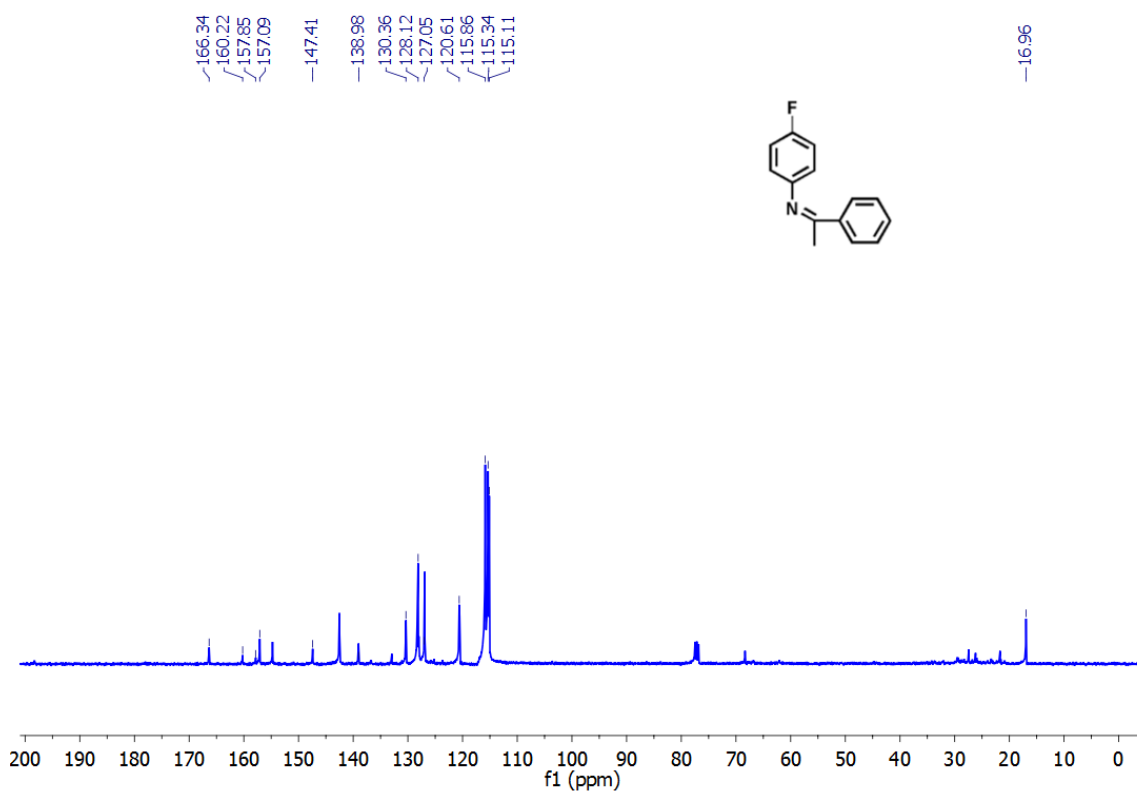


**Fig S36.** <sup>13</sup>C NMR spectrum (100 MHz, CDCl<sub>3</sub>) of *N*-(1-phenylethylidene)-*p*-floroaniline (11).

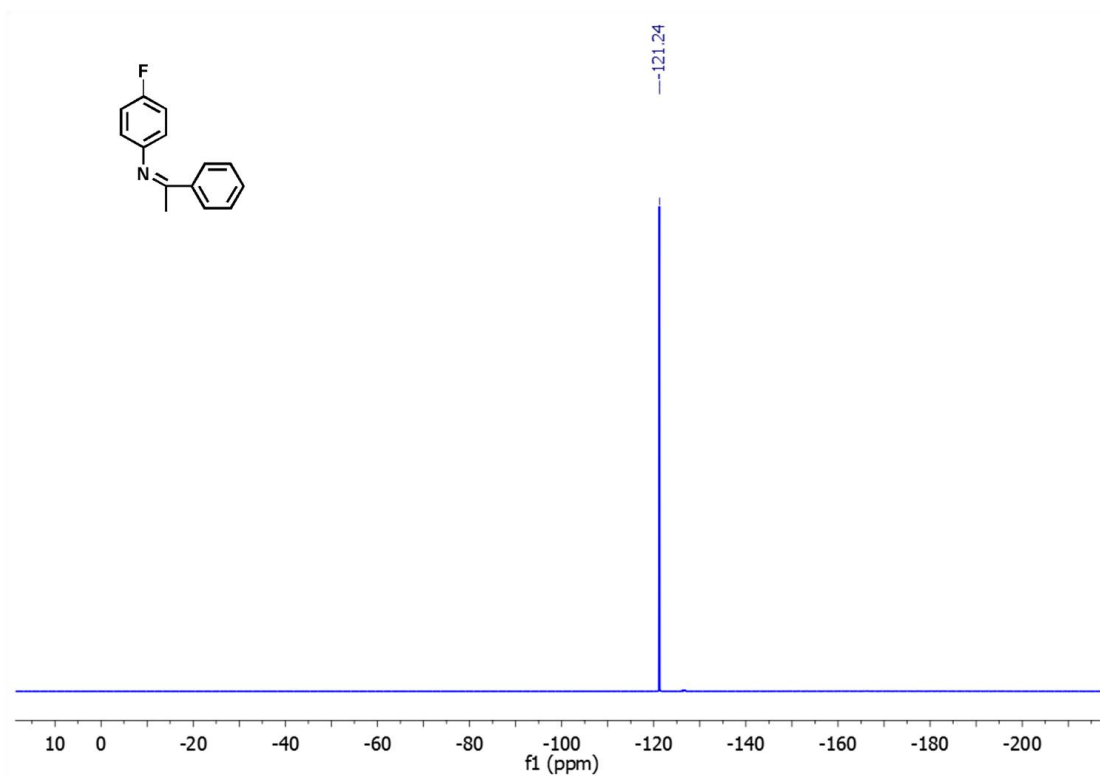


**Fig S37.**  $^{19}\text{F}$  NMR spectrum (376.4 MHz,  $\text{CDCl}_3$ ) of *N*-(1-phenylethylidene)-*p*-floroaniline (**11**).

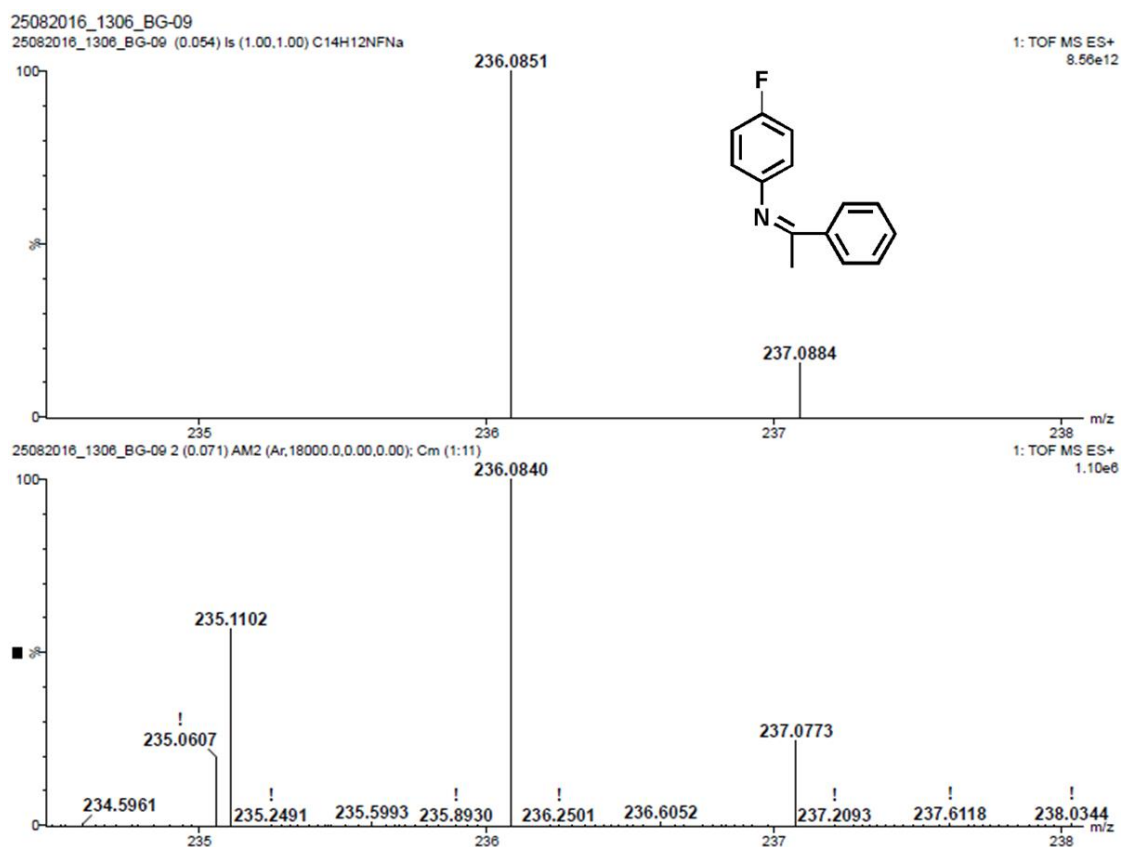


**Fig S38.** HRMS spectrum of *N*-(1-phenylethylidene)-*p*-floroaniline (**11**).



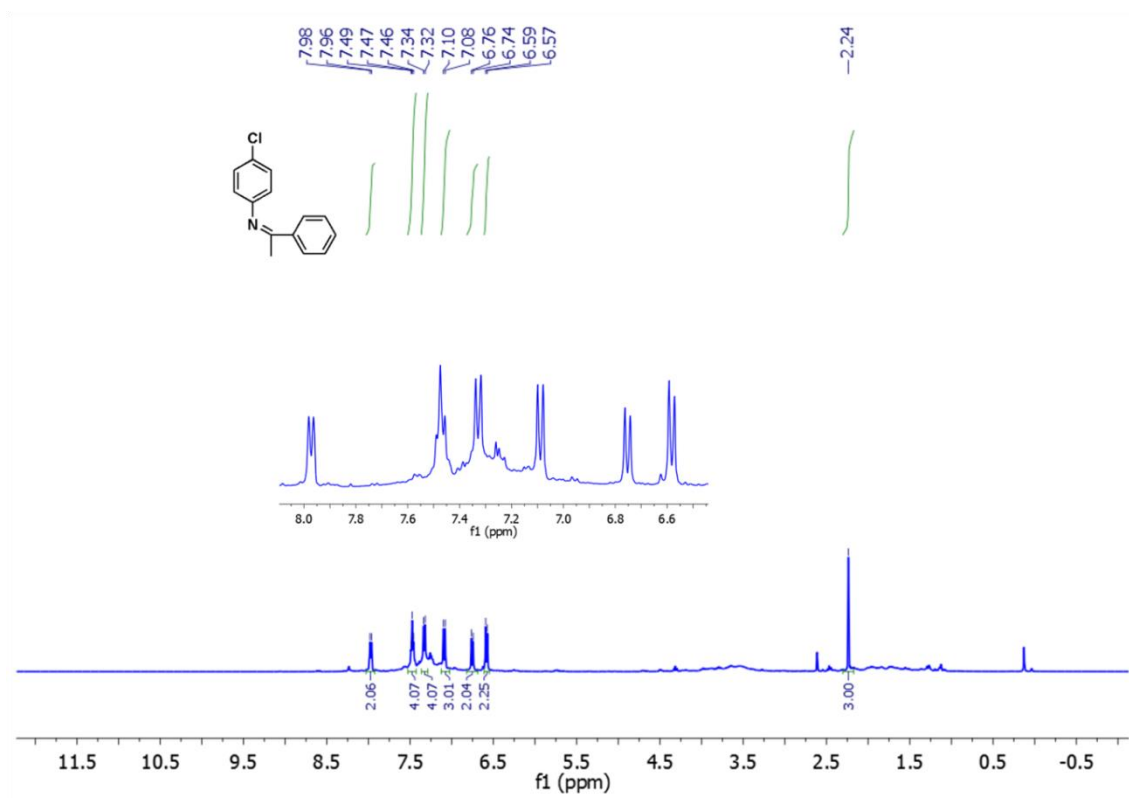


**Fig S39.** <sup>1</sup>H NMR spectrum (400 MHz, CDCl<sub>3</sub>) of *N*-(1-phenylethylidene)-*p*-chloroaniline (12).

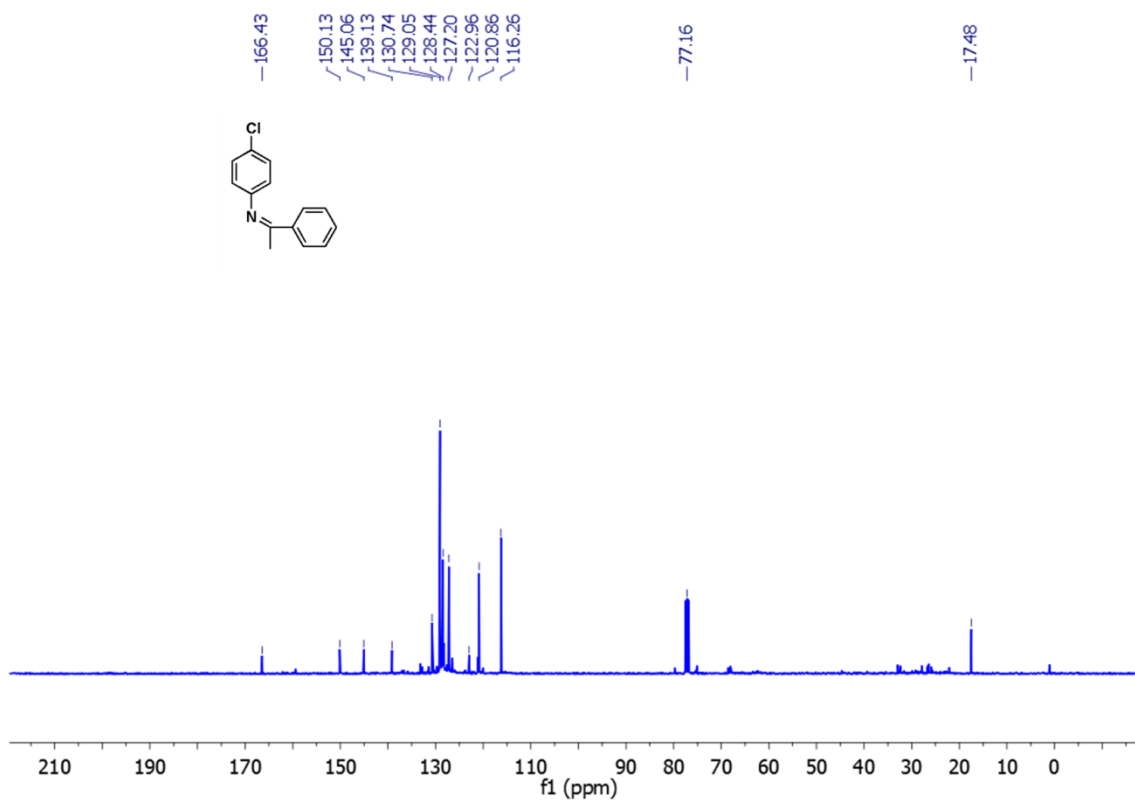


**Fig S40.** <sup>13</sup>C NMR spectrum (100 MHz, CDCl<sub>3</sub>) of *N*-(1-phenylethylidene)-*p*-chloroaniline (12).

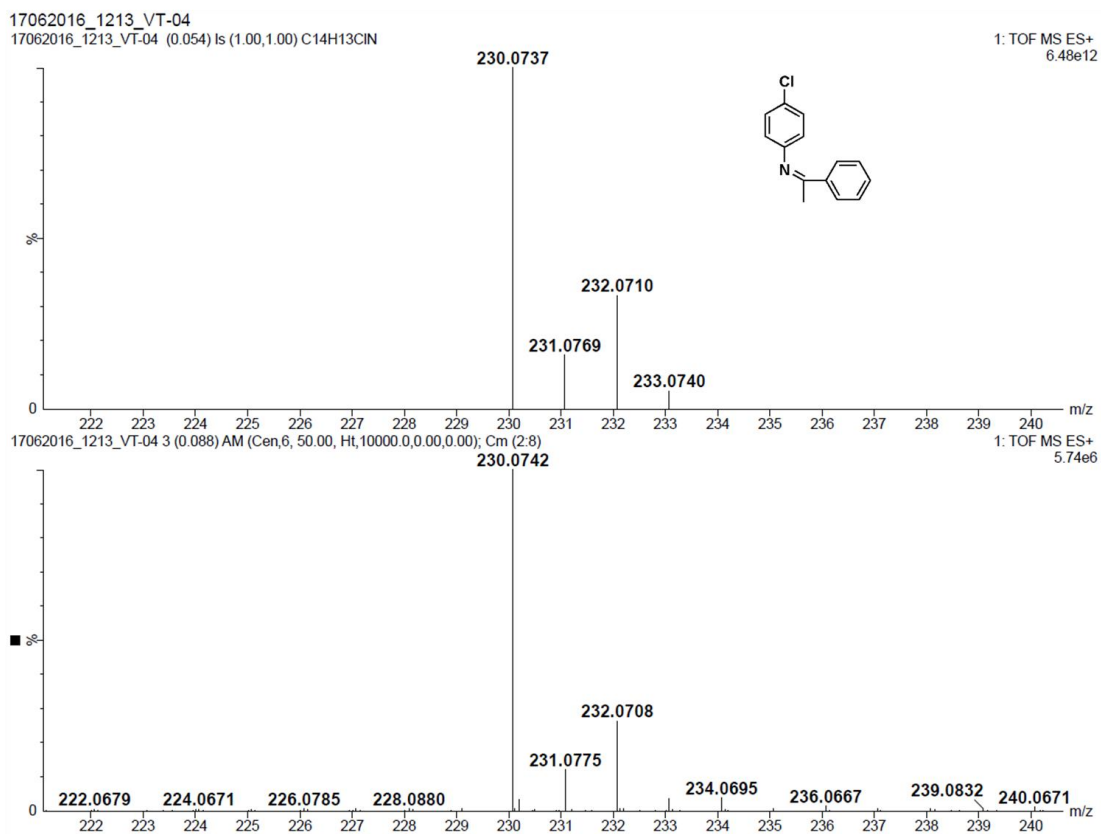


**Fig S41.** HRMS spectrum of *N*-(1-phenylethylidene)-*p*-chloroaniline (**12**).

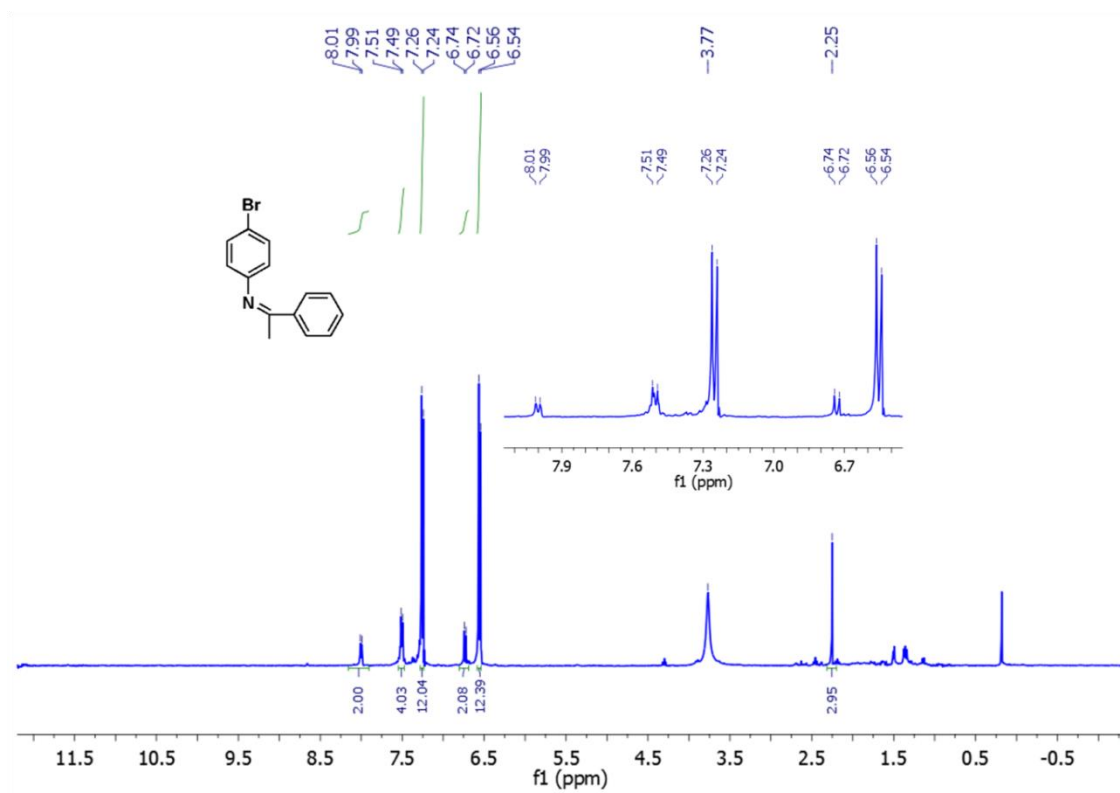


**Fig S42.**  $^1\text{H}$  NMR spectrum (400 MHz,  $\text{CDCl}_3$ ) of *N*-(1-phenylethylidene)-*p*-bromoaniline (**13**).

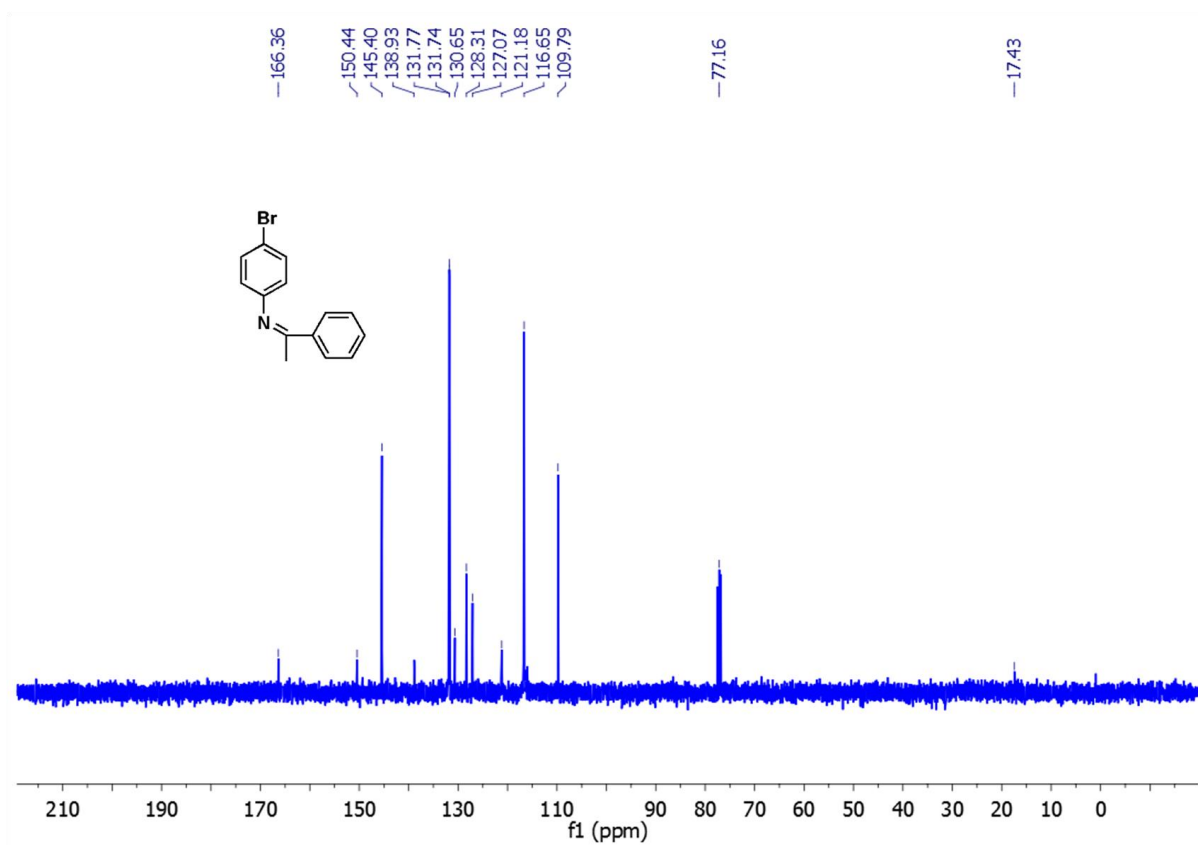


**Fig S43.** <sup>13</sup>C NMR spectrum (100 MHz, CDCl<sub>3</sub>) of *N*-(1-phenylethylidene)-*p*-bromoaniline (13).

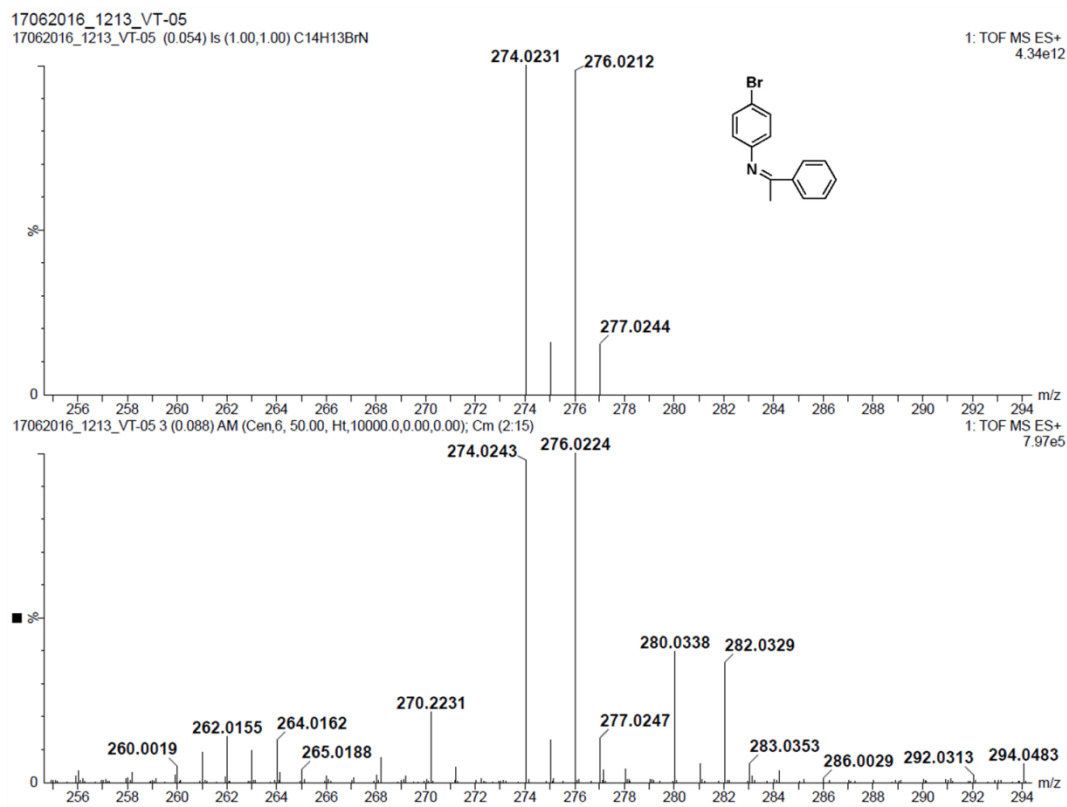


**Fig S44.** HRMS spectrum of *N*-(1-phenylethylidene)-*p*-bromoaniline (13).

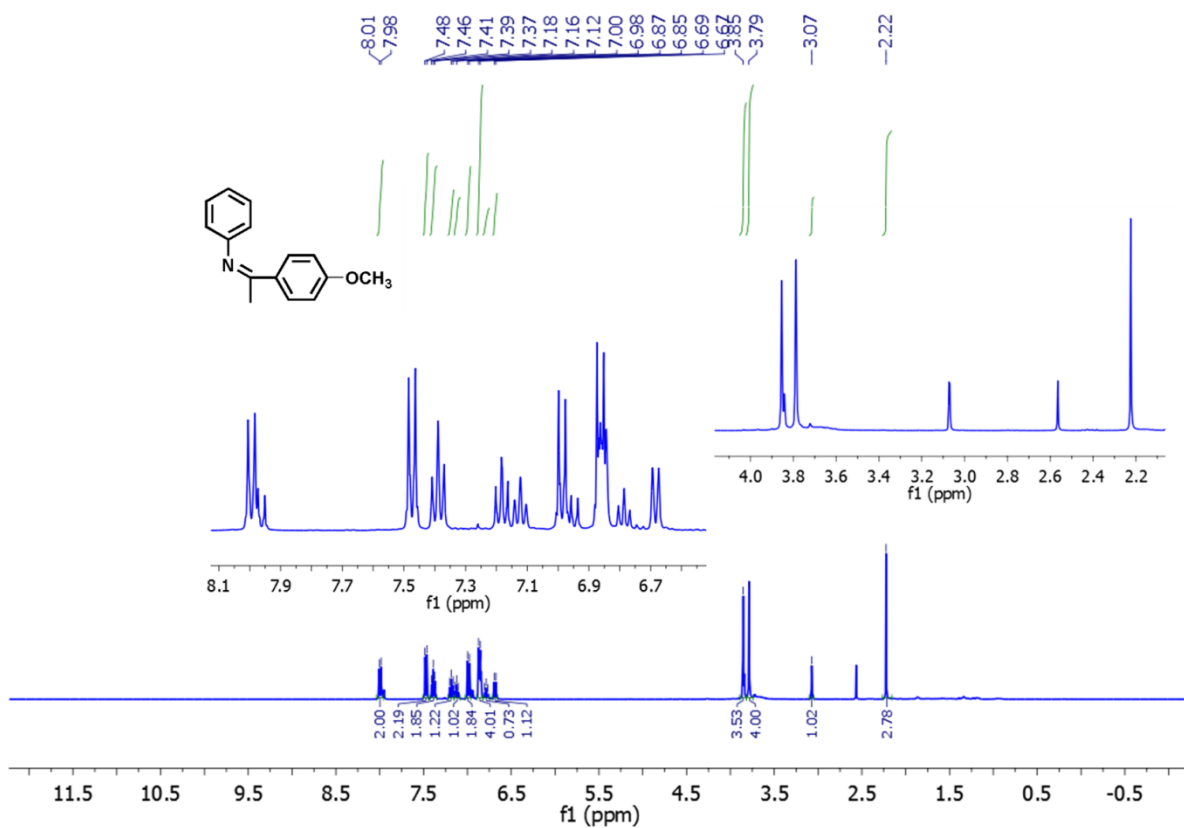


**Fig S45.** <sup>1</sup>H NMR spectrum (400 MHz, CDCl<sub>3</sub>) of *N*-(1-(*p*-methoxyphenyl)ethylidene)aniline (**14**).

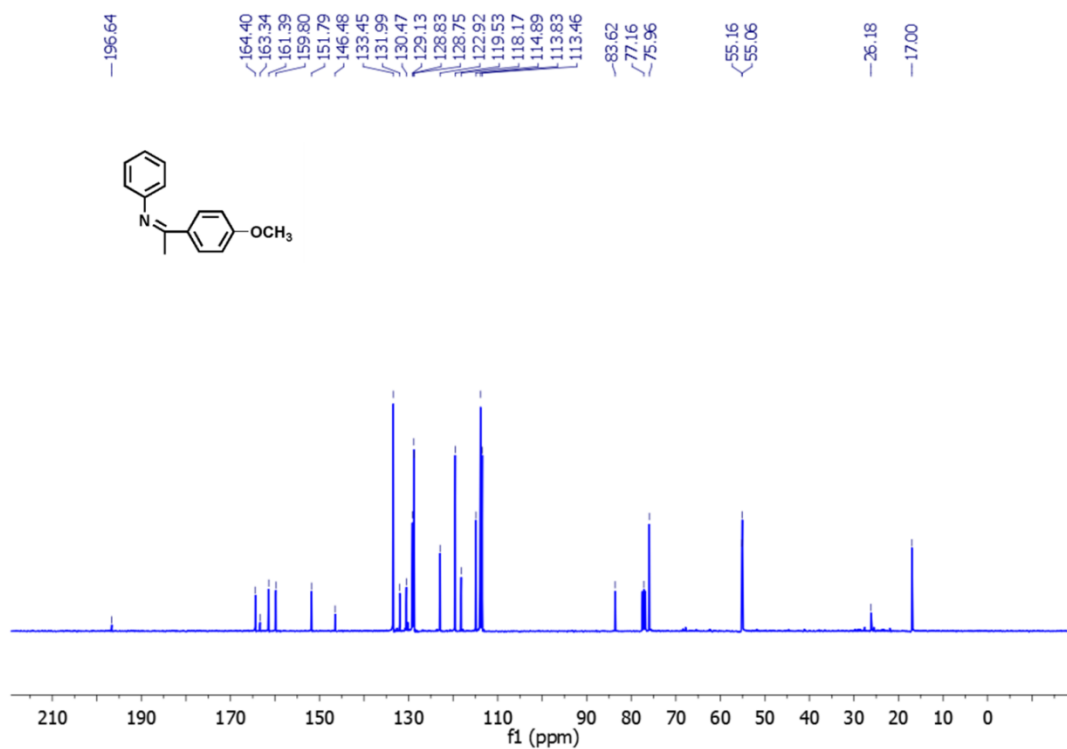


**Fig S46.** <sup>13</sup>C NMR spectrum (100 MHz, CDCl<sub>3</sub>) of *N*-(1-(*p*-methoxyphenyl)ethylidene)aniline (**14**).

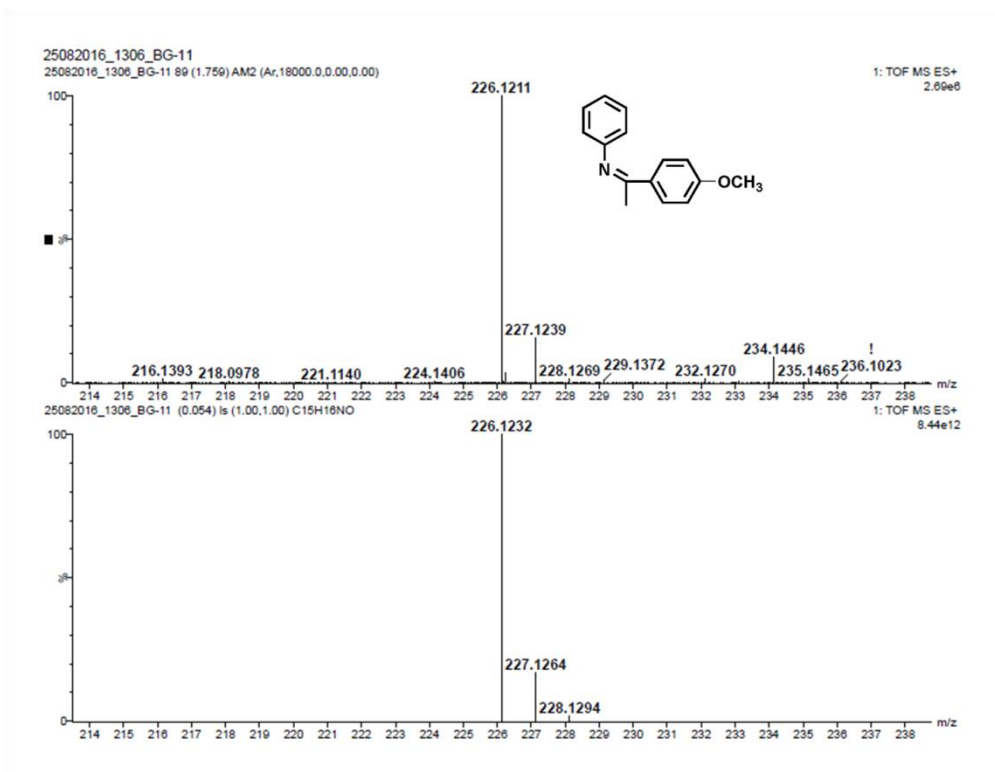


**Fig S47.** HRMS spectrum of *N*-(1-(*p*-methoxyphenyl)ethylidene)aniline (**14**).

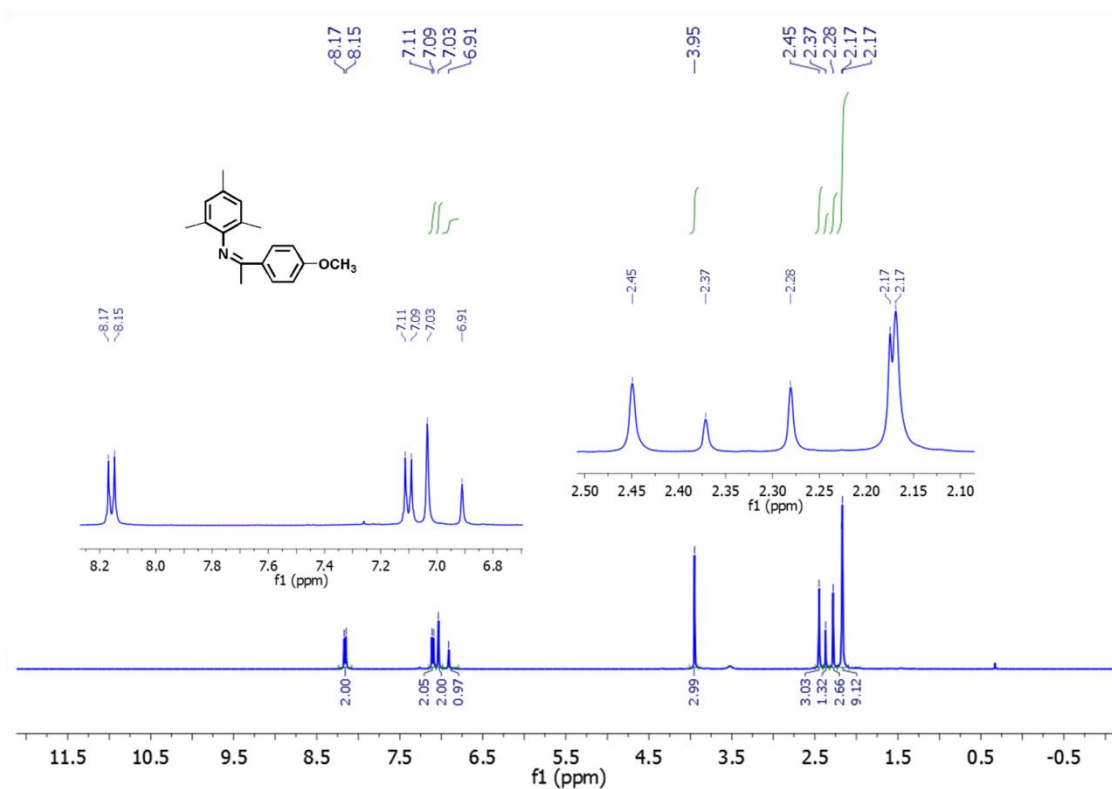
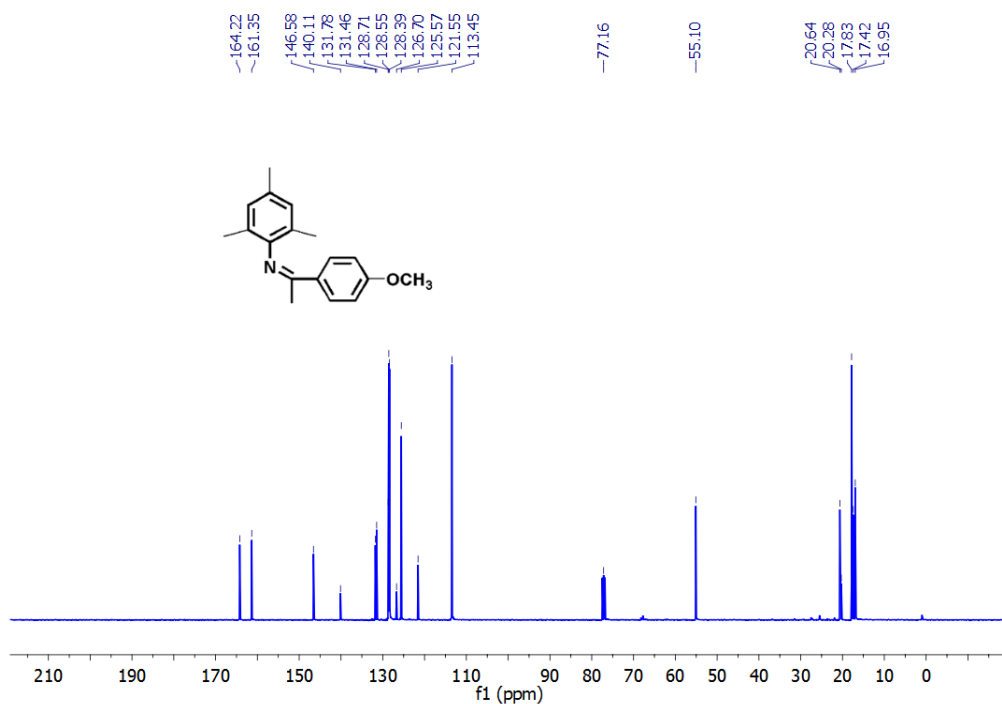


**Fig S48.** <sup>1</sup>H NMR spectrum (400 MHz, CDCl<sub>3</sub>) of *N*-(1-(*p*-methoxyphenyl)ethylidene)-2,4,6-trimethylaniline (**15**).



**FigS49.**  $^{13}\text{C}$  NMR spectrum (100 MHz,  $\text{CDCl}_3$ ) of *N*-(1-(*p*-methoxyphenyl)ethylidene)-2,4,6-trimethylaniline (**15**).

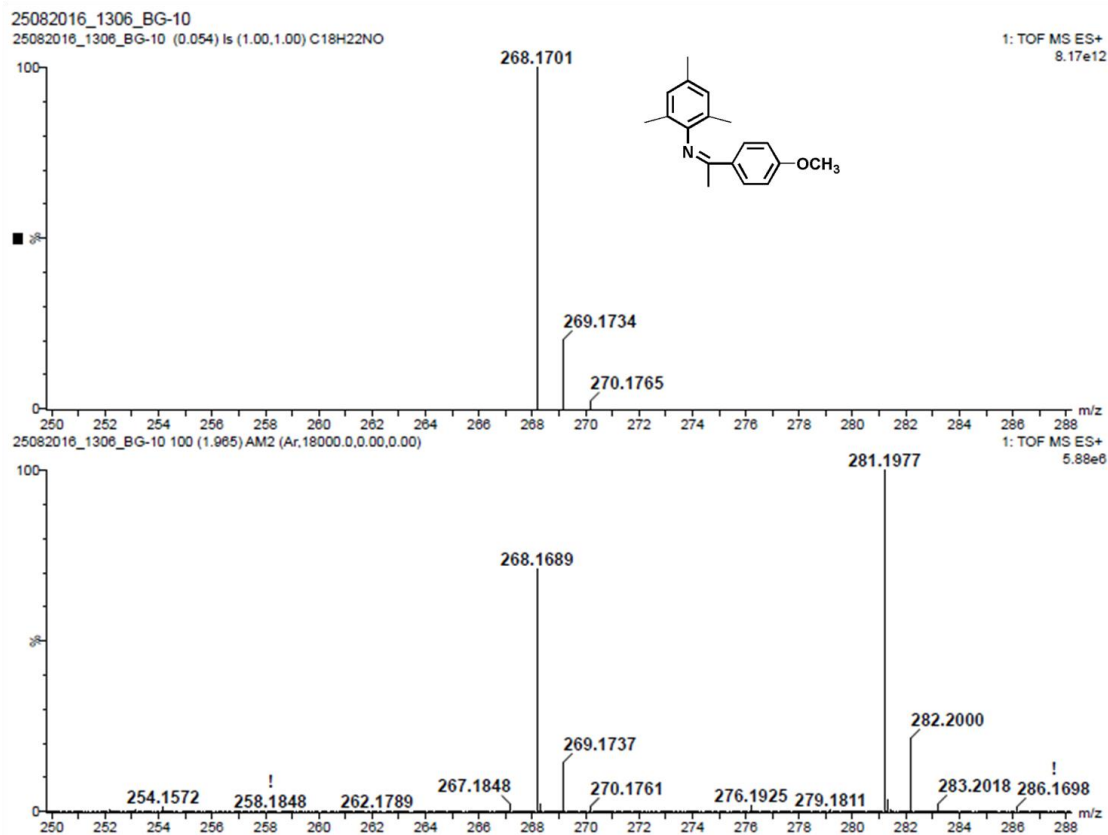


**Fig S50.** HRMS spectrum of *N*-(1-(*p*-methoxyphenyl)ethylidene)-2,4,6-trimethylaniline (**15**).

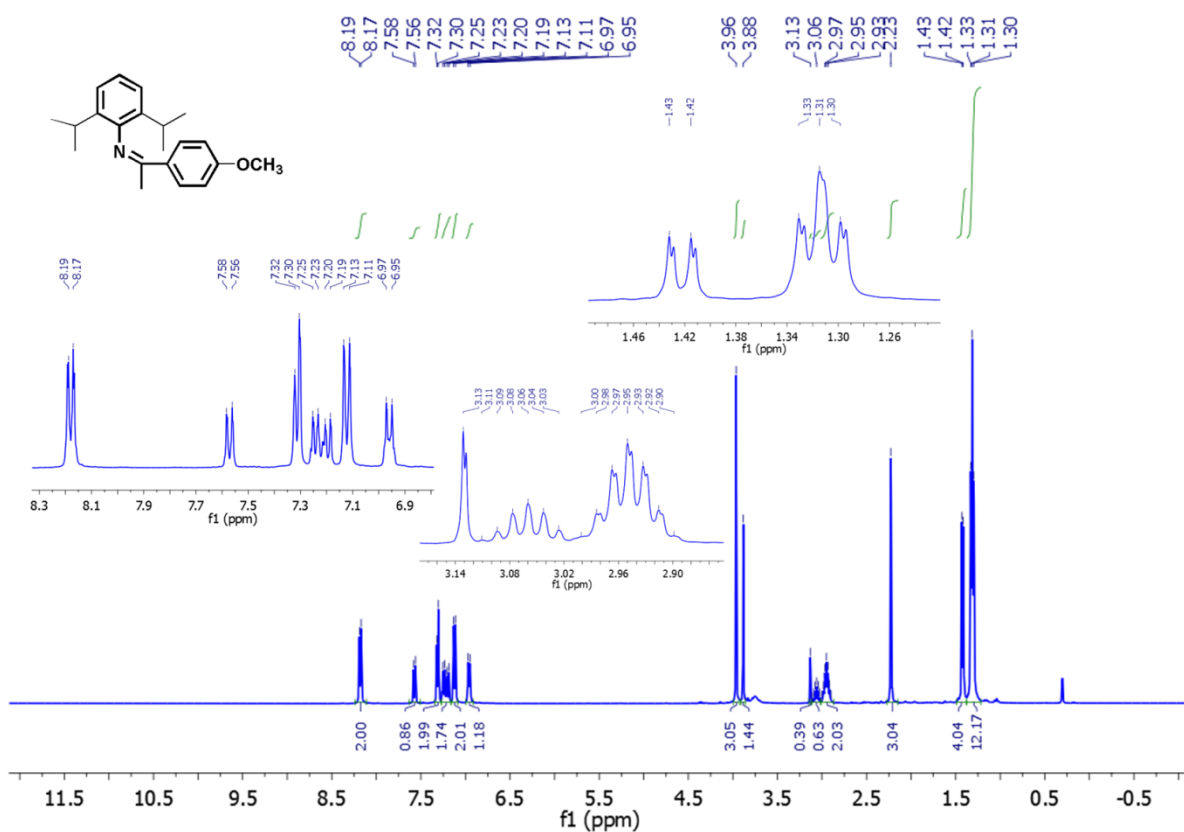


**Fig S51.** <sup>1</sup>H NMR spectrum (400 MHz, CDCl<sub>3</sub>) of *N*-(1-(*p*-methoxyphenyl)ethylidene)-2,6-diisopropylaniline (**16**).

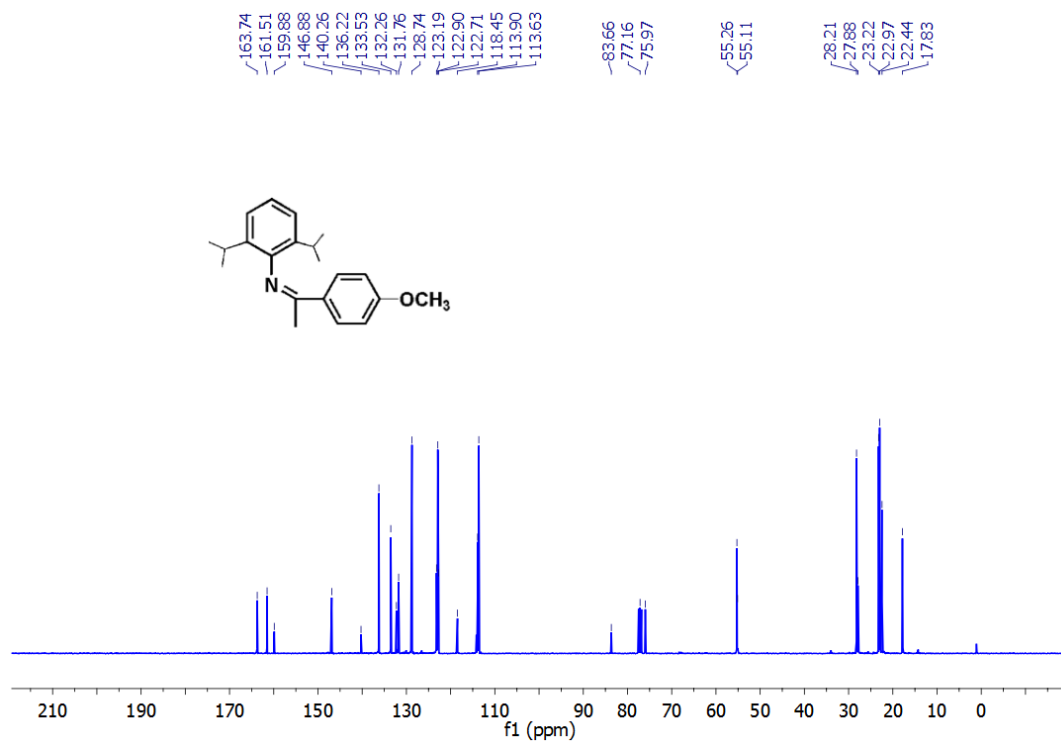


**Fig S52.** <sup>13</sup>C NMR spectrum (100 MHz, CDCl<sub>3</sub>) of *N*-(1-(*p*-methoxyphenyl)ethylidene)-2,6-diisopropylaniline (**16**).

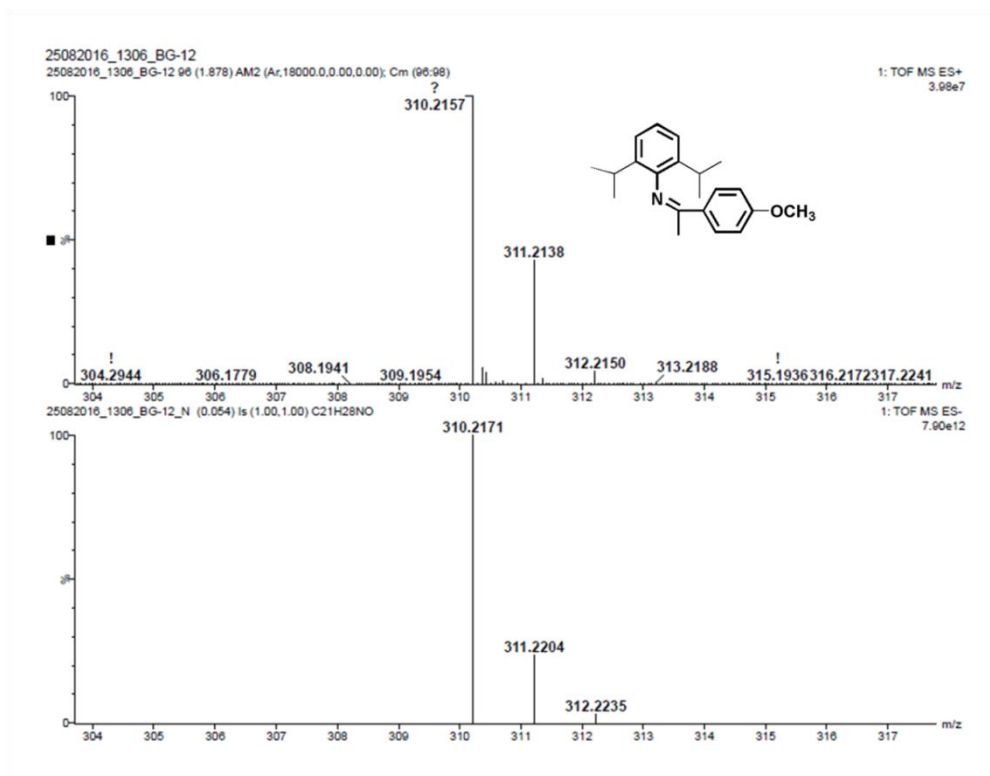


**Fig S53.** HRMS spectrum of *N*-(1-(*p*-methoxyphenyl)ethylidene)-2,6-diisopropylaniline (**16**).

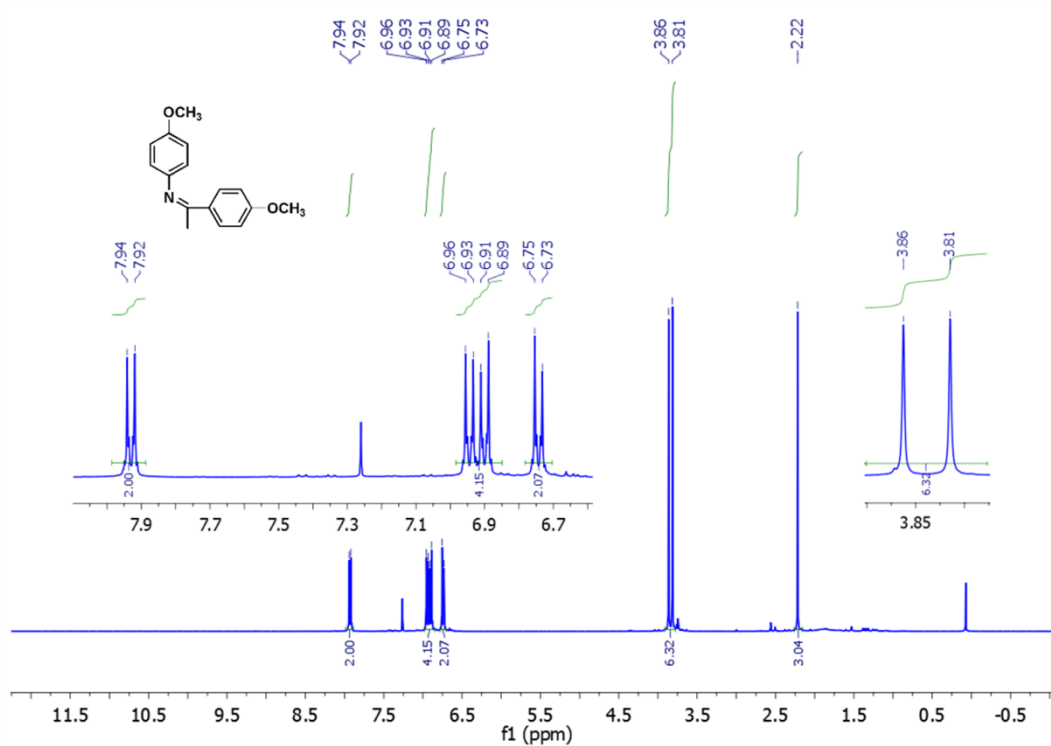


**Fig S54.**  $^1\text{H}$  NMR spectrum (400 MHz,  $\text{CDCl}_3$ ) of *N*-(1-(*p*-methoxyphenyl)ethylidene)-*p*-methoxyaniline (**17**).



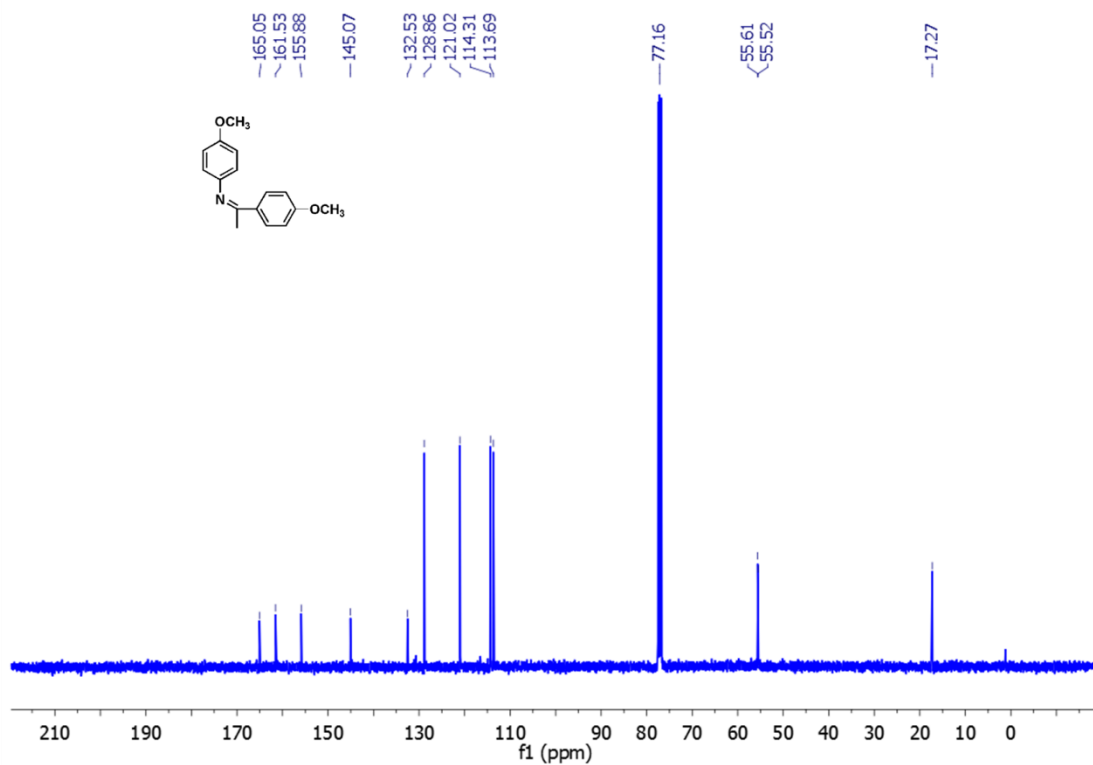


**Fig S55.** <sup>13</sup>C NMR spectrum (100 MHz, CDCl<sub>3</sub>) of *N*-(1-(*p*-methoxyphenyl)ethylidene)-*p*-methoxyaniline (**17**).

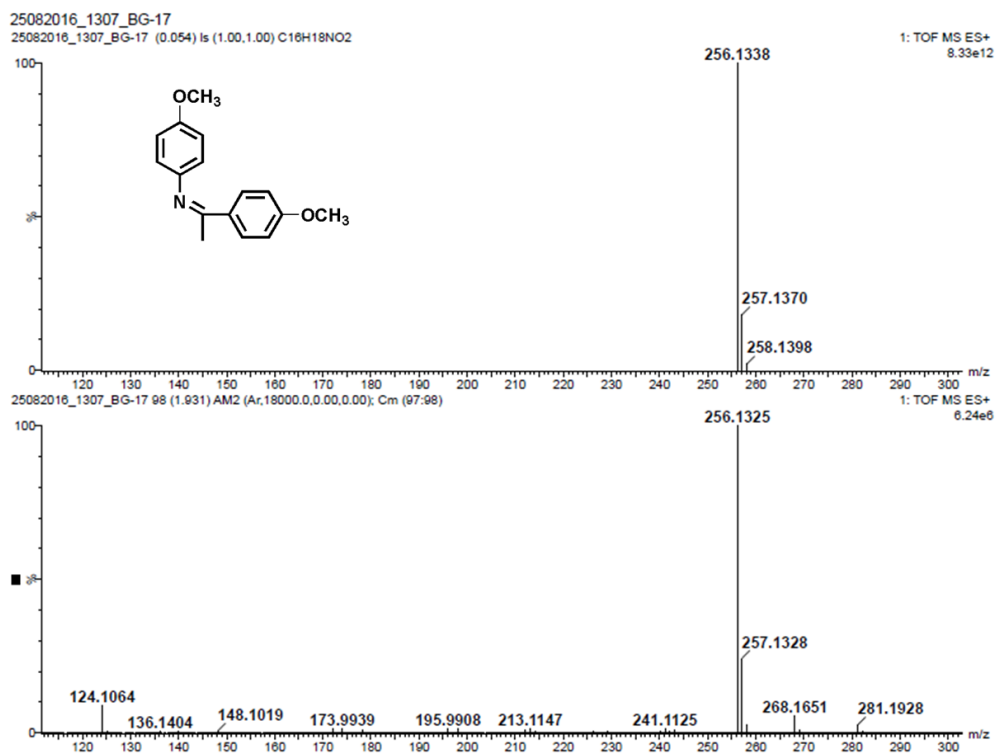


**Fig S56.** HRMS spectrum of *N*-(1-(*p*-methoxyphenyl)ethylidene)-*p*-methoxyaniline (**17**).

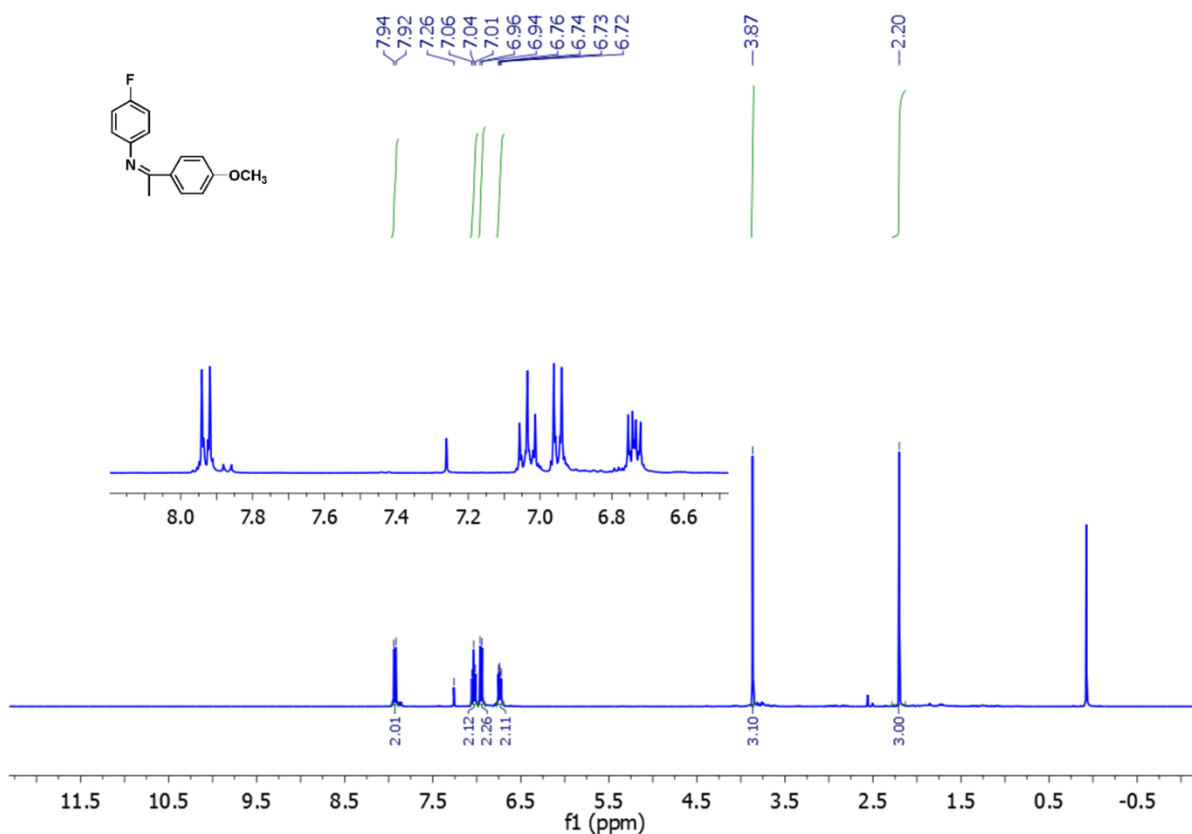


**Fig S57.** <sup>1</sup>H NMR spectrum (400 MHz, CDCl<sub>3</sub>) of *N*-(1-(*p*-methoxyphenyl)ethylidene)-*p*-floroaniline (18).

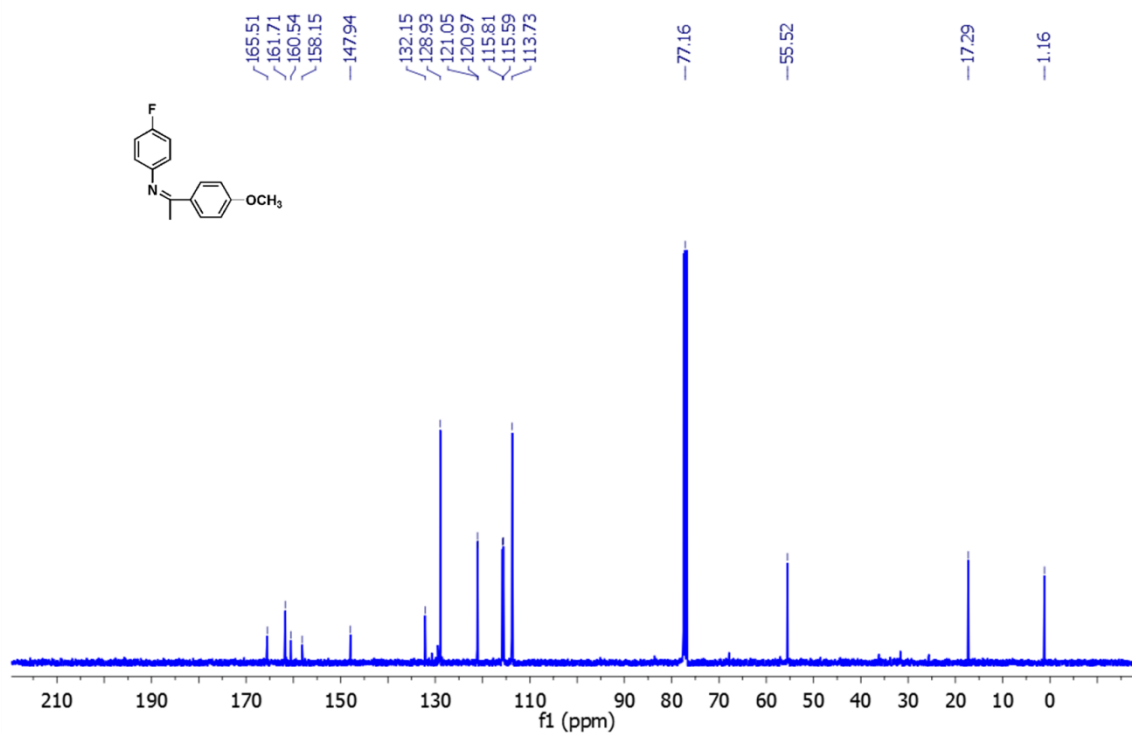


**Fig S58.** <sup>13</sup>C NMR spectrum (100 MHz, CDCl<sub>3</sub>) of *N*-(1-(*p*-methoxyphenyl)ethylidene)-*p*-floroaniline (18).

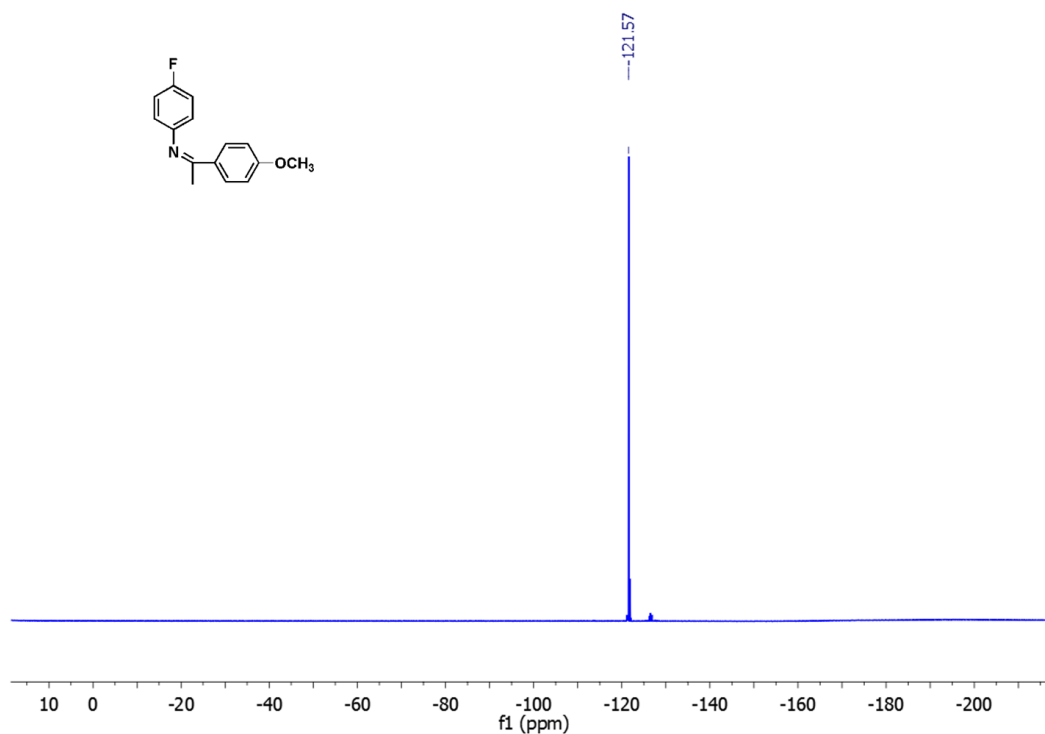


**Fig S59.**  $^{19}\text{F}$  NMR spectrum (376.4 MHz,  $\text{CDCl}_3$ ) of *N*-(1-(*p*-methoxyphenyl)ethylidene)-*p*-floroaniline (**18**).

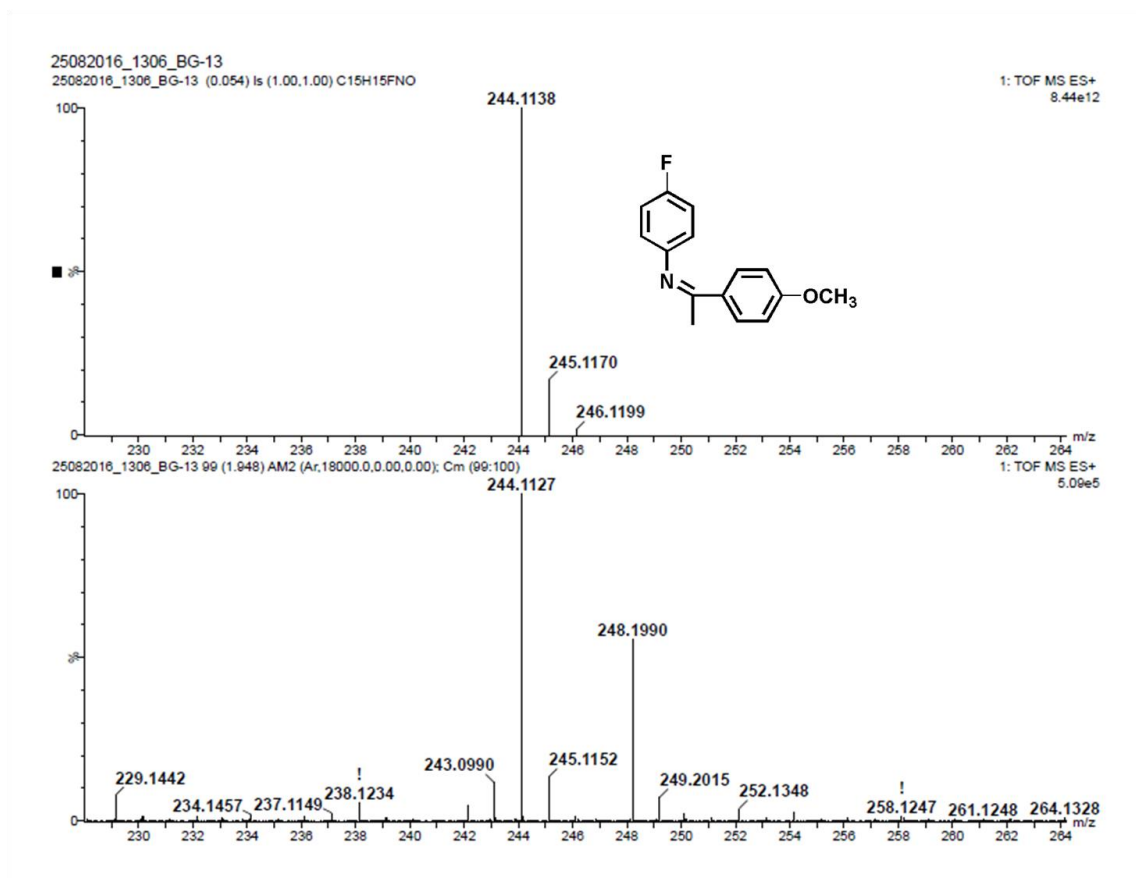


**Fig S60.** HRMS spectrum of *N*-(1-(*p*-methoxyphenyl)ethylidene)-*p*-floroaniline (**18**).

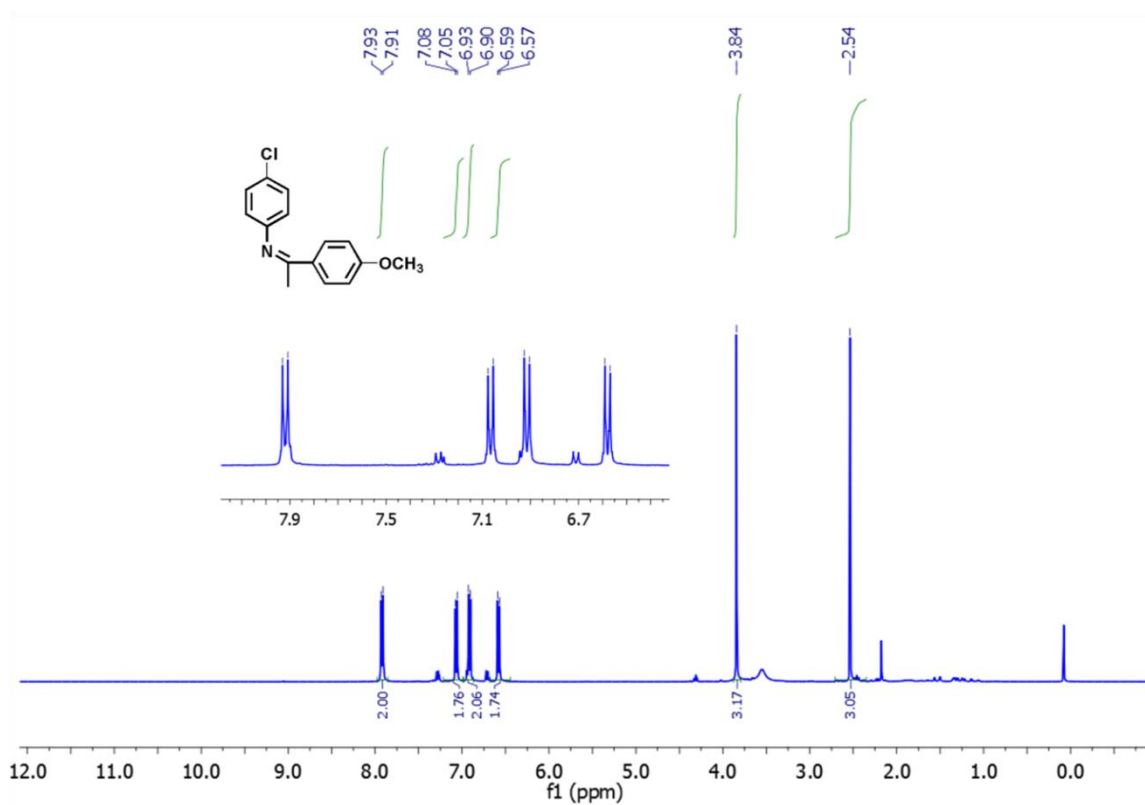


**Fig S61.** <sup>1</sup>H NMR spectrum (400 MHz, CDCl<sub>3</sub>) of *N*-(1-(*p*-methoxyphenyl)ethylidene)-*p*-chloroaniline (19).

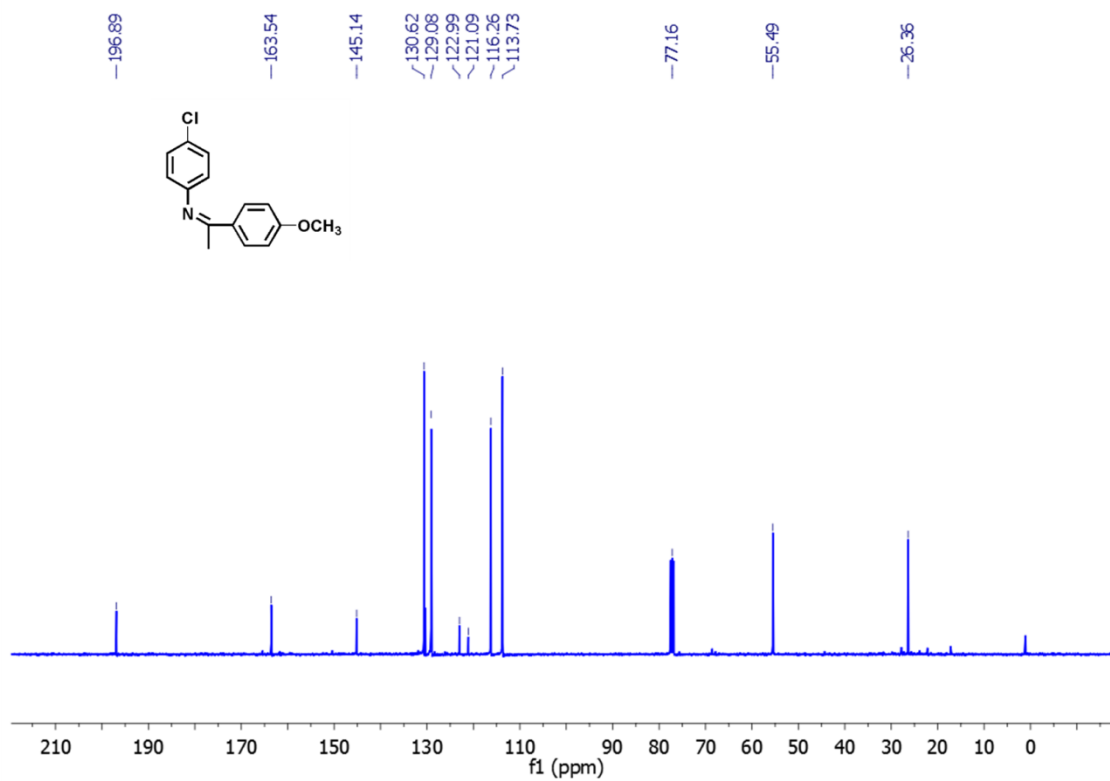


**Fig S62.** <sup>13</sup>C NMR spectrum (100 MHz, CDCl<sub>3</sub>) of *N*-(1-(*p*-methoxyphenyl)ethylidene)-*p*-chloroaniline (19).

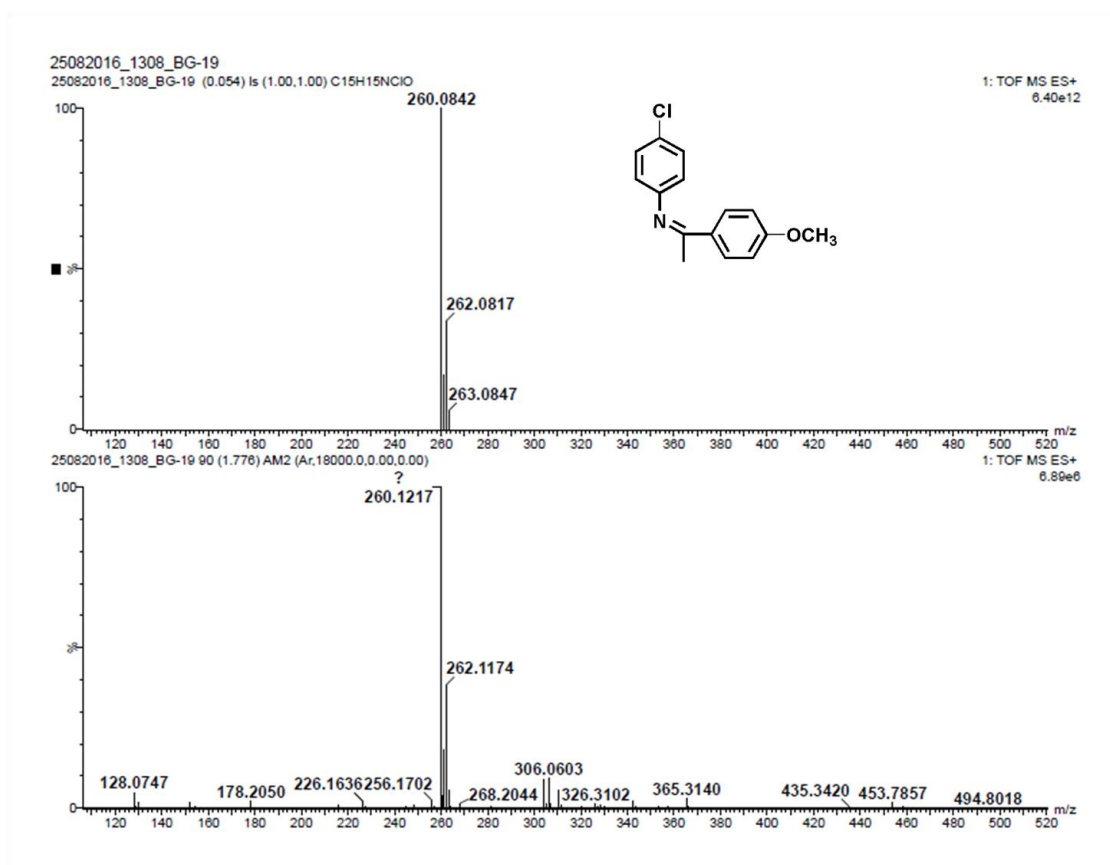


**Fig S63.** HRMS spectrum of *N*-(1-(*p*-methoxyphenyl)ethylidene)-*p*-chloroaniline (19).

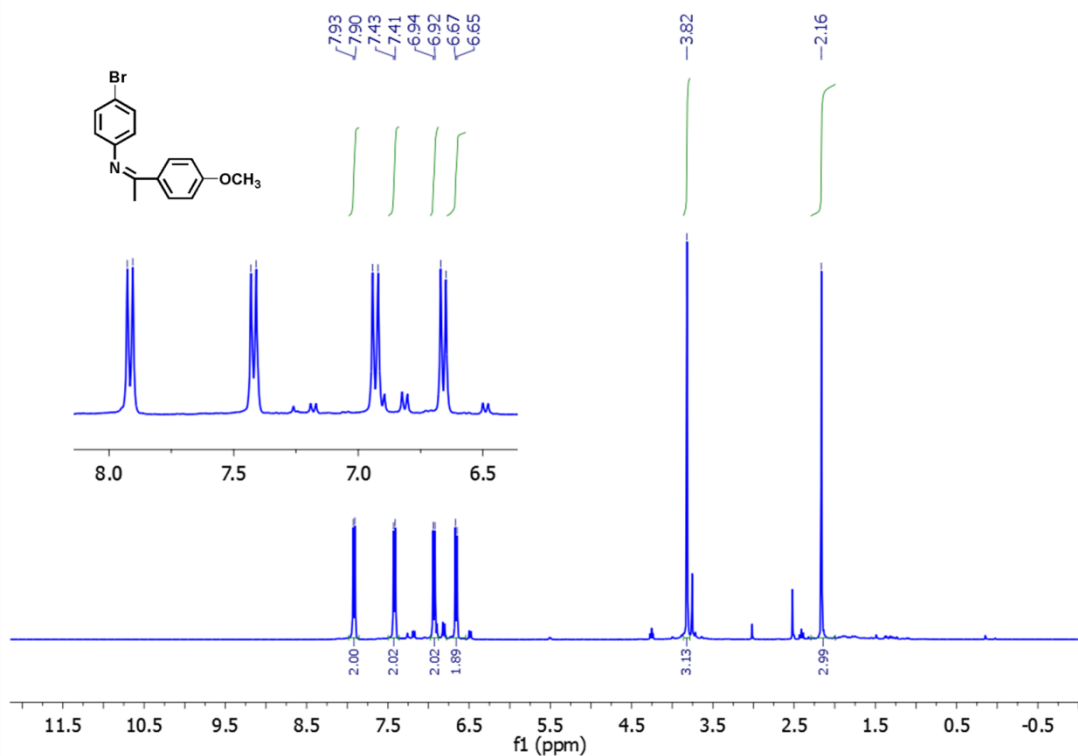


**Fig S64.** <sup>1</sup>H NMR spectrum (400 MHz, CDCl<sub>3</sub>) of *N*-(1-(*p*-methoxyphenyl)ethylidene)-*p*-bromoaniline (20).

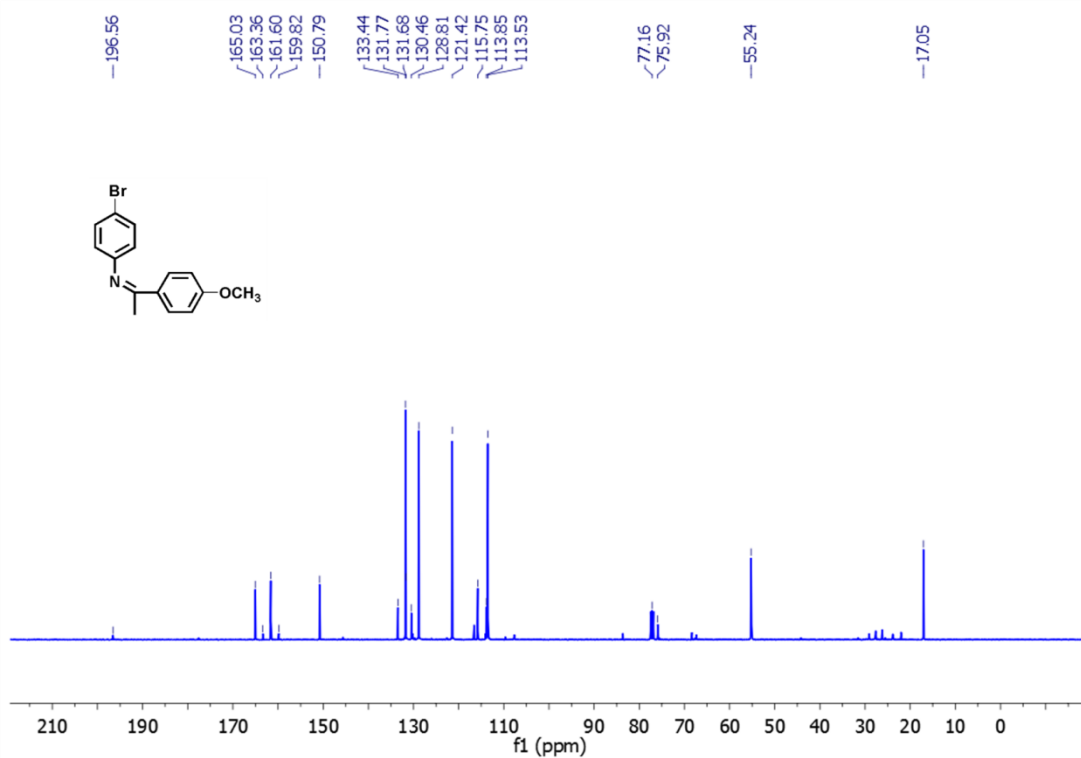


**Fig S65.** <sup>13</sup>C NMR spectrum (100 MHz, CDCl<sub>3</sub>) of *N*-(1-(*p*-methoxyphenyl)ethylidene)-*p*-bromoaniline (20).

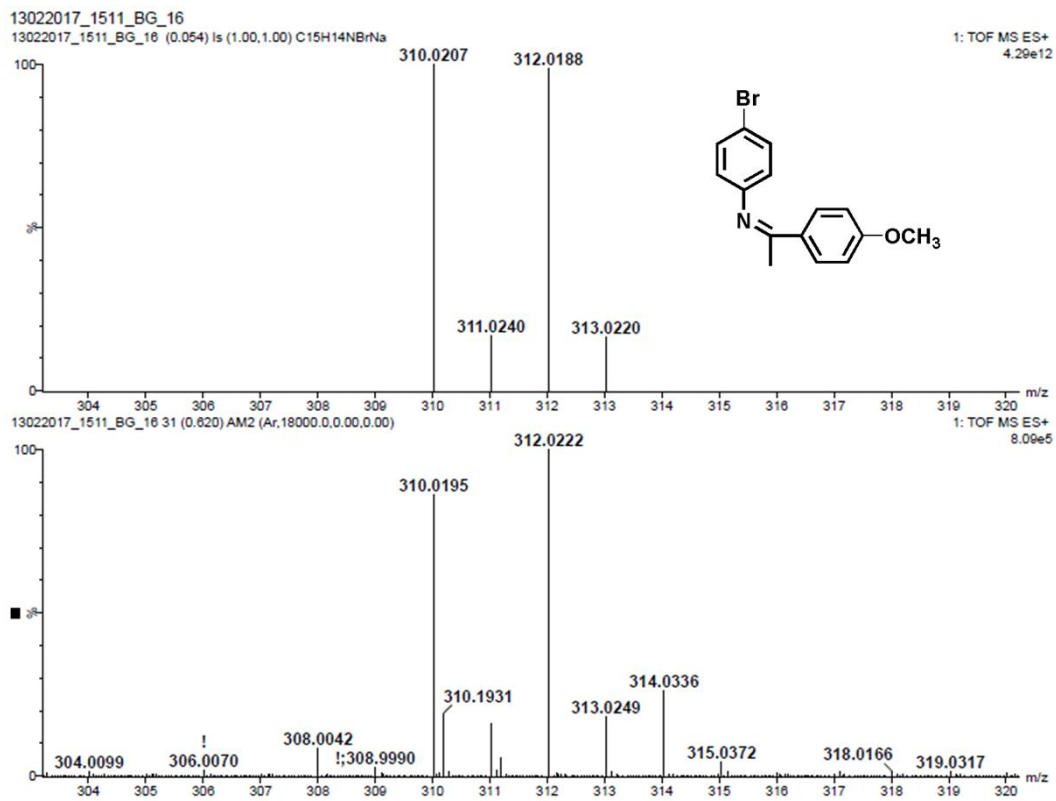


**Fig S66.** HRMS spectrum of *N*-(1-(*p*-methoxyphenyl)ethylidene)-*p*-bromoaniline (20).

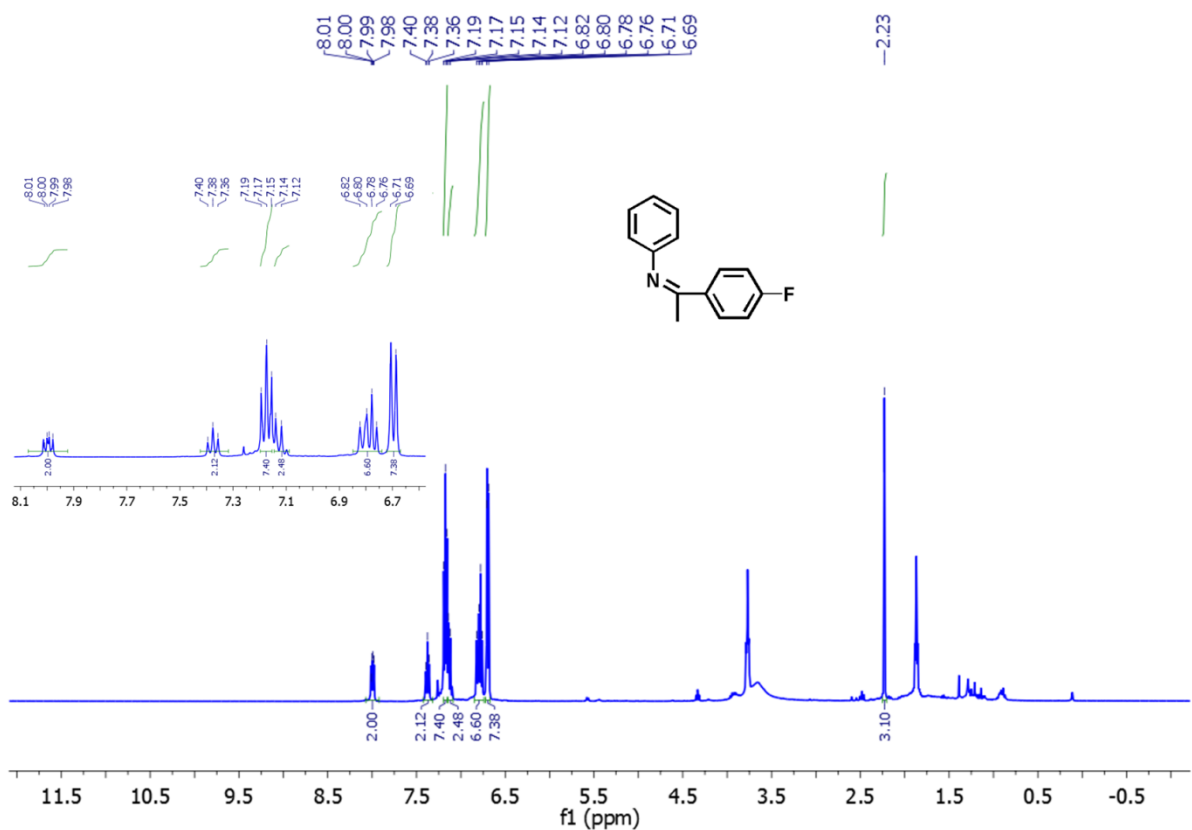


**Fig S67.** <sup>1</sup>H NMR spectrum (400 MHz, CDCl<sub>3</sub>) of *N*-(1-(*p*-florophenyl)ethylidene)aniline (21).

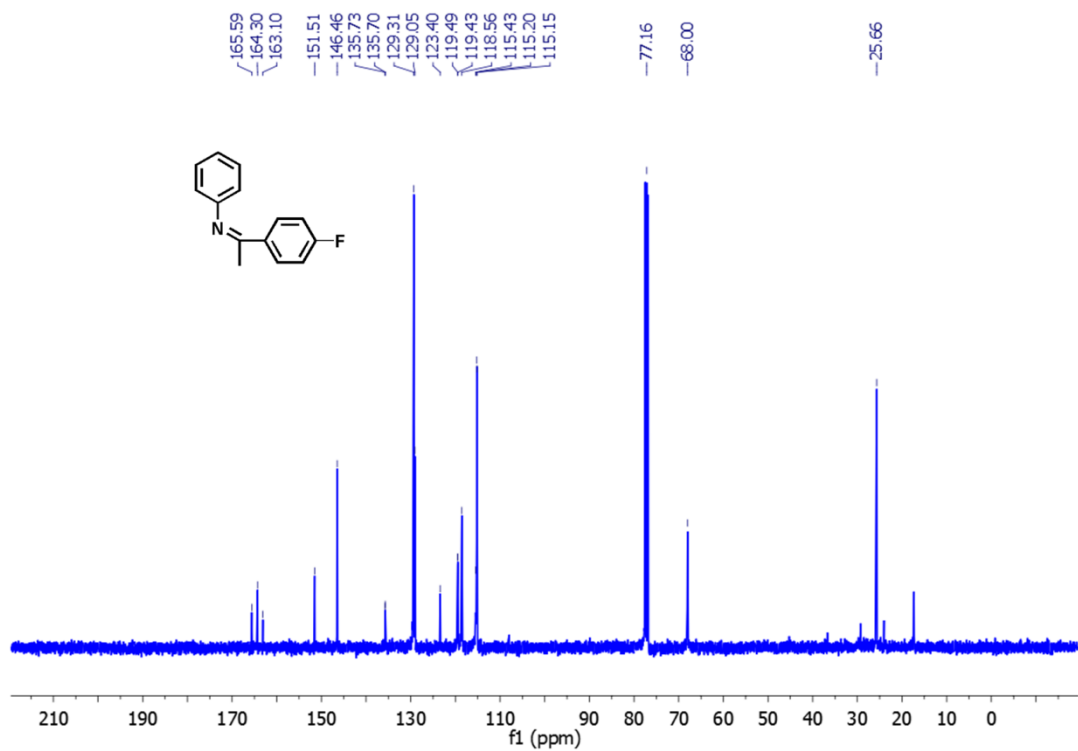


**Fig S68.** <sup>13</sup>C NMR spectrum (100 MHz, CDCl<sub>3</sub>) of *N*-(1-(*p*-florophenyl)ethylidene)aniline (21).

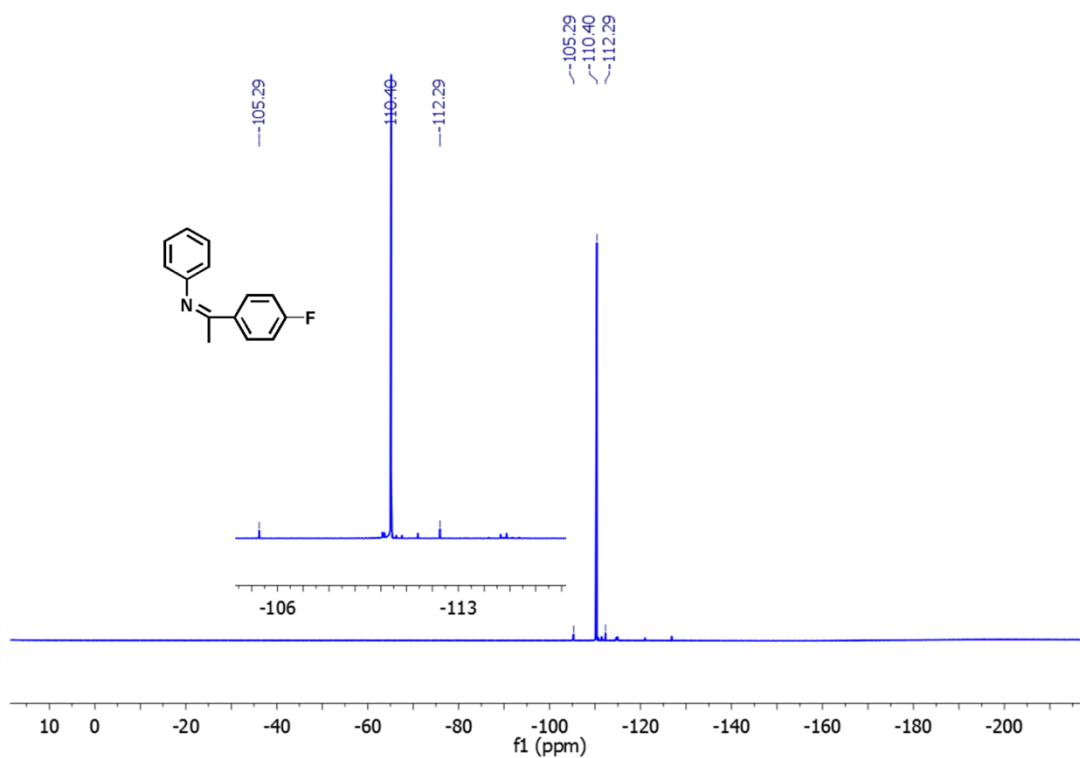


**Fig S69.**  $^{19}\text{F}$  NMR spectrum (376.4 MHz,  $\text{CDCl}_3$ ) of *N*-(1-(*p*-florophenyl)ethylidene)aniline (**21**).

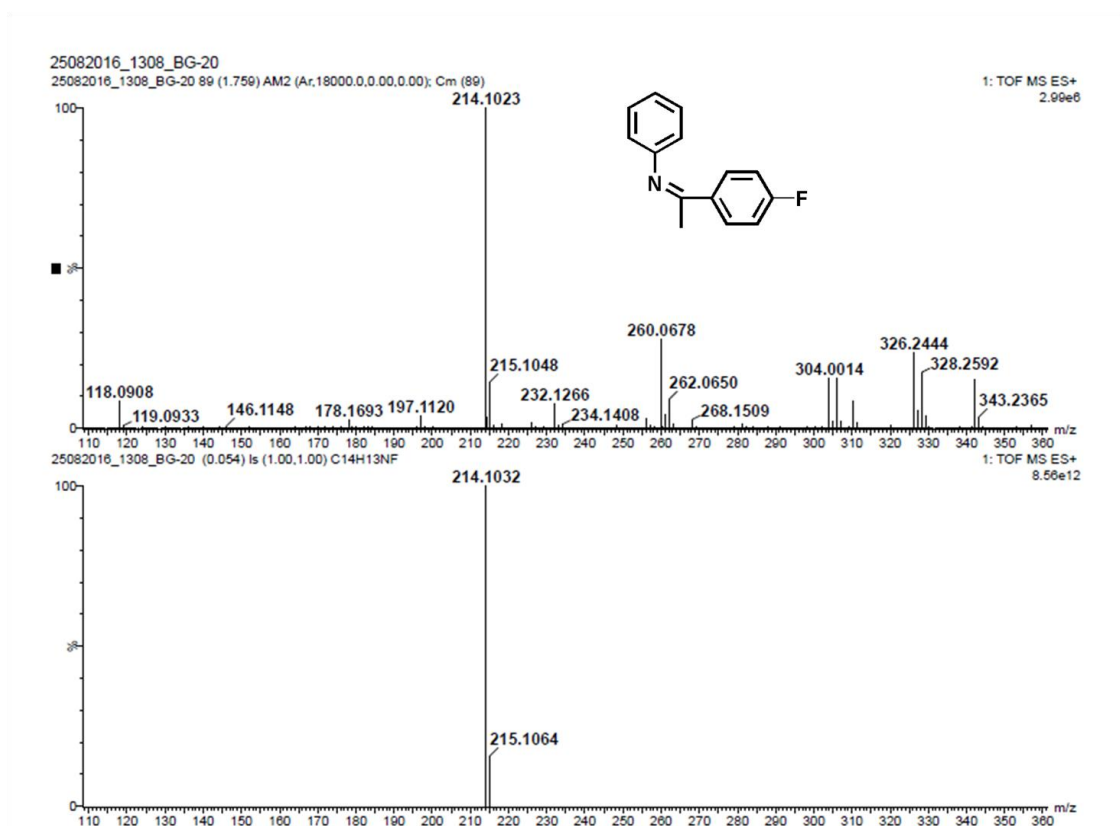


**Fig S70.** HRMS spectrum of *N*-(1-(*p*-florophenyl)ethylidene)aniline (**21**).



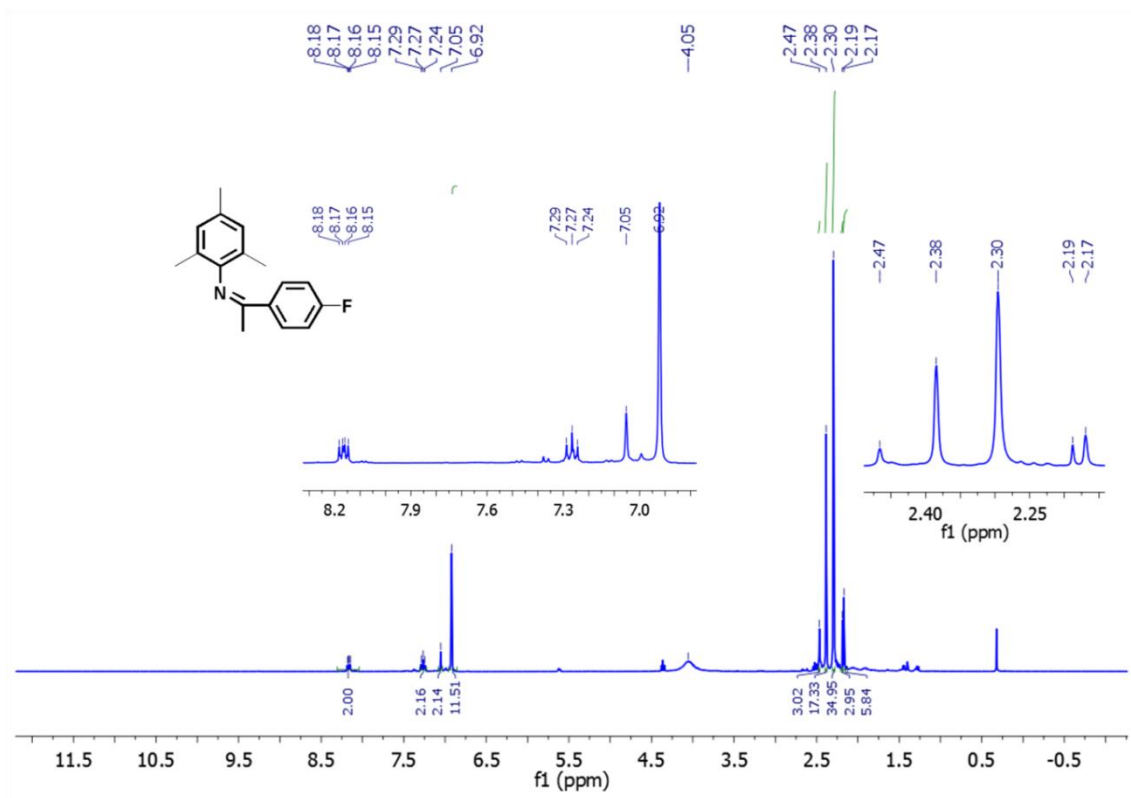


**Fig S71.** <sup>1</sup>H NMR spectrum (400 MHz, CDCl<sub>3</sub>) of *N*-(1-(*p*-florophenyl)ethylidene)-2,4,6-trimethylaniline (**22**).

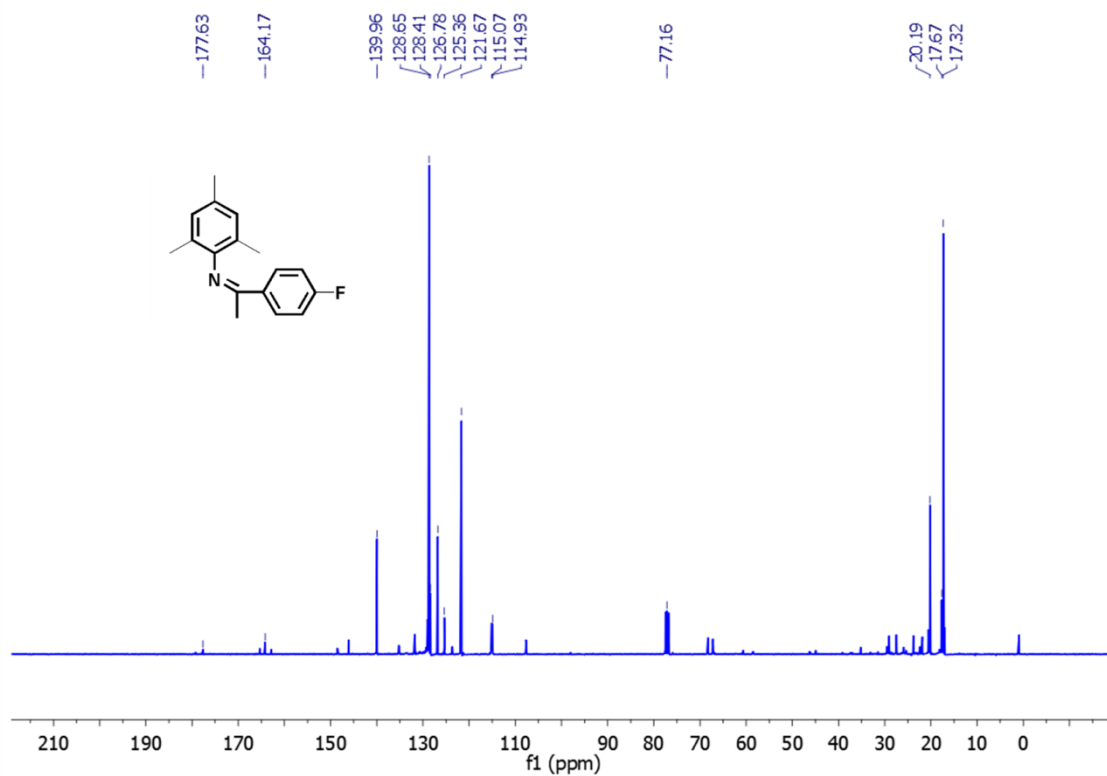


**Fig S72.** <sup>13</sup>C NMR spectrum (100 MHz, CDCl<sub>3</sub>) of *N*-(1-(*p*-florophenyl)ethylidene)-2,4,6-trimethylaniline (**21**).

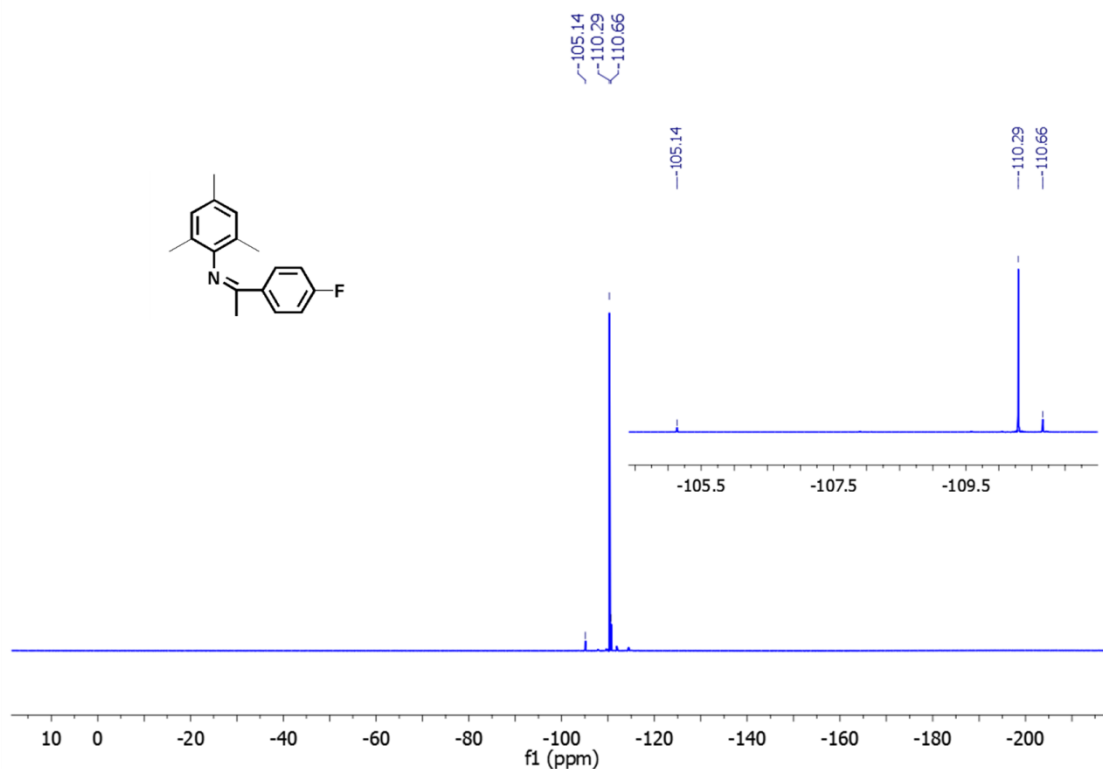


**Fig S73.**  $^{19}\text{F}$  NMR spectrum (376.4 MHz,  $\text{CDCl}_3$ ) of *N*-(1-(*p*-florophenyl)ethylidene)-2,4,6-trimethylaniline (**22**).

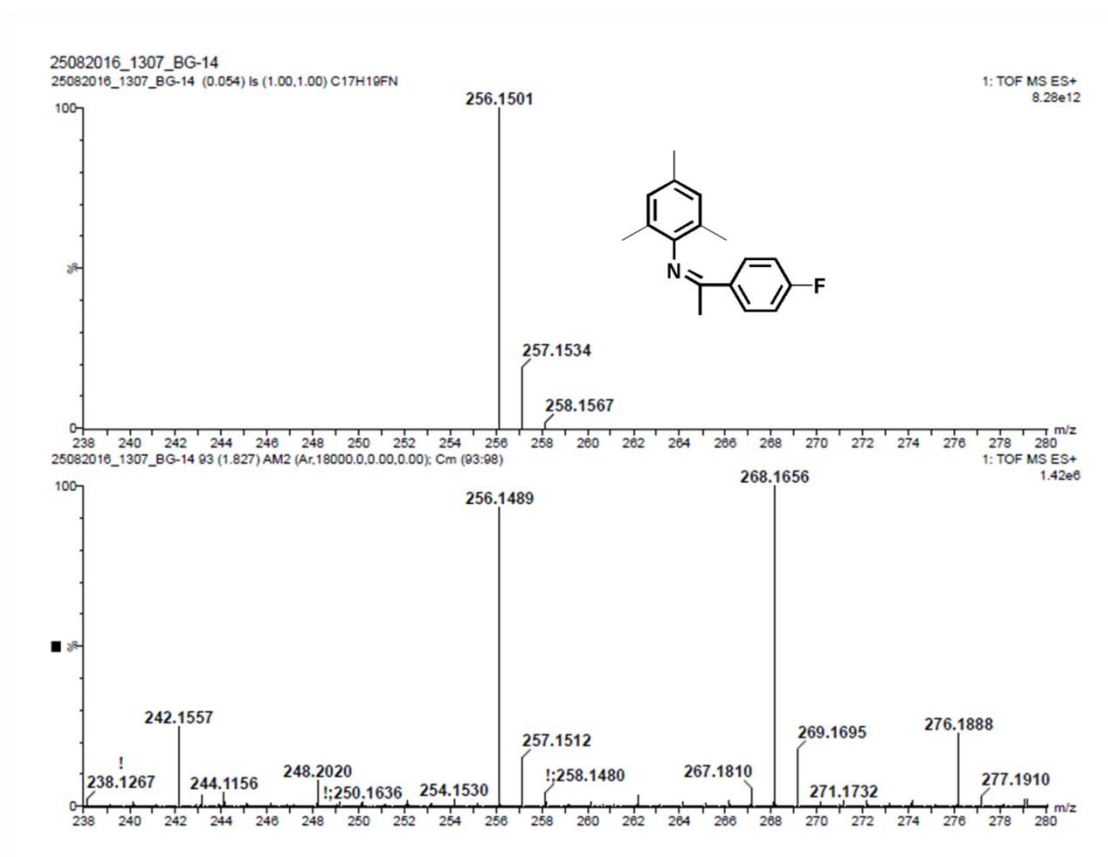


**Fig S74.** HRMS spectrum of *N*-(1-(*p*-florophenyl)ethylidene)-2,4,6-trimethylaniline (**21**).

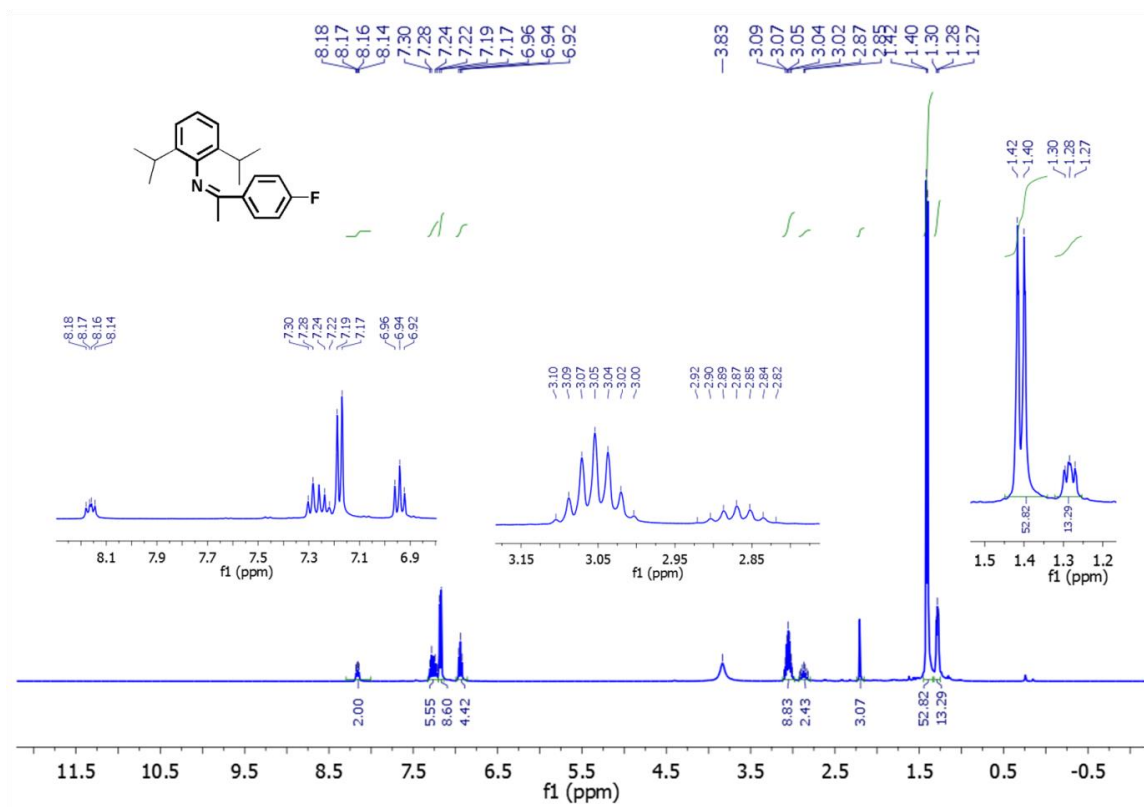


**Fig S75.** <sup>1</sup>H NMR spectrum (400 MHz, CDCl<sub>3</sub>) of *N*-(1-(*p*-florophenyl)ethylidene)-2,6-diisopropylaniline (**22**).

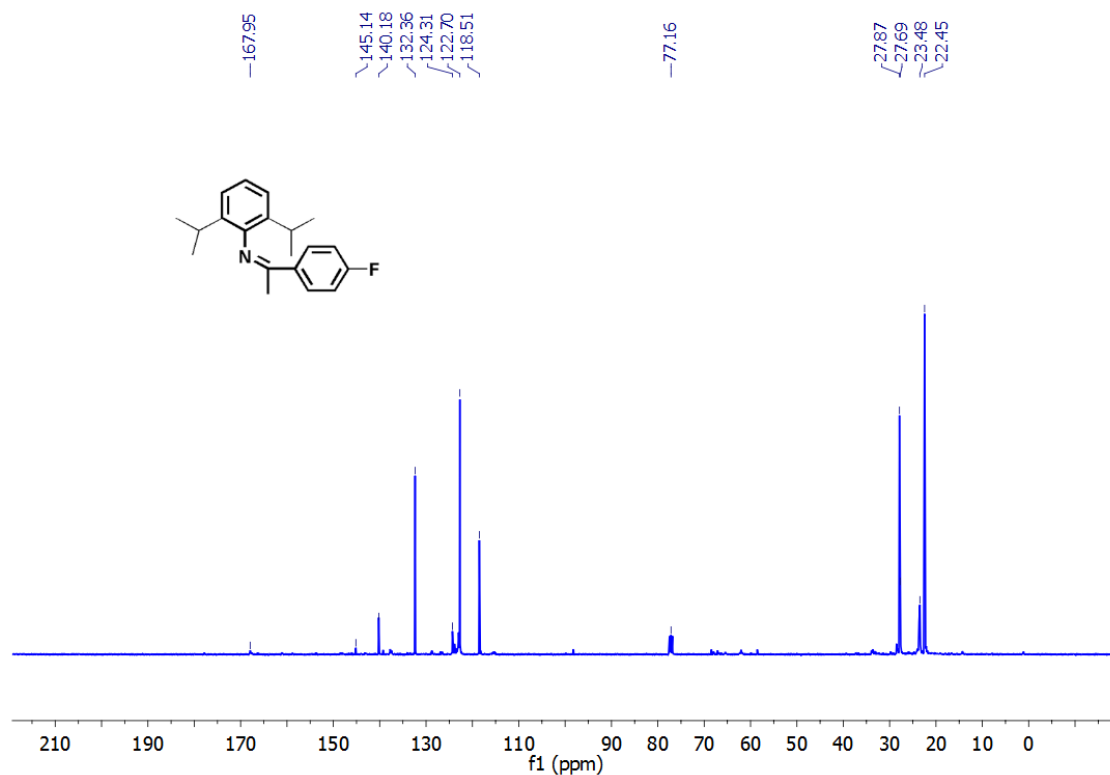


**Fig S76.** <sup>13</sup>C NMR spectrum (100 MHz, CDCl<sub>3</sub>) of *N*-(1-(*p*-florophenyl)ethylidene)-2,6-diisopropylaniline (**22**).

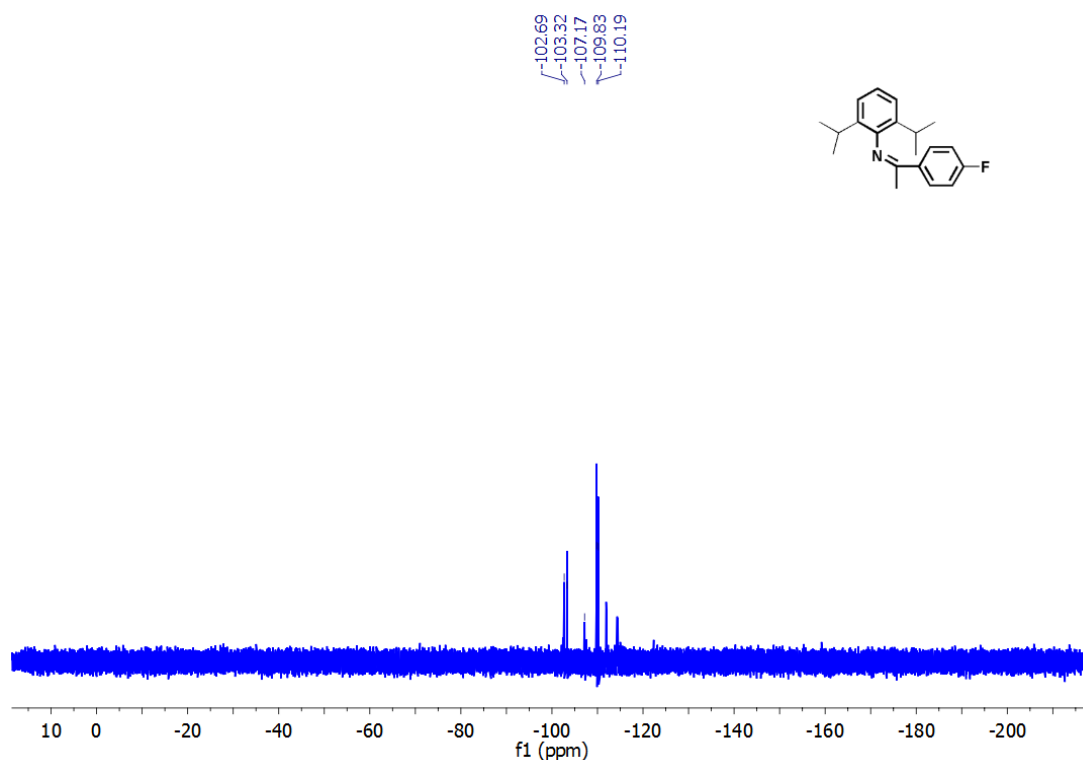


**Fig S77.**  $^{19}\text{F}$  NMR spectrum (376.4 MHz,  $\text{CDCl}_3$ ) of *N*-(1-(*p*-fluorophenyl)ethylidene)-2,6-diisopropylaniline (**22**).

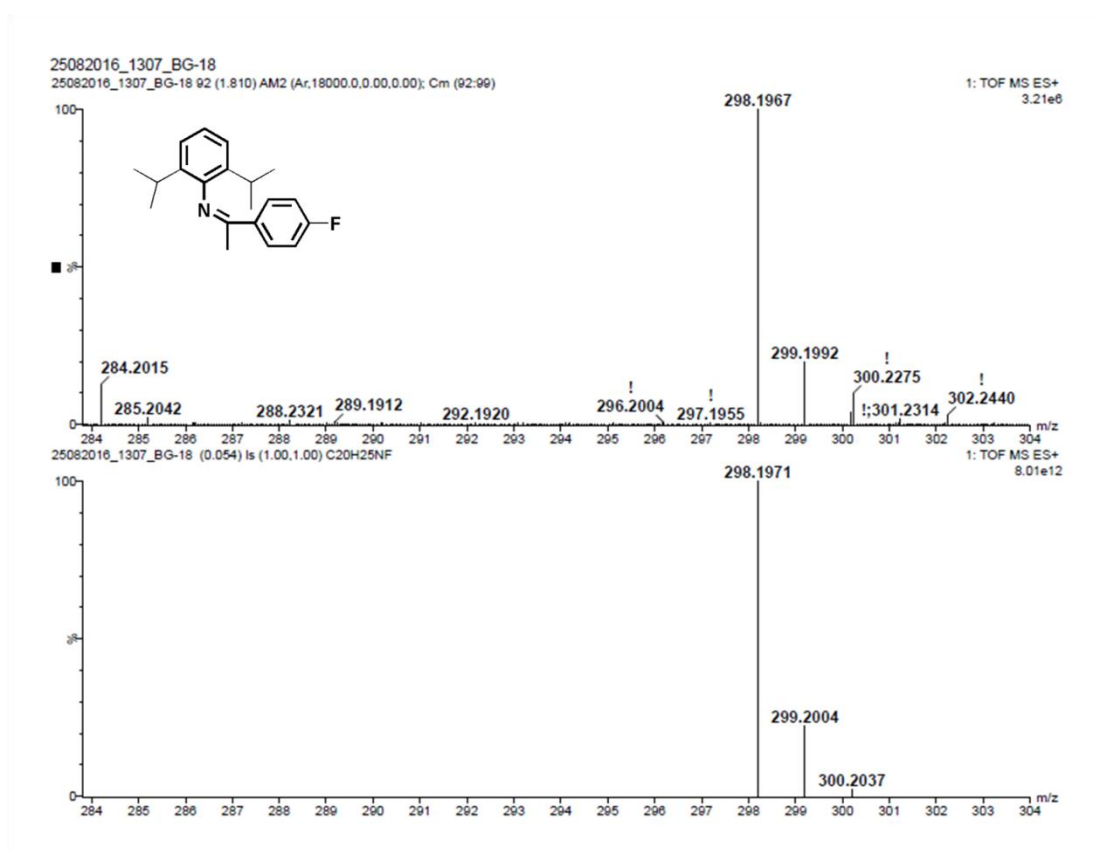


**Fig S78.** HRMS spectrum of *N*-(1-(*p*-fluorophenyl)ethylidene)-2,6-diisopropylaniline (**22**).

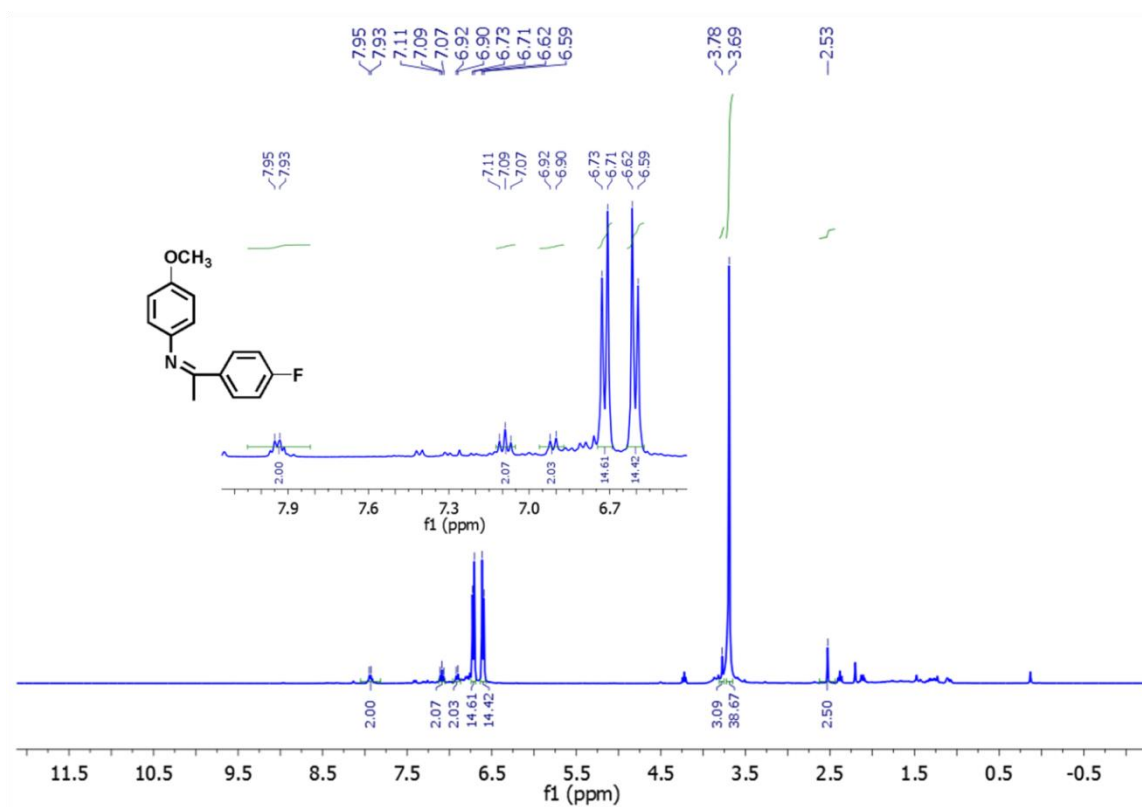


**Fig S79.** <sup>1</sup>H NMR spectrum (400 MHz, CDCl<sub>3</sub>) of *N*-(1-(*p*-florophenyl)ethylidene)-*p*-methoxyaniline (**23**).

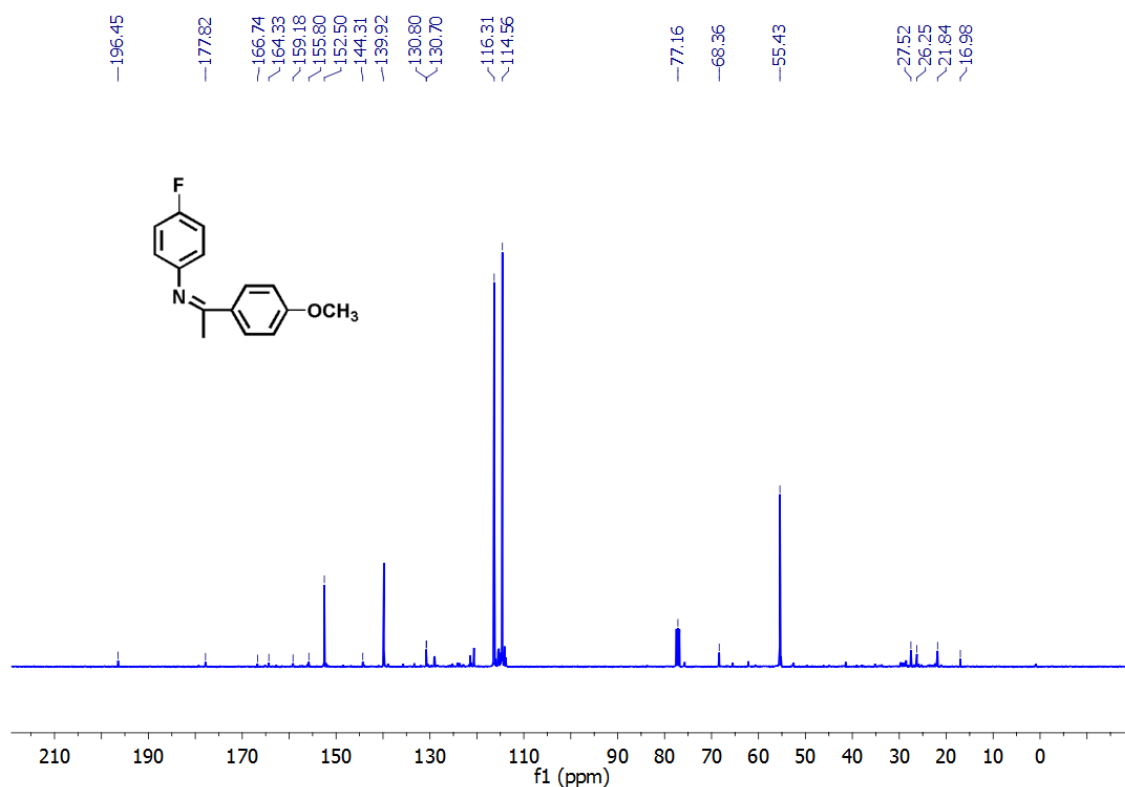


**Fig S80.** <sup>13</sup>C NMR spectrum (100 MHz, CDCl<sub>3</sub>) of *N*-(1-(*p*-florophenyl)ethylidene)-*p*-methoxyaniline (**23**).

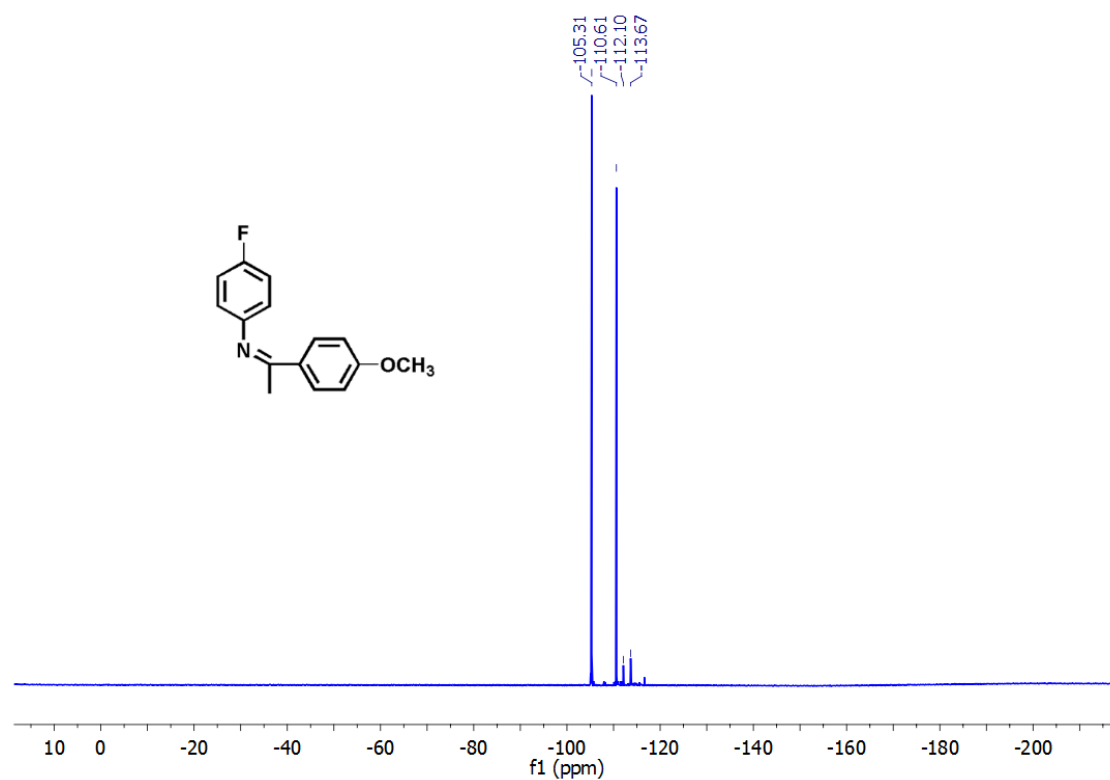


**Fig S81.**  $^{19}\text{F}$  NMR spectrum (376.4 MHz,  $\text{CDCl}_3$ ) of *N*-(1-(*p*-florophenyl)ethylidene)-*p*-methoxyaniline (**23**).

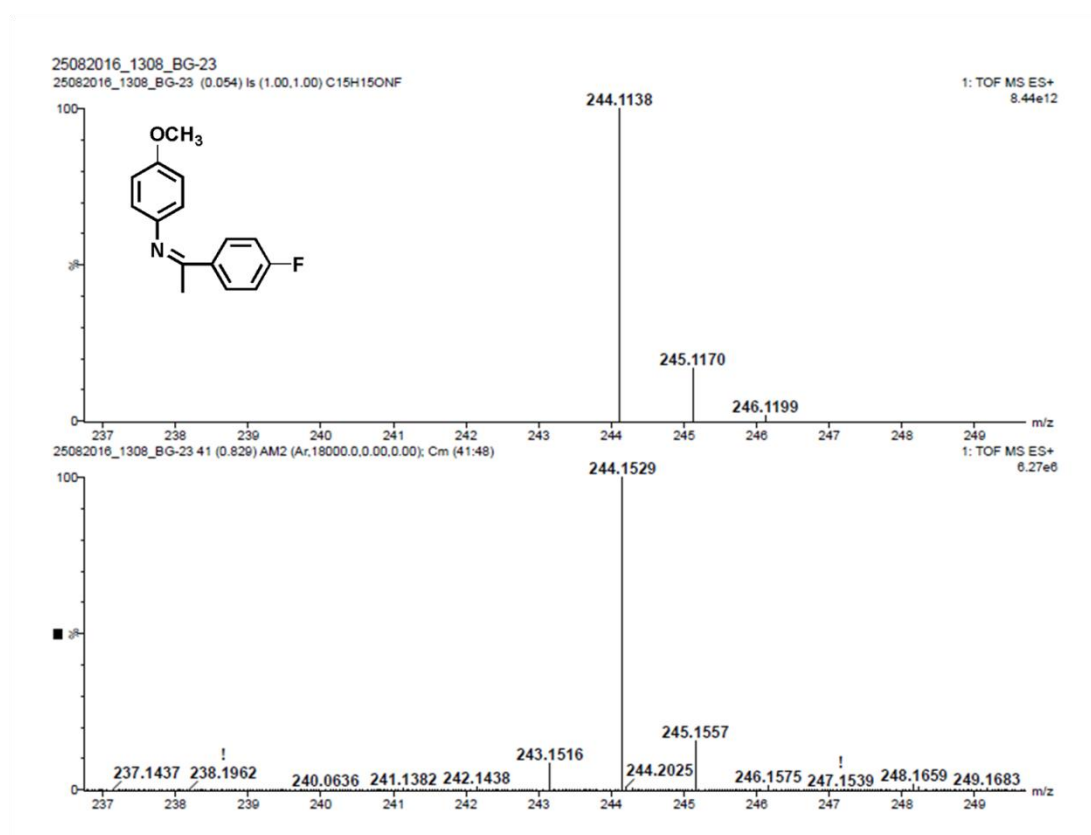


**Fig S82.** HRMS spectrum of *N*-(1-(*p*-florophenyl)ethylidene)-*p*-methoxyaniline (**23**).

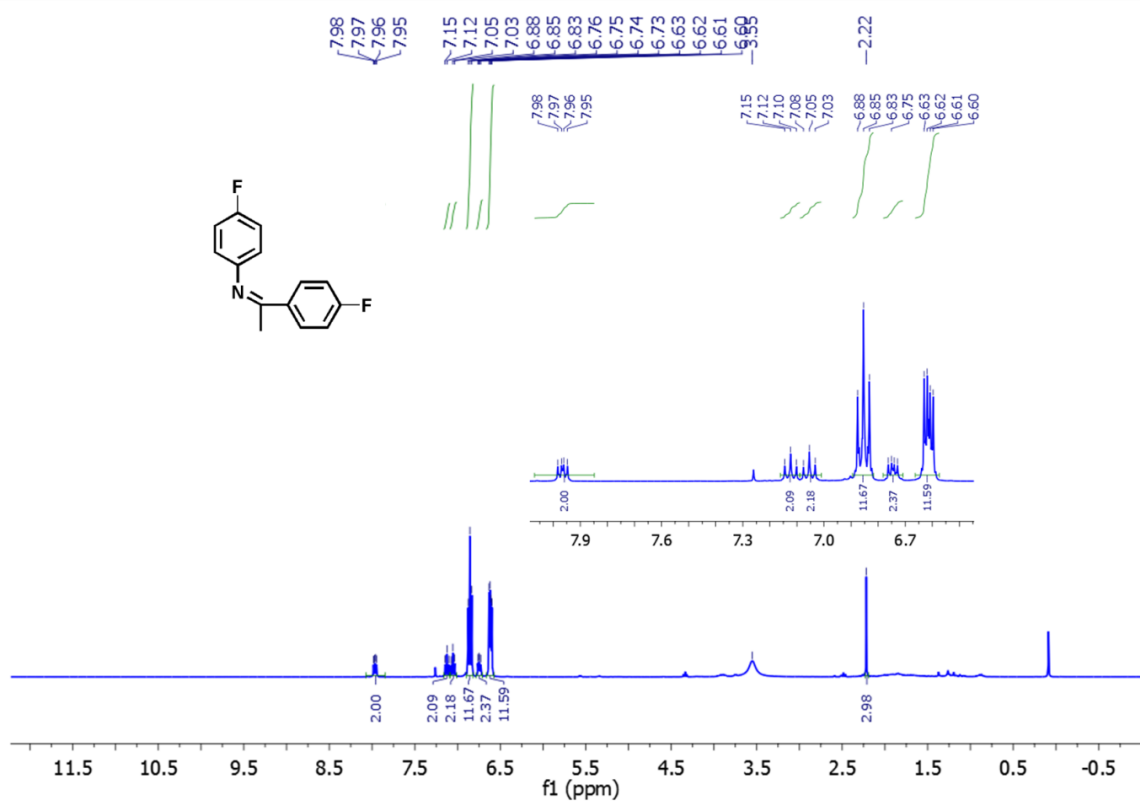


**Fig S83.** <sup>1</sup>H NMR spectrum (400 MHz, CDCl<sub>3</sub>) of *N*-(1-(*p*-florophenyl)ethylidene)-*p*-floroaniline (**24**).

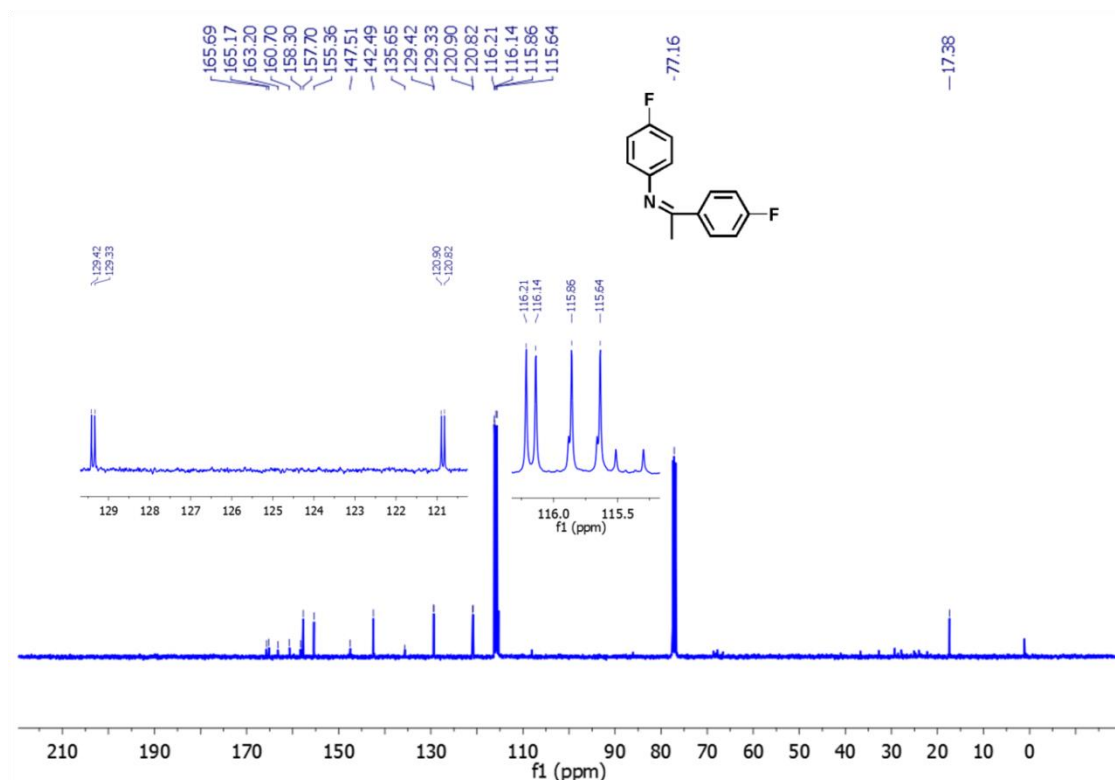


**Fig S84.** <sup>13</sup>C NMR spectrum (100 MHz, CDCl<sub>3</sub>) of *N*-(1-(*p*-florophenyl)ethylidene)-*p*-floroaniline (**24**).

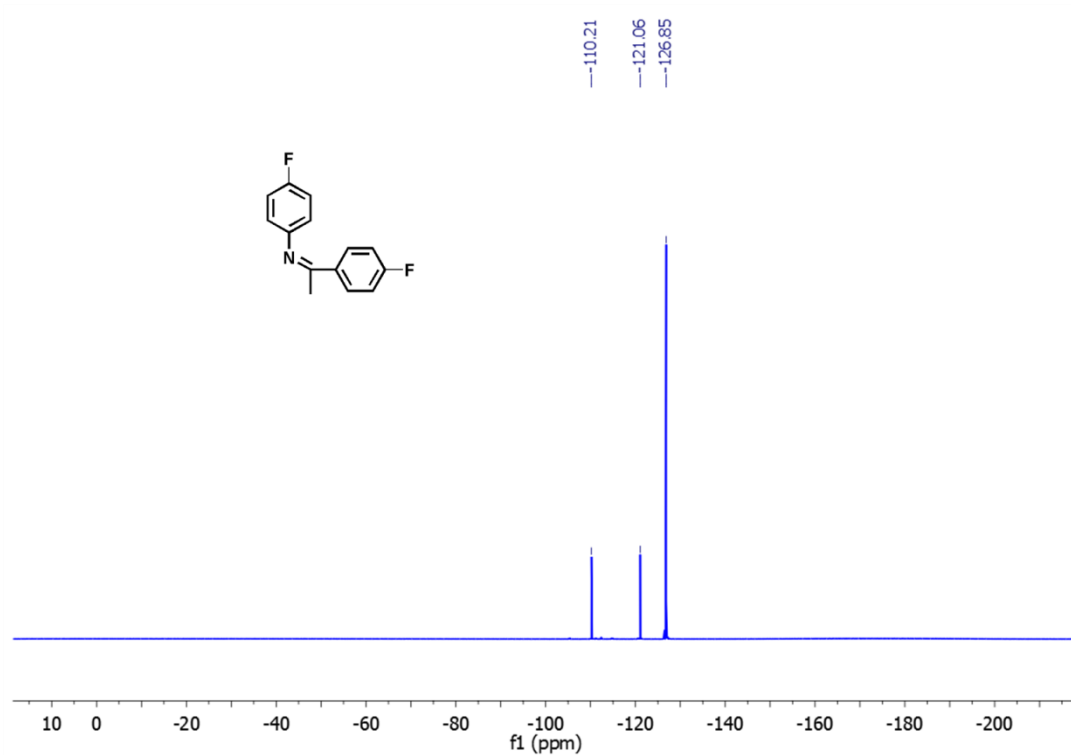


**Fig S85.**  $^{19}\text{F}$  NMR spectrum (376.4 MHz,  $\text{CDCl}_3$ ) of *N*-(1-(*p*-florophenyl)ethylidene)-*p*-floroaniline (24).

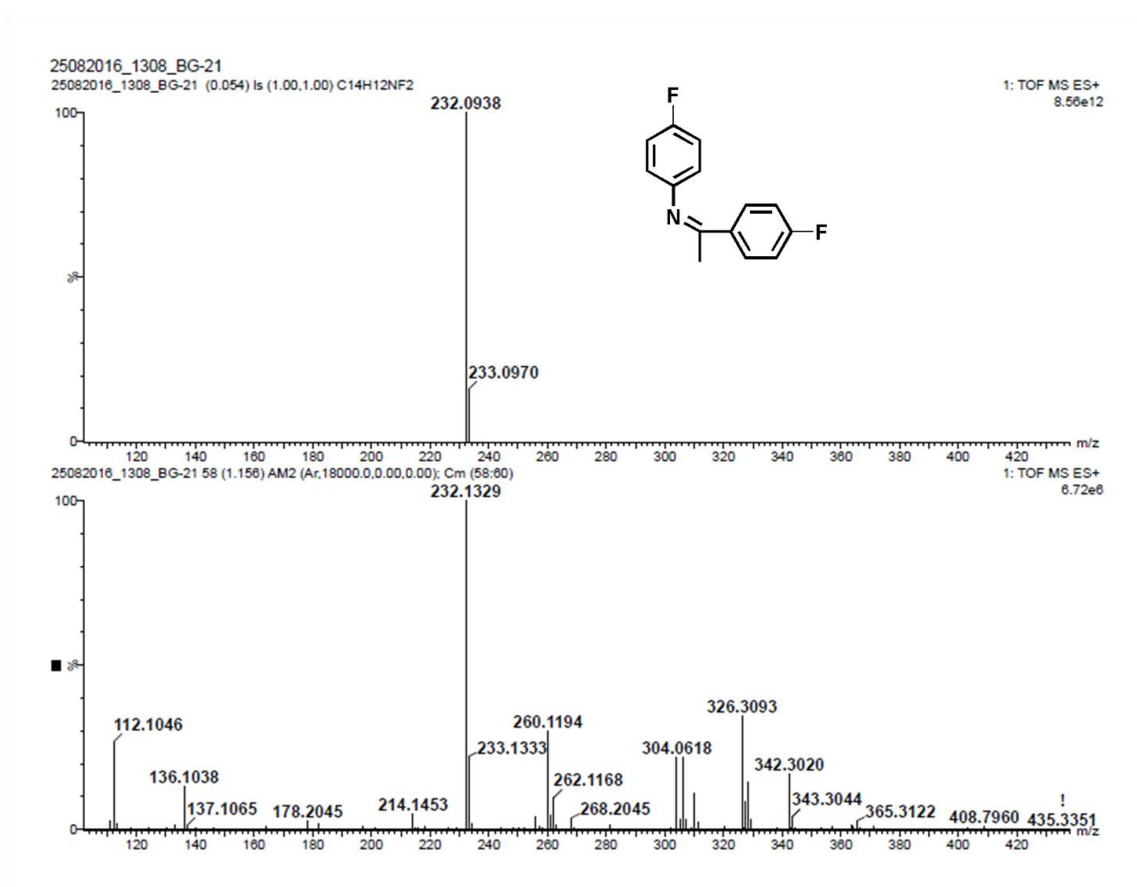


**Fig S86.** HRMS spectrum of *N*-(1-(*p*-florophenyl)ethylidene)-*p*-floroaniline (24).



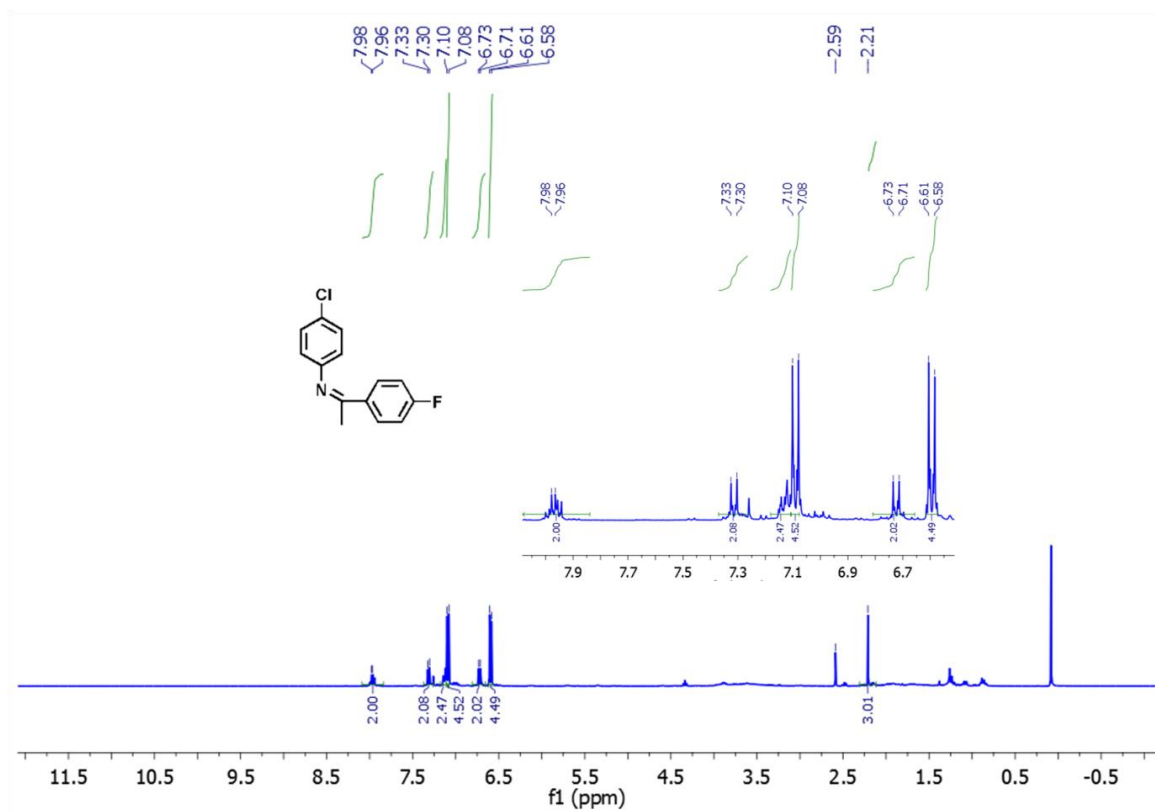


**Fig S87.** <sup>1</sup>H NMR spectrum (400 MHz, CDCl<sub>3</sub>) of *N*-(1-(*p*-florophenyl)ethylidene)-*p*-chloroaniline (25).

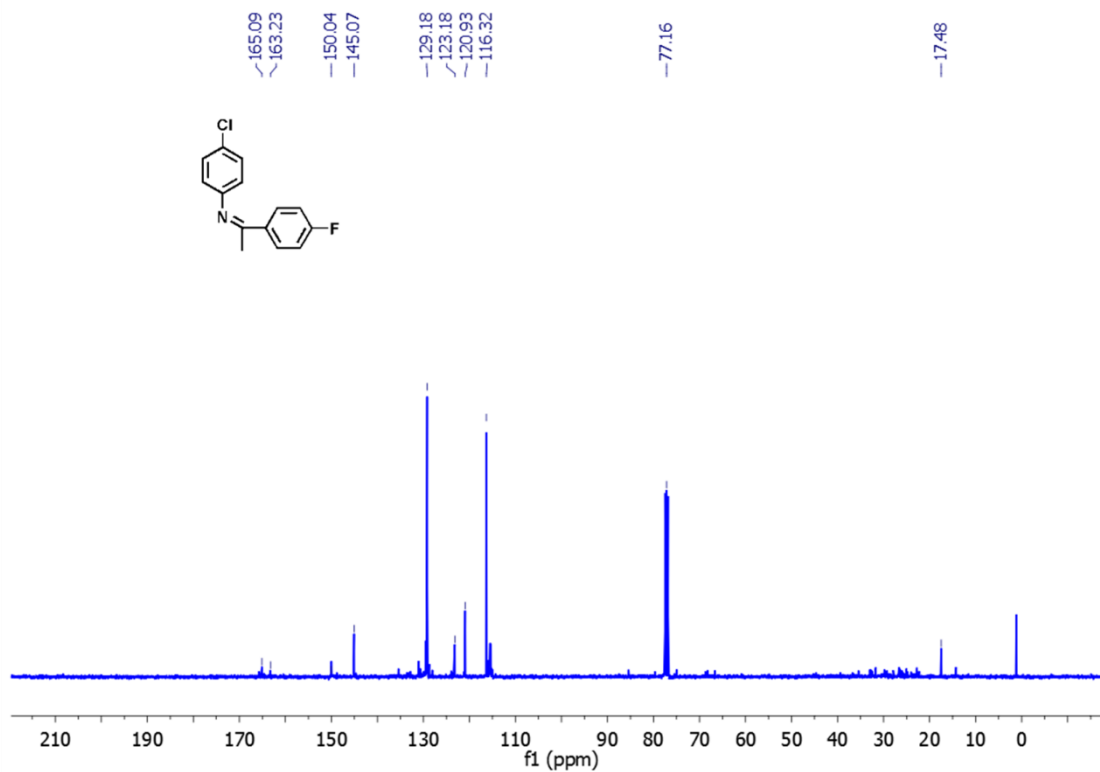


**Fig S88.** <sup>13</sup>C NMR spectrum (100 MHz, CDCl<sub>3</sub>) of *N*-(1-(*p*-florophenyl)ethylidene)-*p*-chloroaniline (25).

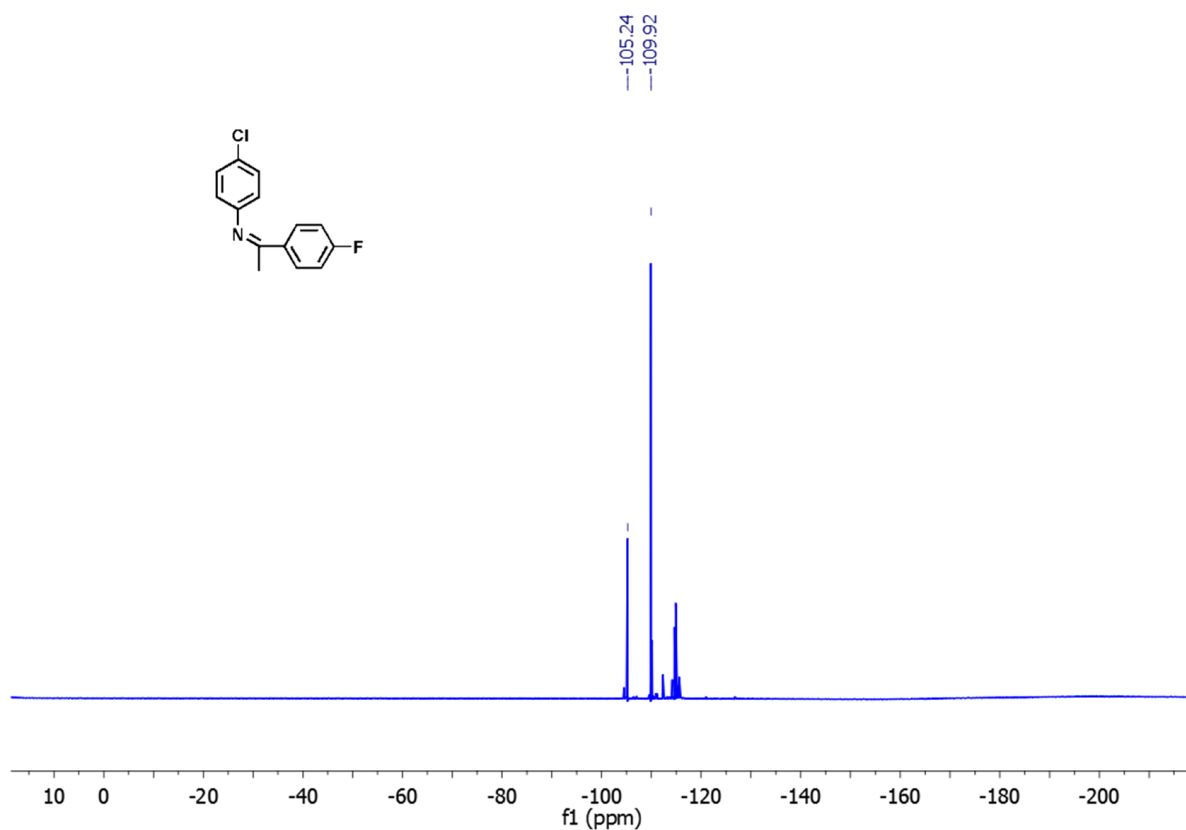


**Fig S89.** <sup>19</sup>F NMR spectrum (376.4 MHz, CDCl<sub>3</sub>) of *N*-(1-(*p*-florophenyl)ethylidene)-*p*-chloroaniline (25).

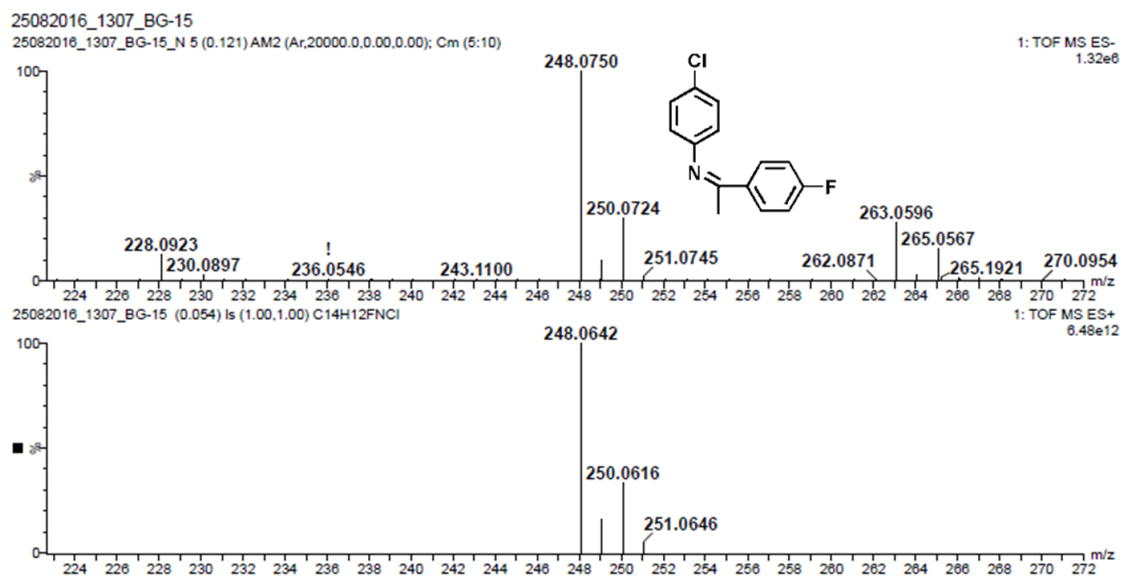


**Fig S90.** HRMS spectrum of *N*-(1-(*p*-florophenyl)ethylidene)-*p*-chloroaniline (26).

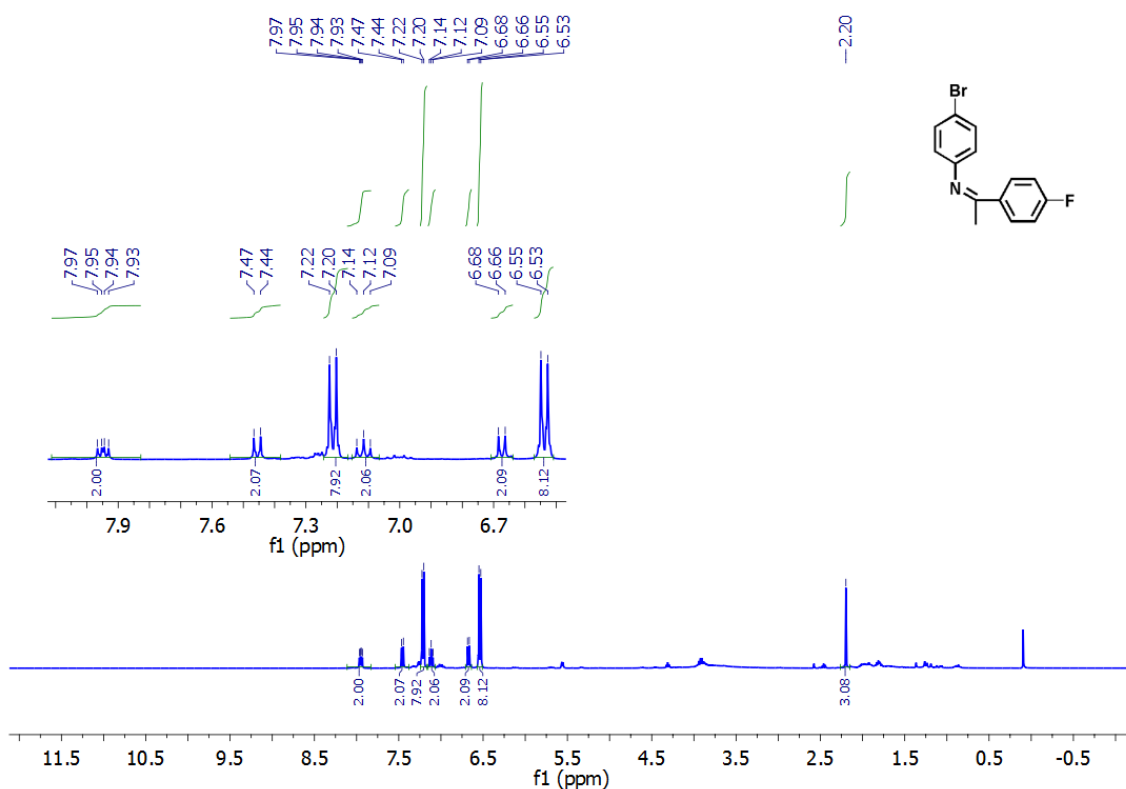


**Fig S91.** <sup>1</sup>H NMR spectrum (400 MHz, CDCl<sub>3</sub>) of *N*-(1-(*p*-florophenyl)ethylidene)-*p*-bromoaniline (27).

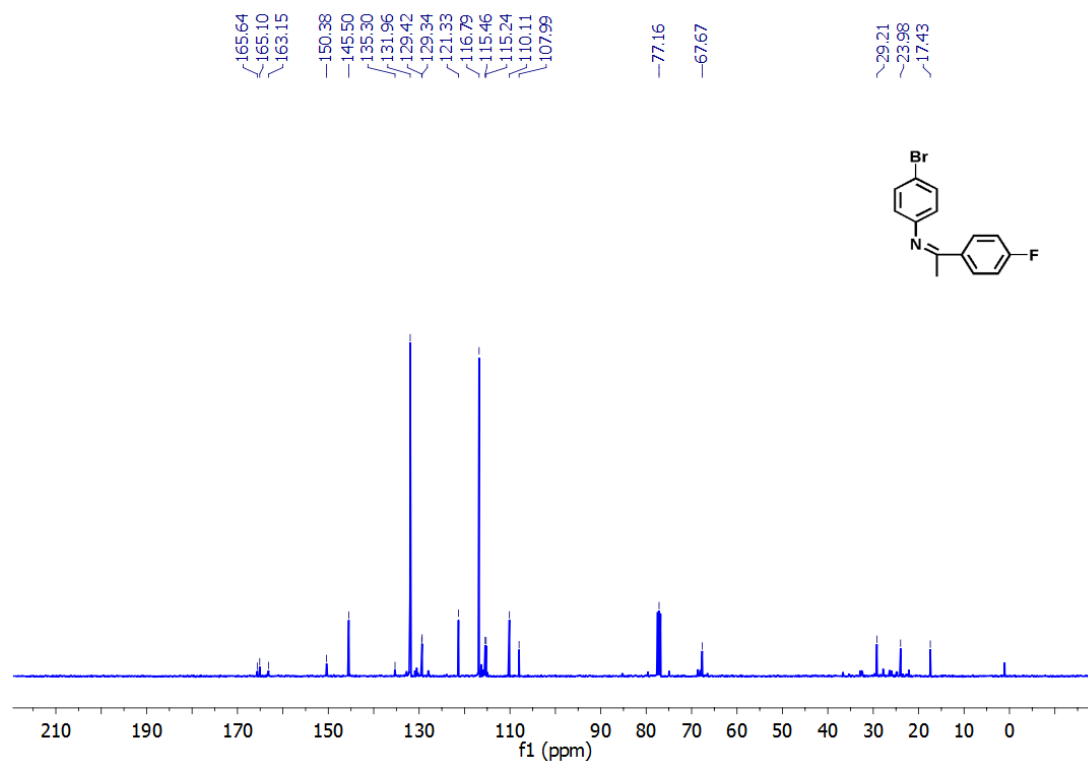


**Fig S92.** <sup>13</sup>C NMR spectrum (100 MHz, CDCl<sub>3</sub>) of *N*-(1-(*p*-florophenyl)ethylidene)-*p*-bromoaniline (27).

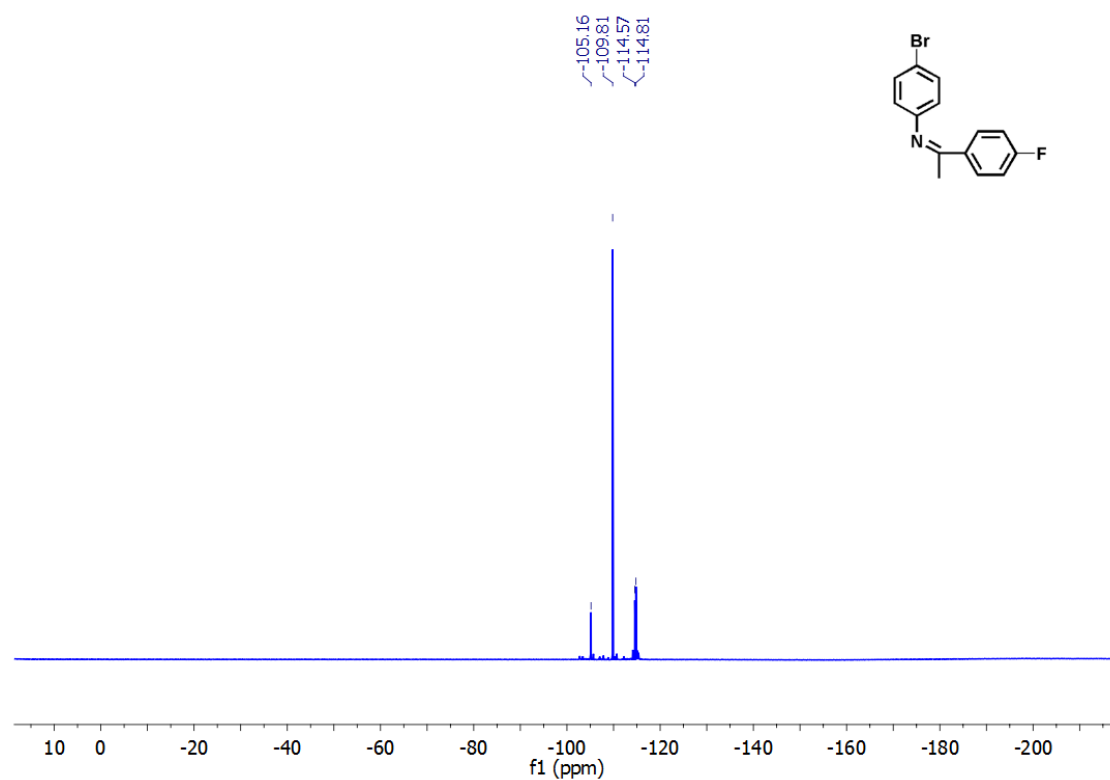


**Fig S93.**  $^{19}\text{F}$  NMR spectrum (376.4 MHz,  $\text{CDCl}_3$ ) of *N*-(1-(*p*-florophenyl)ethylidene)-*p*-bromoaniline (27).

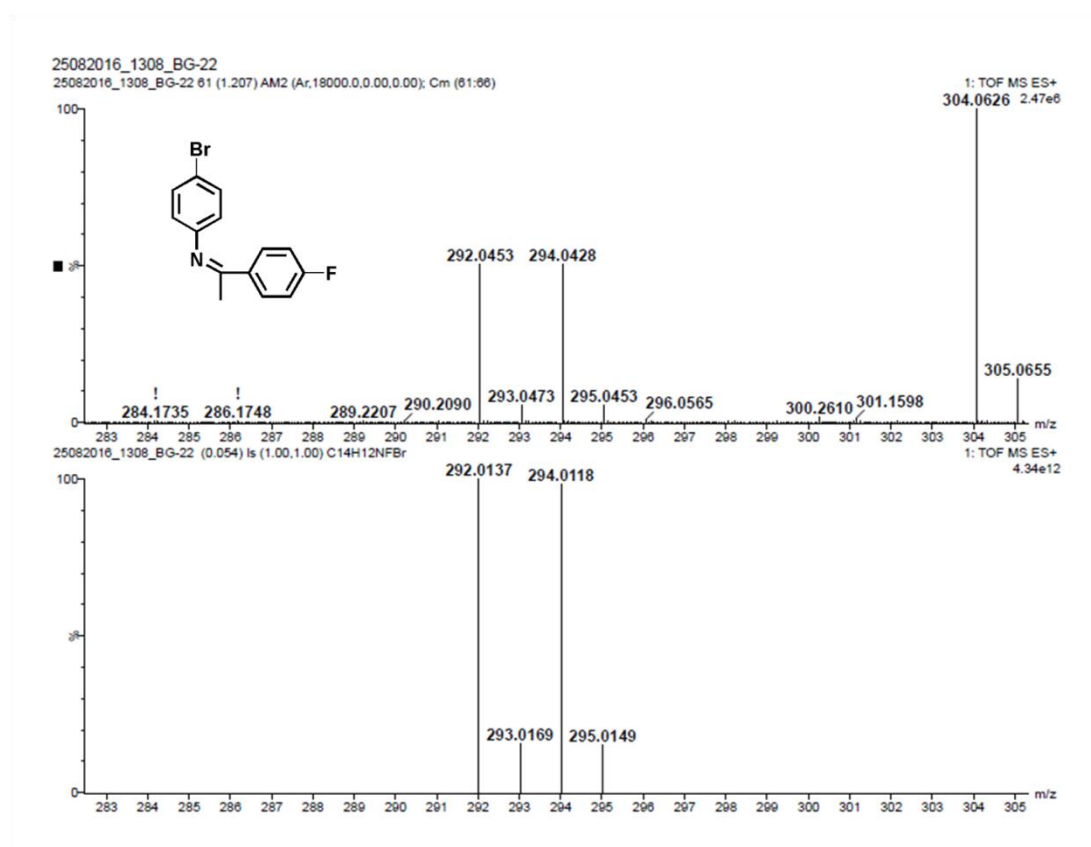


**Fig S94.** HRMS spectrum of *N*-(1-(*p*-florophenyl)ethylidene)-*p*-bromoaniline (27).